DESIGN AND MANUFACTURING OF A NEW CNC GANTRY MACHINE WITH DOUBLE MOTION FEED DRIVE SYSTEM

SEYED REZA BESHARATI

THESIS SUBMITTED IN FULFILLMENT OF
THE REQUIREMENTS FOR
THE DEGREE OF DOCTOR OF PHILOSOPHY

FACULTY OF ENGINEERING
UNIVERSITY OF MALAYA
KUALA LUMPUR

2015

ORIGINAL LITERARY WORK DECLARATION

UNIVERSITI MALAYA

Name of Candidate: **Seyed Reza Besharati** (I.C/Passport No:)

Registration/ Matric No: **KHA110013**

Name of Degree: **PhD of Engineering**

Title of Project Paper/Research Report/Dissertation/Thesis ("this Work"):

Design and manufacturing of a new CNC gantry machine with double motion feed drive system

Field of Study: **Manufacturing**

I do solemnly and sincerely declare that:

(1) I am the sole author/writer of this Work;
(2) This Work is original;
(3) Any use of any work in which copyright exists was done by way of fair dealing and for permitted purposes and any excerpt or extract from, or reference to or reproduction of any copyright work has been disclosed expressly and sufficiently and the title of the Work and its authorship have been acknowledged in this Work;
(4) I do not have any actual knowledge nor do I ought reasonably to know that the making of this work constitutes an infringement of any copyright work;
(5) I hereby assign all and every rights in the copyright to this Work to the University of Malaya ("UM"), who henceforth shall be owner of the copyright in this Work and that any reproduction or use in any form or by any means whatsoever is prohibited without the written consent of UM having been first had and obtained;
(6) I am fully aware that if in the course of making this Work I have infringed any copyright whether intentionally or otherwise, I may be subject to legal action or any other action as may be determined by UM.

Candidate's Signature Date

Subscribed and solemnly declared before,

Witness's Signature Date

Name:
Designation:

ABSTRACT

The CNC machine tools are spatial machines that are able to control computer. There are two types of machine tools structure, C-frame and gantry-frame. A CNC gantry machine tool is defined as a computer numerically controlled machine that is programmed and controlled through a computer. Its CNC controller offers very short setup time flexibility to run batches of one to several thousand. Today, the CNC gantry machines are widely used in manufacturing combined with software programs to efficiently and consistently create different products for large companies or even single consumers. The CNC gantry machine is used in the manufacturing sector including drilling, milling, reaming, boring and counter boring. Parts can be grooved and threaded with CNC milling centers; they can be transformed into CNC lathes, CNC drill and tap areas; for CNC grinding; and used in conjunction with routers to make CNC wood engravers and letterers. The CNC gantry machine can be used to machine small, large, short and lengthy components. Currently, there are two types of such machines in the market. The first type has a moving worktable and fixed gantry and the second type has a moving gantry and fixed worktable. Each type has advantages and disadvantages. In this study, a new concept is proposed to improve the specifications and applicability of the first type of CNC gantry machine.

In the new concept, reciprocal and simultaneous motion of the gantry and worktable is proposed as the gantry machine's X-axis double motion mechanism. At the beginning of this study, the double motion mechanism is designed based on a rack and pinion system. A new anti-backlash system is proposed to compensate for transmission error and backlash (simultaneously) and for use in the double motion mechanism. The simulation results of the new anti-backlash system are discussed. Due to manufacturing limitations of the rack and

pinion systems, a new double motion mechanism based on a ball screw system is proposed. Then, various designs of a new CNC gantry machine are presented. In this improvement process the problem is solved with the new design of a completed CNC gantry machine. The dynamic and static behavior of the final CNC gantry machine design is investigated via modal and static structural analysis using ANSYS software. The gantry's natural frequency is designed to be 202 Hz in the first vibration mode, making the machine capable of working at higher speeds of up to 11530 rpm, which is suitable not only for rough cutting but also for finishing. The final design of the new CNC gantry machine is updated according to the obtained results. The increase in natural frequency during gantry design modification affects complexity, increasing the weight and manufacturing cost of the gantry. As such, five different gantry designs are selected for comparison. Four parameters, i.e., the first four natural frequencies, total deformation due to mechanical forces, weight and manufacturing cost are considered performance indices. One is selected among five designs mathematically and optimized by MOGA (multi-objective genetic algorithm) in ANSYS software. In the optimization process, the gantry's natural frequency is maximized, thus minimizing the total gantry weight and deformation against mechanical forces. CNC gantry machine documents for manufacturing are prepared, followed by modeling, casting, machining and assembly. To evaluate and verify the design and analysis, an experimental modal test is performed. The experimental results show less than 11% error between the dynamic analysis and experimental test.

ABSTRAK

Alat mesin kawalan berangka komputer (CNC) adalah mesin spatial yang boleh dikawal menggunakan komputer. Ada dua jenis struktur alat mesin, iaitu rangka-C dan rangka gantri. Sebuah alat mesin gantri kawalan berangka komputer di definisikan sebagai sebuah mesin di kawal menggunakan pengiraan komputer. Kawalan CNC-nya menawarkan tempoh persediaan mesin yang singkat dan fleksibiliti untuk penghasilan secara berkelompok daripada satu sehingga beberapa ribu kelompok. Kini, mesin-mesin gantri CNC ini banyak digunakan di dalam proses pembuatan dengan kombinasi perisian komputer untuk menghasilkan produk secara efisyen dan konsisten untuk syarikat-syarikat besar mahupun kegunaan peribadi. Penggunaan mesin-mesin ini dalam sektor pembuatan meliputi proses penggerudian, pengisaran, *reaming*, menggerek dan menggerek-balas. Alur dan bebenang boleh di hasilkan kepada produk menggunakan fungsi mesin larikan berpusat CNC, dan mesin turut boleh diubahkan untuk menjalankan fungsi mesin larikan CNC, mesin gerudi dan torehan CNC, pengisaran CNC dan mengukir atau mengabjad kayu dengan menyertakan penghala. Mesin gantry CNC ini boleh digunakan untuk menghasilkan komponen kecil dan besar, pendek mahupun panjang. Sehingga kini, ada dua jenis mesin seperti ini dalam pasaran. Jenis yang pertama mempunyai meja kerja yang bergerak dengan gantri yang pegun, manakala jenis yang kedua mempunyai gantri bergerak dengan meja kerja pegun. Kedua-duanya mempunyai kelebihan dan kekurangan. Di dalam kajian ini, sebuah konsep baru dicadangkan untuk menambahbaik spesifikasi dan aplikasi mesin gantri CNC jenis pertama.

Di dalam konsep baru ini, satu mekanisme pergerakan pada paksi-X mesin gantri diperkenalkan iaitu pergerakan gantri dan meja kerja secara bersaling dan serentak, dikenali

sebagai mekanisme gerakan berganda. Pada permulaan kajian ini, mekanisme gerakan berganda ini telah direka berasaskan sistem rak dan pinan. Suatu sistem *anti-backlash* baharu diperkenalkan untuk mengadakan kompensasi terhadap ralat transmisi dan *backlash* (serentak) untuk memanfaatkan mekanisme gerakan berganda. Keputusan simulasi bagi sistem *anti-backlash* yang baharu ini dibincangkan. Disebabkan had pembuatan sistem rak dan pinan, mekanisme gerakan berganda dicadangkan untuk sistem *ballscrew*. Kemudian, pelbagai jenis rekabentuk mesin gantri CNC dipersembahkan. Di dalam proses pembaikan ini, masalah-masalah telah diselesaikan dengan rekabentuk baharu untuk menyiapkan mesin gantri CNC yang baharu. Kelakuan statik dan dinamik bagi rekabentuk akhir mesin gantri CNC disiasat melalui kaedah analisis struktur secara mod dan static menggunakan perisian komputer ANSYS. Mesin gantri ini direka untuk beroperasi pada frekuensi asli 202 Hz dalam mod getaran pertama bagi memungkinkan mesin untuk beroperasi pada kelajuan yang tinggi sehingga 12000 rpm supaya ianya bukan sahaja sesuai digunakan untuk menjalankan pemotongan kasar, bahkan untuk pemprosesan bagi tujuan kemasan. Rekabentuk akhir bagi mesin gantri CNC dimodifikasi berdasarkan keputusan yang didapati. Peningkatan frekuensi asli gantri semasa modifikasi rekabentuk telah mendatangkan kesan kepada kerumitan rekabentuk, peningkatan berat dan kos pembuatan gantri. Berdasarkan sebab-sebab ini, lima rekabentuk gantri telah dipilih bagi tujuan perbandingan Empat parameter iaitu empat frekuensi asli yang pertama, perubahan bentuk total disebabkan daya mekanikal, berat dan kos pembuatan dipertimbangkan sebagai indeks prestasi. Salah satu daripada lima rekabentuk telah dipilih menggunakan kaedah matematik. Rekabentuk yang dipilih telah menjalani proses pengoptimuman menggunakan kaedah MOGA (*multi-objective genetic algorithm*) yang merupakan kaedah algoritma genetik pelbagai objektif melalui perisian ANSYS. Dalam proses pengoptimuman, frekuensi asli bagi gantri telah dimaksimakan, selain perubahan bentuk total disebabkan daya mekanikal dan berat dikurangkan. Dokumen bagi tujuan pembuatan mesin gantri CNC disediakan. Kemudian, pemodelan, pembuatan acuan, pemesinan dan pemasangan mesin dibuat. Sebagai penilaian dan pengesahan rekabentuk dan analisis, suatu eksperimen ujian modal telah dilakukan. Keputusan eksperimen menunjukkan kurang 11% perbezaan atau ralat antara eksperimen dan analisis dinamik.

ACKNOWLEDGMENT

In the name of ALLAH the most compassionate, the most merciful

I thanksgiving ALLAH and I send my greeting to Prophet Muhammad and his family and followers.

I appreciation to my dear supervisors, Associate Prof. Dr. Ahmed Aly Diaa Mohammed Sarhan, Prof. Dr. Javad Akbari and Prof. Dr. Mohd Hamdi Bin Abd Shukor, who really supported me during my Ph.D. program and their invaluable comments really helped me in building up this thesis. I would also like to appreciate my dear friend Mr. Vahid Dabbagh for his sincere helps and I would like thank Prof. Mohammadreza Movahedi and his research group from Sharif University, for their useful advices. I would like to appreciate from *AMMP* group for helping and supporting me.

Finally, I am constantly indebted to my wife and my family for their endurance, understanding and encouragement throughout my achievement.

TABLE OF CONTENT

LIST OF FIGURE

LIST OF TABLE

LIST OF ABBREVIATIONS

CN	Numerical Control
CNC	Computer Numerical Control
MOGA	Multi-Objective Genetic Algorithm
2D & 3D	2 & 3 Dimension
L	Linear Motion
R	Rotary Motion
CAD	Computer Aided Design
CAM	Computer Aided Manufacturing
RPS	Roller Pinion System
DTE	Dynamic Transmission Error
ODE	Ordinary Differential Equations
Rpm	Revolution Per Minute
µm	Micro Meter
FFT	Fast Fourier Transform
UMCIC	University of Malaya Center of Innovation and Commercialization
FEM	Finite Element Method
GBCM	Gear Backlash Compensation Mechanism
MRR	Maximum Metal Removal Rate
AHP	Analytical Hierarchy Process
PEG -MCDM	Pareto –Edgeworth- Grierson(Multi Criteria Decision Method)
DM	Decision Maker's
TOPSIS	Technique for Order of Preference by Similarity to Ideal Solution
ELECTRE	Elimination and Choice Expressing Reality

GRA	Generic Risk Assessment
C.I	Consistency Index
C.R.	Consistency Ratio
MSE	Calculating Mean-Square-Error
Eq.	Equation
TPM	Technology Park Malaysia
EMA	Experimental Modal Analysis

LIST OF SYMBOLS

Kg	Kilogram
mm	Millimeter
g	Gram
N	Newton
HZ	Hertz
kPa	Kilopascal
M	Momentum
F	Force
V	Velocity
P	Presser
ms	Millisecond
KHz	Kilo Hertz
m/s	Meter per Second
MP a.	Mega Pascal
j_t,	Circular Backlash
j_t,	Normal Backlash
j_r	Center Backlash
j_θ	Angular Backlash
ft/sec	Feet per Second
GPa	Giga Pascal
N.F.	Natural Frequency

CHAPTER 1

1 INTRODUCTION

1.1 General Background

Machine tools are spatial mechanisms with several degrees of freedom and require sufficient workspace to coordinate workpiece and tool movement for the machining operation (Reuleaux., 2007). The function of these machines is to move either the tool or the workpiece, or both at the same time (simultaneously) for machining.

During the industrial development, John T. Parsons invented the first numerical control (NC) machine around 1950 (Arnold, 2001; IOS, 2001). This NC machine had some problems. Although it worked automatically and produced workpieces with a high degree of accuracy, it was complicated and expensive (Sematech, 1997). The first generation of numerical control was this NC machine introduced in 1950, which was developed for CNC machines after a few years. CNC technology has a radical effect on manufacturing expansion across the globe (Newmana, 2008). This technology offers the advantage of producing a huge array of complex, different size components, from micro- to multi-meters, as well as various types of materials such as aluminum and titanium alloys (Newmana, 2008). Between the 1970s and 1980s, for producing more complex components, CNC machine manufacturers felt the CNC machine needed to have additional axes for wider usage and flexibility (Xu, 2006). Moreover, a high-accuracy CNC milling machine was required for many industrial purposes due to the growing demand for component precision and consistency of quality. However, for industrial requirements, CNC machine makers added extra axes consecutively. After the three-axis CNC machine, five-axis CNC machine tools became increasingly popular owing to their ability to efficiently machine free-form surfaces (Lei, 2007). Five-axis CNC machines have most widely been used in machining complex surfaces. Five motions are simultaneously and continuously controlled with a five-axis machine. This machining ability can be useful in different, complex machining processes. The three-axis CNC machine is complemented by two additional rotary axes to adjust the tool orientation relative to the workpiece. The benefits of the five-axis CNC machine include: better tool accessibility, high material removal rate (MRR), surface quality, less workpiece setup time and significantly lower production costs (W.T. Lei, 2002). One of the important applications of the five-axis CNC machine is in industrial die and molds; this machine tool has been widely used to machine complex parts in this field. Five-axis CNC machines are not only applicable in milling operations but can be general-purpose, such as for boring, turning and grinding (Teo, 2007).

1.2 Importance of Study

Five-axis CNC machine applications are crucial to the development of nearly all industrial fields. Industrialized countries aim to have CNC five-axis machine technologies because CNC production is profitable. Nowadays, five-axis CNC machines yield huge profits worldwide and their price is rising. Nonetheless, five-axis CNC machine technology is very complicated and is rapidly undergoing development.

There are two ways to obtain this technology: reverse engineering or reverse design. The reverse engineering method is a famous means of producing many things, but it is not addressed in this thesis. CNC gantry machine design has been considered for achieving the technology. The importance of this study lies not only in the design of a CNC gantry machine but also in significantly improving the specifications of existing CNC gantry machines.

Some of the main goals are to improve precision while reducing size and cost and enhancing abilities. Small machine size and particular specifications are required to obtain results. Therefore, this research provides the design of a new CNC gantry for industrial purposes. New specifications are considered in designing a five-axis CNC gantry machine with a double motion mechanism and high speed machining as some of this machine's characteristics.

1.3 Research Problem Statement

Designing five-axis CNC machines is challenging due to the technical complexity. Design information of existing machines is not readily available, nor is it completely found in books. Nevertheless, the required knowledge must be found, which will take a long time. Unfortunately, machine manufacturers do not disclose the main CNC gantry machine technology knowledge and seldom can this science be found in papers or books. A number of problems are evident in the first type of existing CNC gantry machine, such as machine worktable length, precision and industrial space length. These must be solved by improvements through our proposed gantry machine, which is the main target. Therefore, a new five-axis CNC gantry machine design is required to solve the problems with the specifications, so a fundamental redesign of the machine is essential. This research is an attempt to solve these problems in this study by designing a new CNC gantry machine. The process of understanding and solving design problems is part of the difficulty with this technology.

1.4 Study Objectives

In this work, a novel type of CNC gantry machine will be designed. There are two main objectives:

i. Design a new type of CNC gantry machine with a double motion feed drive system (for moving both the gantry and table simultaneously). The design includes details of the machine structure, gantry, worktable, carriages and components, besides selecting suitable standard components.

ii. Prototyping of a semi-industrial size of new type of the CNC gantry machine which complies with standard components.

1.5 Research Methodology Flowchart

The flowchart of the research activities is shown in Figure 1.1.

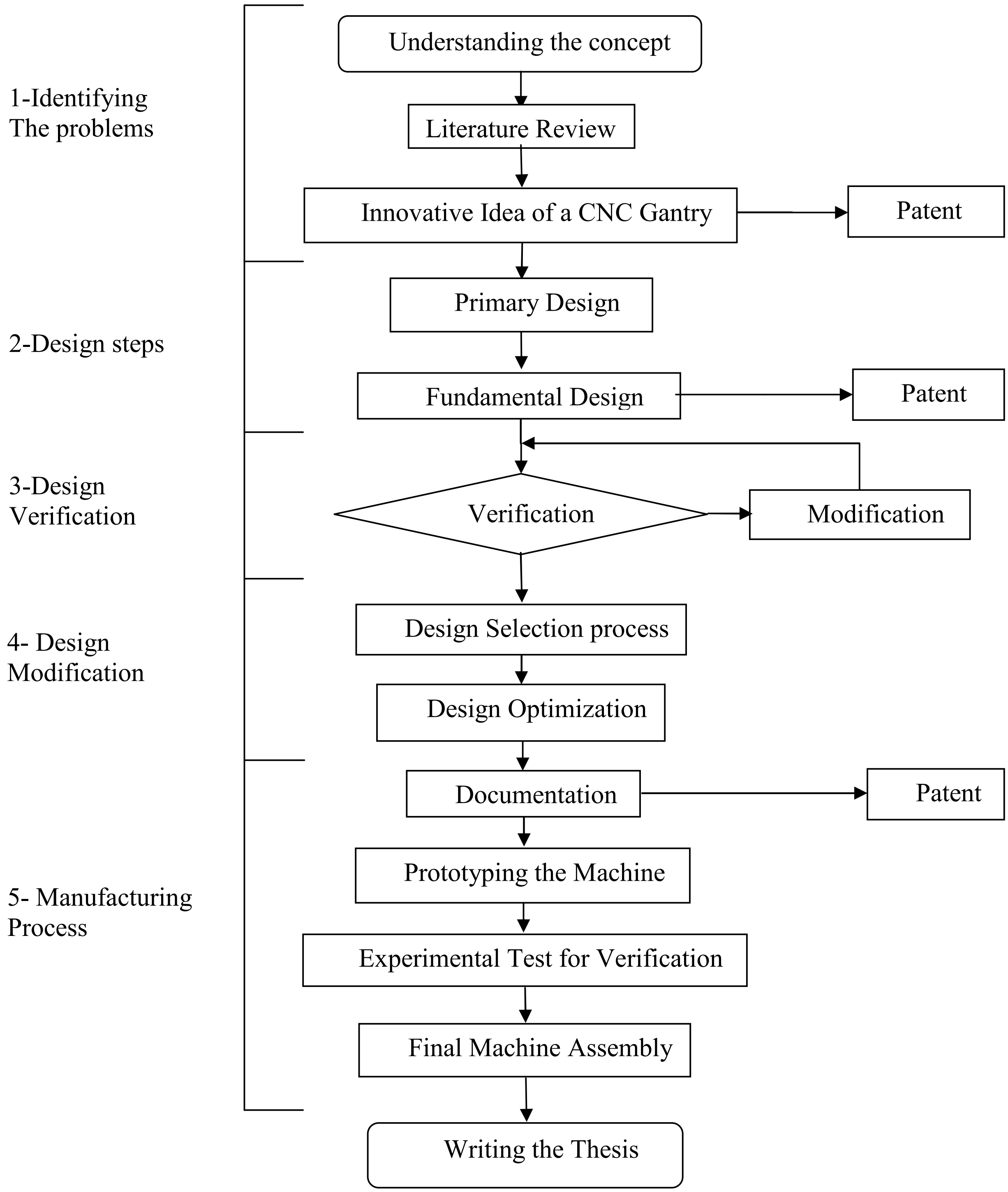

Figure 1.1 Study Flowchart

1.6 Research Activity Explanation

i. Understanding the Concept

The objective of this work is to design a new type of CNC gantry machine with high-performance features. The performance of existing CNC gantry machine types can be enhanced. In fact, the feed drive motion of the new machine is totally different from existing types. The gantry and table can move together simultaneously in this design. For a briefing of the main concept, current types of CNC gantry machine must be explained.

ii. Literature Review

The literature review of prior experience about CNC gantry machine design based on available resources (e.g., the Internet, journals and conference proceedings) can help achieve the desired goal. The main objective of this study is to identify the capabilities of each machine type, such as structures, motion mechanisms and applications to designing new types. Therefore, the researcher must investigate the main different types of existing CNC gantry machine to conceive the new idea of developing them.

iii. Innovative Idea of a CNC Gantry Machine

The new idea of a CNC gantry machine based on the conceptual design is presented. This type of machine is made to further develop the CNC gantry machine.

iv. Patent Process

All documents related to the design novelty are prepared and submitted to the UMCIC section for patenting.

v. **Primary Design Step**

The primary design of the new type of CNC gantry machine from the conceptual design is discussed in this section. The overall machine design is considered.

vi. **Fundamental Design Steps**

The fundamental design of a CNC gantry machine with a double motion mechanism from the primary design is considered and discussed. The different machine designs are presented and compared in this section to find the best design of a new gantry machine based on certain requirements.

vii. **Analysis Process**

Design verification via modal, harmonic and static analysis methods are considered, and the result is applied for further machine modification.

viii. **Modification Process**

The design target is for the machine to be capable of tolerating around 200 Hz of natural frequency in the first mode of vibration. Therefore, a gantry modification process is performed. In this process, the modified design will be compared with the final modification results to find a solution to increase performance, such as design dynamics and static behavior.

ix. **Design Selection Process**

In this section, several gantry designs will be selected for performance comparisons. Some gantry specifications include the natural frequencies of the first of four modes, total deformation of the gantry under working forces, gantry weight and manufacturing costs. The optimum design will be presented through special optimization methods.

x. **Optimization Process**

The selected design will be optimized with MOGA (multi-objective genetic algorithm) via ANSYS software. In this process, gantry performance will be investigated. Some gantry technical specifications must be maximized while others must be minimized. Optimized design documents will also be prepared for the fabrication process.

xi. Documentation

All design documents required for manufacturing are prepared and presented in this section. 3D and 2D documents for making patterns, casting, machining and assembly are made.

xii. **Manufacturing Process**

The prototyping steps for a new CNC gantry machine are presented in this section. A concise report about the processes of pattern making, casting, machining and assembly of the new CNC gantry machine will be presented and discussed. The manufactured detail components and purchased standard components of the machine have been shown in Appendix (A and F).

xiii. Experimental Test for Verification

Following gantry prototyping, to verify the design process an experimental analysis test will be performed on the prototyped gantry using related instruments. The differences between experiment results and design analyses are investigated.

xiv. **Final Machine Assembly**

All fabricated machine components will be assembled in this section.

1.7 Scope of Work

The main objective of this project is to design and manufacture a new type of CNC gantry machine, with the aim of solving the problems of existing CNC gantry machines by creating a new design in this project. The main advantages of the new design are presented below.

i. Increase Worktable Length

In the first type of gantry machine the worktable length is limited to the length of the ball screw. Using a double motion mechanism for feed drive motion should solve the problem.

ii. Decrease the Total Length of the Machine

The total length of the existing type of gantry machine is nearly twice that of the worktable and in the new design it is reduced to almost one and a half times the worktable.

iii. Improve Total Precision of the Machine

In the current type of gantry machine the total precision is dependent on the total length of the ball screw. In the new design a shorter ball screw is used, hence machine precision is increased.

iv. Increase Machining Rapid Speed

The X-axis rapid speed in the existing type of gantry machine is dependent on the worktable or gantry speed. In the new design, the rapid speed is increased to the total speed of the worktable and gantry.

v. **Considerably Increase Machine Efficiency**

In the new CNC gantry machine design, the total efficiency will be increased on account of the double motion mechanism.

vi. Simplify Machine Manufacturing

In the new CNC gantry machine design, the total machine length will be decreased significantly to simplify the manufacturing process.

vii. Significantly Decrease the Total Cost of the Machine

With the new CNC gantry machine design, the total manufacturing cost will be decreased due to simplifying the process.

1.8 Organization of the Thesis

This research is divided into seven chapters.

CHAPTER 1: INTRODUCTION

Chapter one presents a general background and the importance of the study, the research problem, statement of study objectives, research methodology, an explanation of research activities, scope of study, the concept and how the contents are organized.

CHPTER 2: LITERATURE REVIEW

Chapter two comprises an introduction, a general background of machine tool design, machine kinematic chain design, common configurations of a five-axis machine, CNC gantry machine types and accessories, machine structure, design-related key words for a CNC machine gantry, such as modification, optimization, feed drive, anti-backlash with a new anti-backlash system proposed and the conclusion.

CHAPTER 3: CONCEPTUAL DESIGN OF A NEW GANTRY MACHINE

Chapter three includes an introduction and the conceptual design of a new type of CNC gantry machine. The advantages of the new type are explained, a CNC gantry machine feed drive motion is proposed and a feed drive design (double motion mechanism) based on rack and pinion is proposed. The design of a new CNC gantry based on a double motion mechanism is presented and then the characteristics of the double motion mechanism and its problems are investigated. A new anti-backlash mechanism with a new idea for solving the first problem of the double motion mechanism is proposed and a new anti-backlash (GBCM) mechanism is designed. Subsequently, three new CNC gantry machine designs based on the new anti-backlash are proposed. Nonlinear dynamic analysis of the new anti-backlash gear mechanism design for less dynamic transmission error is carried out and the nonlinear dynamic model is discussed. The chapter ends with a conclusion.

CHAPTER 4: STRUCTURAL DESIGN OF A GANTRY MACHINE TOOL

Following the introduction, chapter four presents the design of a double motion mechanism based on a ball screw system. The double motion mechanism and its modified characteristics are discussed. The gradual design of the new type of CNC gantry machine is proposed based on the new motion system. The third CNC gantry machine design process is described and analyzed. Further modification is done based on dynamic and static results and the behavior of the modified gantry under cutting force and natural frequency below 12000 RPM is evaluated. The fourth design is introduced and a fifth gantry machine design is proposed based on crossbeam modifications. The best gantry design is selected according to the initial gantry design. The selection parameters are defined for the selection process and finally, the chapter concludes.

CHAPTER 5: OPTIMUM SELECTION SEEKING USING MULTI-CRITERIA DESIGN MAKING (MCDM) AND MULTI-OBJECTIVE STRUCTURAL OPTIMIZATION OF A GANTRY

Chapter five begins with an introduction and continues with seeking the optimum design using AHP and PEG-MCDM. The optimization objectives are investigated, the optimization methods and gantry parameters for the optimization process are evaluated and the sensitivity of the gantry parameters is assessed as well. Gantry optimization is carried out based on the MOGA method and the chapter finishes with conclusions.

CHAPTER 6: GANTRY MACHINE MANUFACTURING PROCESS AND TESTING

Chapter six starts with an introduction, which is followed by the design preparation of the new CNC gantry machine documents. The machine fabrication technology and its materials will be investigated and the experimental result of vibration of the gantry will be prepared. In addition the final assembly process of the CNC gantry machine will be discussed. Finally the CNC controller of the machine will be introduced.

CAPTER 7: THESIS CONCLUSION

Chapter seven comprises the thesis conclusions, directions for future research, future works and recommendations.

CHPTER 2

2 LITERATURE REVIEW

2.1 Introduction

Machine tools have an important role in manufacturing and have undergone considerable productivity, precision and durability in the past few decades. The requirements for the operational and technological properties of materials employed have also increased significantly (Shevchuk, 2008). Surface roughness is a major consideration in modern Computer Numerical Control (CNC) machines (Lan, 2010). It is desirable that the negative effects such as vibration and noise in the machine tools used today be brought to a minimum. Desired machine tool properties include high static stiffness for bending and torsion, good dynamic characteristics, good dimensional stability, low coefficient of expansion, low cost and low material requirements (Rahman, 2001.Bazul,).

In this thesis, designing a “new type” of gantry machine tool is accomplished using several concept and methods. Static and dynamic machine tool characteristics affect the final attainable accuracy and therefore, relevant literature is investigated in this chapter. In addition to static and dynamic characteristics, the cost of production and weight are considerable matters in designing machine tools. To attain optimal results, optimization and decision making methods could be exploited. Such methods provide scientific procedures for obtaining the optimal design and at the same time reduce the time invested in the design stage. Accordingly, relevant research regarding optimization and multi-criteria decision making is investigated.

2.2 Concepts of Machine Tool and Gantry Machine Tool Technology

A machine tool is a special device capable of cutting away surplus material from a workpiece in accordance to the specimen's shape and size, as well as required degree of accuracy and surface finish. The machine tool should meet these requirements and must be able to uphold the cutting tool and workpiece provide sufficient power to enable the tool to cut the material from the workpiece and position the tool and workpiece relative to each other. The positioning must be controlled with a certain degree of accuracy. There are many categories of machine tools, such as turning, milling and so on, with gantry machine tools belonging to the milling category.

2.2.1 **General Background of Milling Machine Tool Design**

Lopez de Lacalle, Bohez and their colleagues are recognized for advancing the design procedure of CNC milling machines. Therefore, it is necessary to become familiar with their basic notions about machine kinematics and the definition of machine axis motion (Bohez, 2002; Lamikiz, 2009).

Generally, the main specifications of a milling machine tool must satisfy the following principles(Bohez, 2002; Lamikiz, 2009):

- The machine kinematics should provide sufficient flexibility for the orientation and positioning of the tool and workpiece.
- Orientation and positioning must be accomplished with the highest possible speed and accuracy.
- The tools and workpiece must be furnished for the fastest potential change.

- The machine cutting tool must be designed with the highest possible material removal rate (MRR).

Mainly, the number of axes of a milling machine tool or the number of independent controllable motions of movable parts is defined in terms of degrees of freedom. ISO 84/2001 recommends following the right-hand rule for defining the nomenclature of an axis coordinate system to the corresponding Z-axis (tool axis). Hence, a three-axis milling machine has three linear motions for the main parts (X-, Y- and Z-axis), which can be positioned anywhere within a particular range that is limited by an over-travel limit switch. In a three-axis CNC machine, the tool's direction will be fixed during the machining process. According to this limitation, the flexibility of the tool orientation will be related to the workpiece, therefore several different setups will be needed for machining (Lamikiz, 2009). To decrease the number of setups, more degrees of freedom must be added to the machine's axes to increase tool flexibility and workpiece orientation. For this purpose, rotational-movement axes can be added to conventional three-linear axis machines to obtain more flexibility in the machining process. A manual five-axis machine is a mechanical five-axis milling machine, which can use a rotary tool with five degrees of freedom that can move in any workspace orientation and position. Figure 2.1 represents a DMG 60 U five-axis manual milling machine.

2.2.2 **Milling Machine Kinematic Chain Diagram**

The five-axis CNC milling machine is actually similar in structure to two robots (Lamikiz, 2009), one of which is responsible for carrying the workpiece and the other the tool. Bezier (Be´zier, 1972) and Held (Held, 1991) presented an introduction to five-axis milling, machine applications and multi-axis machining regarding kinematics and axis orientation.

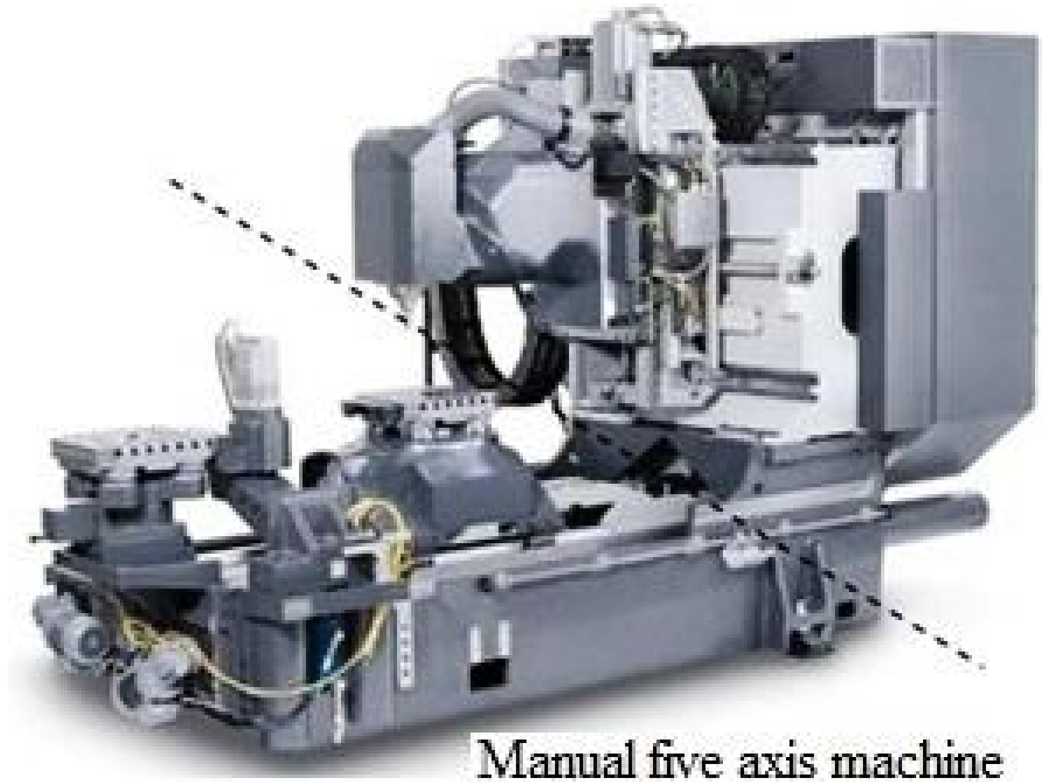

Figure 2.1 : The “DMG 60 U” Five-axis Manual Milling Machine (Lamikiz, 2009)

They explained that for orienting two rigid bodies in space relative to each other, six degrees of freedom are required for each body (tool and workpiece). Hence, twelve degrees of freedom are needed for the orientation altogether. However, six degrees of freedom can be reduced in number rather than each relative common orientation. For sufficient flexibility orientation between tool and workpiece, at least five degrees of freedom are required(Bohez, 2002), meaning that the tool and workpiece can be oriented relative to each other under any angle via five degrees of freedom.

According to the kinematic (chain) diagram, two axis groups are prevalent. In milling machine tools some axes are responsible for carrying the tool and others the workpiece(Bohez, 2002). Hence they can be divided into workpiece axis carriers and tool axis carriers. Furthermore, (L) and (R) introduce the axes, where L means a linear axis and R a rotational axis. Figure 2.2 presents the milling machine's kinematic configuration as (RRLLL), meaning the workpiece is carried by four axes (*RRLL*) and the tool only by one axis (*L*) (Bohez, 2002; Lamikiz, 2009). In Figure 2.2, according to the kinematic chain design, the first axis of the classical five-axis milling machine usually defines other axes. However, the best kinematic design is the one in which the workpiece is carried by just one axis of freedom and the other axes carry the tool.

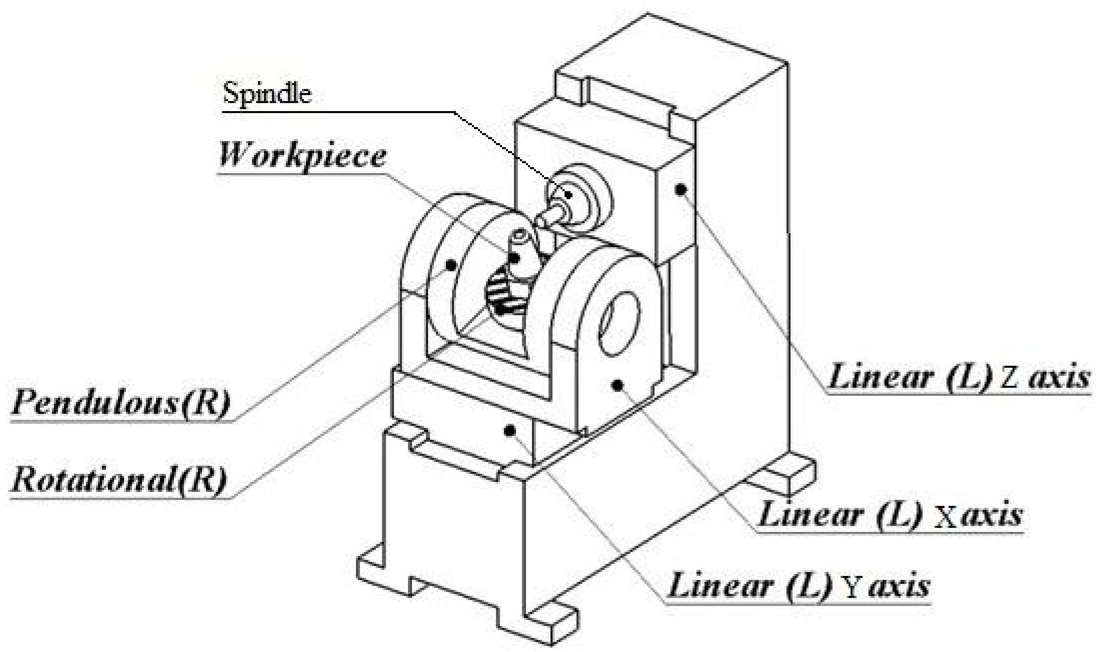

Figure 2.2 : Kinematic Configuration (RRLLL)(Bohez, 2002)

2.2.3 **Common Five-axis Machine Configurations**

Based on the kinematic chain in a five-axis milling machine, there are three common configurations starting from the workpiece and moving towards the tool tip (Lamikiz, 2009) as follows.

2.2.3.1 **RRLLL Configuration**

This configuration is normally applied in small, compact machines (Lamikiz, 2009). The table (workpiece) is supported by a double rotation (RR) table, pendulous and rotational simultaneously. One is a swiveling motion and the other is a rotation around the axis perpendicular to the plate and three linear axes provided by the tool. Figure 2.3 shows the RRLLL configuration.

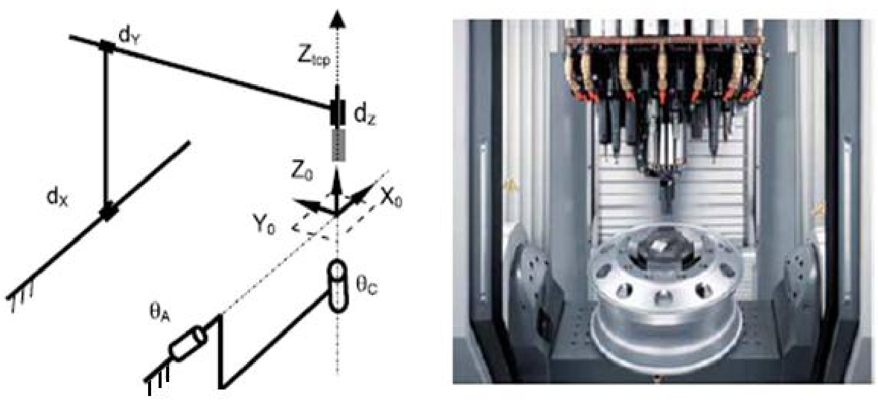

Figure 2.3 : RRLLL Configuration (Lamikiz, 2009)

2.2.3.2 **RLLLR Configuration**

This five-axis machine configuration is very suitable for tall and cylindrical workpieces)Díaz, 2009; L.N, 2009(. The table (workpiece) is supported by a rotary turning table (R) as well as Y-axis motion (L). Two other axes (X and Z) have linear motion (LL) and the headstock provides swiveling (R) of freedom. Figure 2.4 illustrates the RLLLR configuration.

This configuration is used for machining large gantry machine tools, usually big industrial molds and dies (Díaz, 2009; L.N, 2009). Three linear motions (LLL) by the X-, Y-, Z-axis whose Cartesian motions are produced either via the tool axes or machine table (workpiece) and two rotary motions (RR) by the headstock and spindle are produced Figure 2.5 shows the LLLRR configuration. The different types of CNC gantry machine tools will be discussed next.

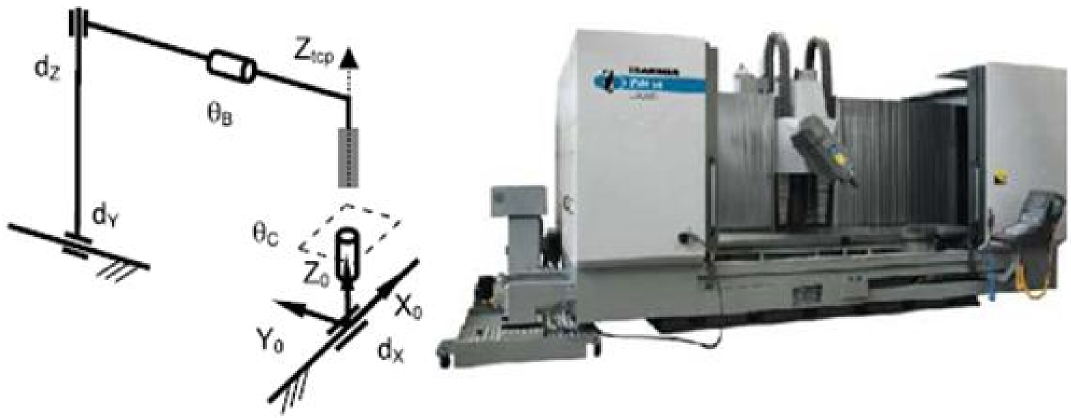

Figure 2.4 : RLLLR Configuration (Lamikiz, 2009)

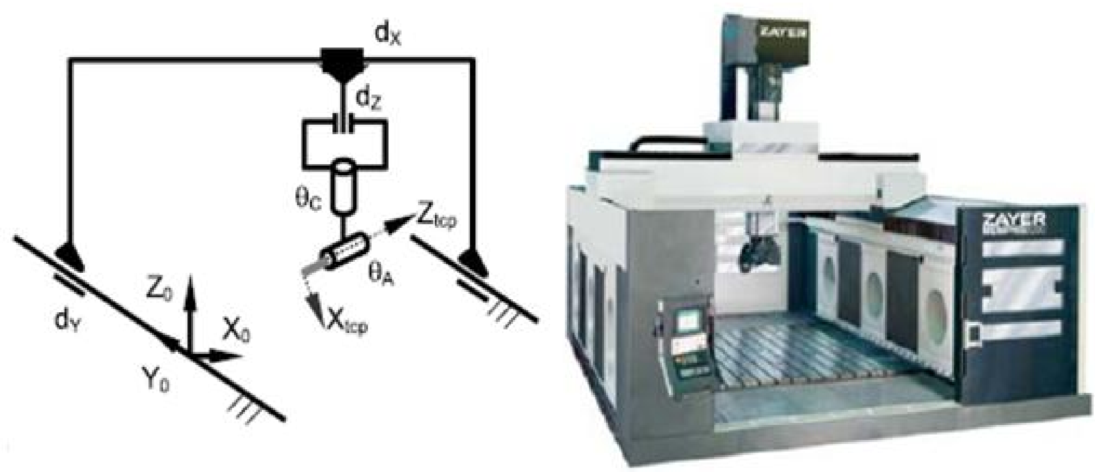

Figure 2.5: LLLRR Configuration (Lamikiz, 2009)

2.3 Types of CNC gantry machine tool

There are different milling machine structure categories, such as the C-frame gantry frame. CNC gantry machines can be used for making large workpieces. Gantry machine tools are widely applied for machining complex components in the industrial field (B.

Sencer, 2008). For instance, in recent years, CNC machine center and gantry milling machines are the indispensable processing equipment for energy, aerospace, shipbuilding, automobile, railway and engineering machinery and tools.

The general configuration of these machines is LLLRR. Three linear motions, namely X-axis via worktable or gantry, Y and Z-axis carriages and two rotational motions via a rotary headstock, which is a CNC machine accessory, make the chain kinematic configuration of CNC gantry machines. Among several accessories for CNC gantry machines are the rotary headstock, automatic tool changer (ATC) and automatic pallet changer (APC). These accessories are used for easy machining and easy tool and component changing in the manufacturing process. The rotary headstock is one of most important accessories of a five-axis CNC gantry machine. Figure 2.6 shows a classic example of a rotary headstock, the "twist and swivel head." The twist head facilitates greater accessibility and positioning to traditional 3-axis machines. However, this head does not have high stiffness, so in terms of accuracy and dynamics it is not suitable for high power applications. Over the last few years, the traditional gear transmission for two rotational axes has been replaced by a torque motor (L.N, 2009). The torque motor is directly inserted into the rotary joints. Eliminating the gears leads to stiffness enhancement, avoiding backlash and more precise rotation.

Torque motors are mainly designed for low speed applications. Their combined advantages are performance, high torque levels, high dynamic response (due to small electrical time constants), high efficiency (due to permanent magnets), high angular rotation and dynamic stiffness. Prior to designing a new type of gantry, it is essential to familiarize with different available types and their condition. At the moment, there are two types of gantry machine in the world (Tsann-Huei Chang, 2004). In the first type, the gantry is fixed and the worktable is moving, while in the second type the worktable is fixed and the gantry is moving.

Figure 2.6: Rotary headstock (158 JIXIE)

The Y and Z axes can move on the gantry in both types. Figure 2.7 shows the two existing types of CNC gantry machine.

2.3.1 **Fixed Gantry with Moving Worktable (First Type)**

In general, the first type of gantry machine adopts a fixed gantry and moveable worktable. It means the machine worktable can be moved while the gantry remains fixed. High accuracy machining is one of the advantages, because the ball screw is used for X-axis movement. The length limitation of the worktable and total machine length are two disadvantages of these machines.

Actually, the total precision of the ball screws depends on their length. In addition, the total machine length must be more than twice the worktable length. In terms of optimizing industrial space, the space occupied by the machine is a big problem. Therefore, CNC gantry machine performance is enhanced in this project by introducing a new idea to mitigate the two problems. Figure 2.8 presets the moving worktable type of gantry machine. Figure 2.9 presents a moving table type gantry machine with working space length twice the table length.

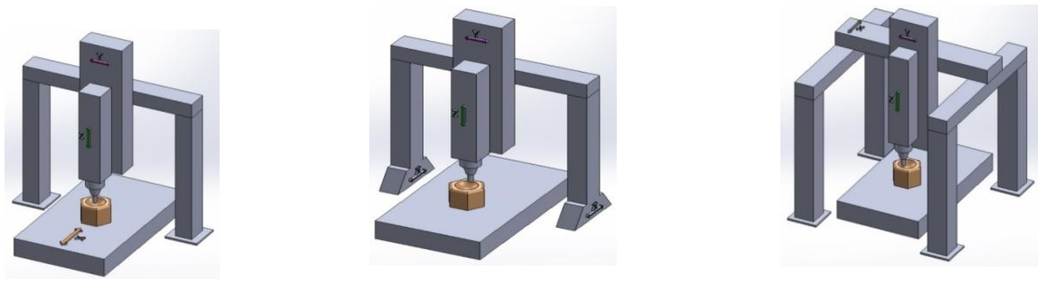

(a) Fixed Gantry

(b) Fixed Table (integrated gantry)

(c) Fixed Table (disintegrate gantry)

Figure 2.7 : The Two Types of CNC Gantry Machine

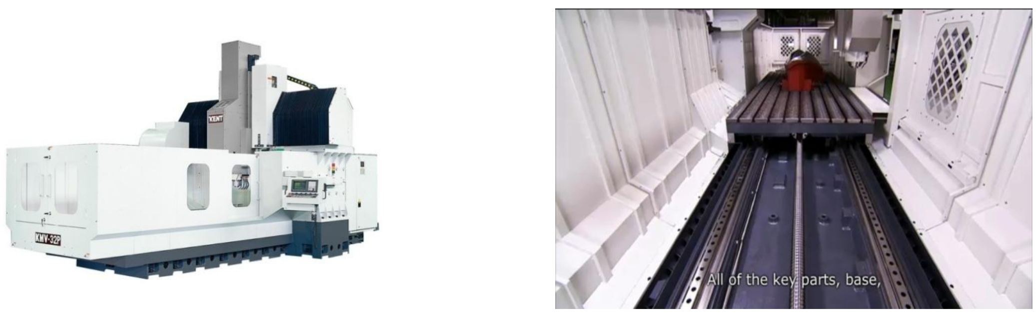

(a) Fixed Gantry

(a) Fixed Gantry

Figure 2.8: Moving worktable and fixed gantry (Macrotec Machine tools LTD)

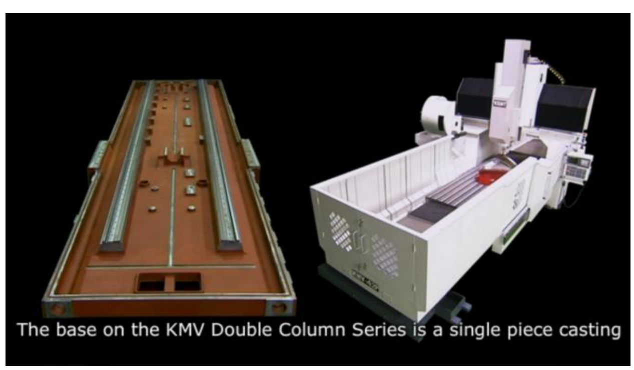

Figure 2.9: Working Space of the First Type of Gantry Machine (Macrotec Machine tools LTD)

The total machine length is typically more than twice the worktable. For example, for a 5 m worktable, the machine length will be more than 10 m. In this type, X-axis movement (L) normally belongs to the worktable and the gantry supports the other two axes (L, L). Figure 2.10 shows the Y and Z-axis movement in the fixed gantry.

2.3.2 **Fixed Worktable -- Moving Gantry (Second Type)**

The machine worktable is fixed in this type. The gantry can be moved along the worktable length and the gantry's (L, L, L) configuration supports the other axes.

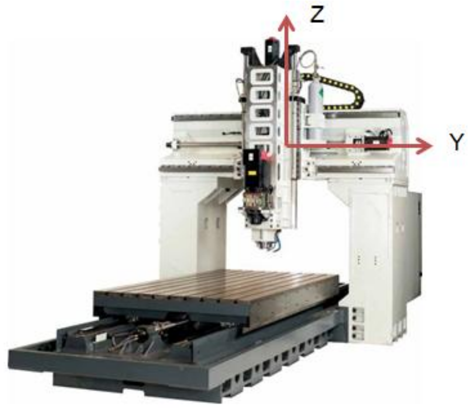

Figure 2.10: Y and Z Axes of the Second Gantry Type (Macrotec Machine tools LTD)

In the moving gantry (second type), the static form of gantry machining can help avoid large worktable area and workpiece movement and influence the dynamic characteristics of the machine tools (Guan, 2010; Jianrun, 2005; Liu Fang, 2007; Ni Xiangyang, 2005). Compared to the first type of gantry machine with a moving worktable and fixed gantry, the new gantry machine tool exploits a fixed worktable and moving gantry, which leads to higher speed and precision with lower energy consumption. High static and dynamic stiffness of the gantry are of concern in achieving high speed and high precision machining. Figure 2.11 shows the fixed worktable type CNC gantry machine.

2.4 CNC Gantry Machine Tool Structural Design

The most important research is related to CNC gantry design. In investigating previous research works on machine tool design, key words including gantry design, modification, optimization, feed drive mechanism and anti-backlash are considered in the following sections.

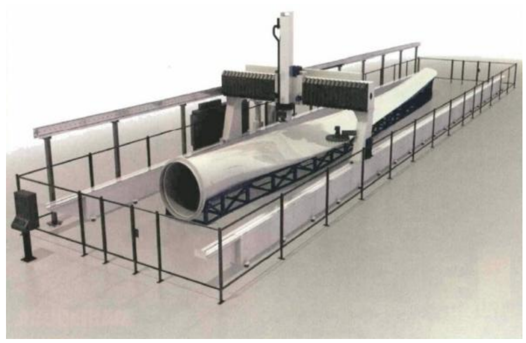

Figure 2.11: The Second Type of CNC Gantry Machine (Fixed Worktable) (Tomasent)

2.4.1 **Different Gantry Designs Proposed**

The ideas proposed for industrial gantry applications are introduced in this section. Concerning CNC gantry machine design, some research has been done as follows.

K. Erkorkmaz and colleagues (2010) proposed a new X–Y (300 x 300 mm) stage concept for "precision machine tools" using a T-type gantry (Erkorkmaz, 2010). The worktable is located on the gantry and the T-type gantry is supported on a vacuum preloaded air bearing on top of a reference granite surface. Figure 2.12 provides the schematic and prototype of this design.

L. Uriarte and colleagues (2013) reviewed the designs, engineering principles and applications of machine tools developed for large parts. They believe such large dimensions produce an amplification factor of any error source. Thus, to evaluate and solve these problems they investigated several suggestions.

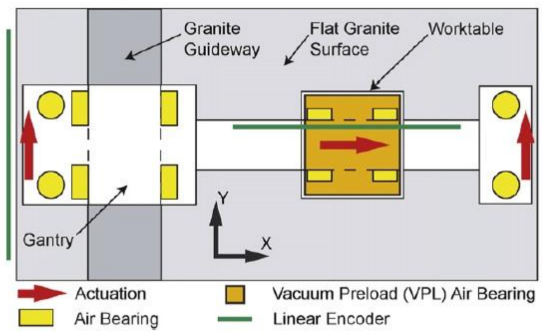

(a) Schematic

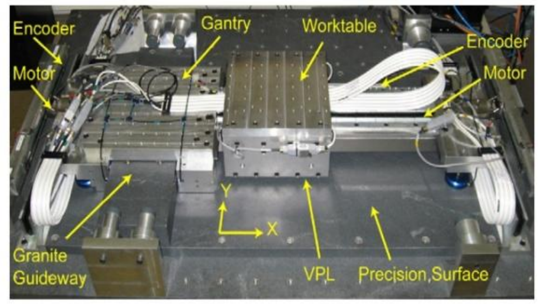

(b) Prototype

Figure 2.12: New Concept of T-type Gantry X–Y for Precision Machine Tools (Erkorkmaz, 2010)

Hao-Bo Cheng and colleagues (2005) presented a “six-axis machining system” design that is applicable to fabricating large off-axis spherical mirrors with sub aperture (Cheng, 2005). For fabricating high accuracy spherical and conformal optics (free form surface shapes and geometry), they proposed a “CNC machining system.” Figure 2.13 shows the overall structure and CNC machining system.

According to the schematic view of the gantry, the machine is fixed and the worktable has one rotational and one linear motion and the tool axis carriage has two linear and one rotational motion. Hence, the kinematic configuration of this machine is RLLLR; this is actually a five-axis machine, but the machine’s CNC controller may even be able to control six axes simultaneously. C. S. Teo and colleagues (2006) presented a dynamic model and adaptive control of an H-type gantry stage (Teo, 2007). Among the various high precision Cartesian robotic system configurations, one of the most useable is the H-type moving gantry with parallel slides supported by two motors. Figure 2.14 illustrates two precision gantry stage types.

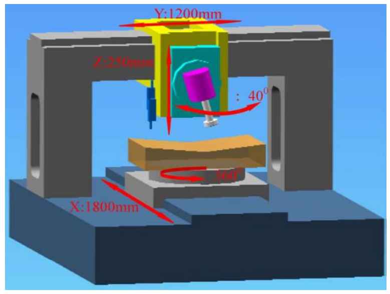

(a) Schematic view

(b) CNC machining system

Figure 2.13: Six-axis CNC Machining System (Cheng, 2005)

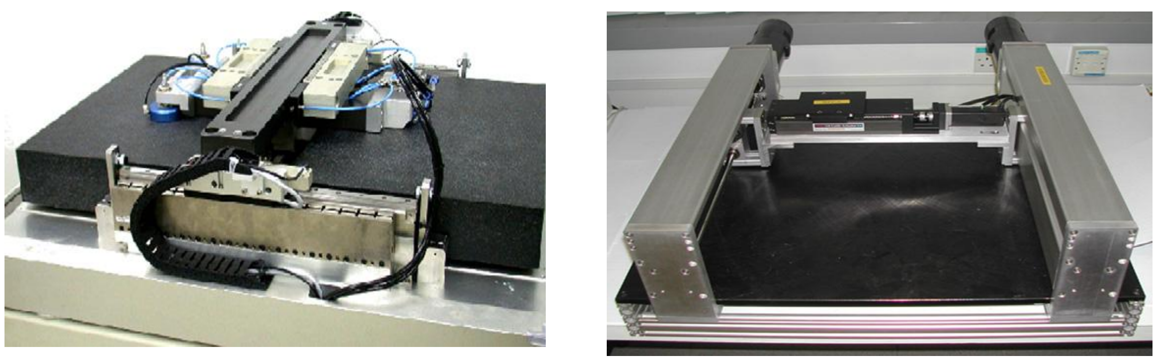

Figure 2.14: Two Precision Gantry Stage Types (Teo, 2007)

N.Đ. Zrnić and colleagues proposed a combined finite element and analytical method for obtaining transverse and longitudinal vibrations of a gantry crane system (Zrnić, 2014). They studied factors such as speed, acceleration, the influence of structural damping and suspension characteristics of a moving gantry. They believed the obtained results can be used in the design process of gantry cranes. Figure 2.15 presents the gantry and FE modeling.

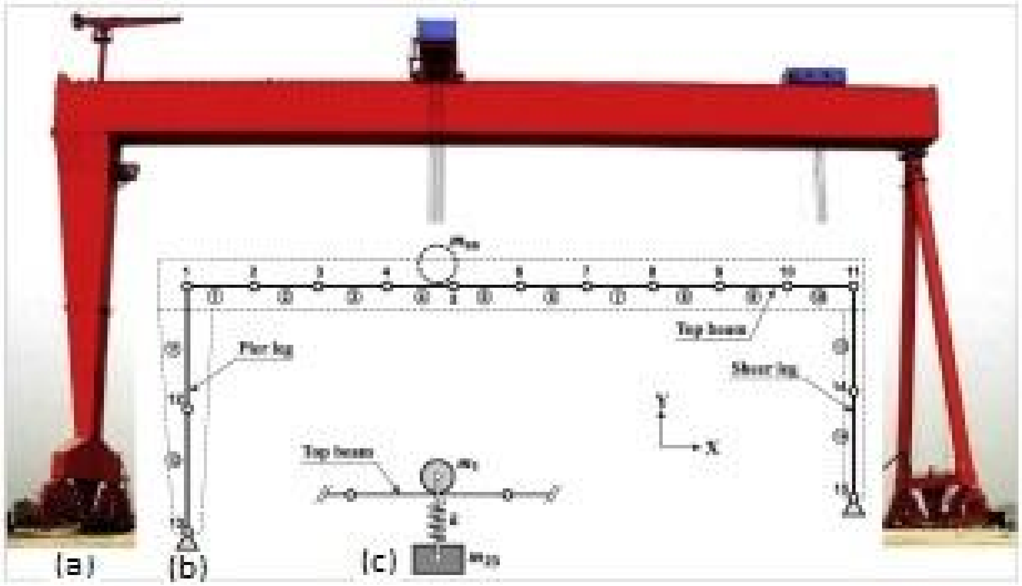

Figure 2.15: (a) Gantry Crane, (b) FE Model of the Gantry and (c) Moving System

Ling Zhao and colleagues (2011) proposed a method to design lightweight and high efficiency large gantries by introducing a natural bionic structure (Zhao, 2011). They made a laboratory model to test it and a number of gantry performances, such as natural frequency and improved weight.

Figure 2.16 shows the idea and testing of the lightweight gantry design.

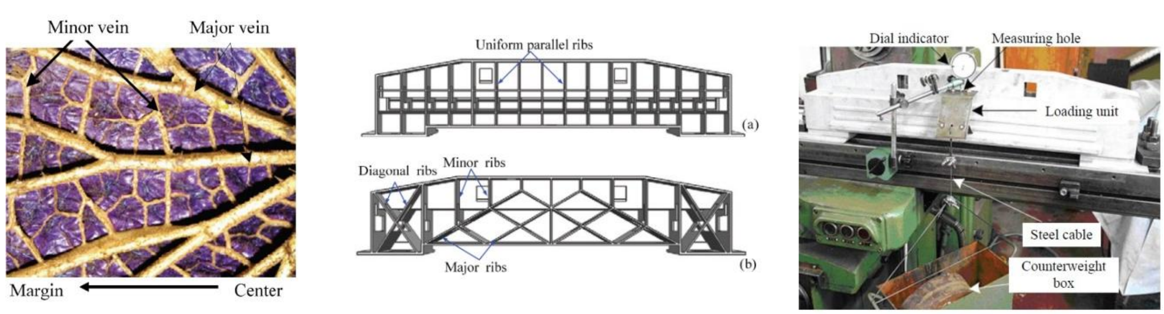

Giant water lily leaf and its vein distribution

(a) The conventional ribs of original model
(b) Improved bionic model

Setup for the static test

Figure 2.16: The Idea and Laboratory Static Testing of a Lightweight Gantry (Zhao, 2011)

2.4.2 **Gantry Design Modification**

Highly accurate CNC machine tools are also needed due to the growing demand for precision and consistent quality machining. The geometry of CNC gantry machines has normally been designed for easy machining of long and high components. However, the rigidity of the machine's gantry gets reduced under severe load during machining operations. Thus, vibration or deformation will occur during machining. After designing a gantry, some of its characteristics are often not satisfactory and depending on the target, the design must be modified. Manufacturers attempt to modify designs in order to achieve the strongest machine gantry for stability in the machining process because vibration negatively affects product quality. The first natural frequencies of previous gantry designs are seldom higher than 100 Hz (Ming, 2010; Shubo Xu, 2010). But for high finishing processes, machine tools are required to reach more than 8000 rpm. Therefore, the minimum natural frequency of a machine's gantry must be higher than 140 Hz. For the finishing process, a high speed spindle is normally needed. Milling machines with less than 150 Hz natural frequency are not capable of high speed machining, so lower quality surface is used. Hence, the design of a CNC machine gantry with rapid machining ability requires an appropriate gantry. Some researchers have explored gantry performance modification methods that can sustain vibration during high speed machining. Several software tools are available for gantry modification purposes and will be discussed next.

2.4.2.1 **Computer-Aided Design (CAD) software for designing and drawing**

The comprehensive CAD (computer-aided design) application for different industrial purposes yields enhanced modification methods. Recently, design and modification processes done via CAD systems have covered all designer requirements according to requests. Numerous researchers have tried to develop the CAD application software for industrial purposes. Lin and colleagues have attempted this and described a newly developed algorithm for CAD using coordinate measuring machines (CMMs) (Lin, 2001). Many different CAD software types have been produced to help with designing and modifying a subject.

2.4.2.2 **Computer-aided analysis via FEM software (dynamic and static)**

High static and dynamic stiffness are typically required when the gantry is moving. It is difficult to predict the static and dynamic behavior of a gantry by traditional methods (Dhupia, 2007; Lee, 2006; Ra Jeev S, 2003; S. Haranath, 1987; Stamper, 1997). Therefore, novel ideas must be applied to the design of gantry machine tools as well as the modification process to improve gantry characteristics. The following is a summary of research focusing on modification via FEM (finite element method) for rapid improvement of machine tool performance.

C. Yongqing performed finite element analysis of a structure for a 2400t gantry with ANSYS software and obtained the stress and deformation of key components in a variety of conditions (C.Yongqing, Jan. 2007). Z. Dewen accurately calculated the arch degrees of bridge type crane girders based on FEM. This method facilitated all sorts of deflection calculation means for bridge type crane girders and deduced the calculation formula of webs baiting arch degrees curve before the girder was made (Z.Dewen, 2006). F. Junlian applied a modification program to modify the main girder and proposed a research method for bridge crane girder structure analysis and optimal design (FJunlian., 2006). S. V. Sorokin analyzed and optimized the energy flow of a structure comprising a crossbeam element

(Sorokin, 2001). K. M. Khuberyan analyzed underground farm arched tents supported by crane crossbeams and the analysis showed that the deformation and stress conditions of the arch-supported wall affected the overall structure analysis results, so the impact of the supported wall should be added to the analysis (Khuberyan, 1972). Large span crossbeams are complex, so it is difficult to experimentally obtain a range of parameters; therefore, according to the structure's characteristics, Guhua (Han, 2011) analyzed and modified the crossbeam of a heavy NC machine moving gantry and milling machine. It had a certain reference value to the design and analysis of large span machines.

2.4.3 Structural Optimization of a Machine Tool

Gantry machine tools with the advantage of extensive machining span, high machining precision and good rigidity have been broadly applied in manufacturing industries and subsequently, their development has been rapid. In China, major scientific and technological projects of "high-grade CNC machine tools and basic manufacturing equipment" with gantry machine tool R&D have been undertaken as an important study issue. Focus is on structural dynamic optimization design techniques for the gantry machine tool's main components and parts. An important part of a gantry machine tool, the crossbeam achieves Y-axis feed motion and supports the spindle system to achieve Z-axis feed motion. The crossbeam's structural and dynamic properties directly affect the gantry machine tool's overall stiffness and machining precision. Therefore, the crossbeam's structural optimization design for the gantry machine tool has become a research focus of more and more scholars. Luo and Li (2006) analyzed the stiffness of a crossbeam with different rib plate shapes by finite element method (Luo, 2006). Shi (2009) conducted static, modal and harmonic analyses for the gantry machine centre's crossbeam and identified the weakness for further optimization design(Liu Fang, 2007) . Wang et al. (2009) conducted topology optimization for the crossbeam by studying the layout of the rib plates, so the static stiffness and anti-vibration performance were greatly improved (Wang XY, 2009). Guan et al. (2010) discovered the weak link in a gantry machine tool's crossbeam by using FEM and put forward a modification scheme, which enhanced the crossbeam's static and dynamic performance (Guan, 2010). Zhao et al. (2008) carried out structural bionic optimization for the stiffener plate of a gantry machine tool's crossbeam based on giant waterlily vein distribution, so the crossbeam achieved a lightweight performance design and its dynamic performance was further improved (Zhao, 2008).

Currently, the optimization of structural components for machine tool design is usually done through the static and dynamic stiffness as well as the structure's natural frequency as the optimized objective function. The majority of researchers have employed the finite element method (FEM) to optimize the main structural components of machine tools and also scientifically analyzed flutter during machining. In the US, Vance from Iowa State University and Yeh from the IsU Research Center optimized the design of a machine's structural shape by virtual reality technologies (Gimenez, 1995). Jiang and Chiredast from Michigan University presented a math model to simulate a joint form of the machine tool structure, set up a whole machine model and then did topology optimization on the locations and quantities of connecting pieces (e.g. solder joints, bolts) between the machine's bonding surfaces (Liu, 1995; Liu Fang, 2007) .

Gantry optimization is the process of altering parameters to obtain the best results under given conditions. In the steps of the design process or updating any engineering system, engineers are faced with many important technological decisions. The final goal of such decisions is to either minimize the effort required to maximize the desired benefit or vice versa. A practical situation can express the required effort or desired benefit as a function of certain decision variables. The optimization process can be defined as the conditions that yield the maximum or minimum value of a function. There are several available optimization methods for solving problems and a number of them have been developed to solve various types of problems (Krishna, 2009; Rao, 2009).

Mathematical programming techniques are useful to minimize or maximize a function of several variables based on certain limitations. For analyzing the problems described by a set of random variables, also known as probability distributions, stochastic process techniques can be used. Statistical methods can be used to analyze experimental data and to build practical models to obtain the most accurate representation of a physical situation (Guang-Yuan, 1985; Majid, 1974).

As demand for high speed, high precision machining of large components rises, the gantry machine tool with the advantages of large machining span, high precision and high speed, meets the demand of crucial industries, such as aerospace, military, ship building and other large machine building industries. Due to the extensive application of these strategic gantry machine tools, many manufacturers invest in them to develop high speed, high precision gantry machine tools, something that requires various developments in the design stage of gantry machine tools.

Liu et al. (Liu, 2014) investigated the structural design of the gantry beam using multi-criteria decision making with grey relational analysis and Analytical Hierarchy Process (AHP). Design criteria include static, anti-vibration and lightweight performance. The optimal crossbeam design scheme was chosen among four initially proposed schemes. Six optimal, non-inferior solutions based on the dynamic optimization of the selected scheme were obtained. The final optimal solution was recovered using gray relational analysis. The first four natural frequencies also increased around 17%.

The application of finite element software for modeling, optimizing and redesigning key gantry machine components has been investigated by many researchers (Guan, 2010; Han, 2011; Weule, 2003; Xiuheng, 2010; Y. Guan, 2010; Yanhua, 2009; Zhao, 2011). Guan et al. (Guan, 2010) proposed the finite element model of a GMCU2060 gantry machine center. According to the FE model, static and dynamic stiffness of the crossbeam were obtained. Based on analysis, weak points were discovered and through modification, the static and dynamic stiffness was enhanced.

In another research conducted by Guan et al. (Y. Guan, 2010), the weak links of a five-axis gantry milling machine were detected using modeling and analysis of key machine tool components. Accordingly, the static stiffness increased to 68.4 $N/\mu m$ and the first natural frequency increased from 30 Hz to 42 Hz with a mass reduction of 632 kg.

By applying the bionic approach inspired by giant waterlily leaf ribs and cactus stem structure, Zhao et al. (Zhao, 2011) aimed to improve the structural characteristics of a Lin MC6000 gantry machine center crossbeam. The results demonstrated the effectiveness of the bionic approach with static deformation and weight reductions of 16.22% and 3.31%, respectively and an increase in the first four natural frequencies.

Machine tool design often comprises many conflicting criteria, such as static, dynamic, weigh and cost performance. Several multi-criteria decision making methods proposed including AHP, ANP, TOPSIS, ELECTRE, PROMETHEE, GRA, PEG-MCDM (Grierson, 2008; Yanhua, 2009) have been successfully applied by numerous researchers in the design stage (Ayağ, et al., 2011; Taha, 2012).

To date, most researches have intended to enhance the static and dynamic performance of the gantry machine tool crossbeam, which results from the high rigidity of the gantry machine's fixed wall. However, in moving the gantry machine's columns, the topology and structural properties of the columns directly affect the ultimate machine performance. Therefore, in this study, static, anti-vibration, light weight and low cost performance of the gantry head consisting of a crossbeam and columns were investigated. Prior to optimization, the AHP method, a well-known multi-criteria decision making method, was employed for selecting the best design scheme proposed by gantry designer experts. Sensitivity analysis was conducted prior to multi-objective optimization to discover influential parameters. Using the design exploration toolbox of ANSYS Workbench, multi-objective optimization of the selected gantry machine tool was achieved by applying the multi-objective genetic algorithm (MOGA). In order to choose the ultimate design among non-inferior solutions proposed by MOGA, the PEG-MCDM method was employed. To validate the simulation results, experimental modal analysis was carried out on the gantry prototype by comparing the first four natural frequencies obtained from simulation and experiments. The results proved the effectiveness of the proposed design methodology for designing a gantry machine with high performance moving columns.

2.4.4 **Applying Multi-Criteria Decision Making In the Machine Design**

Multi-objective decision making (MODM) is aimed at optimal design problems in which several (conflicting) objectives are to be achieved simultaneously. The characteristics of MODM are a set of (conflicting) objectives and a set of well-defined constraints.

Therefore, MODM is naturally associated with a method of mathematical programming for dealing with optimization problems. However, it is evident that two main difficulties involving the trade-off and scale problems complicate the MODM problems through the mathematical programming model.

In the trade-off problem, since a final optimal solution is usually obtained through mathematical programming, multiple objectives must transform it into a weighted single objective. Therefore, a process of obtaining trade-off information between the considered objectives should first be identified. If the trade-off information is unavailable, Pareto solutions should be derived. With the scaling problem, on the other hand, as the number of dimensions increases beyond capacity, the curse of dimensionality problem arises, i.e., the computational cost increases tremendously. Recently, many evolution algorithms, such as genetic algorithms (Holland, 1975), genetic programming (Koza, 1992) and evolution strategy (Rechenberg, 1973) have been suggested to handle this.

With the globalization of businesses, the competitive manufacturing companies must invest and improve production facilities, especially regarding the introduction of new equipment to the market. Therefore, machine tool selection for investing and improving facilities is an important decision that plays on the survival of developing manufacturing facilities. Improperly selected machines can negatively impact the overall system performance, such as productivity, precision, flexibility, adaptation and responsiveness. As such, this is a time-consuming and intractable problem and it is the largest drawback for engineers and managers due to the lack of deep knowledge, experience and technological understanding (Budak, 2004; Ertuğrul, 2007).

The progress of the production economy always requires companies to find replacement manufacturing solutions to respond to and satisfy customer demand. One of the significant strategies to attain optimal operational performance is to apply production automation through flexible manufacturing system (FMS) implementation (Taha, 2011). FMS achieves the efficiency of an automatic batch manufacturing system while having the flexibility of a manual job shop to simultaneously machine several part types. FMS structure comprises many CNC machine tools, workstations and material handling systems mechanically linked together and electrically controlled by a computer-centered system (Stecke, 1983). However, FMS investment cost is very high. Thus, small and medium enterprises (SMEs) in developing countries usually choose flexible manufacturing cells (FMCs) as a competitive strategy for improving technology and productivity. Machine tools are system-centered equipment and the critical connection responsible for transforming raw materials into finished discrete components to be assembled into end products. Machine tool selection plays a crucial role in improving FMC performance (Abdel-Malek, 2000).

Researchers have made different contributions by offering decision-making solutions for selecting the most suitable candidate machines. For example, Ayağ and Özdemir (Z. Ayağ, 2006) used the fuzzy AHP to select the best machine tool from alternatives on the market. The multi-criteria decision making (MCDM) model is constructed based on quantitative and qualitative factors. Fuzzy logic is utilized to solve the vague and imprecise information of uncertain expert judgment. The fuzzy AHP method serves to evaluate the weights of criteria and ranking of alternatives. Finally, Benefit/Cost (B/C) ratio analysis is implemented for each alternative and the ultimate machine tool candidate responds to the highest B/C ratio. The decision support system (DSS) for selecting the machine tool in the implementation of FMC using fuzzy AHP and artificial neural network (ANN) was proposed by Taha and Rostam (Taha, 2011). ANN with feedback propagation is utilized to learn and verify the fuzzy AHP results for predicting the candidate ranking. Önüt et al (Önüt, 2008) described the hybrid fuzzy MCDM approach for machine tool selection based on the integration of fuzzy AHP with fuzzy TOPSIS (Technique for Order Preference by Similarity to Ideal Solution) in order to evaluate the vertical CNC machining centers. The criteria priorities are obtained by fuzzy AHP to handle the qualitative criteria and the alternatives ranking result is quantified by fuzzy TOPSIS. Besides, Ayağ (Z. Ayağ, 2007) presented the integration of the AHP and simulation technique for machine tool selection. Taha and Rostam (Z. Taha, 2011) presented DSS using fuzzy AHP and PROMETHEE (Preference Ranking Organization Method for Enrichment Evaluation) to evaluate the best computer numerical controlled (CNC) turning machines in FMC. Dağdeviren (Dağdeviren, 2008) also proposed the integration of AHP with PROMETHEE. Durán and Aguilo (O. Durán, 2008) used fuzzy AHP for machine-tool selection, while Abdi (Abdi, 2009) used fuzzy AHP to evaluate reconfigurable machining system equipment. Ic et al. (Y.T. Ic, 2012) developed a component-based machining center selection model using AHP for the MCDM process in machine tool alternatives.

Lin and Yang (Lin, 1996) also employed AHP to evaluate machine selection. Ic and Yurdakul (Y.T. İç, 2009) developed DSS to choose the most appropriate machining center, involving the integration of fuzzy AHP and fuzzy TOPSIS. In particular, the priorities of criteria are determined by fuzzy AHP while fuzzy TOPSIS is employed to calculate the ranking of alternatives. Qi (Qi, 2010) proposed a fuzzy MCDM model based on the modified fuzzy AHP and grey theory to determine the weights of criteria and the performance of each alternative through the Sugeno fuzzy integral.

2.5 Static and Dynamic Behavior of CNC Gantry Machine Tools Structure

Globally competing manufacturing companies tend to build their products on the edge of technically feasibility. This trend leads to increasing demand for high stiffness production systems. Machine tools have to function accurately and highly dynamically to keep up with the requirements of modern machining processes like high speed cutting. Besides technical issues, the time for marketing production systems is continuously becoming shorter. Machine tool manufacturers have to predict machining stiffness without building real prototypes, which calls for a method that enables the prediction of large machine movements and dynamic positioning. These technical characteristics are essential for the quality and manufacturing time of machined workpieces.

2.5.1 The CNC Gantry Machine Structure- Errors Sensitivities

CNC machine tool structure should hold all machine components and must tolerate against forces induced by the machining process. It must have enough stiffness to preserve the machine precision requirement. High damping ratio and low thermal distortion are expected of the machine structure as well. Errors that affect the machine tool accuracy can be classified as geometric errors, thermal errors and cutting force-induced errors. Spindle is the core component of a CNC machine tool and it is also the important contributor to the total thermal errors (around 70 percent) and that is due to the large amounts of heat from its high-speed revolution and cutting process (Krulewich, 1998). Therefore the study on thermal deformations of the spindle is the most important activity for reducing the total machine errors.

In addition a machine tool must be statically and dynamically rigid simultaneously to attain a satisfactory machining process. In fact, the dimensional accuracy of components is related to static stiffness; surface quality and maximum metal removal rate (MRR) which are related to dynamic stiffness (Myers, 2005); and cutting process stability is related to the dynamic performance of the machine's structure (K Fansen, 1999). The unstable phenomena of the cutting process, e.g. chatter, are often the result of a mutual effect of the dynamic behavior between the CNC machine's structure and cutting process (Baradie, 1991; EI Baradie, et al., 1976; M. A. EI Baradie, 1993).

CNC machine structure includes two main parts: the structure (bed) body and main frame. They can be fabricated in one block through a casting process or assembled in several separate sub-frames by a welding process. The machine bed is very important because it is the solid part of the machine that holds the others components.

Two types of design machine structure must be considered due to machining heat, namely open-loop and closed-loop (Lamikiz, 2009). In the open-loop design, heat from the machining process is easily conducted to the ground via the structure but in the closed-loop design heat travels a long way to the ground.

2.5.1.1 **Open-Loop Type**

The C-frame is a common open-loop characteristic of small milling machines. It provides easy access to the work zone but is sensitive to thermal and mechanical loads (torsion and flexion) with an asymmetrical response. Two types of C-frame design are shown in Figure 2.17.

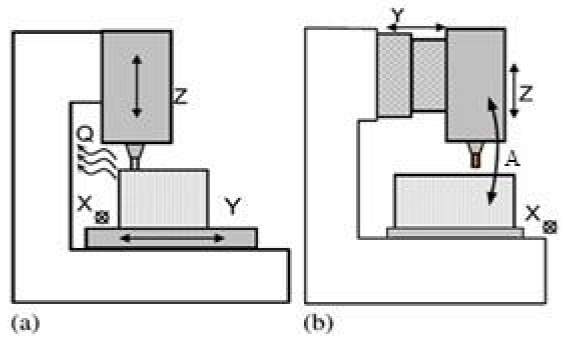

Figure 2.17: Two Types of C-Frame Design (Lamikiz, 2009)

One type of C-frame is the fixed column (a), which is affected by heat from the machining process; the workpiece depends on its weight and can be moved by the Y-axis. In type (b), the headstock can be moved via the Y- and Z-axis and the workpiece via the table (X-axis).

2.5.1.2 Closed-Loop Type

The gantry milling machine is a closed-loop design (Lamikiz, 2009). In this type heat from the machining process is conducted a long way to the ground. Hence, heat remains in the machine gantry. The closed-loop design is shown in **Error! Reference source not found.**Figure 2.18.

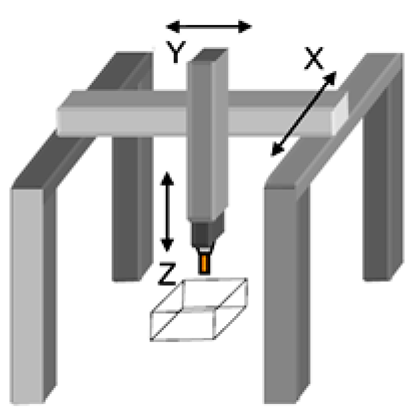

Figure 2.18 : A Closed-loop Design Gantry (Lamikiz, 2009)

2.5.2 Static Behavior of Machine Tools Structure

Prior to manufacturing, static analysis software must be used to study the static behavior of machine tool structure to identify several different types of machining error. Stress, thermal error, deflection and deformation, allowable loads, etc., can be identified with analysis software. Regarding the estimation of the static behavior of machine tool structure, quite some research has been done including by Josef Mayr and colleagues (Mayr, 2014).

2.5.3 Dynamic Behavior of Machine Tools Structure

The dynamic behavior of machine tool structures in each frequency range can be simulated as a set of individual modes of vibration. By modeling the structure with modal parameters, the vibration problem caused by resonance can be investigated (Maia, 1997). It is still impossible to define the dynamic behavior of machine tool structures by drawing only with a special degree of accuracy. However, considerable advances have been achieved in the development of experimental methods to determine the mode shapes of machine tool structures. Researchers (Y. Altintas, 2000; E. Budak, 1994; Tlusty, 1963) have introduced static and dynamic analysis of machine tool structures involved in machining systems by resting using stiffness measurements and modal analysis. Eman and Kim (Eman, 1983) introduced a concept for the modal analysis of machine tool structures based on a parametric representation of the measured responses. Multivariable autoregressive moving average models were utilized in their study. Yuan et al. (Pedrammehr, 2012) presented the finite element method for the modal analysis of machine tool structures. They determined the first ten natural frequencies and mode shapes of the machine tool structure. Patwari et al. (Patwari, 2010) presented experimental and analytical modal analysis techniques for structural dynamic evaluation processes of a vertical machining center. Experimental modal analysis of different milling machine components was carried out in their study and the theoretical mode shape of components was obtained by FEM. Zhijun et al. (Pedrammehr, 2012) proposed an approach to analyze the characteristics of machine tools by modal analysis and harmonic response. They carried out modal experiments to obtain modal frequency, damping and shape. Meanwhile, simulation and modal analysis using FEM served to obtain accurate dynamic characteristics. Baker and Rouch (Baker, 2002) analyzed the instability of the machining process through FEM but the result integrity was not validated by the experimental results.

2.6 CNC Machine Tool Feed Drive Mechanisms

2.6.1 Background

A feed drive is used for positioning and orienting the cutting tool and workpiece during machining (Altintas, et al., 2011). The machine tool carriages must carry the cutting tool and workpiece to the desired operation location. Hence, the quality and productivity of machine tools is determined from their positioning and speed accuracy. A feed drive system is a mechanism that can support machine tool carriage motion via controllable positioning. A general schematic of feed drive hardware and its computer control structure is shown in Figure 2.18

There are two types of feed drive. One is linear, which is powered directly by a linear motor and the other is a rotary feed drive that works with a rotary motor. The ball screw must convert rotary to linear motion in a rotary feed drive. Figure 2.20 shows linear and rotary feed drives. The rotary feed drive consists of a machine worktable installed on the linear guide and a ball screw supported by a servomotor. The rotational motion of the ball screw will be converted into linear motion by a nut installed under the worktable. A CNC controller controls the servomotor driver to position the worktable. The ball screw can be connected directly to the servomotor or to a gear box to reduce rotation and increase feed drive torque when heavy load is required. The servomotor is supported by a specific driver connected to the CNC controller system. The worktable is positioned by a specific program generated with a CAD/CAM system that is loaded onto the CNC machine tool controller. The CNC program defines tool path segments that may consist of linear, circular, Sp-line or other geometric motions.

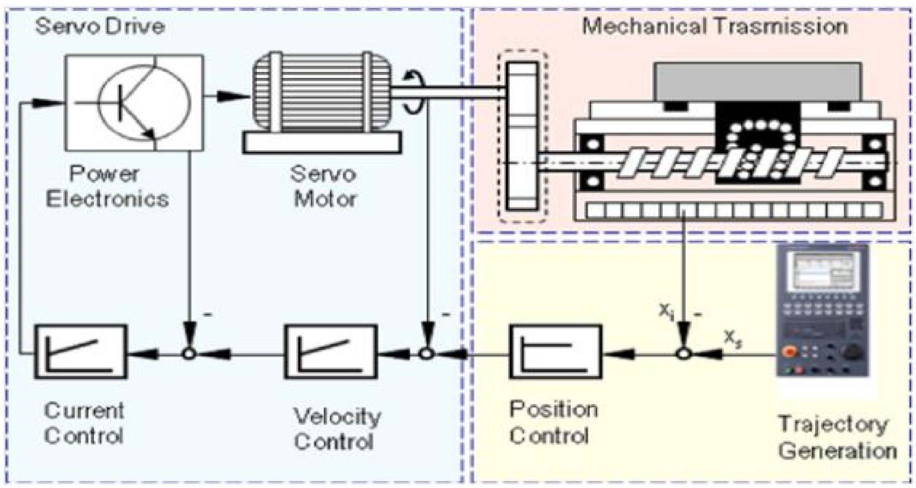

Figure 2.19: Feed Drive Hardware Schematic (Altintas, et al., 2011)

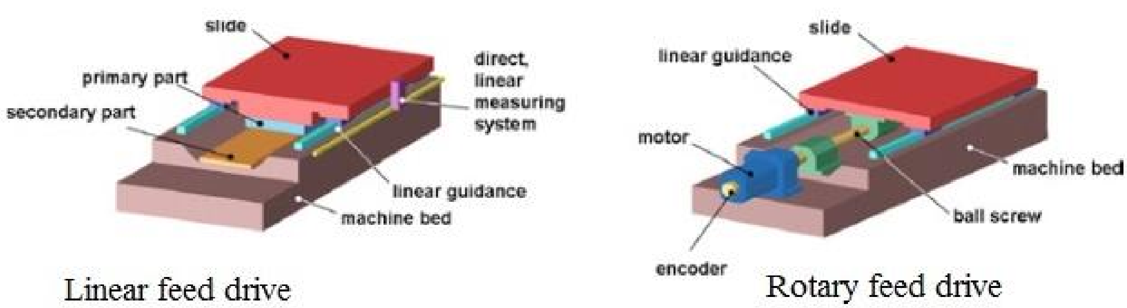

Figure 2.20: Linear and Rotary Feed Drive Systems (Altintas, et al., 2011)

2.6.2 **The Guideway**

The guideway in a machine's feed drive motion is one of the more important components which can be used in this kind of mechanism. Several types of guideway may be used in machine tools. Next, different guideway types are introduced. A slide-way schematic is shown in Figure 2.21.

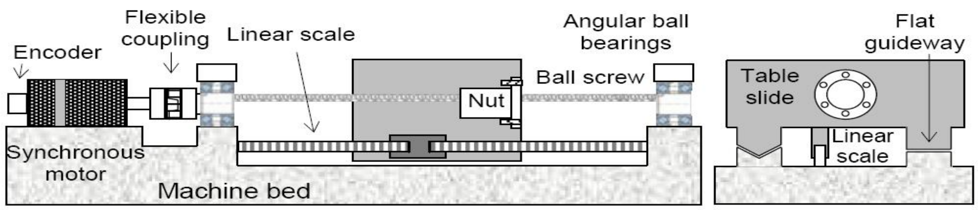

Figure 2.21: Guideway with Lubrication (L.N, 2009)

2.6.2.1 **Slide-Ways (Friction Guides)**

Friction guides have good damping, strength against impact loads and high load capacity of up to 140 MPa. They are primarily used at speeds under 0.5 m/s (Díaz, 2009; L.N, 2009; LNL de Lacalle, 2009). The slide-ways are lubricated by 1 mm deep lubrication slots located on the moving part of the guide. The friction guides can also be coated with a few millimeters of polymers in order to reduce friction. Various friction guide configurations are shown in Figure 2.22.

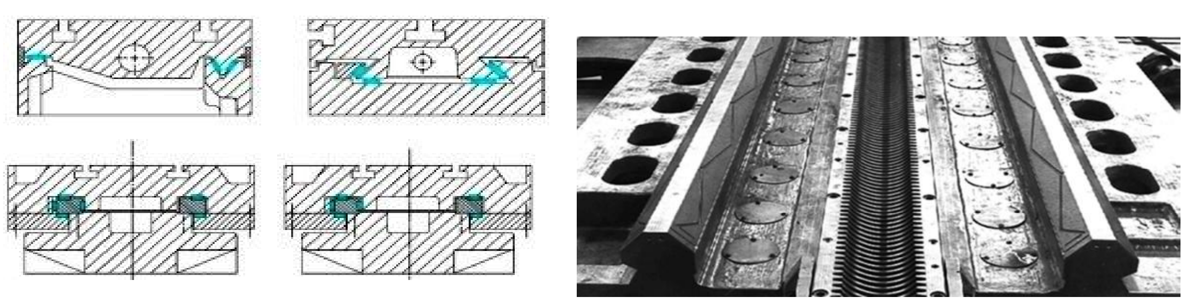

(a) Schematics of Different Slide-Way Types

(b) Real Slide-Way Components

Figure 2.22: Friction slide-way configurations (Altintas, et al., 2011; L.N, 2009)

Different materials can be used to manufacture friction guides, for instance cast iron, steel, bronze and some polymers.

2.6.2.2 Linear Guides

Low friction, high load capacity, stiffness and low structural damping are among the specifications of linear guides. The two linear guide types are ball and rolling guides. Rolling guides are manufactured with different sizes and loads and can be supplied with integrated position sensors or racks to expedite the design and machine tool drive assembly. A ball or roller linear guide is the "linearization" of the rolling bearing concept. Where lubrication is limited, balls or roller linear guides substitute it. Balls are adequate for light loads and high velocities and rollers work well for high loads but lower velocities. The guideways are stiffer than friction slides, with lower opposition to displacement. Easy installation and maintenance by rapid substitution they have for guides or carriages. Machine tool manufacturers can usually buy them already assembled with the required guide length. They must be calculated and preloaded to a specific value for the carriage load to move. The main drawback of this sliding system is low damping due to the direct metal-to-metal contact. Some additional carriages especially designed for high damping using polymers or inducing an oil film, can be inserted among rolling slides.

2.6.2.3 Hydrostatic Guides

To completely avoid metal-to-metal contact in hydrostatic guides, a sufficiently thick oil film must always separate the sliding elements. To maintain the oil film, an external pump continuously injects oil into the bearing. The stiffness of the bearing is proportional to the oil supply pressure. Therefore, the main advantage of oil hydrostatic bearings is the extremely high damping ratio, which is very important when machining hard or brittle materials. The linear guide system is shown in Figure 2.23.

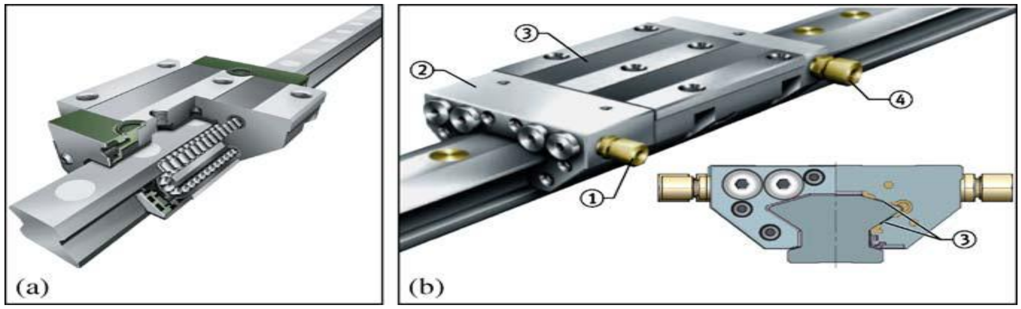

Figure 2.23: Linear Guide: (a) Roller Guide Model (RUE), (b) Special Hydrostatic Guide (Altintas, et al., 2011; L.N, 2009)

2.6.3 **CNC Gantry Machine Tool Feed Drive**

Among the researchers accomplished in this field, Y. Altintas and colleagues (2011) reviewed different designs of machine tool feed drive systems and controls (Altintas, et al., 2011). They discussed machine tool guide designs using friction, rolling elements, hydrostatic and magnetic levitation principles, mechanical drives based on ball screw, linear motors, electrical motors and sensors, the control of both rigid and flexible drive systems and virtual feed modeling.

A. Verl and colleagues (2014 presented a double nut ball screw to improve its operating characteristics (Verl, 2014). According to dynamic applications that often required ball screws with high preloading values, this idea improved the operating characteristics by proposing a novel design principle for ball screws using a double nut and spring. Figure 2.24 shows the idea and prototype of a double nut ball screw.

Cheng-Hsien Wu and colleagues investigated the thermal analysis of a CNC machine feed drive system (Wu, 2003). According to the heat generated by the high-speed drive system from friction at the contact areas, such as the ball screw and nut, they investigated the thermal deformation of a ball screw during the drive process.

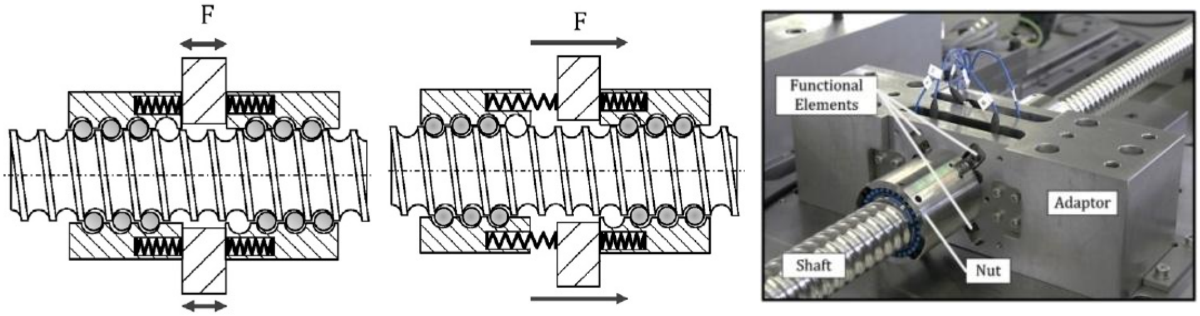

Moderate Load   Overload   Prototype of a double nut ball screw

Figure 2.24: The Idea and Prototype of a Double Nut Ball Screw (Verl, 2014)

J. S. Chen and colleagues (2000) presented a feed drive mechanism to control preload and motion with a ball screw and piezo-electric nut (Chen, 2000). This mechanism was proposed for the motion stage of long-stroke, high-speed and ultra-precision applications. Figure 2.25 illustrates a feed drive mechanism with piezo-electric nut.

Seamus Gordon and colleagues (2005) applied a linear motor as a feed drive motion for high-speed CNC cutting machines (Gordon, 2005).

In the second type of CNC gantry machine the rack and pinion mechanism is used for the X-axis feed drive mechanism. Figure 2.26 presents the second type of CNC gantry machine feed drive mechanism. The rack and pinion motion system is used for X-axis movement.

In this type of machine the gantry columns must be moved by two separate motors simultaneously. Motion coordination in this mechanism is very important and difficult. Such machines are suitable for long machining.

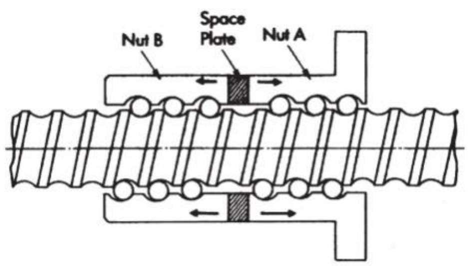

Principle of Ball Screw Preload

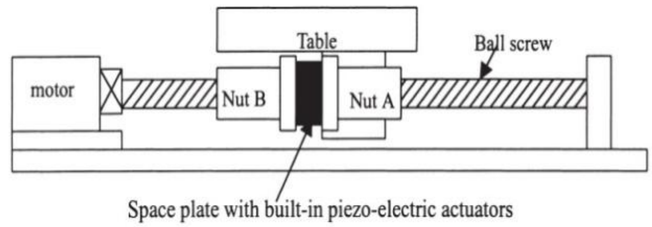

Ultra-precision Stage Construction

Figure 2.25: Feed Drive Mechanism with Piezo-electric Nut (Chen, 2000)

(a) Rack and Pinion System

(b) The Rack

Figure 2.26: Rack and Pinion System for X-axis Gantry Motion

A moving gantry can avoid using large worktables and workpiece movement. The optimum space occupied, fixed worktable and large workpieces are advantages of such machines and lower machining precision is a disadvantage.

2.7 Anti-backlash Mechanism in Feed Drive system

Rack and pinion systems are able to convert rotational motion into linear (Nsk Ltd, 2013). Rack and pinion systems have mainly been used for linear motion in CNC gantry machines (worktable fixed type), robotics and linear motion systems with continuously changing directions. Meanwhile, gears have almost become an integral part of power transmission systems and machine instrumentation. Consequently, any error in gear transmission will affect the performance of such systems (Brauer, 2003). When the system is subjected to non-continuous motion with frequent direction reversal, this negative effect will be conspicuous. Often, most such errors occur in robotic manipulators and the X-axis motion of CNC gantry machines (Shibly, 1988). These mechanical components have non-linear characteristics, such as gear backlash (R. Kalantari, 2009). Backlash is the shortest distance between two teeth in mating gears. When gear teeth are not in contact, the transmission force will be zero but when they are in contact, due to elasticity, the force is usually proportional to the angular position difference between the gears (R. Kalantari, 2009). Backlash in rack and pinion systems generates different problems, such as machining process errors, lower surface quality, noise and increased probability of damage (Li, 2007; Van Dooren, 2001).

Anti-backlash gear systems are extensively used to reduce transmission error and obtain precise, desirable output rotation or displacement. Available anti-backlash gears have been used in many industrial applications, including gantry machine making and aerospace (Shim, 2008). One method of anti-backlash gear design is to cut a gear into two halves, with each half being ½ the thickness of the original gear. One of the gear halves is fixed to the shaft and the other gear half is allowed to rotate on the shaft. Several coil springs are used to push the two gear halves apart (radially) so that the gear teeth fit tightly between the mating gear teeth. The coil springs are sized and compressed above normal operating gear system torque. An example of an anti-backlash gear set is shown in Figure 2.27.

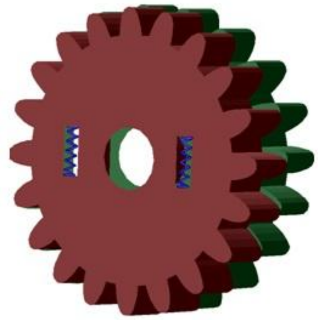

Figure 2.27: Anti-Backlash Gear (Imasaki, 1995)

2.7.1 **Split Pinions**

The simplest zero-backlash drive system utilizes a split pinion, which consists of two pinion halves and an axial spring pack (Hale, 1994). The pinion halves mesh with the opposite tooth flanks on the same rack, eliminating backlash. One pinion half drives the axis while the second pinion half is "preloaded" to remove the backlash. The preload setting of the second pinion half is fully adjustable on the machine by turning the axial spring pack at the end of the pinion shaft. Figure 2.28 shows the split pinion system.

Figure 2.28: Split Pinion System (Atlanta Drive Systems Inc., 2013)

2.7.2 **Controlling Backlash for Ultra-Precise Positioning**

The general idea is to produce precise positioning and repeatability of rack and pinion mechanisms by eliminating backlash, which can be accomplished using two pinions. One pinion drives the axis and the other is for “preload” to remove backlash. Precise positioning must be maintained during acceleration and deceleration, as well as movement direction changes. Several different solutions to achieve a zero-backlash drive system with this idea are presented next.

2.7.3 **Dual Pinion Electrical Preload**

One method to remove backlash in a rack and pinion is to use two motor/reducer assemblies with dual pinions operating on the same rack in a master/slave setup. One pinion drives the axis while the second is "preloaded" to remove the backlash. The preload is created electronically with a special motor controller; these systems can also be set up to drive together during cycles when backlash is not critical. Figure 2.29 shows a dual pinion electrical preload system.

Figure 2.29: Dual Pinion Electrical Preload (Atlanta Drive Systems Inc., 2013)

2.7.4 **Rack and Pinion Drive with Mechanical Preload**

The mechanical preload is the same as the dual pinion electrical preload system, but one motor includes a rotary spring. Figure 2.30 shows the rack and pinion drive with mechanical preload.

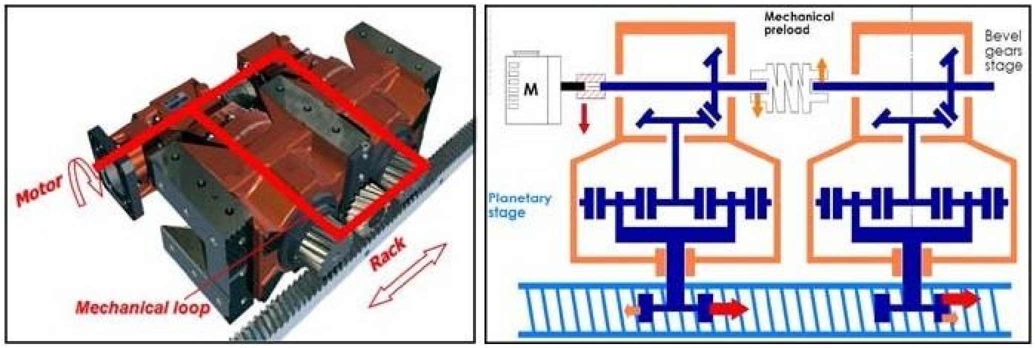

Figure 2.30: Rack and Pinion Drive with Mechanical Preload (Atlanta Drive Systems Inc., 2013 ; Lamikiz, 2009)

2.7.5 **Roller Pinion System**

The roller pinion system is an advanced, new technology that revolutionizes linear motion. The roller pinion system (RPS) provides zero backlash, very high positional accuracy, unlimited length, unique design possibilities as well as the capability to achieve much higher performance levels in machine designs. The RPS line features an innovative rack and pinion technology with extremely accurate positioning. This design eliminates the cumulative error and thermal expansion error problems experienced with ball screw systems. The opposing roller has contact with two or more teeth at the same time. This design eliminates the costly and complex split and dual pinion systems required in most traditional rack and pinion systems to achieve zero-backlash. The RPS line is designed with bearing-supported rollers that move smoothly along the face of each tooth. This reduces noise levels often associated with other motion systems, tooth slap or ball return noise.

The roller pinion system maintains accurate positioning at speeds up to 11 m/sec (36.1 ft/sec). Even at such speeds, the extremely low friction design does not produce heat or wear. Low load application is a drawback of the roller pinion system. Figure 2.31 presents a roller pinion system.

(a) Roller pinion

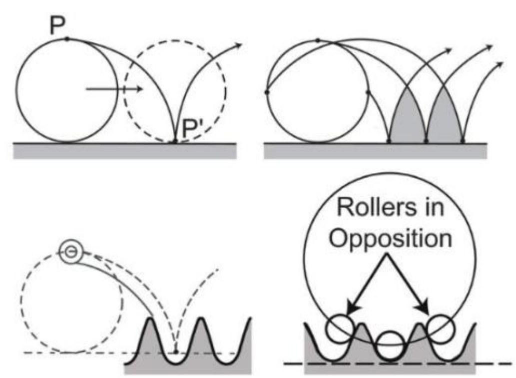

(b) Diagram of a roller pinion system

Figure 2.31: Roller Pinion System (Atlanta Drive Systems Inc., 2013 ; Clark)

2.8 Conclusions and Objectives

In this chapter, a background of CNC was discussed and the most important design processes, such as machine kinematic chain and configurations, were evaluated. The CNC machine kinematic principle showed the best kinematic design, it is the one in which “the workpiece is carried by just one axis”. Different types of existing CNC gantry machine were evaluated and several conceptual designs of new types of such machines have been proposed. The “longitudinal vibation” of the gantry was the important challenge of the works. In these researches the most important key words in CNC gantry design are “the design, modification and optimization" which were evaluated and discussed. Several research works on the feed drive motion of CNC gantry machines have been done and evaluated by the researchers. The rack and pinion with its "backlash" problems was evaluated; existing gear anti-backlash mechanisms were evaluated.

In addition, this chapter summarized the relevant research associated with machine tools, gantry machine tools and design criteria including "static" and "dynamic" behavior, "cost and weight". Tools were investigated, such as optimization and "multi-criteria decision making" for attaining optimal design solutions. The finite element method for achieving rapid and reliable solutions and analysis was also addressed. The content of this chapter pointed out the scientific design methods and procedures that will be considered in subsequent chapters. The conceptual design of a new type of CNC gantry machine will be discussed in the next chapter.

CHAPTER 3

3 CONCEPTUAL DESIGN OF NEW GANTRY MACHINE

3.1 Introduction

The existing types of CNC gantry machine were introduced in chapter two. In the first type, the worktable moves while in the second type, the gantry moves. With the new idea of feed drive motion of a CNC gantry machine, the worktable and gantry can move simultaneously but opposite each other. Basically, in this novel type of CNC gantry machine tool, the feed drive motion is a double motion mechanism that will cause the worktable and gantry to move simultaneously and opposite each other. Because the new CNC gantry machine has no fixed parts, the worktable and gantry are able to move opposite each other simultaneously through the new feed drive motion mechanism. Hence, the total speed of the machine includes the velocity of the worktable and gantry together. In fact, the gantry and worktable will move half of the X-axis distance during any machining operation. Therefore, the space occupied by the worktable will be 1.5 times its length on the structure, the total length of the CNC gantry machine tool will be around 1.5 times of the worktable length, while the total length of the first type of CNC gantry machine becomes more than twice the worktable.

In this section the design steps are presented as follows:

A. The conceptual design of the new type of CNC gantry machine
B. Design of a double motion mechanism for X-axis feed drive motion
C. Initial design of the CNC machine using the double motion mechanism

3.2 The Conceptual Design of the Proposed CNC Gantry Machine

The conceptual design of the proposed CNC gantry machine is based on the concept of the worktable and gantry moving simultaneously and in opposite directions (Figure 3.1). According to the machine's kinematic configuration discussed in chapter two, the configuration of the new gantry machine is (LL) LLRR. It means there are two linear motions for the X-axis (worktable and gantry simultaneously), another two linear motions belong to the Y- and Z-axes and two rotational motions can be used for the rotary headstock (as a machine gantry accessory). In this design, the gantry and worktable can move at the same time with a special mechanism, the double motion mechanism, which is introduced subsequently. The conceptual design of the new gantry machine with two different configurations is shown in Figure 3.1.

As seen in Figure 3.1 (a), a ball screw is used for the machine's worktable feed drive motion. The ball screw will cause the worktable to move and the gantry will move in the opposite direction from the worktable at the same time via the double motion mechanism installed in the gantry columns. Figure 3.1 (b) shows that the gantry employs two servomotors, which will move the double motion mechanism and the worktable will move in the opposite direction from the gantry via the double motion mechanism. In this design, the motion of the gantry is dependent on the worktable. The main feed drive motion is the only difference between these two configurations. The main feed drive motion in the first (a) configuration is via a ball screw supported by the servomotor while the main feed drive motion in the second (b) configuration is via the double motion mechanism that is supported by the servomotor directly. Therefore, the table and gantry can move in opposite directions over the same length. The worktable and gantry will move half of the machining operation. Fig 3.1 (b) shows the main motion drive is the gantry by two servomotors installed on the gantry columns.

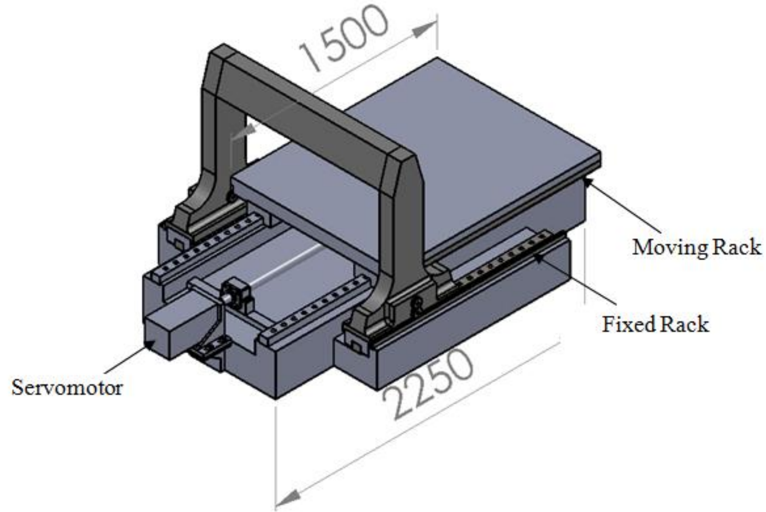

(a) New Gantry Machine with Double Motion Mechanism (Table-based)

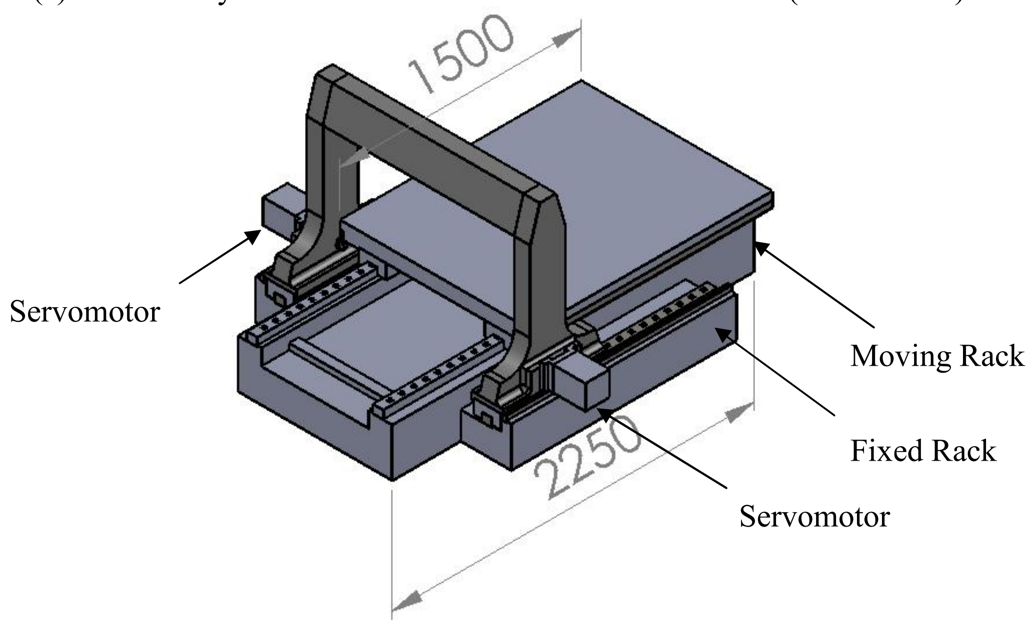

(b) New Gantry Machine with Double Motion Mechanism (Gantry-based)

Figure 3.1: Conceptual Design of the New CNC Gantry Machine with a Double Motion Mechanism

The conceptual design of the new CNC gantry machine was patented by University of Malaysia after document preparation (M. H. S. R. Besharati, 2011). Several important advantages have been obtained from the conceptual design of this new type of CNC gantry machine, including:

1. The total length of the machine is decreased, which affects other achievements, such as the total cost of manufacturing and machine space occupied. In Figure 3.2 this advantage is compared with the first existing CNC gantry machine types.

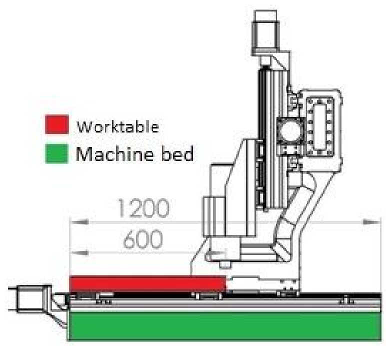

(a) Existing Type of Gantry
(Initial Worktable Position)

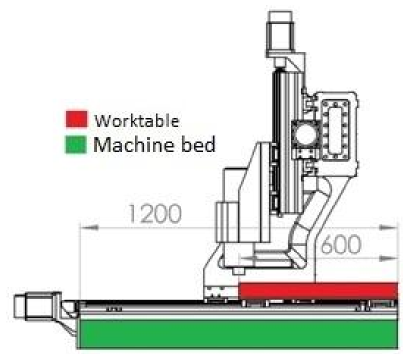

(b) Existing Type of Gantry
(End Worktable Position)

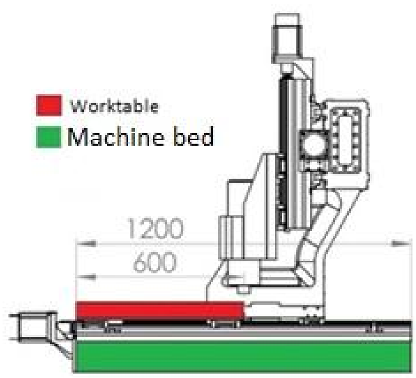

(c) New Proposed Type
(Initial Worktable Position)

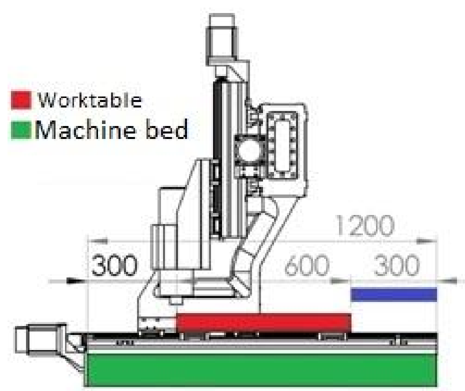

(d) New Proposed Type
(End Worktable Position)

Figure 3.2: Comparison between First Type of Existing Gantry and the New Idea

As seen in Figure 3.2 (a, b) the worktable is 600 mm long and the machine structure must be 1200mm because the worktable must move twice its length. In Figure 3.2 (c, d) the machine structure is 900 mm long because the worktable must move half (300 mm) of its length and the gantry will move half of the balance of its total length but in the opposite direction. Figure 3.3 shows that in the new design, the total length of the machine structure will be around 1.5 times the worktable length.

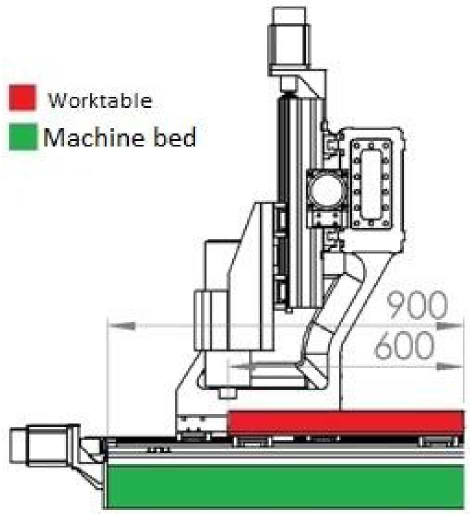

Figure 3.3: Total Machine Structure Length in the New Design

2. The new feed drive motion increases the speed of the X-axis twice, because the worktable and gantry will move together but opposite each other simultaneously. Thus, the total speed of the machine's X-axis is the speed of the worktable plus that of the gantry. This advantage has impact on increasing the machining speed. In addition, for any specified worktable length, using half the ball screw length is required. For example, a one-meter long worktable requires only half the ball screw length. This improves the length limitation of the worktable evident in the first type of existing gantry. In this case, the machine worktable can be produced up to around 10 meters because this length would only need 5 meters of ball screw length. In addition, the total length of the machine will be around 15 meters in this case. One of the significant advantages is the reduction to half the rotation of the ball screw compared to the first type of CNC gantry machine. In this system, the machine is able to use low speed servomotors as well.

3. The total precision of the machine is improved because half of the ball screw length can be used for a worktable of any length. Actually, the total precision of the ball screws depends on their length. Figure 3.4 shows the ball screw lengths in the first and new type of CNC gantry machine.

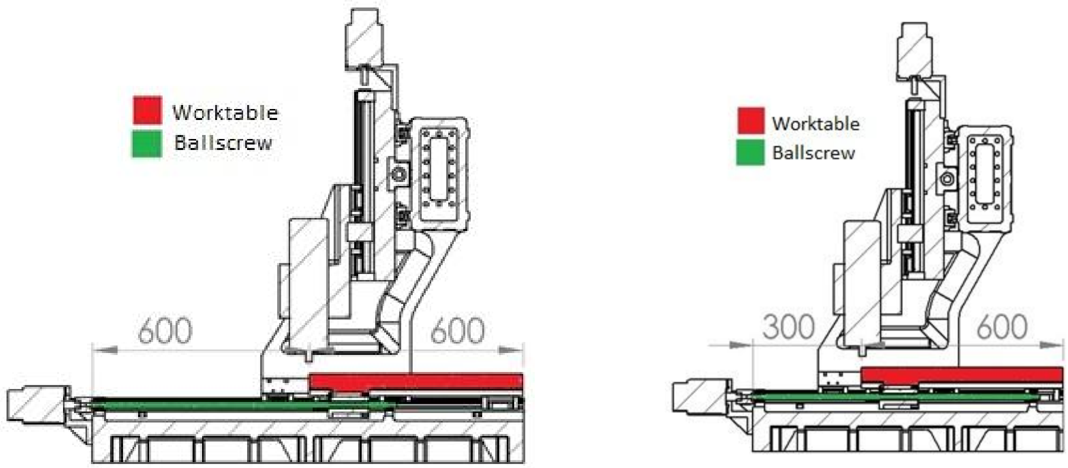

(a) Existing Type of Gantry

(b) New Gantry Design

Figure 3.4: Usage of Ball Screw Length in Existing and New Gantry Types

In the first type of CNC gantry machine the total ball screw length is equal to the worktable length, but in the new type only half the length is needed.

4. The machining table length limitation is improved. In the gantry-fixed type CNC gantry machine, the length of the machine table is exactly the same as the length of the ball screw. Usually, depending on the application and precision requirements, maximum ball screw length is available. However, in the new design, the worktable length can be increased to double that of the ball screw production length.

Other topics requiring investigation in future research on this subject include improving machine efficiency, simplifying machine manufacturing and decreasing the total cost of the machine.

3.3 Proposed Design of CNC Gantry Machine with Double Motion Feed Drive System

The concept of a double motion mechanism entails a special feed drive mechanism that is able to produce motion for the gantry and worktable of the CNC gantry machine simultaneously and in opposite directions. Two types of double motion feed drive system can be designed:

A –double motion mechanism based on a rack and pinion (dependent system),

B -double motion mechanism based on ball screw (independent system).

Both can be used for the same purpose, but there are some differences between them. By the dependent system worktable and gantry they can move dependently and they can’t move separately; this system is suitable for mass production applications. The independent system can be used for universal machine, the worktable and gantry can move simultaneously and separately with the fore axis CNC controller.

3.3.1 Design of Double Motion Mechanism based on a Rack and Pinion system

The design of a double motion mechanism based on a rack and pinion is described in this section and the other one will be described in section (4.2). Although it seems like a simple design, it is not comprehensibly easily because the mechanism (with several pinions and two racks) supports two parts that should move in opposite directions. This device has two gear groups with several functions. The gantry and worktable’s “equal and simultaneous transferring motion" in "opposite directions" are among the gear system functions. Essentially if the table moves, the gantry will move at the same time with a similar measure but in the opposite direction. Therefore, the transfer ratio of the moving rack and fixed rack is very important. The final designed mechanism is shown in Figure 3.5.

To understand how the double motion mechanism works, the layout of a double motion gear system is depicted in Figure 3.5 (a). In the mechanism illustrated, two racks are used. One is fixed and the other is moving; in any circumstance, the length of the moving rack must be two times that of the fixed rack. In this instance, the fixed rack is 300 mm long and is fixed on the machine structure, while a moving rack 600 mm long is installed on the worktable. Two pinions are connected by two shafts and their ratio of transfer is 2/1. There is a special rectangular component, which is representative of the CNC machine gantry's column and is able to carry both shafts. A pinion with 40 teeth is shown in front of the picture and it is fixated to the bottom shaft by a key. On the other side of this shaft the pinion (20 teeth) is free to rotate on the shaft. Two additional gears are fixed on the upper shaft. Although in the conceptual design (Figure 3.1) the gears of the double motion mechanism are installed in the columns, in this step the double motion mechanism has been designed as a separate part (Figure 3.5 (a, b)).

The mechanism functions in the following way. If the large pinion ($Z = 40$) moves 300 mm over the length of the fixed rack, it will rotate around $N=300/ (Z*M*3.14) =1.194$ rev at the end of 300 mm (the gear module is $M = 2$ mm). Furthermore, the upper pinion ($Z=20$) will rotate twice $N = 2.388$ RPM via pinion $Z=40$. Similarly, the corresponding pinion on the other side of the shaft, pinion ($Z=40$) will rotated the same value, $N = 2.388$ rev. Therefore, the engaged pinion ($Z=20$) will rotate around twice the value $N = 4.777$ rev it is freewheel. This pinion will move a distance $L= 599.991$ mm. This means that it will move the total length of the fixed rack in the opposite direction. In other words, if the big pinion (Z = 40 at the front of the picture) rotates counterclockwise, the representative gantry will move to the left and the moving rack (worktable) will move to the right simultaneously.

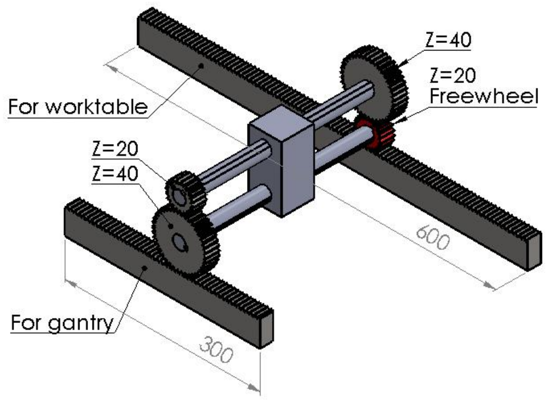

(a) Schematic of the Double Motion System

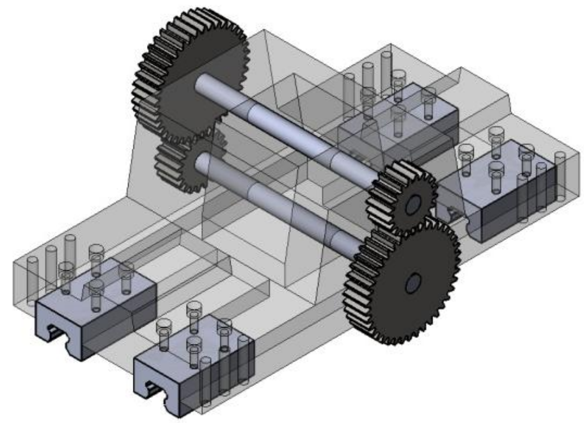

(b) Double Motion Mechanism

Figure 3.5: Double Motion Gear Mechanism

Basically if the machine gantry moves only L= 300 mm, the worktable will move L= 300 mm in the opposite direction. In this case, if the total length of the machining operation is L= 600 mm then the total space occupied by the machine will be L= 900 mm, while the value for the existing type of CNC gantry machine (first type) will be L= 1200 mm.

The double motion mechanism is able to simultaneously support two linear axes of the machine, the worktable and gantry. The ball screw system is used to drive the X-axis (worktable) of the machine and the gantry can be simultaneously moved using the double motion mechanism. Figure 3.6 shows the first design of the double motion mechanism as well as its installation on the new machine structure.

In this design the gears are installed on the double motion body and the column is assembled at the top of the mechanism. It can be installed without columns on the main machine structure as well as before gantry assembly. The gantry installation onto the mechanism follows the double motion body, which is tapered in the installation area (guide method).

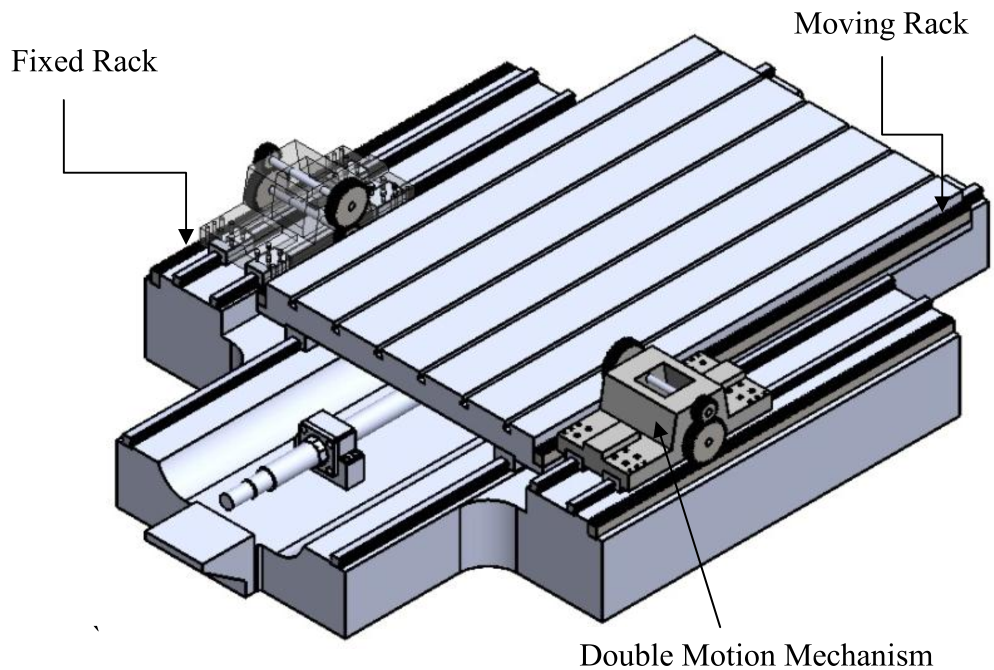

Figure 3.6: The First Design of a Double Motion Mechanism and its Installation on the New CNC Gantry Structure

Clearly, the ball screw drives the worktable, which is supported by a servomotor. The motion will transfer to the double motion mechanism via the rack installed on two slats at the left and right sides of the worktable. The motion will finally be transferred to the gantry through the double motion mechanism. Standard linear guideways are used for all linear motion systems. In this case three-axis CNC controllers must be used to control the X-, Y- and Z-axes because the gantry's motion is dependent on the X-axis through the double motion mechanism and not the separate axis as shown in Figure 3.7. Therefore, the machine has three simultaneously controllable axes.

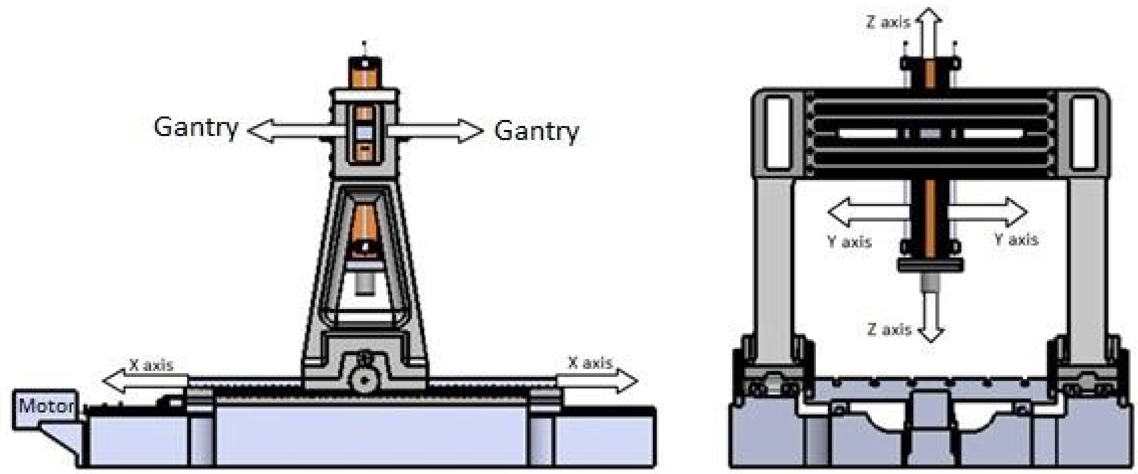

Figure 3.7: The X-, Y- and Z-axes of the New CNC Gantry Machine

3.3.2 The Characteristics of the Double Motion Mechanism Based on Rack and Pinion

This mechanism has three important characteristics:

1. The motion of the gantry is dependent on the motion of the worktable and vice versa.

2. The gantry and the worktable can be controlled by one axis (the X-axis). However, the CNC gantry machine's kinematic configuration is (LL) LLRR (four linear and two rotational motions).

3. There is a backlash problem because a rack and pinion is used in this system.

3.3.3 Double Motion Mechanism Backlash Problem

The major problem with rack and pinion systems is backlash. It causes high transmission error, decreases precision and causes unsatisfactory surface quality in the manufacturing process. Hence, solving the problem requires designing a complementary device for the double motion mechanism. In fact, any error in the rack and pinion will lead to low machine performance (Brauer, 2003). The major deficiency of rack and pinion systems is in the free play between the rack and pinion teeth (Lassâad Walha, 2009). When the system is subjected to non-continuous motion with frequent direction reversal there will be significant error. Nonetheless, there are many anti-backlash mechanisms to remove or control backlash, as presented in chapter two.

3.4 Proposing a New Anti-backlash Mechanism in Rack and Pinion System

Various anti-backlash systems have been proposed for various applications, such as industrial robots, precision machining tools, radar antennas and precision servomotors. Anti-backlash gear systems reduce the transmission error. As a result, precise and desirable output rotation or displacement is gained. The double electric motor method, double helical gear anti-backlash method, adjusting center distance method and spring-loaded anti-backlash method (Allan, 1980; Boyuan, 2001; C. W. Cairnes, 1953; Guoming, 2001; Imasaki, 1995; Kwon, 2004; Shim, 2008) are among the approaches used to eliminate backlash in gear, rack and pinion systems.

Among the above-mentioned methods utilized to omit backlash, the spring-loaded anti-backlash technique is widely employed in numerous fields. In this method, the coefficient of the spring needs to be determined so that the mated teeth are always in contact for all input torque. However, high preload in the system causes high contact and bending stress, which may reduce gear lifespan. Other drawbacks of this method include complex manufacturing and installation, low transfer torque and high friction. In addition, if the teeth are assumed to be rigid and static transmission error is neglected, the dynamic transmission error (DTE) would always be in the system due to torsional spring deformation triggered by the input torque.

In order to gain thorough insight into the dynamic and vibration behavior of gear systems, their modeling has been studied since 1920. Numerous investigations have been conducted and accomplishments achieved regarding the dynamic modeling and analysis of gear systems, with summaries compiled by Wang et al (Wang, 2003) and Özgüven and Houser (Nevzat Özgüven, 1988).

More realistic and exact gear models with multi parameter excitation have been studied in recent research works (Eritenel, 2012; He, 2007; Moradi, 2012). In addition, nonlinear gear system dynamics have been vastly taken into account. For instance, the interactions between time-varying mesh stiffness and clearance nonlinearities, as well as nonlinear dynamics of a gear rotor-bearing system with multiple clearance and dynamic transmission errors (DTE) made by tooth deflection, which consequently lead to vibration, have been investigated (Gregory, 1963; Kahraman, 1991a, 1991b). A relation between gear noise, transmission error and vibration has been established in (Gill-Jeong, 2007; Wang, 2007). In the mentioned research, the role of transmission error and dynamic behavior was considered in order to reduce gear noise. Typically, due to difficulty in solving nonlinear equations, the vibration response of dynamic gear models has been determined either by integrating or applying other prevalent numerical methods (Kahraman, 1991a; Padmanabhan, 1996).

Until now, only few studies have been performed on nonlinear modeling, contact stiffness and dynamic transmission error (DTE) in anti-backlash systems. For example, in (Guoming, 2001) a simplified torsional dynamic model was established and the natural frequency was analyzed. An approach was proposed to estimate the minimum preload torque required to attain satisfactory step response for spring-loaded anti-backlash systems (Allan, 1980).

A new anti-backlash system with a unique feature was proposed (S. R. Besharati, et al., 2012). In this new mechanism, assuming that all teeth are rigid and static transmission error is negligible, dynamic transmission error (DTE) is zero for every input torque -- a unique trait never proposed before. Nevertheless, dynamic nonlinear system modeling with regard to time-varying stiffness and backlash modeling is investigated in order to thoroughly perceive the system's dynamic behavior. Based on a dynamic model, the minimum required preload is also specified to eliminate backlash for different input torques. Eventually, an approximate relation for determining the minimum preload necessary to eliminate backlash is proposed. The developed equations are based on dynamic transmission error (DTE) and numerical methods are employed to solve them.

Backlash, or dead zone, is characteristic of gear trains and general mechanisms. From an analysis point of view, backlash is a nonlinear behavior and excessive backlash can reduce mechanism performance, causing system instability. Due to inherent deficiency in gear machining, there is always clearance between gear teeth, as shown in Figure 3.8 (a, b). In this figure, the input gear must travel a (b/2) distance before contacting the output gear. When the input gear has contacted the output gear, to reverse direction, the input gear must travel a (b) distance before the output gear moves.

Backlash occurs for different reasons, but it cannot be evaluated before the machining process. The general goal of reducing backlash is to prevent transmission error and noise. Any increase in the amount of backlash will increase the possibility of errors and jamming during machining. Consequently, smaller amounts of backlash in gear systems lead to better precision. Gear runout, error in profile, pitch and tooth thickness, helix angle and center distance are all influential on increasing the amount of backlash. Excessive backlash must be removed, particularly when the drive is frequently reversed or high load is proposed.

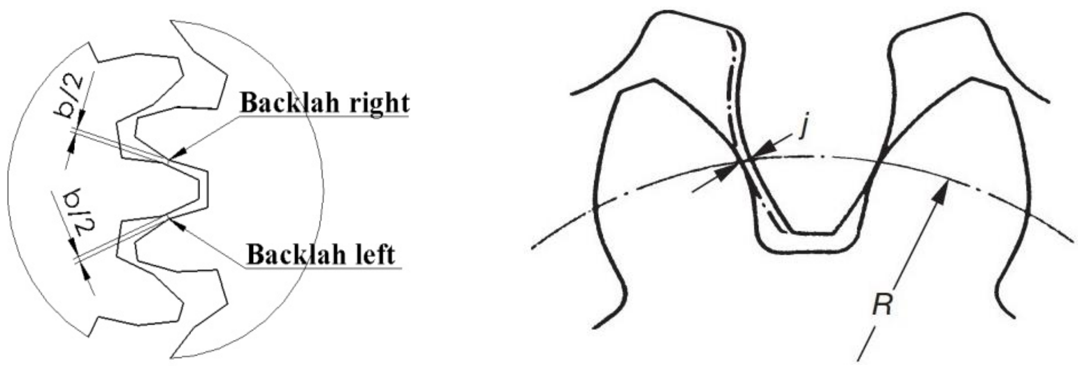

(a) Backlash Schematic (b) Backlash, j, between Two Gears

Figure 3.8: Gear Backlash Schematic

However, high cost is needed to reduce backlash during gear manufacturing. Thus, machining accuracy will be affected when decreasing backlash. Any increase or decrease in the distance of the centers between two gears will be transformed into backlash. There are different ways to design backlash in gears, with several kinds in rack and pinion: circular backlash j_t, normal backlash j_n, center backlash j_r and angular backlash j_θ (°) (Figure 3.9).

3.5 New Anti-backlash Design in a Rack and Pinion System

To solve the backlash problem it is necessary to design suitable anti-backlash for the double motion mechanism. A new concept for a gear backlash compensation mechanism (GBCM) is introduced for the first time. It is applicable for any other industrial application purposes. As such, a combination of three pinions and one rack is used. The design of the new concept is explained next. Figure 3.10 presents the novel gear backlash compensation mechanism (GBCM) used in the double motion mechanism.

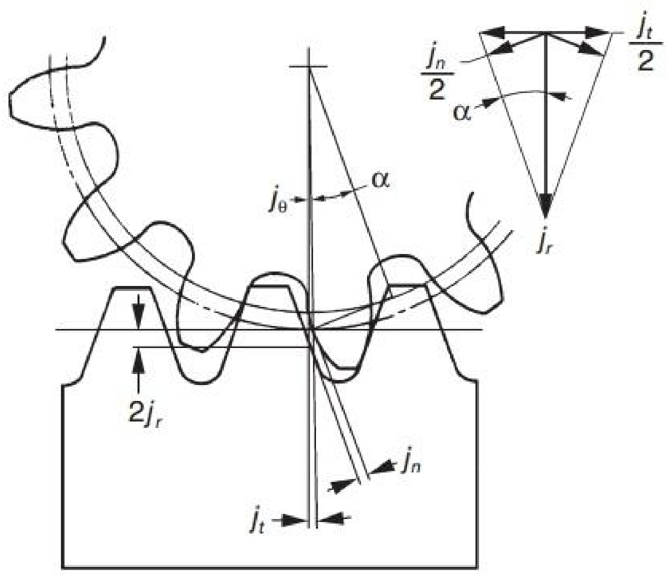

Figure 3.9: Kinds of Backlash in Rack and Pinion

This anti-backlash mechanism is an adjustable system, meaning that it is able to adjust the clearance or remove backlash without heavy preload. The GBCM system can be used for two purposes owing to the combination of three pinions: first, transferring motion from the feed drive mechanism to the rack and second, removing the backlash. For removing backlash, the distance between two racks that engage the pinions (with the racks) is adjustable.

Upon any increase or decrease in distance between these pinions, the backlash in all racks and pinions will automatically change. This means that a mechanism can be managed to control the distance between the two rack-engaged pinions, in order to control the backlash in the mechanism. Therefore, the GBCM and double motion mechanism together must serve the following functions.

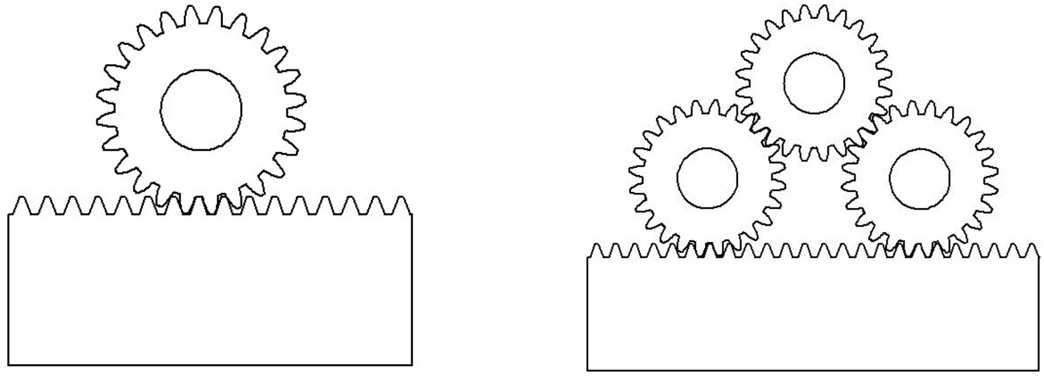

Figure 3.10: The Novel Concept of a Gear Backlash Compensation Mechanism(GBCM)

- Transfer motion from the gantry to the worktable or vice versa

- Change the direction of the gantry and table

- Transfer the ratio of motion

- Control clearance or remove backlash

According to the initial concept of controlling backlash, the backlash compensation mechanism for use in rack and pinion systems has been innovated and designed. These mechanisms can be adjusted in terms of different gear specifications. The gear backlash compensation mechanism (GBCM) can be used to reduce or remove gear free play down to zero. The GBCM is very important for the precision of linear motion systems. This mechanism has to be used mainly in CNC gantry machines for X-axis motion feed drive of the gantry or any linear motion systems. The GBCM performance is shown in Figure 3.11.As Figure 3.11 depicts, there are three adjustable brackets in the GBCM mechanism that can be adjusted by a screw. The left and right brackets can move opposite each other with the screw and they carry two big pinions. One adjustable bracket on top of the small pinion is to carry this pinion and the bracket can move up and down. Two bearing holders are shown in this figure as well, which can change rotationally around the center of the small pinion's axis. There are three shafts for the pinions and each bearing holder has two roller bearings to keep the shafts. In this mechanism all the pinions are installed on the shafts and can rotate smoothly.

The distance between the two large pinions can change -- it can be increased or decreased when the adjustable bracket of the small pinion moves up or down. Thus, these two big gears can move opposite each other thanks to the adjustable brackets, so the total backlash between the rack and pinions will be compensated for as well. Figure 3.12 shows the entire GBCM that can be used in linear motion systems.

The advantages of the GBCM over other similar systems are mentioned as follows.

a) In the new anti-backlash mechanism, the numerous gear teeth are engaged with others simultaneously. This means that more power and torque can be transferred by this mechanism. Most existing systems are functional for normal torque and power, like anti-backlash gear.

b) The contact area of the gear teeth is greater in the new mechanism, so movement will be fluent.

c) The gear backlash is easily controlled by the combination of three pinions.

d) The backlash can be controlled or removed without heavy preload requirement. All other anti-backlash systems that can be used in CNC gantry machine feed drive motion require heavy preload to remove the backlash.

e) The requirement of clearance is adjustable, whereas in existing systems this is not possible.

f) One motor is exploited to drive the GBCM, which is one of most important advantages of this innovation.

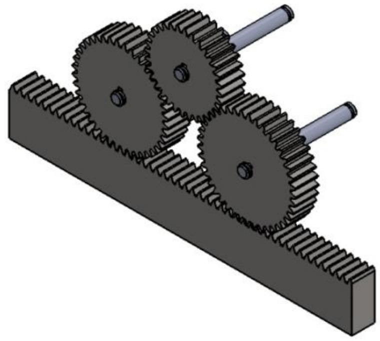

(a) Rack and Pinion System

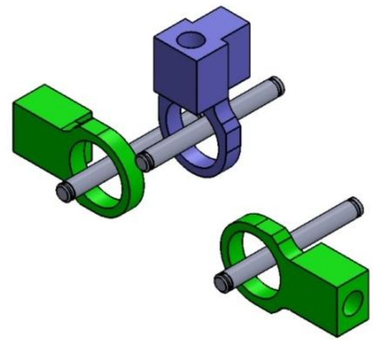

(b) The Slats

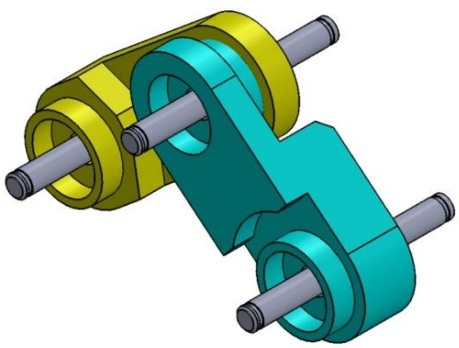

(c) The Brackets

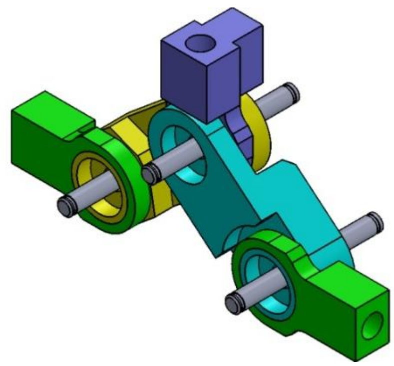

(d) Assembly of Slats and Brackets

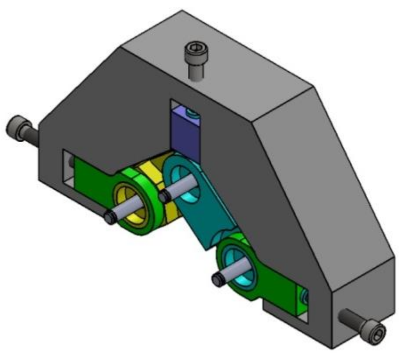

(e) The GBCM Body

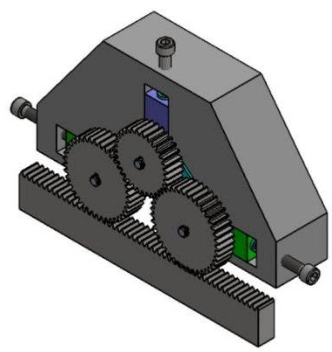

(f) The GMCM Mechanism

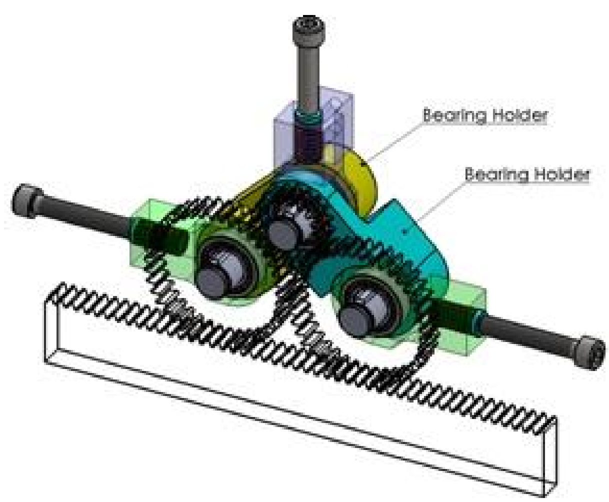

Figure 3.11: The Gear Backlash Compensation Mechanism (GBCM)

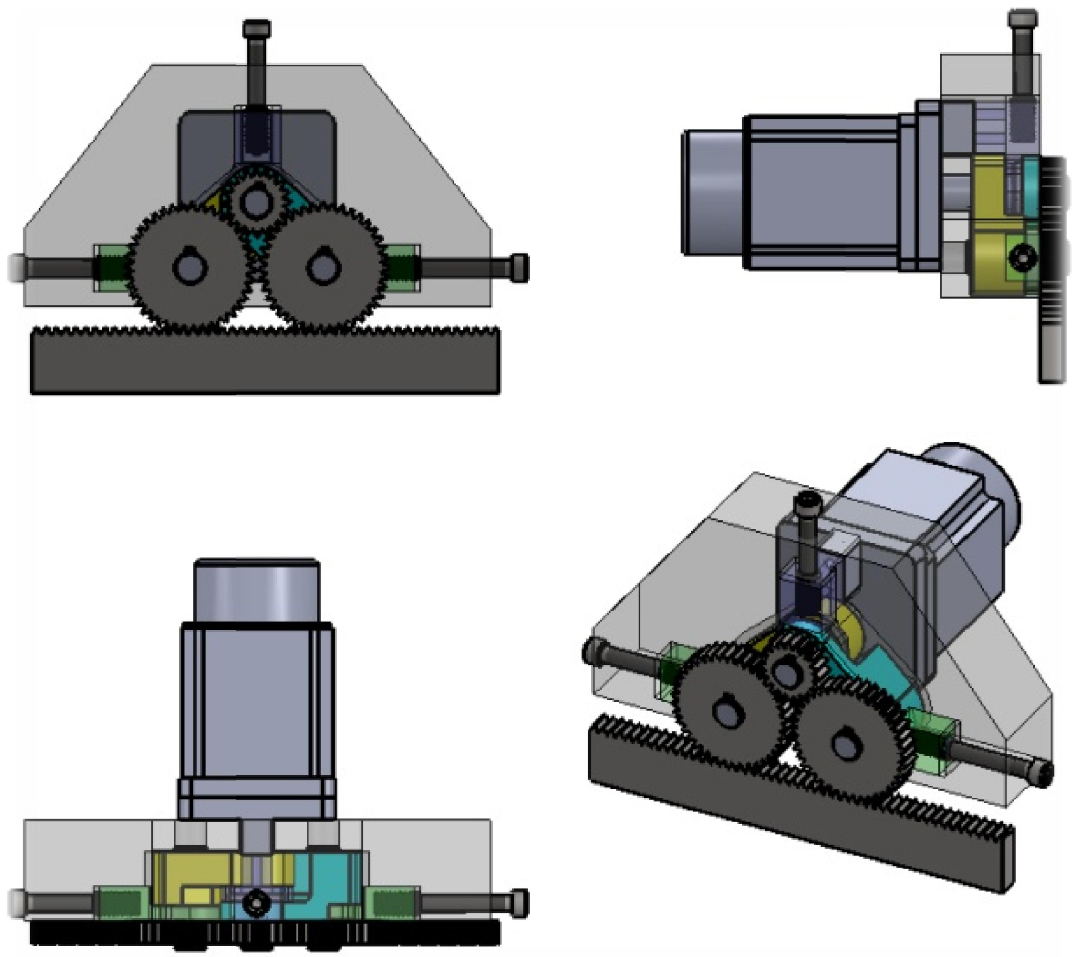

Figure 3.12: The Complete GBCM System

g) Production cost is lower than some other systems.

h) The right or left tooth setting is adjustable, so it is suitable for GBCM system calibration (existing anti-backlash systems cannot do this). Figure 3.13 shows Schematic of (Left and Right) GBCM Adjustment shows two types of GBCM adjustment.

The deigned GBCM document has been prepared for patent application and submitted to UMCIC, which the GBCM (Gear backlash compensation mechanism (GBCM) in rack and pinion system) has got patent (S. R. Besharati, et al., 2012).

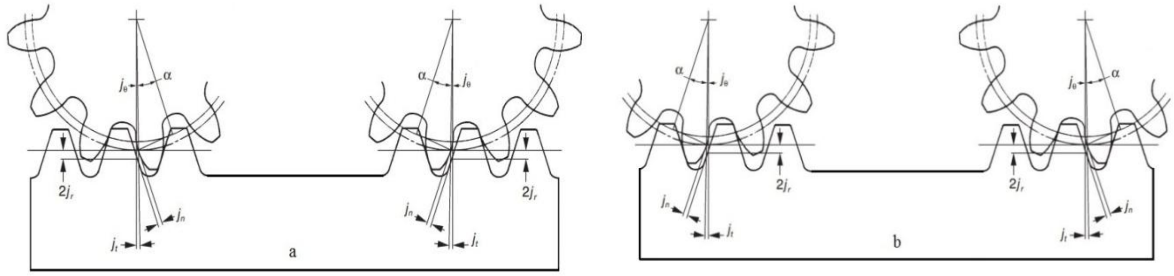

(a) Internal Adjustment (b) External Adjustment

Figure 3.13 : Schematic of (Left and Right) GBCM Adjustment

3.6 Proposed Double Motion Feed Drive with Anti-backlash Mechanism in Rack and Pinion System

The GBCM was installed in the double motion mechanism to avoid the backlash problem of the rack and pinion system. First, for moving the pinions to the left, right, up and down, six separate brackets were designed.

Furthermore, four suitable double brackets for rotational angular movement were designed; then the new CNC double motion system was installed in the new type of CNC gantry machine structure as shown in Figure 3.14.

In this design, the structure has been modified based on the new double motion mechanism. Also, the ball screw will be derived the worktable and the motion will become a double motion in this way. Then the gantry will be moved by the new, double motion mechanism without backlash. For easy gantry assembly, a special plate has been added to install linear blocks (Figure 3.14) and the double motion mechanism will be assembled on top of this plate and the gantry columns on top of the double-motion mechanism.

3.7 Nonlinear Dynamic Analysis of Anti-Backlash Gear Mechanism for Less Dynamic Transmission Error

Subsequently, a new anti-backlash gear mechanism design (GBCM) comprising three pinions and a rack is introduced. This mechanism offers several advantages compared to conventional anti-backlash mechanisms, such as lower transmission error as well as lower required preload.

The nonlinear dynamic modeling of this mechanism is developed to acquire insight into its dynamic behavior. It is observed that the amount of preload required to diminish the backlash depends on the applied input torque and nature of periodic mesh stiffness. Then an attempt is made to obtain an approximate relation and find the minimum required preload to preserve the system's anti-backlash property and reduce friction and wear on the gear teeth. The mesh stiffness of the mated gears, rack and pinion is achieved via finite element method using ANSYS workbench and is approximated by Fourier series in the equation of motion.

A numerical method is used to solve the differential equation of motion and the total transmission error of the system and spectral content is computed.

Assuming that all teeth are rigid and static transmission error is negligible, dynamic transmission error (DTE) is zero for every input torque, which is a unique trait, not yet proposed in previous research.

Gear mechanisms are used extensively in modern power transmission systems owing to their remarkable advantages. Some gear system applications include power generation, mining, transportation and refining industries.

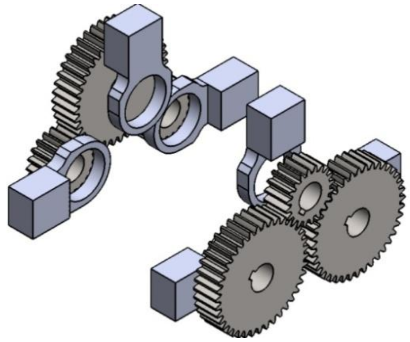

(a) The Slats

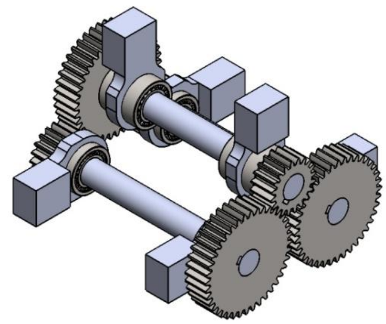

(b) The Shafts and Angular Bearings

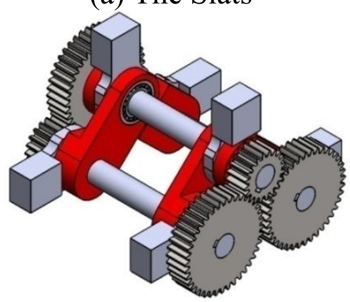

(c) The Brackets

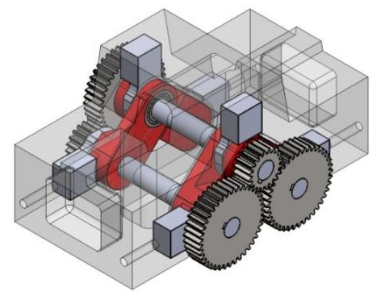

(d) Double Motion Mechanism with GBCM

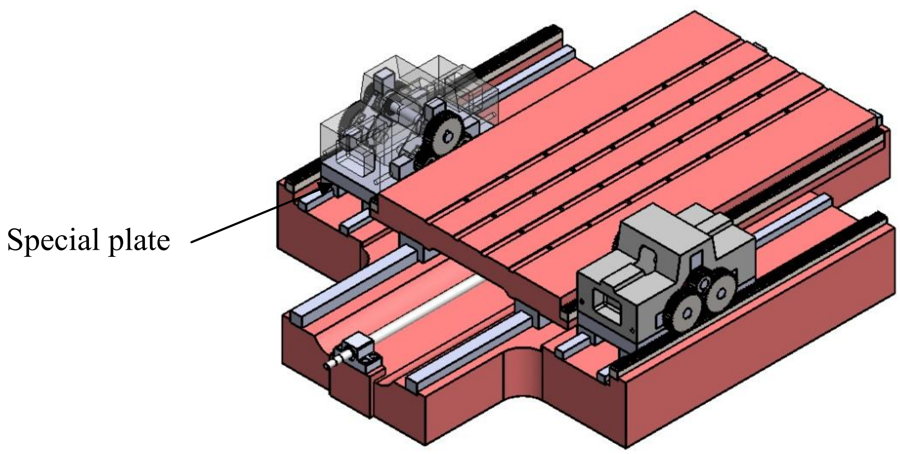

Figure 3.14: The Double Motion Mechanism with the GBCM

3.7.1 **The Concept**

The configuration of the new anti-backlash mechanism comprises three pinions, one rack, two bearing holders and three adjustment slides, as shown in Figure 3.15.

In this mechanism, the main pinion is the driver to which input torque is applied. An optimum amount of preload is exerted on the main pinion by an adjusting system to ensure that all gear teeth remain in contact in various operating conditions. Afterward, the distance between the transmission pinion and the rack is fixed using a mount screw. Contact among the teeth of the mated gears ensures that the rotation transmission will be continuous.

In fact, transferring clockwise and counterclockwise rotation is accomplished using the right and left transmission pinions, respectively. It is not essential to use a spring to provide the required preload and it is sufficient to use a screw to supply an accurate amount of preload. Compared with a spring-loaded mechanism, assuming that teeth are rigid and static transmission error is zero, this system would provide zero transmission error. In order to verify the applicability of the mechanism concept to eliminate backlash, a simulation of the mechanism in Motion Analysis of Solidworks CAD software has been investigated.

Figure 3.15 shows the modeled mechanism and preload as well as rotational motor applied on the mechanism. The contact constrains were applied between the adjacent gears and rack. First, force was applied as preload to ensure contact between adjacent teeth.

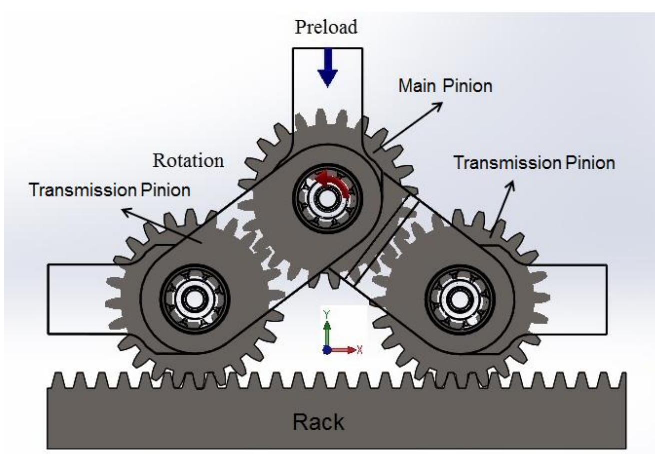

(a) The Main Mechanism

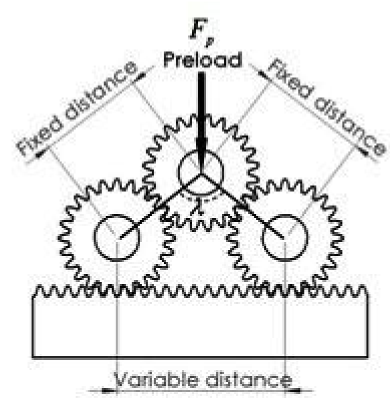

(b) Gear Configuration

Figure 3.15: Configuration of the New Anti-backlash Mechanism

Next, the motor began rotating the main pinion clockwise and with constant angular velocity at the 1st second and altered the direction at the 3rd second as well as Motor Rotation (Clockwise from 1st Second and Counterclockwise from 3rd Second) on Main Pinion Figure 3.16 shows the linear displacement of the rack. The small variation in rack displacement before the 1st second, results from the applied preload, which attempts to eliminate the initial clearance between teeth. As seen in this figure, the rack begins to move immediately after motor initiation. This result verifies the anti-backlash characteristics of the proposed mechanism for both directions.

There is a possibility of tooth separation due to the system's dynamic complicity, which depends on internal (variable mesh stiffness) and external system excitation (input torque). In order to better understand the dynamic behavior of the system and determine the optimum amount of preload, the next section deals with nonlinear dynamic system modeling assuming variable mesh stiffness. For investigating the dynamic behavior of the new anti backlash mechanism, the modal analysis is required to extract the natural frequency of the mechanism.

Modal analysis is mainly a technique used to obtain the vibration characteristics of a structure. Hence, the dynamic behavior of the new anti backlash mechanism with Steel "ASTM-A36" was analyzed to identify the minimum natural frequencies. The entire modal analysis process was done using ANSYS (engineering simulation software) by finite element method. In order to make a finite element model, a three dimensional model of the new anti backlash mechanism with ANSYS Workbench was considered. The three dimensional model with SolidWorks software was performed. The model was exported to ANSYS Workbench and the necessary input data as material properties like modulus of elasticity, Poison ratio and density was applied. Then, elements of the model were made under Solid element.

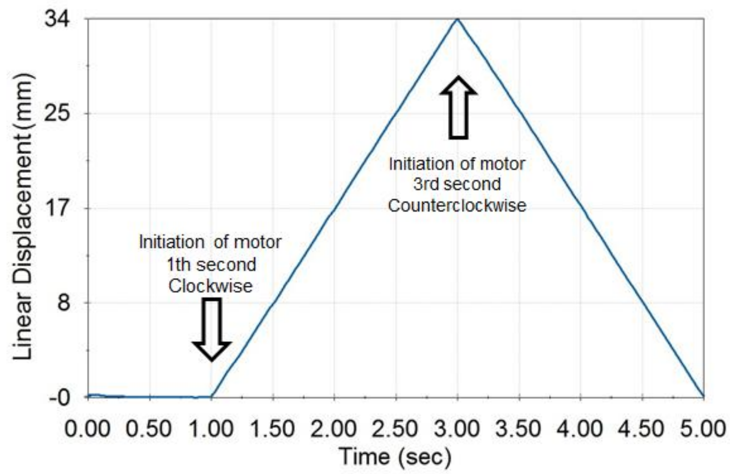

Figure 3.16: Linear Displacement of the Rack by Applying Preload
(from Beginning of Simulation)

This model has 187616 elements and 345694 nodes. Relevant boundary conditions are applied on the earth connection of the rack. Finally, modal analysis was performed to obtain natural frequencies of the mechanism.

The modal analysis shows that the mechanism vibrates at a natural frequency of around 140.18 Hz in the X-axis direction in the first mode. The modal analysis evaluation is shown in Figure3.17

The modal analysis results are shown that the minimum natural frequency of the gears is 140.18; it means that the gears can be rotating around 8400 RPM without any vibration. Mainly the rack and pinion systems are able to change the rotational motion to linear and they can be used for CNC gantry machine X axis travel and many other applications. The X travel of existing CNC gantry machine in the market is up to 10000 mm/min of rapid speed. Therefore the new anti backlash pinions must be rotated at 66.34 RPM to accommodate 10000 mm for this case. Hence according to minimum natural frequency (140.18Hz equivalent 8448.6 RPM) of the new anti backlash mechanism, it doesn't have any vibration during rapid traveling process.

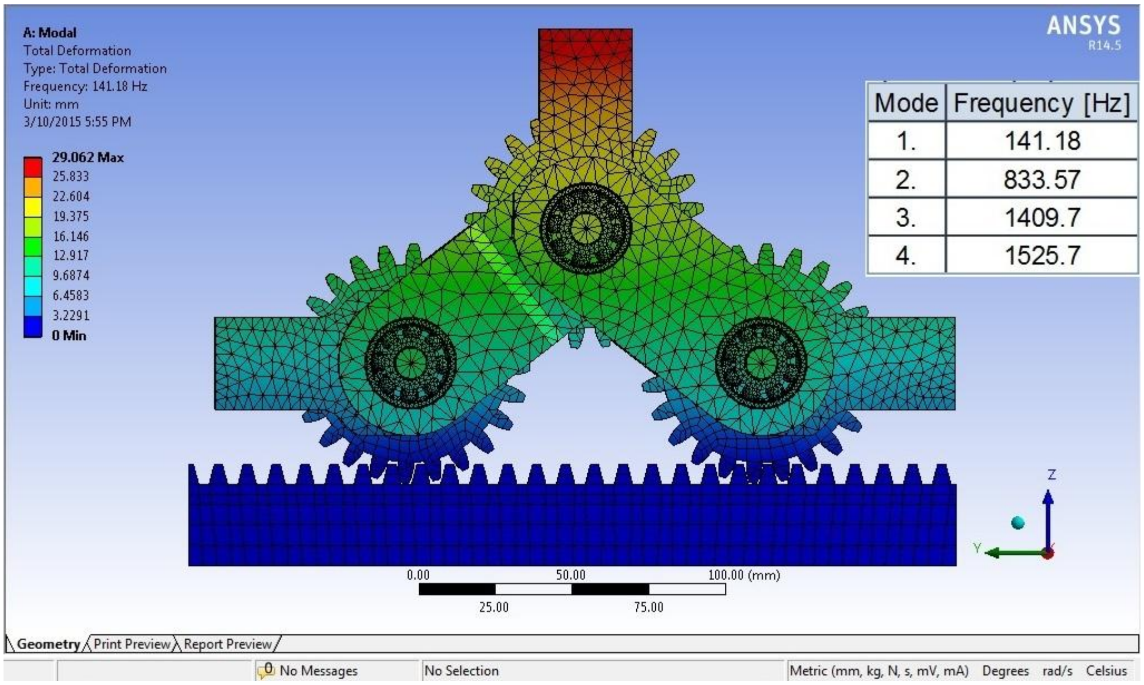

Figure3.17: Modal Analysis Results of new Anti Backlash Mechanism

3.7.2 **Nonlinear Dynamic Model**

The spur gears, rack and pinion are modeled using a disk and mass coupled with nonlinear mesh stiffness and damping (Figure 3.18).

The mesh compliance is considered by periodic variable springs (k(t)) and energy loss in the mesh is achieved by the damping elements (c_1, c_2). Mesh stiffness is evaluated using the finite element method for the pinions in contact and rack and pinions separately. In order to obtain motion equations based on the transmission errors of the relevant gears, the following definitions are first stated:

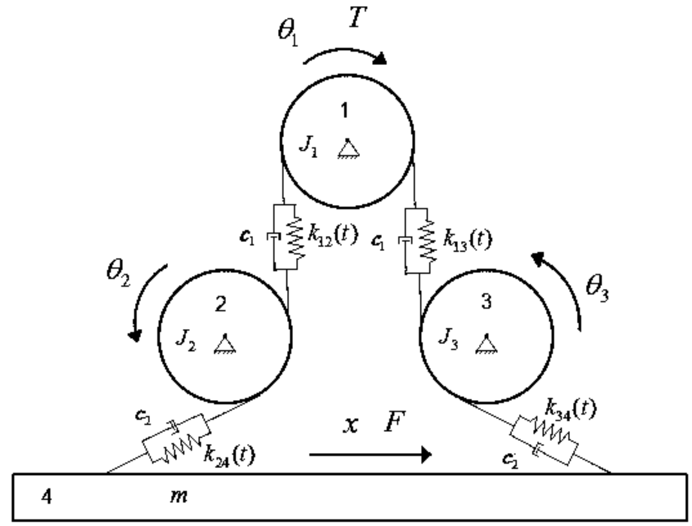

Figure 3.18: Model of Anti-backlash Gear Mechanism

$$x_{12} = -R_1\theta_1 + R_2\theta_2 \tag{3.1.a}$$

$$x_{13} = R_1\theta_1 - R_3\theta_3 \tag{3.1.b}$$

$$x_{24} = -R_2\theta_2 + x \tag{3.1.c}$$

$$x_{34} = R_3\theta_3 - x \tag{3.1.d}$$

where x_{12}, x_{13}, x_{24} and x_{34} are relative transmission error between pinions 1 and 2, 1 and 3, pinion 2 and rack and pinion 3 and rack, respectively. R_1, R_2, R_3 are gear radii, $\theta_1, \theta_2, \theta_3$ are the gears' rotational displacements and x is the rack's linear displacement. These relations are defined such that compression always gives positive transmission error.

For simplicity, Eq. (3.1) can be stated in matrix form as follows:

$$\{x\} = [P]\{\theta\} \tag{3.2.a}$$

where

$$\{x\}=\begin{Bmatrix} x_{12} \\ x_{13} \\ x_{24} \\ x_{34} \end{Bmatrix}\ ,\ \{\theta\}=\begin{Bmatrix} \theta_1 \\ \theta_2 \\ \theta_3 \\ x \end{Bmatrix}\ ,\ [P]=\begin{bmatrix} -R_1 & R_2 & 0 & 0 \\ R_1 & 0 & -R_3 & 0 \\ 0 & -R_2 & 0 & 1 \\ 0 & 0 & R_3 & -1 \end{bmatrix} \tag{3.2.b}$$

Using the Newtonian laws of motion and assuming that the shafts and bearings are rigid, the dynamic equations for the gears and rack are obtained separately, as in Eq. (3.3). In the following equations, J_1, J_2, J_3 represent the mass inertial moment of gears 1, 2, 3 respectively; m is the mass of the rack; and T and F are torque applied on gear 1 and external force applied on the rack, respectively.

$$J_1\ddot{\theta}_1 = c_{12}\dot{x}_{12}R_1 - c\dot{x}_{13}R_1 + k_{12}(t)f(\delta_1 + x_{12})R_1 - k_{13}(t)f(\delta_1 + x_{13})R_1 + T \tag{3.3.a}$$

$$J_2\ddot{\theta}_2 = -c_1\dot{x}_{12}R_2 + c_2\dot{x}_{24}R_2 - k_{12}(t)f(\delta_1 + x_{12})R_2 + k_{24}(t)f(\delta_2 + x_{24})R_2 \tag{3.3.b}$$

$$J_3\ddot{\theta}_3 = c_1\dot{x}_{13}R_3 - c_2\dot{x}_{34}R_3 + k_{13}(t)f(\delta_1 + x_{13})R_3 - k_{34}(t)f(\delta_2 + x_{34})R_3 \tag{3.3.c}$$

$$m\ddot{x} = -c_2\dot{x}_{24} + c_2\dot{x}_{34} - k_{24}(t)f(\delta_2 + x_{24}) + k_{34}(t)f(\delta_2 + x_{34}) + F \tag{3.3.d}$$

where δ_1 is mesh compression displacement of gears 1-2 and 1-3 and likewise, δ_2 is mesh compression displacement of gear 2-rack and gear 3-rack due to applied preload. δ_1 and δ_2 are computable using $\delta_1 = F_p / 2\sin(\lambda / 2)$ and $\delta_1 k_{12} = \delta_2 k_{24}$ or $\delta_1 k_{13} = \delta_2 k_{34}$ which result from static analysis for the main pinion and transmission pinions. F_p and λ represent the preload and angle between the center lines of the main and transmission pinions shown in Figure 3.15b, respectively and f is a nonlinear displacement function due to backlash and is defined as:

$$f(\zeta)=\begin{cases}\zeta & , \quad \zeta>0 \\ 0 & , \quad -b<\zeta\le 0 \\ \zeta+b & , \quad \zeta\le -b\end{cases} \tag{3.4}$$

where b is backlash.

Equation (3.3) can be expressed in matrix form as follows:

$$\{\ddot{\theta}\}=[C]\{\dot{x}\}+[K(t)]\{f(\delta+x)\}+\{F\} \tag{3.5}$$

where

$$\{f(\delta+x)\}=\begin{Bmatrix} f(\delta_1+x_{12}) \\ f(\delta_1+x_{13}) \\ f(\delta_2+x_{24}) \\ f(\delta_2+x_{34}) \end{Bmatrix}, \quad [K(t)]=\begin{bmatrix} \frac{k_{12}(t)R_1}{J_1} & -\frac{k_{13}(t)R_1}{J_1} & 0 & 0 \\ -\frac{k_{12}(t)R_2}{J_2} & 0 & \frac{k_{24}(t)R_2}{J_2} & 0 \\ 0 & \frac{k_{13}(t)R_3}{J_3} & 0 & -\frac{k_{34}(t)R_3}{J_3} \\ 0 & 0 & -\frac{k_{24}(t)}{m} & \frac{k_{34}(t)}{m} \end{bmatrix}$$

$$[C]=\begin{bmatrix} \frac{c_1R_1}{J_1} & -\frac{c_1R_1}{J_1} & 0 & 0 \\ -\frac{c_1R_2}{J_2} & 0 & \frac{c_2R_2}{J_2} & 0 \\ 0 & \frac{c_1R_3}{J_3} & 0 & \frac{-c_2R_3}{J_3} \\ 0 & 0 & -\frac{c_2}{m} & \frac{c_2}{m} \end{bmatrix}, \quad \{F\}=\begin{Bmatrix} \frac{T}{J_1} \\ 0 \\ 0 \\ \frac{F}{m} \end{Bmatrix}$$

By multiplying both sides of Eq. (3.5) by $[P]$ defined in (3.2.b), the following equation that is completely based on the relative transmission error vector is obtained:

$$\{\ddot{x}\}=[K'(t)]\{f(\delta+x)\}+[C']\{\dot{x}\}+\{F'\} \tag{3.6}$$

where

$$[K'(t)]=[P][K(t)]$$

$$[C'] = [P][C]$$

$$\{F'\} = [P]\{F\}$$

Finally, it is possible to obtain the total transmission error of the mechanism using the following relation:

$$T.E. = x - R_1\theta_1 = x_{24} + x_{12} = -(x_{13} + x_{34}) \tag{3.7}$$

3.7.3 **Determining the Approximate Preload Requirement (No-backlash Condition)**

In being aware of the minimum amount of preload needed to preserve tooth contact between mated gears, it is important to ensure that no excess amount of compression load is present in the system. In practice, it is necessary to induce a certain amount of compression by displacement in the mated gears so that no separation may occur during all states of applying and maintaining loads. Next, the aim is to obtain a simplified relation that provides insight into the minimum amount of preload required for the anti-backlash condition. First, it is assumed that the system is in a normal situation, meaning no separation occurred. Therefore, according to Eq. (3.4), it is possible to use ζ instead of $f(\zeta)$. Thereafter, due to the mechanism's inherent symmetry, the effect of compression displacement vanishes, yielding a linear version of the equation of motion that will be used in this section to discover a limiting case of separation.

For further simplification, it is assumed that $k_{12} = k_{13} = k(t)$ and $k_{24} = k_{34} = \alpha k(t)$, where α is a constant number. This condition is achievable by tuning the mechanism prior to employing it. It is fairly reasonable for the variable mesh matrix to be expressible only by the constant and periodic cosine wave as follows:

$$[K(t)] \approx k_m (a_0 + a_1 \cos \omega t)[\gamma] \tag{3.8}$$

where ω is mesh frequency and $[\gamma] = \frac{1}{k(t)}[K(t)]$. It is assumed that the transmission error vector and rotation vector are expressed as:

$$\{x(t)\} \approx \{x_0\} + \{x_1\} \sin \omega t + \{x_2\} \cos \omega t \tag{3.9.a}$$

$$\{\theta(t)\} \approx \{\theta_0\} + \{\theta_1\} \sin \omega t + \{\theta_2\} \cos \omega t \tag{3.9.b}$$

By substituting relations (3.8), (3.9.a) and (3.9.b) in the linear form of Eq. (3.5), the following equation is obtained:

$$\begin{aligned} &-\omega^2 \{\theta_1\} \sin \omega t - \omega^2 \{\theta_2\} \cos \omega t = [C](\omega \{x_1\} \cos \omega t - \omega \{x_2\} \sin \omega t) + \\ &k_m (a_0 + a_1 \cos \omega t)[\gamma](\{x_0\} + \{x_1\} \sin \omega t + \{x_2\} \cos \omega t) + \{F\} \end{aligned} \tag{3.10}$$

By collecting similar terms and equating them with each other we have:

$$k_m a_0 [\gamma]\{x_0\} + \{F\} = 0 \tag{3.11.a}$$

$$[\omega^2 \{\theta_1\} - \omega [C]\{x_2\} + k_m a_0 [\gamma]\{x_1\}] \sin \omega t = 0 \tag{3.11.b}$$

$$[\omega^2 \{\theta_2\} + \omega [C]\{x_1\} + k_m a_1 [\gamma]\{x_0\} + k_m a_0 [\gamma]\{x_2\}] \cos \omega t = 0 \tag{3.11.c}$$

Considering the fact that in steady state response the natural frequency of a system is very large compared to mesh frequency, it can be assumed that the damping and inertial forces are much smaller than the spring force and are negligible, therefore:

$$k_m a_0 [\gamma]\{x_0\} = -\{F\} \tag{3.12.a}$$

$$k_m a_0[\gamma]\{x_1\} = 0 \;\rightarrow \{x_1\} \approx 0 \tag{3.12.b}$$

$$k_m a_1[\gamma]\{x_0\} + k_m a_0[\gamma]\{x_2\} = 0 \rightarrow \{x_2\} = -\frac{a_1}{a_0}\{x_0\} \tag{3.12.c}$$

Multiplying both sides of Eq. (9.a) by $k_m a_0[\gamma]$ gives:

$$k_m a_0[\gamma]\{x(t)\} \approx k_m a_0[\gamma]\{x_0\} + k_m a_0[\gamma]\{x_1\}\sin\omega t + k_m a_0[\gamma]\{x_2\}\cos\omega t \tag{3.13.a}$$

Using the results obtained in Eq. (3.12) yields the following relation:

$$k_m a_0[\gamma]\{x(t)\} \approx -\{F\} + k_m a_0[\gamma](-a_1 / a_0)\{x_0\}\cos\omega t = -\{F\} - a_1 k_m[\gamma]\{x_0\}\cos\omega t \rightarrow$$
$$k_m a_0[\gamma]\{x(t)\} \approx -\{F\} + (a_1 / a_0)\cos\omega t\{F\}$$
(13.b)

In order to obtain the maximum amount of transmission error, the maximum value of the right side of Eq. (3.13.b) was considered. Therefore, the following equation is inferable:

$$k_m a_0[\gamma]\{x_{\max}\} \approx -(1 + a_1 / a_0)\{F\} \tag{3.13.c}$$

With insight to Eq. (3.8) using (3.13.c), we obtain the following relation:

$$[K_{eq}]\{x_{\max}\} = -\{F\} \tag{3.13.c}$$

where $[K_{eq}]$ is the equivalent stiffness matrix in which $k(t)$ is replaced by $k_{eq} = \dfrac{k_m}{(1 + a_1 / a_0)/a_0}$.

Equation (13.c) states that the maximum absolute transmission error considering the system's dynamic behavior due to the periodic variation of mesh stiffness is obtainable by replacing k_{eq} by $k(t)$ in the system and carrying out static analysis instead of dynamic analysis for the main pinion and rack considering external torque and load. In fact, this relation lets us analyze the system statically rather than using sophisticated dynamic analysis to gain insight into the dynamic behavior. Performing static analysis thus yields maximum transmission error, which must be covered by initial compression displacement to eliminate tooth separation. The next relation obtained keeping the explained viewpoint in mind, indicates that the initial compression displacement applied in the system through the preload must be more than the minimum compression displacement in the system considering the equivalent mesh stiffness is k_{eq} :

$$\delta > \max\left(\frac{T}{2k_{eq}R}, \frac{F}{2\alpha k_{eq}}\right) \tag{3.14}$$

Assuming that sufficient preload is applied in the system so no separation will occur, the amount of additional preload will not have any influence on the transmission error value and the equation of motion, (3.3), will become completely linear.

3.7.4 **Case Study for Pinion-pinion and Rack-pinion**

In this section a numerical example is discussed to obtain transmission error variation considering step torque input and variable mesh stiffness.

3.7.4.1 **Mesh Stiffness of Pinion-Pinion and Pinion-Rack**

Many investigations on gear mesh stiffness have been carried out and it has been concluded that the mesh stiffness of mated gears is periodic, non-constant and dependent on the applied torque. The varying mesh stiffness is one of the important sources of internal system excitation and it also affects the transmission error value. The mesh stiffness value comprises bending, shear, gear body torsion and Hertzian contact stress, which act in series to form mesh stiffness. Due to the complexity of calculating mesh stiffness, the finite element method is normally employed to achieve accurate results.

For a numerical investigation, the mesh stiffness of mated gears and mated rack and pinion was computed with the finite element method. ANSYS workbench was used to obtain the deformation that occurred for the prescribed force and torque. Mesh stiffness was then computed by dividing the applied torque or load by the resulting rotational or linear displacement. Table 3.1 presents the physical parameters applied in the calculation.

Table 3.1: Physical parameters used in the calculation

	Number of teeth Z	Module m, mm	Mass (kg)	Face width (mm)	Diameter of pitch circle (mm)	Length (mm)	Height (mm)
Gear	24	2	0.222	20	48	-	-
Rack	75	2	0.683	20	-	150	32

The modeling and analysis of two mated gears as well as rack-pinion are shown in 3.19. The relevant mesh stiffness results obtained are given in Figure 3.20. The alternation of mesh stiffness with rotation is due to the transition from a single to a two-tooth contact region. This phenomena will be repeated by 360/N, where N is the number of gear teeth. The frequency of mesh stiffness is $r*N$, where r is the gear's rotational speed.

Due to the periodic nature of mesh stiffness, its representation is approximated by Fourier series and its coefficient is utilized to calculate initial compression displacement by substituting in Eq. (3.14). However, in simulation, instead of approximation, direct use of mesh stiffness as presented in 3.19 is applied to ensure simulation result accuracy. For further simplification, it is assumed that pinion-pinion mesh stiffness can be derived by multiplying the mesh stiffness of the rack-pinion by α as follows:

$$k_{12}(t) = k_{13}(t) = \alpha k_{24}(t) = \alpha k_{34}(t) = k_{\mathrm{m}}(b_0 + \sum_{i=1}^{i=2} b_i \cos \omega t) \tag{3.15}$$

where $\alpha = 0.76$ and $k_m = 523000\, N/mm$, $b_0 = 0.9494$, $b_1 = 0.08264$, $b_2 = -0.03548$ are determined with the curve fitting method using the MATLAB curve fitting toolbox.

3.7.4.2 **Transmission Error**

The numerical method is applied to solve the matrix form of the equation of motion (3.6). For simulation purpose, it is assumed that all pinions are identical. The parameters employed in the simulation are presented in Table 3.2 for pinions and rack. The Rung-Kutta method, one of the most important iterative solvers of ordinary differential equations (ODE), was employed in MATLAB through the ode45 command. The time increment selected was 0.0001 seconds (the increment is selected upon rotational speed and number of gear teeth, 1000(RPM)/60=16.6 revolutions per second, every rotation takes 0.06 seconds, 0.06/24(teeth) = 0.0025, that should be divided to 15 degrees, 0.0025/15=0.000166 seconds) while the applied step torque was 24N.m and the rack was assumed to be free of external force. The rotational speed was 1000 rpm.

An initial compression displacement of 5 μm due to preload was assumed and the damping constant, c, was 1000 N.s/m. Table 3.2 presents a summary of the simulation parameter values. Figure 3.21 illustrates the time response and FFT of transmission error (x_{12} , x_{13} , x_{24} , x_{34}) and total transmission error computed using Eq. (3.7).The results comprise transient and steady portions. The steady part of the results is periodic and emerged from the periodic variation of mesh stiffness; no separation occurred during simulation.

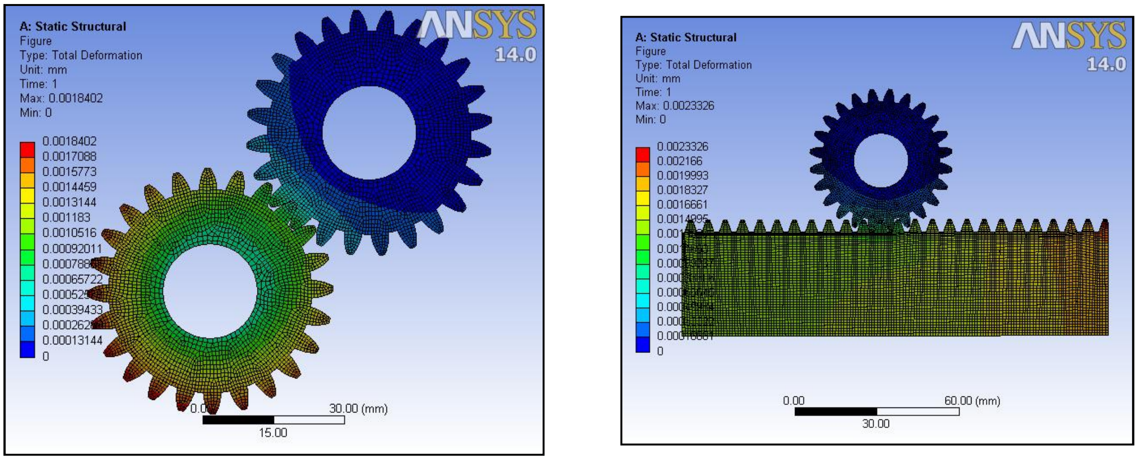

(a) Two Gears

(b) Rack and Pinion

Figure 3.19: Finite Element Modeling and Analysis of (a) Pinion-Pinion and(b) Rack-Pinion for Computing Mesh Stiffness with(534672 of nodes and 488620 of elements)

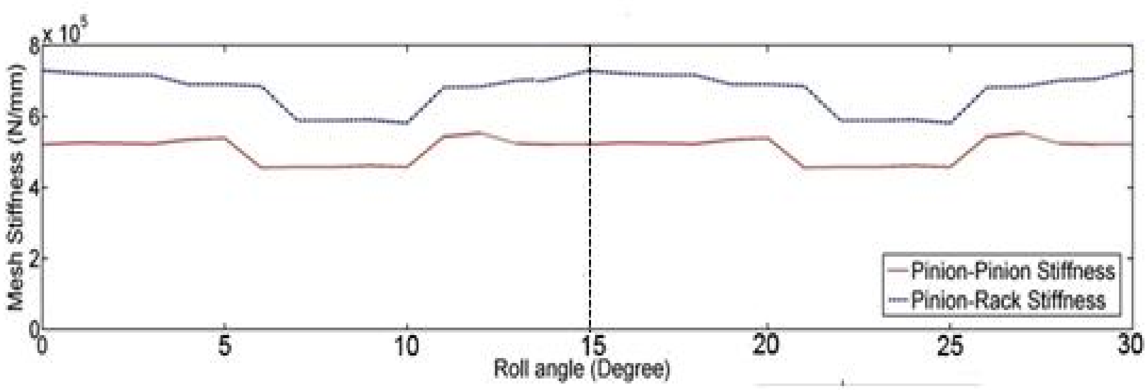

Figure 3.20: Mesh Stiffness of Pinion-Pinion and Rack-Pinion Variation Relative to Roll Angle

According to the results presented in Figure 3.22 the minimum value of relative transmission error belongs to $x_{12}(t)$ with around 1.018µm.Therefore, in order to maintain an anti-backlash system, at least 1.018 μm initial compression displacement needs to be applied.

Table 3.2: Parameters used in simulation

Parameter	Value	Parameter	Value
Applied torque, T(N/m)	24	α	0.76
Applied force on rack, F(N)	0	$k_m\,(N/mm)$	523000
Rotational speed of pinions, n (rpm)	1000	b_0	0.9494
Initial compression displacement between mated pinions, $\delta_1\,(\mu m)$	5	b_1	0.08264
Damping coefficient, $c_1 = c_2\,(N.s/m)$	1000	b_2	-0.03548

According to Eq. (3.14), the approximated amount of compression displacement is 1.15 μm and if the modification of mesh stiffness were not applied, the minimum compression displacement value would be 0.95 μm, which is less.

Thus, the method suggested in this work to evaluate the approximate required initial compression displacement is effective and simple and does not need lengthy and tedious simulation.

In order to investigate the alternation of transmission error under tooth separation, the initial compression displacement was reduced to 0.9 μm to activate the nonlinearity in the equation of motion associated with tooth separation. Figure 3.22 shows the transmission error associated with initial compression displacement of 5 μm and 0.9 μm, respectively. This figure indicates that the absolute value of transmission error increases as the initial compression crosses the limit.

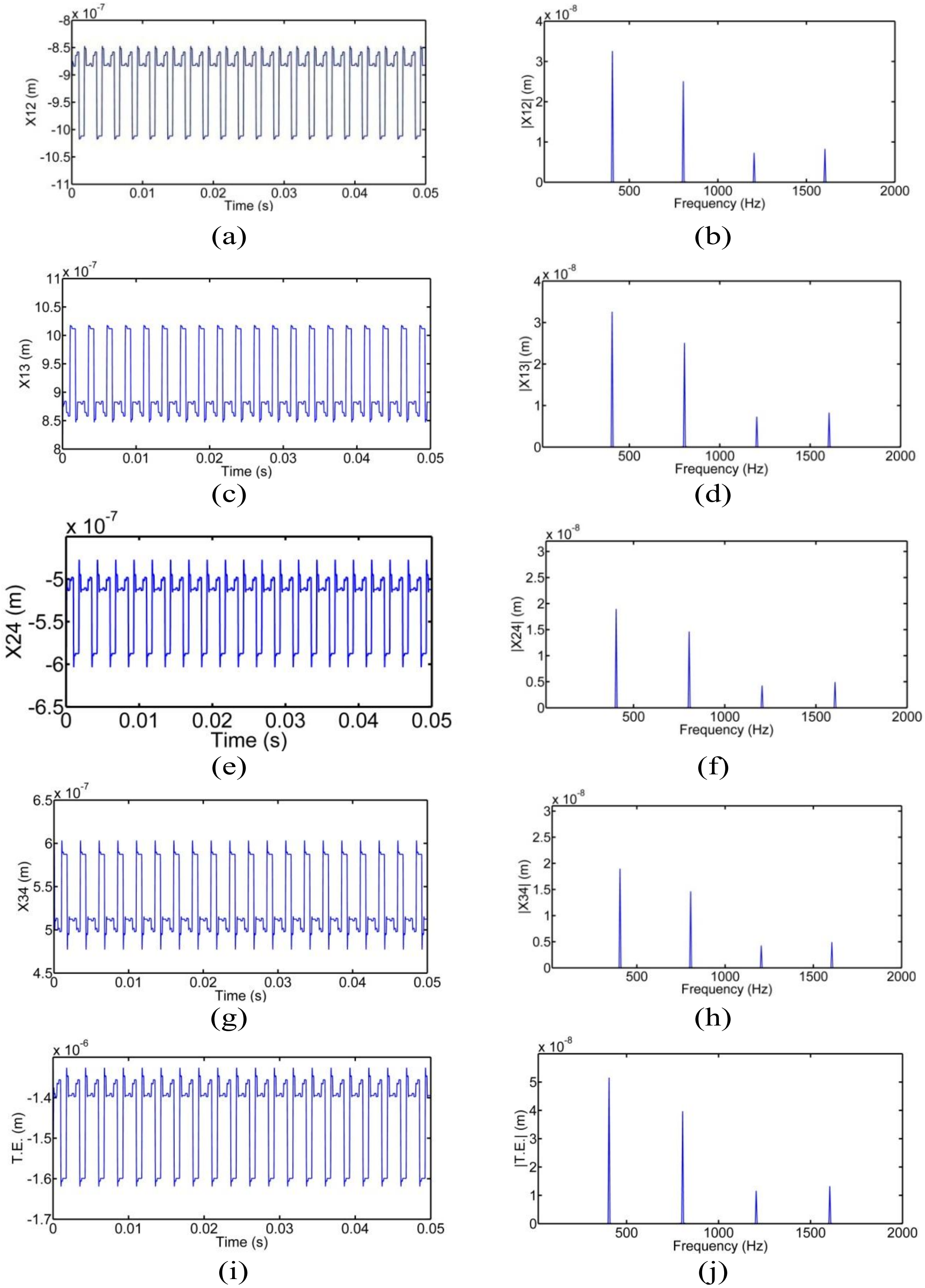

Figure 3.21: Time Response and FFT of Transmission Errors:

(a,b) $x_{12}(t)$, (c,d) $x_{13}(t)$, (e,f) $x_{24}(t)$, (g,h) $x_{34}(t)$ and (i,j) T.E.

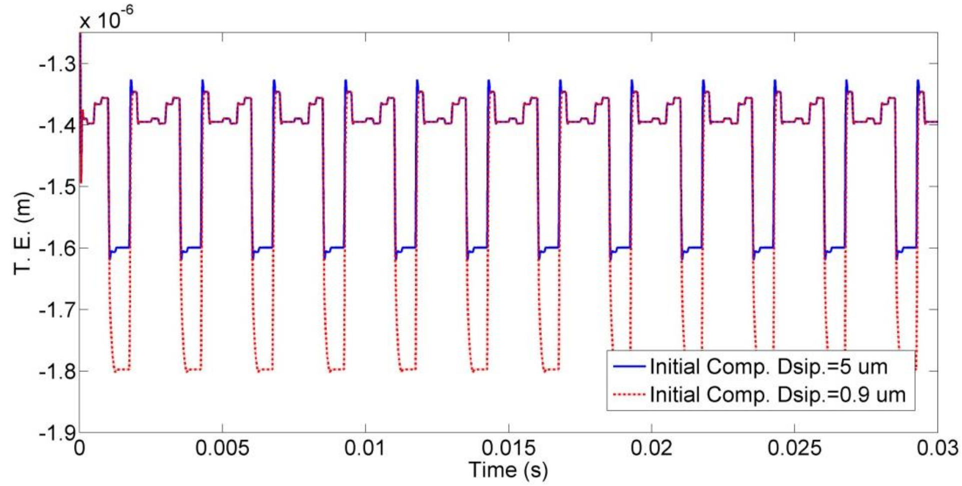

Figure 3.22: Transimision Error Under the Linear ($\delta_1 = 5\,\mu m$) and Nonlinear Region ($\delta_1 = 0.9\,\mu m$)

Since the preload and initial compression displacement are in direct relation, then, by increasing the preload the absolute value of transmission error will be reduced in the nonlinear region.

3.8 Conclusion

In this chapter, the conceptual design of a new CNC gantry machine with (LL) LLRR kinematic configuration and its advantages was presented. According to the design of this new type of gantry machine, the new feed drive motion (double motion mechanism) was designed. In response to the problem with the rack and pinion used in the double motion mechanism for removing backlash, a new concept of a double motion mechanism with an anti-backlash device with a combination of three gears and one rack was introduced. The advantages of the new double motion mechanism were explained. A nonlinear dynamic analysis of the new anti-backlash system was presented to gain insight into the system's dynamic behavior. The validity of the concept of eliminating backlash was examined with Motion Analysis of Solidworks CAD software. The mesh stiffness of mated gears and rack-pinion was evaluated with the finite element method and a motion equation was solved.

Assuming that the gear and rack teeth are rigid and static transmission error is negligible, the total transmission error of the new mechanism is zero, which is one of the more significant features of this system. The minimum amount of preload at which the system remains anti-backlash during operation was estimated. This depends on applied torque, external load on the rack and varied mesh stiffness behavior. Total system transmission error was obtained by solving the differential equation of motion using the Runge-Kutta method.

Finally, it is expected that the proposed mechanism will find numerous applications in industry, such as industrial robots and precision machine tools, due to its low transmission error and low preload.

Further development and investigations of the relative advantages of this new mechanism through experimentation could be a subject of future research. The structural design steps of the new type of CNC gantry machine are discussed in the next chapter

CHAPTER 4

4 STRUCTURAL DESIGN OF THE GANTRY MACHINE TOOL

4.1 Introduction

To design the new type of CNC gantry machine, designer expertise is required in the initial stage. The different designs for the new CNC gantry machine proposed are introduced in this section according to designer experience. Following the expert design step, the additional improvement process of the final design using FEM software will be discussed.

The first design introduced is based on a new system with a double motion mechanism. As discussed in Section 3.3, there are two types of double motion mechanism. The first type is designed based on a rack and pinion and the second type is based on a ball screw. In this chapter, the second type of double motion mechanism is introduced. In this system, the motions of the gantry and worktable are independent. Actually, in the new double motion feed drive system the worktable and gantry motions are dependent during machining but independent if workpiece set-up is required. Hence, the double motion mechanism based on the rack and pinion system cannot fit this motion requirement.

4.2 Double Motion Mechanism Based on a Ball Screw System

For the second type of double motion mechanism, the ball screw system is proposed. Hence, the gantry and worktable of the CNC machine can be moved separately by this system. The U-axis has been added to the machine and consequently, the gantry moves on the U-axis and the worktable moves on the X-axis. The gantry CNC machine controller must control both independently. In this stage, many industrial applications require flexible feed drive system such as worktable and gantry move simultaneously or individually. As a result, we decided to use double motion based on independent system. Hence the most important achievement is the combination of three types of CNC gantry machine into one machine with the double motion mechanism based on a ball screw system, as shown in Figure 4.1.

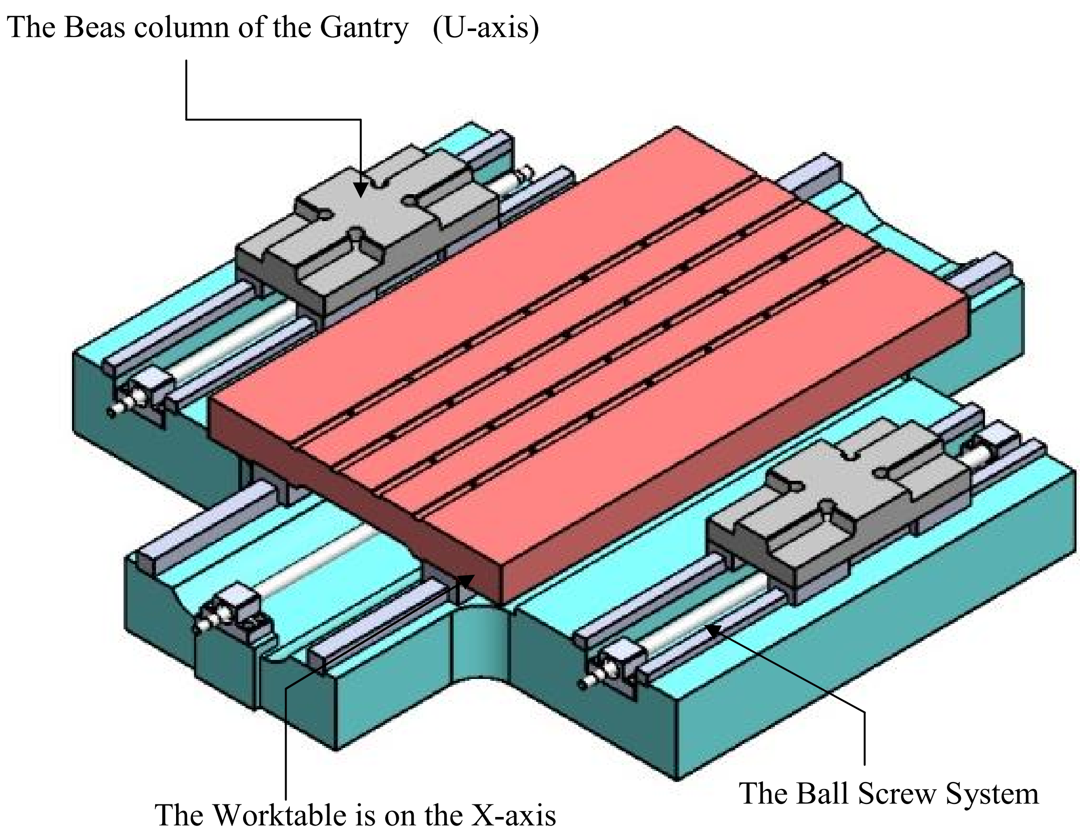

Figure 4.1: The combination of 3 types of CNC gantry machine with a double motion mechanism

The new CNC gantry machine can be used for three kinds of application. The "fixed gantry," "fixed worktable," and "moving gantry and worktable" together form the combination of three types of CNC gantry machine. These three application types are provided by the new double motion system based on a ball screw. Therefore, the total longitudinal motion of the machine has been converted to the X- and U-axes. The double motion mechanism based on a ball screw system has two characteristics:

1. The motion of the gantry is independent of the worktable and vice versa. With this advantage, the machine can employ three types of CNC gantry together (fixed gantry, fixed worktable and double motion system). It is suitable for academic use by different researchers in machining processes using three types of CNC gantry machine.

2. The gantry and worktable can be controlled by two axes (X & U) separately. The CNC gantry machine's kinematic configuration is LLLLRR (four separate linear motions and two rotational motions relative to a standard CY spindle), meaning that the CNC gantry machine needs to have a six-axis CNC controller.

4.3 Gradual Design of a Gantry Machine Tool Using the Ball Screw System

In this section, the gradual gantry design including the design of the structure, axis parts, gantry, crossbeam, feed drive motion and other parts, is investigated. The final design has been chosen for the following process that is utilized to further improve the design using well-known scientific methods.

Regarding the design of a CNC machine gantry, two initial, different design methods for a gantry are introduced. One is the crane design method, which is normally used for designing cranes (discussed in chapter 2). The second is the common gantry design method, using normal and slant crossbeams. The gantry crane, columns and crossbeam, main structure, double motion mechanism, Y- and Z- axes parts and the gantry crane type designed are shown in Figure 4.2.

The common gantry design has two types, normal and slant crossbeams. The slant crossbeam is shown in Figure 4.3.

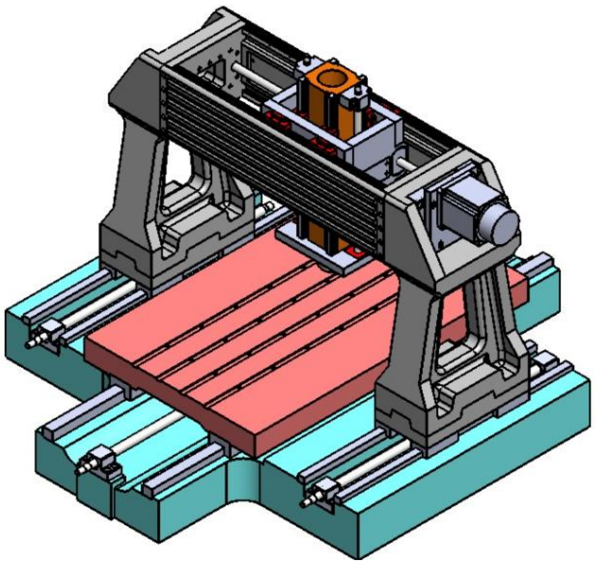

Crane type gantry

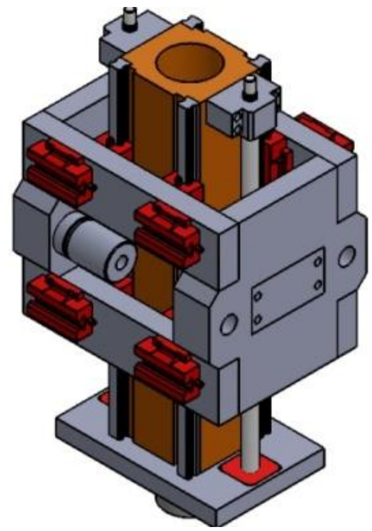

Y- & Z-axes parts

Figure 4.2: Crane Type Gantry Design

The manufacturing process of a slant crossbeam is difficult. In addition, some parts of the Y- and Z-axis components, such as the Y-axis motion system, must be located inside the crossbeam; this usually creates some problems for gantry machine assembly. However, the slant crossbeam has some advantages, such as suitable gantry center of gravity location. In addition, the cutting force in the machining process can be distributed to vertical and horizontal forces on the crossbeam -- a condition that is suitable for linear guides that must be installed on the crossbeam.

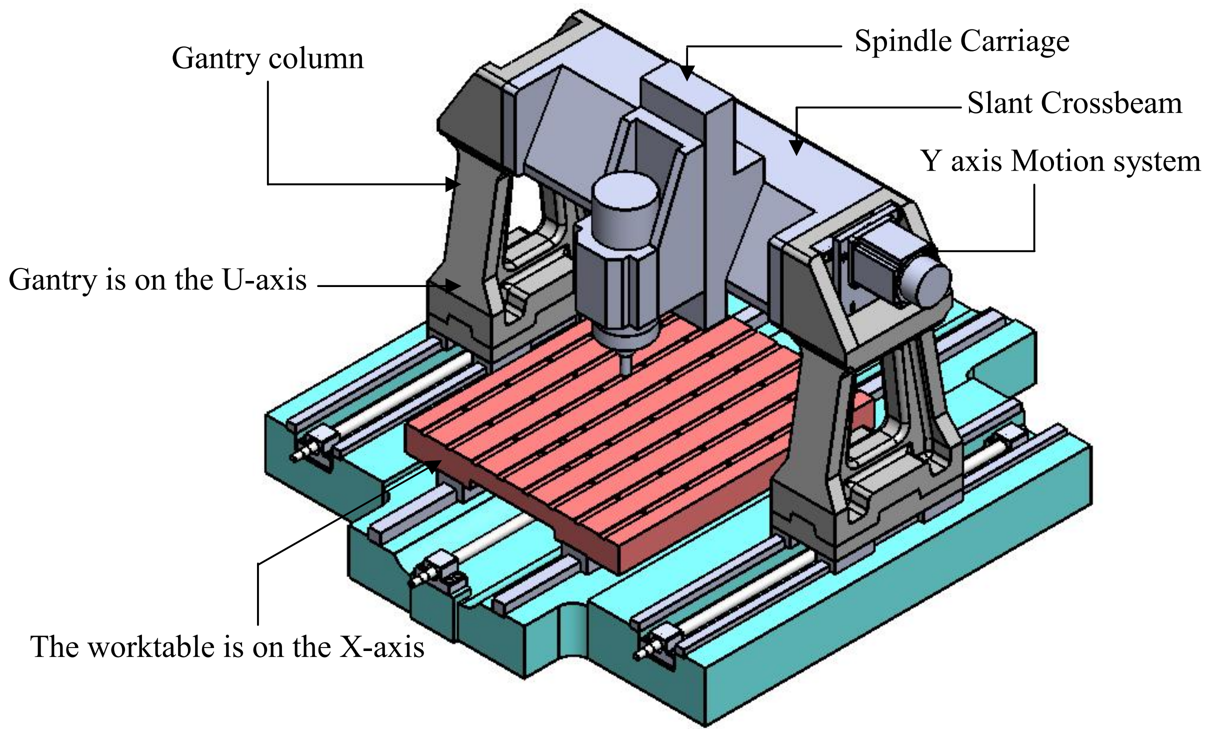

Figure 4.3: Gantry with a Slant Crossbeam

Actually, it is easy to manufacture the normal crossbeam with this method, but the gantry's center of gravity must be improved by applying design modifications. This method is a common, standard approach, which is why it was chosen to design the new CNC gantry. Based on this discussion, the normal crossbeam is used in the design of the new CNC gantry machine. The gantry with a normal crossbeam is shown in Figure.4.4

The normal crossbeam has a key disadvantage as discussed previously. The centers of gravity of the spindle carriage and holder are far from the gantry's center of gravity. This will cause a problem for linear motion guides installed under the gantry columns that will probably get damaged during operation because of the cutting forces produced by the cutting tools.

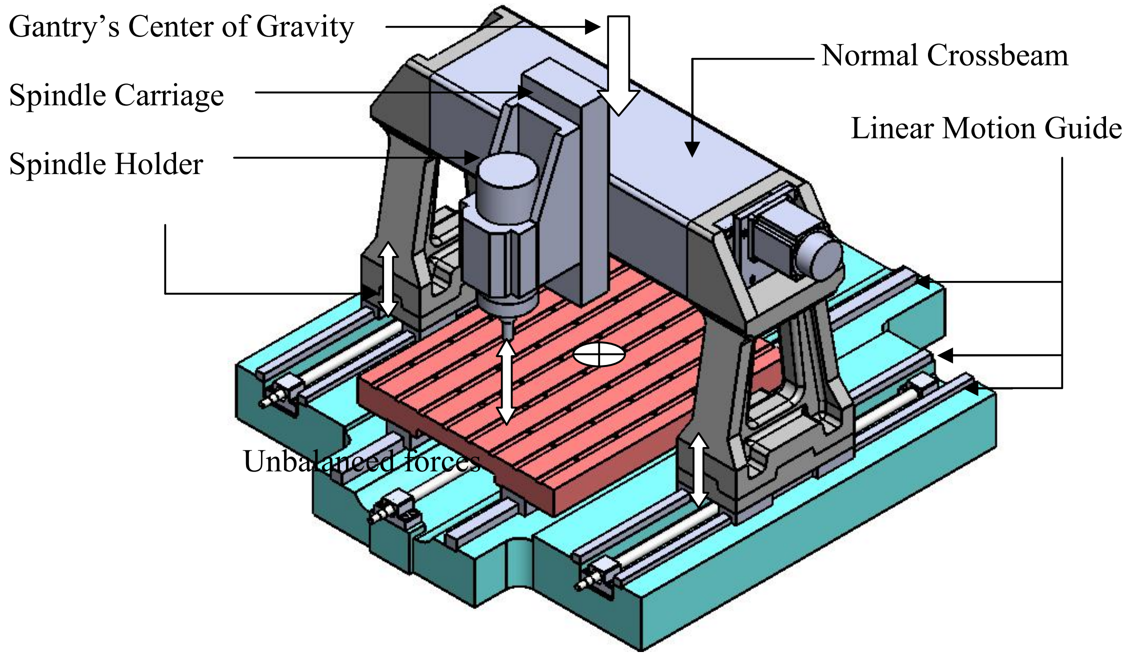

Figure 4.4: Gantry with a Normal Crossbeam

In order to solve this problem, the spindle carriage and holder's centers of gravity must be shifted to the gantry's center of gantry; hence, the shape of the gantry columns must be designed for this purpose. To control the unbalanced forces, the centers of gravity of all gantry parts (including the gantry, spindle carriage and spindle holder) must be close to the gantry's center of gravity.

4.3.1 **First Proposed Gantry Machine Design**

In the first design based on experience, the different column shapes are proposed and the gantry crossbeam is designed as well. This is the first major design as previously discussed, to improve the gantry's center of gantry as well as the gantry design method (Figure 4.5).

This design did not significantly improve the gantry's center of gravity, meaning that it did not solve the major problem yet. Clearly, the crossbeam has been designed as a rectangular shape and the Y-axis ball screw and its servomotor are located on the crossbeam. The

Y-axis part comprises the body and standard components such as spindle carriage linear blocks and spindle holder with two main components, the body and holder. The spindle holder's linear guide is installed onto the spindle carriage and the spindle holder servomotor is installed on top of the spindle carriage body. The initial design of the new CNC gantry machine is shown in Figure 4.5. In the first design, three servomotors support the X- and U-axes' (worktable and gantry) feed drive motions. They connect to the ball screws using flexible couplings.

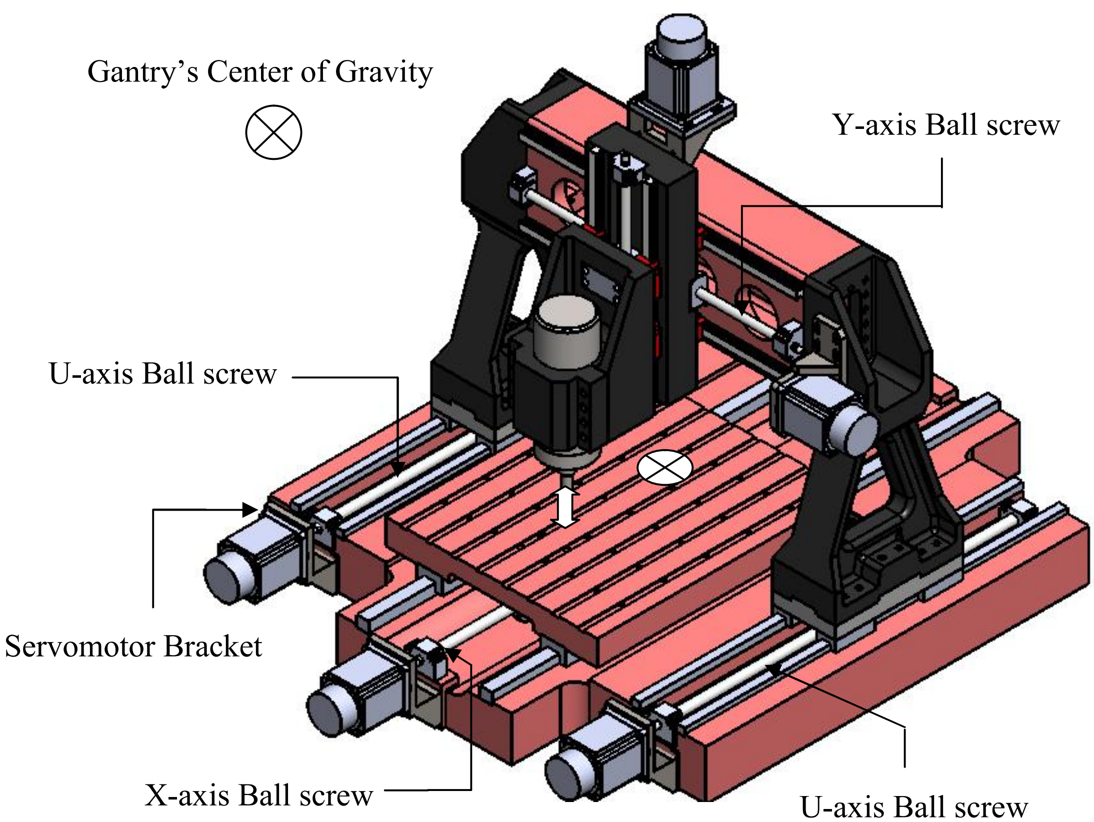

Figure 4.5: The First Gantry Machine Design Proposed

Although the feed drive motions of the gantry and worktable parts are supported by this system, two other feed drive motions (Y- and Z-axes) are supported by a belt in this design. Usually, for better performance the servomotor must support the ball screw directly via flexible coupling. The servomotors' brackets of X- and U-axes were designed and installed onto the structure. The gantry's center of gravity was still not acceptable and had to be improved in the next design. Additional changes to the column shape should perhaps improve the design for enhanced performance. The spindle carriage and spindle holder are shown in Figure 4.6, with standard components such as linear guides and ball screw selected and added to the design. The Y- and Z-axis parts of the CNC gantry machine are clearly visible.

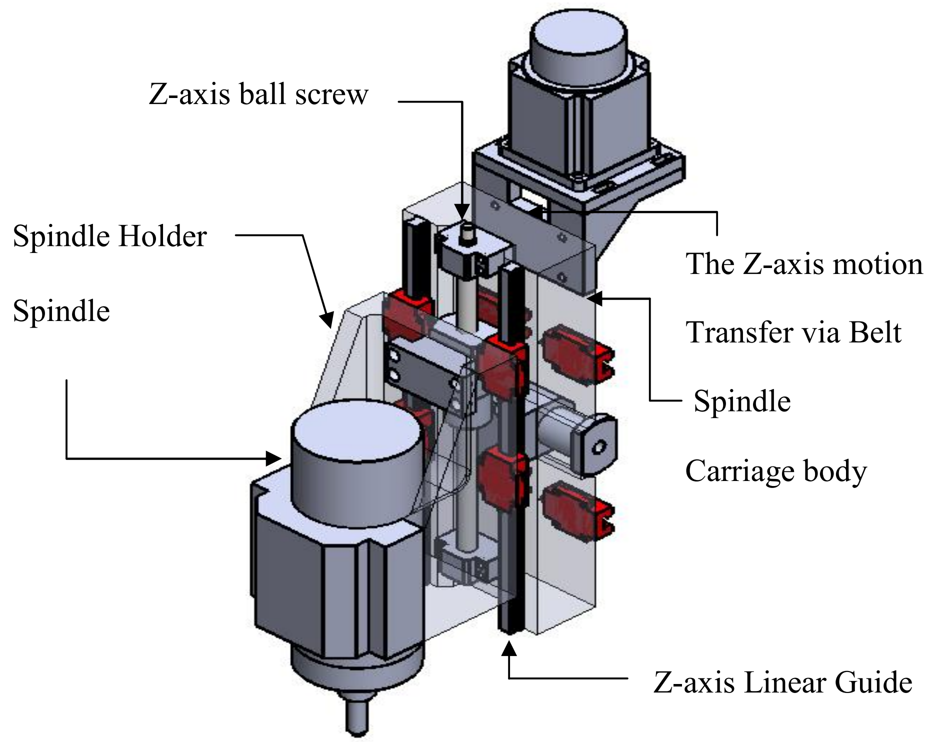

Figure 4.6: The Y- and Z-axis parts

4.3.2 **Second Proposed Gantry Machine Design**

In this CNC gantry machine design, two important changes are applied.

1. To improve the gantry's center of gravity, the shape of the columns has been changed (Figure 4.7). Changing the columns' shape improved the position of the gantry's center of gravity, whereby the center of gravity has shifted to the center of the gantry.

2. As discussed in section 4.2, to incorporate three types of CNC gantry machine in one machine, the gantry must be able to move nearly the entire structure length. Hence, the machine structure has been modified for this purpose. The overall dimensions of the CNC gantry machine and machining space have been finalized in this design.

Figure 4.7 shows the second design of the new CNC gantry machine.

4.3.3 **Third Proposed Gantry Machine Design**

In the third design, more modifications have been done to improve the gantry's center of gravity location. Most changes were done to the machine gantry. This design is the final modification of the CNC gantry machine using designer experience and is shown in Figure 4.8.

In this design, additional changes have been applied to the gantry components, such as columns and crossbeam, for easy manufacturing and assembly. For example, the Y-axis servomotor was placed inside the gantry for easy assembly; with this modification, the Y-axis servomotor can be installed to the ball screw directly using flexible coupling. The Z-axis servomotor bracket was designed, which can also be installed to the ball screw directly by flexible coupling. In this design the gantry's center of gravity has nearly shifted to the center of the gantry. It can be seen in Figure 4.9 that the first and final designs are comparable. The next steps in the design process entail modifications based on the dynamic and static design requirements using finite element analysis.

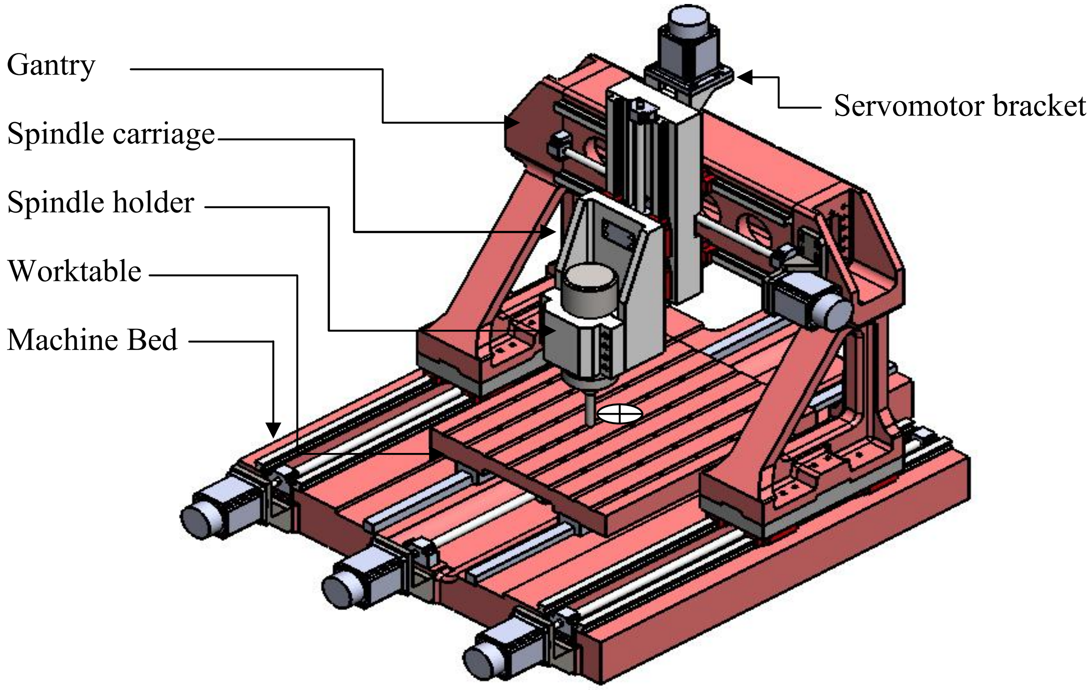

Figure 4.7: The Second Proposed Gantry Machine Design

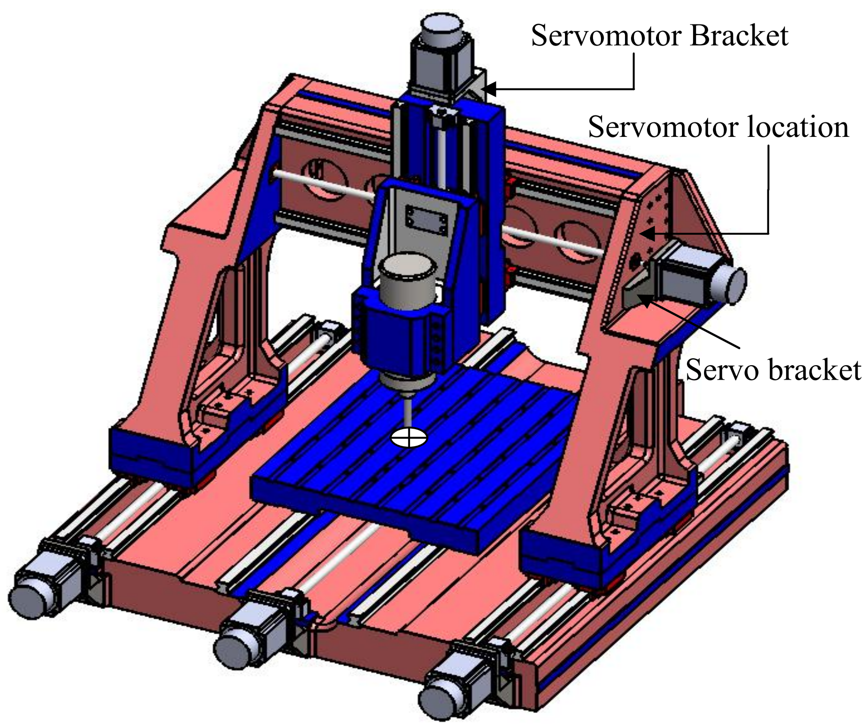

Figure 4.8: The Third Gantry Machine Design

4.4 Further Design Modifications Based on Dynamic and Static Analysis

A machine tool must be statically and dynamically rigid simultaneously to attain a satisfactory machining process. In fact, the dimensional accuracy of components is related to static stiffness; surface quality and maximum metal removal rate (MRR) are related to dynamic stiffness (Myers, 2005); and cutting process stability is related to the dynamic performance of the machine's gantry (K Fansen, 1999). The unstable phenomena of the cutting process, e.g. chatter, are often the result of a mutual effect of the dynamic behavior between the CNC machine's gantry and cutting process (Baradie, 1991; EI Baradie, et al., 1976; M. A. EI Baradie, 1993). The Chatter Theory was developed more than a hundred years ago (Tobias, 1965). In order to evaluate the machine tool's resistance to chatter and vibration, it is necessary to analyze the dynamic behavior of the machine's gantry design.

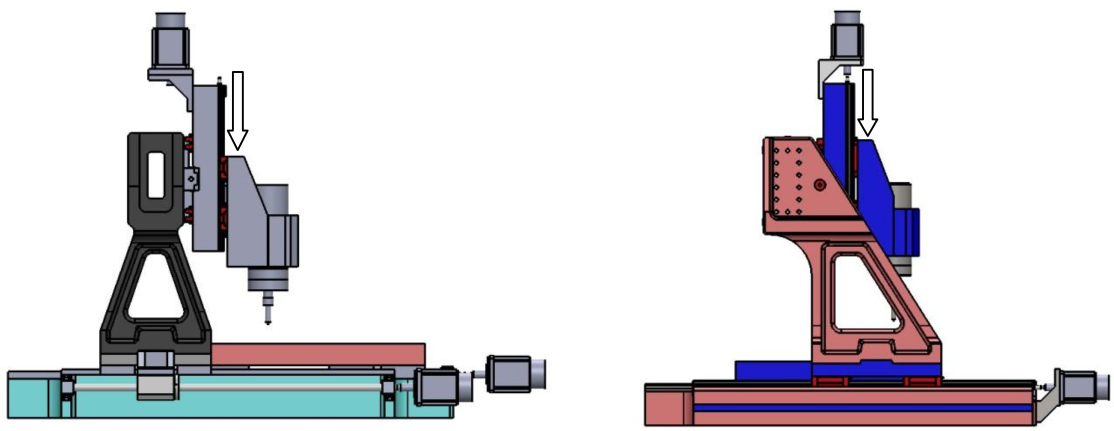

(a) First proposed design (b) Final proposed design

Figure 4.9: Improved Gantry Center of Gravity in the Design Process

In this chapter, an evaluation of the gantry design is first presented in section 4.3.3 and was performed using an analysis process. The evaluation continues with gantry "modification" followed by a "selection" process of the best gantry design. The analysis process is presented as follows:

A) Modal analysis of the gantry is carried out in order to extract the natural frequencies and mode shapes.

B) Harmonic analysis of the gantry is done according to the cutting process performance, which is defined for the machine design (L.N, 2009).

C) The gantry is statically analyzed to extract the maximum deformation under the weight and cutting force.

4.4.1 **Dynamic Analysis of the Gantry**

Sufficient gantry stiffness and damping lead to a stable cutting process and the performance is achievable by dynamically modifying the machine tool (Zhang, 1996).

In the modification process using modal analysis, the following procedure was done sequentially.

- The gantry's 3D design was converted into simulation software format
- The dynamic behavior of the gantry was evaluated by modal analysis; the first natural frequency of the gantry was extracted in this step.
- The results were compared with the initial requirement of 200 Hz natural frequency.
- The modification process for the gantry was performed based on the modal analysis results.
- The gantry was statically analyzed.

In the modification process, around 12,000 rpm (200 Hz natural frequency) for the machine spindle and 10-micron spindle tip accuracy are requirements that must be achieved in the dynamic analysis step. Other machine requirements, such as what kind of materials can be machined or the machine's material removal rate (MRR) value are discussed in the static analysis step**.** The design modification process flow chart is shown in Figure 4.10

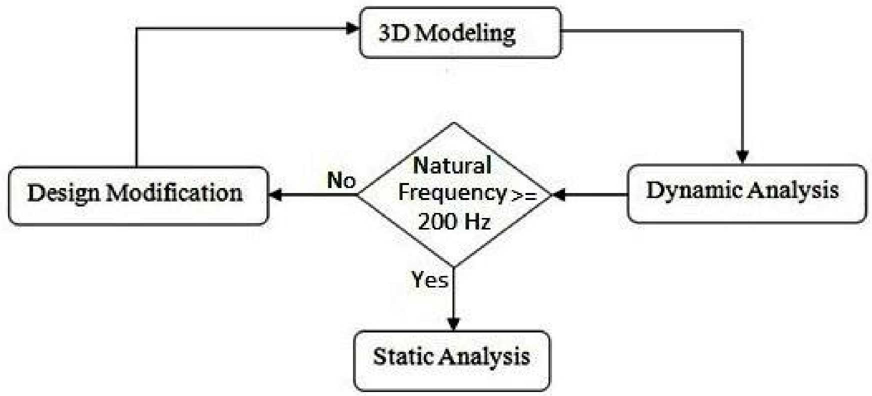

Figure 4.10: Design Modification Process Flow Chart

The entire analysis process was done in ANSYS (engineering simulation software) by finite element method. In order to make a finite element model, a three dimensional model of machine's gantry with ANSYS Workbench has been under consideration. The three dimensional model with SolidWorks software is executed. The model is exported to ANSYS Workbench and the necessary input data as material properties like modulus of elasticity, Poison ratio and density is applied. Then, elements of the model are made under Solid element. This model has 85985 elements and 154081 nodes. Relevant boundary conditions are applied on the earth connection of the gantry. Finally, modal analysis is performed to obtain natural frequencies of the gantry. During analysis, the total weight of the gantry was 417 kg; each column was 93.55 kg, the crossbeam was 118 kg and the spindle carriage and holder were 118 kg. The third gantry design is shown in Figure 4.11.

Modal analysis is mainly a technique used to obtain the vibration characteristics of a structure. Therefore, in observing the dynamic behavior of the designed gantry, its first natural frequency and modes were extracted by modal analysis. The natural frequency differs with varying gantry materials.

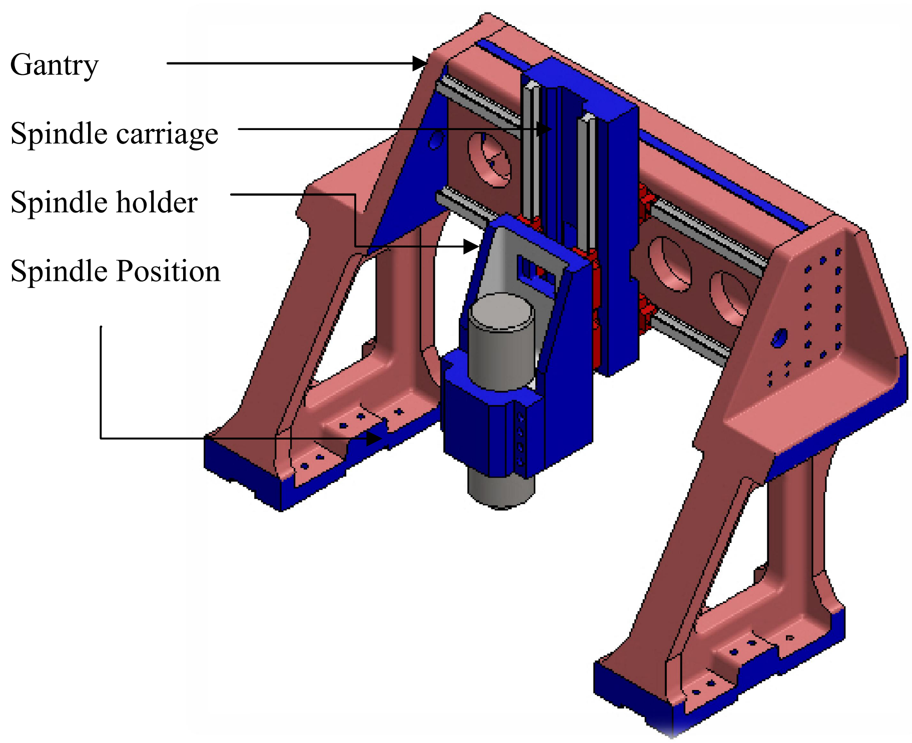

Figure 4.11: The Third Proposed Gantry Design

Hence, the dynamic behavior of a gantry with different materials (gray cast Iron with 120 GPa modulus, 7850 kg/m^3 density and 0/05 shrinkage (T. Murakami, 2006) and Steel “ASTM-A36”) was analyzed to identify the minimum frequencies. For evaluating the critical position of the moving parts, the position of the spindle carriage and holder was adjusted to the lowest location at the middle of the gantry crossbeam. The modal analysis results of the third design show that its rigidity is insufficient and the gantry vibrates at a natural frequency of around 100 Hz in the X-axis direction in the first mode. An example of this modal analysis evaluation is shown in Figure 4.12 and the modal analysis results for two different gantry materials (gray cast Iron and Steel) are shown in Figure 4.13 (a, b). The results indicate that the minimum natural frequency of a gantry with steel is better than cast iron, but still, neither meets the initial design target of 200 Hz.

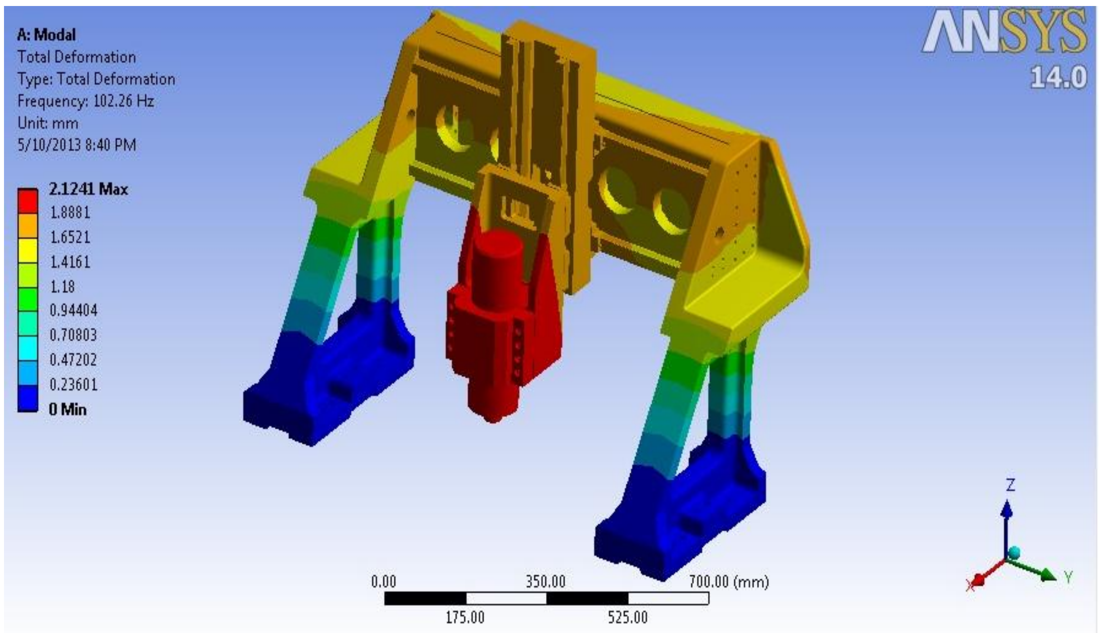

Figure 4.12: Modal Analysis Results for the Third Design

The dynamic analysis process must be resumed because the result is not acceptable. For this reason, more design modifications are required to meet the design requirements.

Various column and crossbeam shapes have been proposed to improve the gantry's natural frequency. Many changes have also been made to the columns and crossbeam in the modification process to enhance the natural frequency (Figure 4.14). In order to increase the natural frequency it is necessary to enhance the stiffness of the structure. Increasing the stiffness requires enlarging the cross selection area. In contrast, increasing the area leads to greater structure mass, which consequently decreases the structure's natural frequency. Therefore, increasing the stiffness shall be conducted bearing in mind the dynamic structure and its mode shape. The most significant parts of the structure that have the highest impact on natural frequency should be identified prior to applying changes.

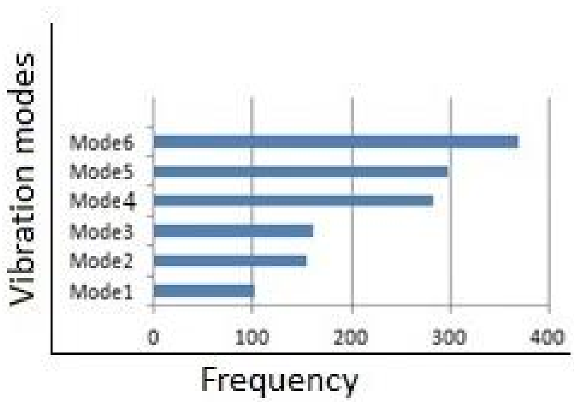

Mode	Frequency [Hz]
1.	102.26
2.	154.92
3.	158.31
4.	282.95
5.	297.71
6.	364.21

Frequency Modes

(a) Using Cast Iron

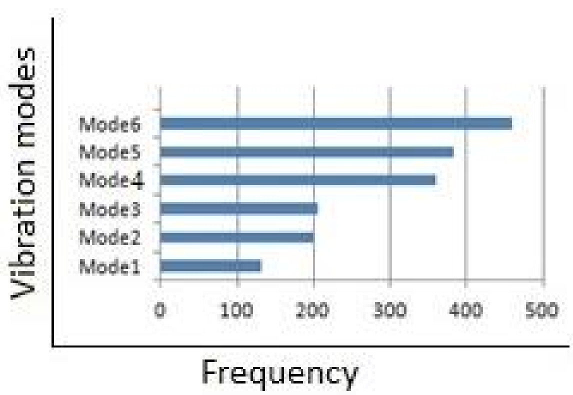

Mode	Frequency [Hz]
1.	131.95
2.	198.54
3.	205.76
4.	360.85
5.	383.38
6.	458.53

Frequency Modes

(b) Using Steel

Figure 4.13: Modal Analysis Results for the Third Design

With respect to the first shape mode of the structure, the most effective part for enhancing the stiffness and natural frequency is the column's cross section. As seen in ure 4.14, the cross section of the columns increased -- something that caused an increase in the natural frequency. The FEM results also validate the concept and support the changes.

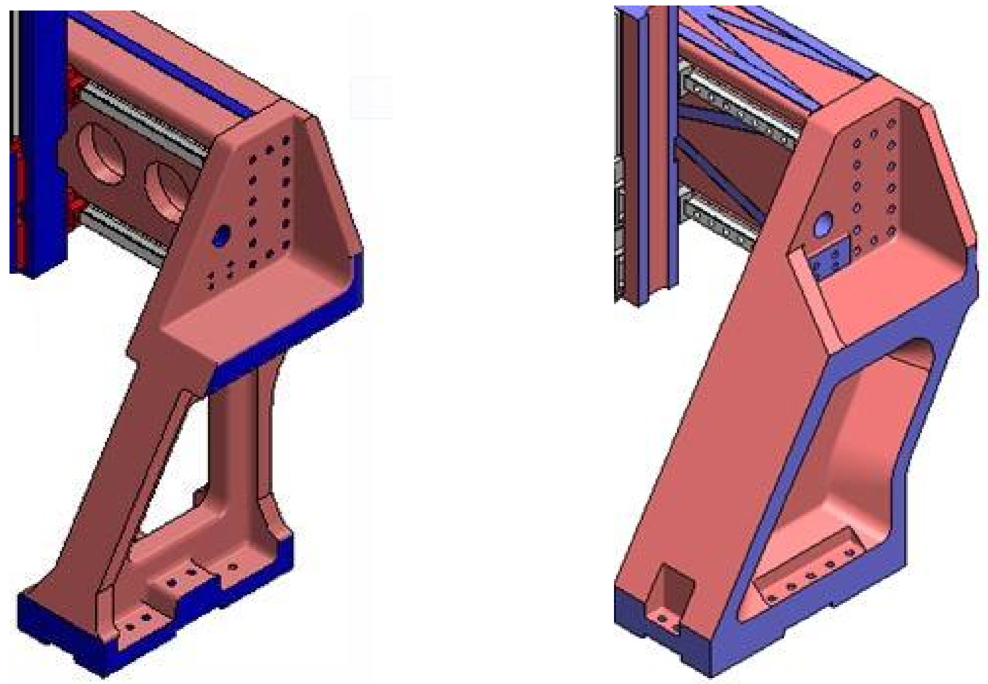

(a) The Previous Gantry Design

(b) The Proposed Gantry Modification

Figure 4.14: Modification of the gantry's columns and crossbeam

The modified gantries with cast Iron and Steel (Figure 4.15) are analyzed and the analysis results are shown in Figure 4.16. The modified design seemed to be close to the design target, as Figure 4.16 (a) shows the minimum natural frequency of the gantry obtained was less than 200 Hz, but (b) shows it was more than 200 Hz. Although the results for Steel demonstrate high frequency performance and the design requirement (200 Hz natural frequency) is met, the steel structure has some problems, such as high processing and machining cost and low damping. Hence, the combination of steel and cast iron (gray cast Iron with 120 GPa modulus and steel "ASTM-A36") was chosen as the best solution.

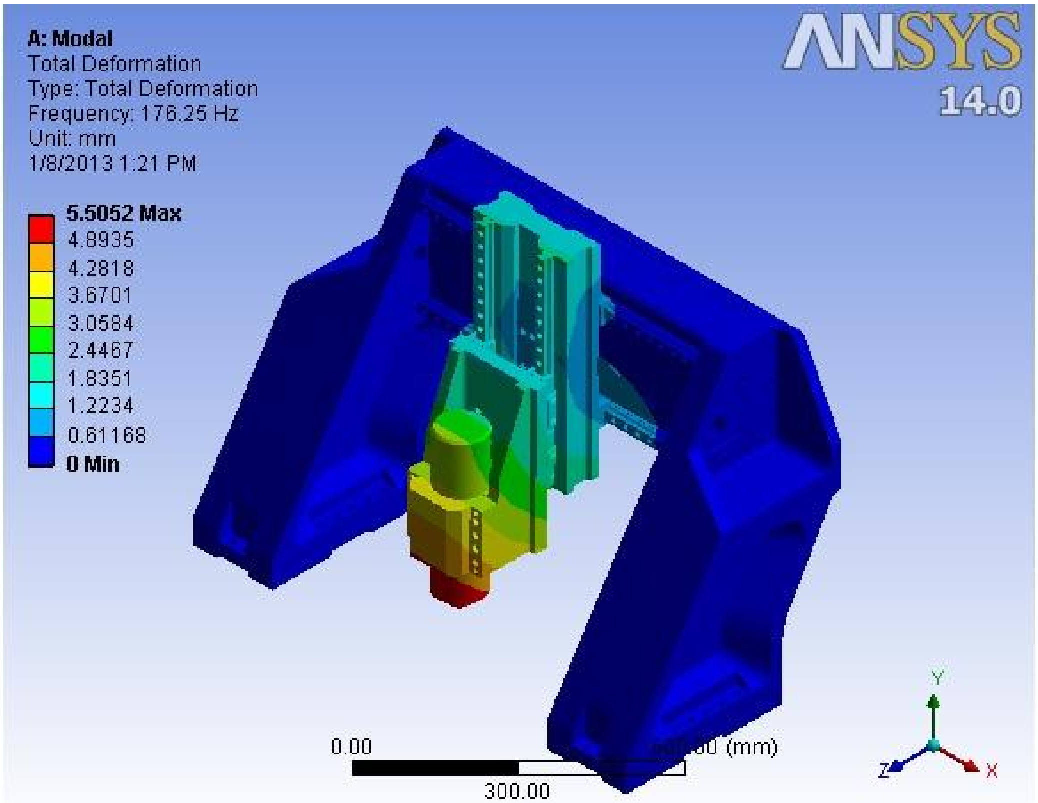

Figure 4.15: Final Analysis Results

Therefore, the crossbeam material was converted to steel for this purpose. The modal analysis of the new combination of gantry materials performed is shown in Figure 4.17.

The analysis results of the new combination of gantry materials are shown in Figure 4.18. The modal analysis results indicate that the design target (200 Hz) was achieved. However, the modification process caused an increase in the gantry's weight.

The reason steel was applied in the crossbeam is that steel weights less than cast Iron and therefore reduces the weight associated with the system and increases the natural frequency. On the other hand, decreasing the weight of the crossbeam rather than the columns has greater effect on increasing the natural frequency since in the first mode the crossbeam has more vibration than the columns.

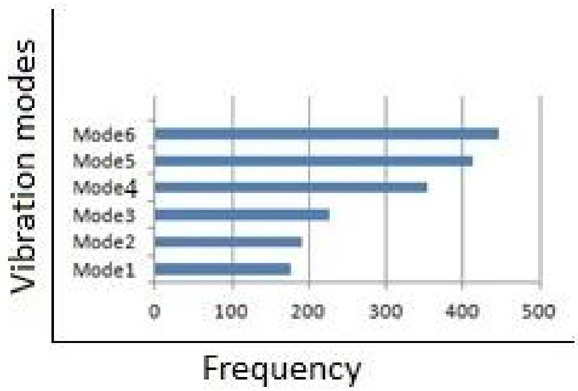

Mode	Frequency [Hz]
1.	176.25
2.	190.97
3.	227.46
4.	354.45
5.	412.98
6.	446.63

Frequency Modes

(a) Modal Analysis Results for the Modified Gantry using Cast Iron

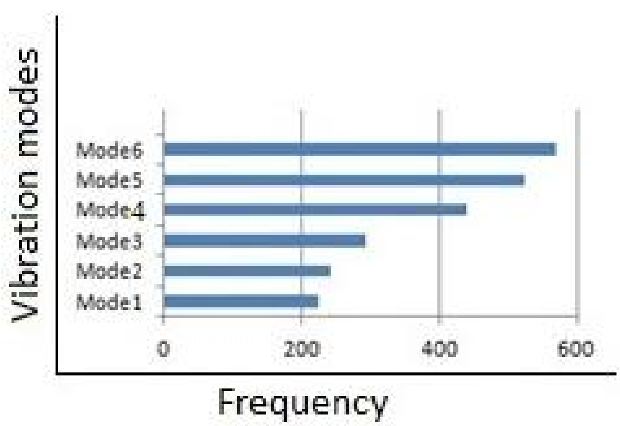

Mode	Frequency [Hz]
1.	223.55
2.	241.7
3.	291.57
4.	439.35
5.	523.03
6.	569.2

Frequency Modes

(b) Modal Analysis Results for the Modified Gantry using Steel

Figure 4.16: Modal Analysis Results for the Gantry Modification Process

(Cast Iron and Steel)

A major challenge in gantry design is the changing position of the moving elements, such as the spindle carriage and holder. The dynamic behavior of the gantry will be affected by the different positions, as the gantry's mass distribution and stiffness change.

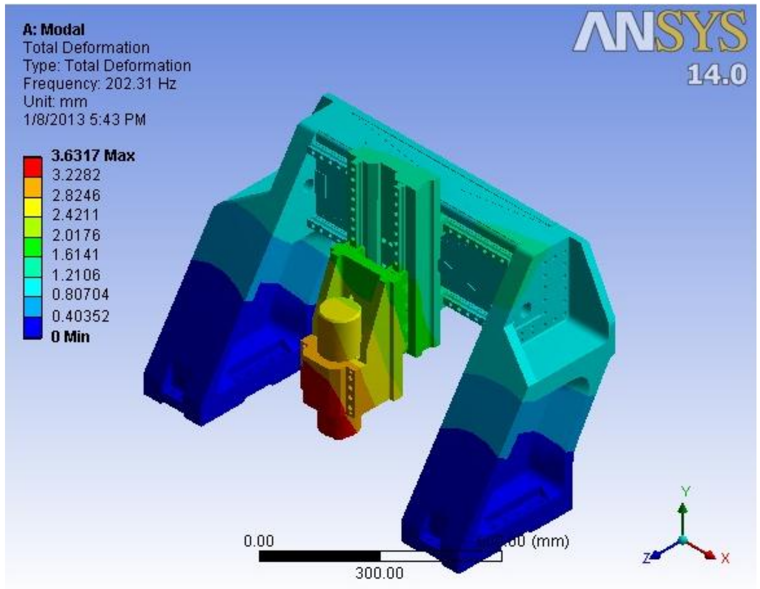

Figure 4.17: Modal Analysis Results of the Gantry using a Combination of Cast Iron and Steel

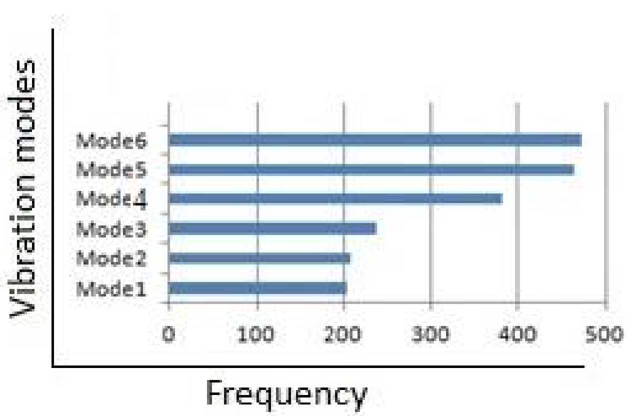

Mode	Frequency [Hz]
1.	202.31
2.	206.51
3.	237.08
4.	380.08
5.	462.61
6.	472.51

Frequency Modes

Figure 4.18: Modal Analysis Results of the Gantry using a Combination of Cast Iron and Steel

To investigate the dynamic behavior of the gantry relative to the different moving part positions, two new spindle carriage and holder positions were evaluated by modal analysis.

Two positions for the moving parts (spindle carriage and spindle holder) were selected to evaluate the dynamic behavior of the gantry in this case. The spindle carriage is extreme left side of middle of the gantry crossbeam when the spindle holder is at the end of the spindle carriage. The modal analysis of the gantry when the moving parts are on the extreme left side of the crossbeam is shown in Figure 4.19 and the modal analysis results for the extreme left side position of the moving parts are shown in Figure 4.20. The results show that the gantry's minimum natural frequency did not change significantly, but the minimum frequency occurred when the Y-axis was at the extreme left of the crossbeam. Although the first natural frequency almost did not change in this position, the other frequency modes increased significantly.

The modal analysis for the middle position of the gantry crossbeam when the spindle holder is at the middle of the spindle carriage is shown in Figure 4.21 and the analysis results are shown in Figure 4.22. According to the modal analysis results, the first natural frequency in the middle position increased significantly, meaning that the moving parts (spindle carriage and holder) could help increase the crossbeam stiffness in the middle position.

As seen in Figure 4.22, the gantry's natural frequencies in the middle gantry crossbeam position are higher in all frequency modes. Therefore, the natural frequencies of all positions, even the critical gantry position that was selected at the first, are higher than the design requirement of 200 Hz.

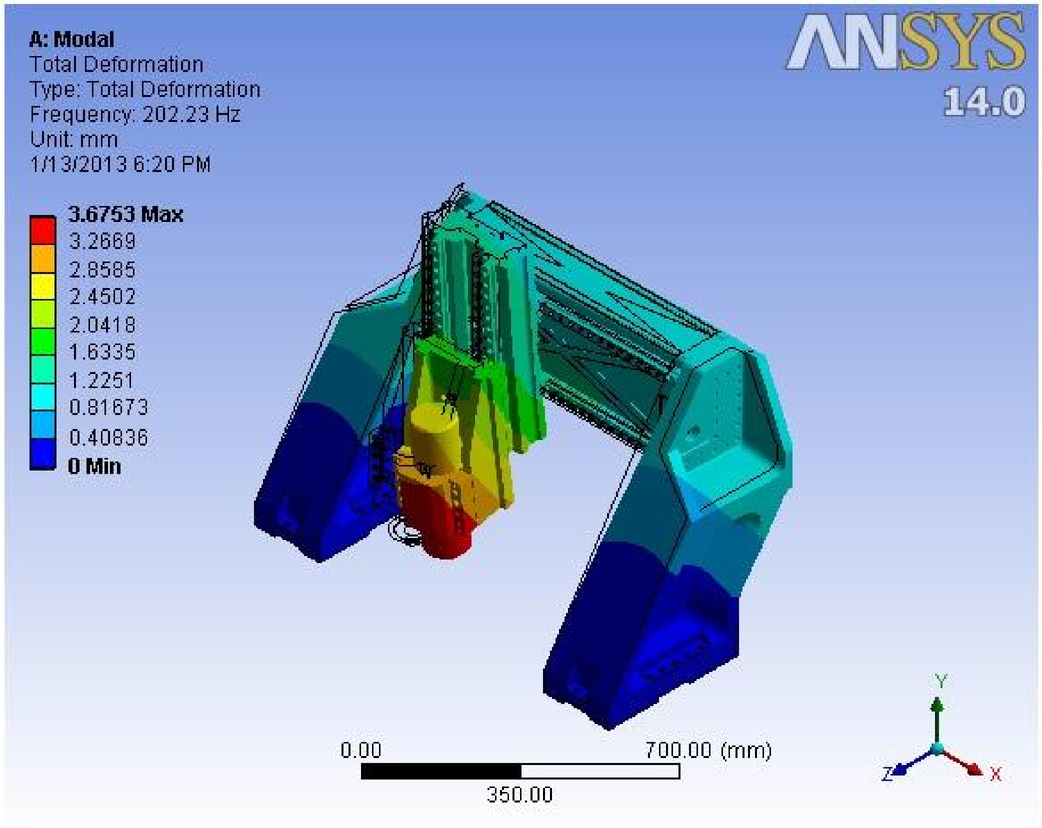

Figure 4.19: The Extreme Left Positions of the Spindle Carriage and Holder

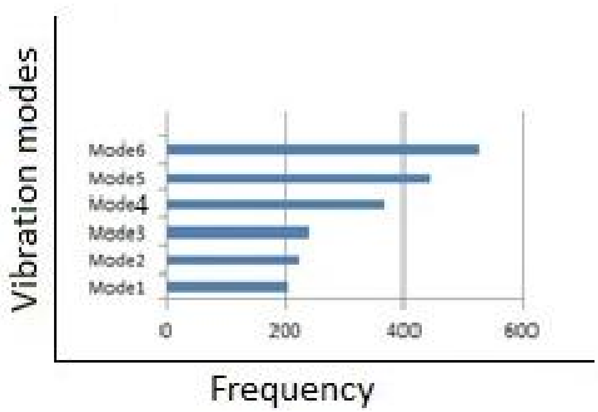

Mode	Frequency [Hz]
1.	202.23
2.	224.85
3.	241.55
4.	369.19
5.	442.65
6.	524.95

Frequency Modes

Figure 4.20: Modal Analysis Results for the Extreme Left Position of the Moving Parts

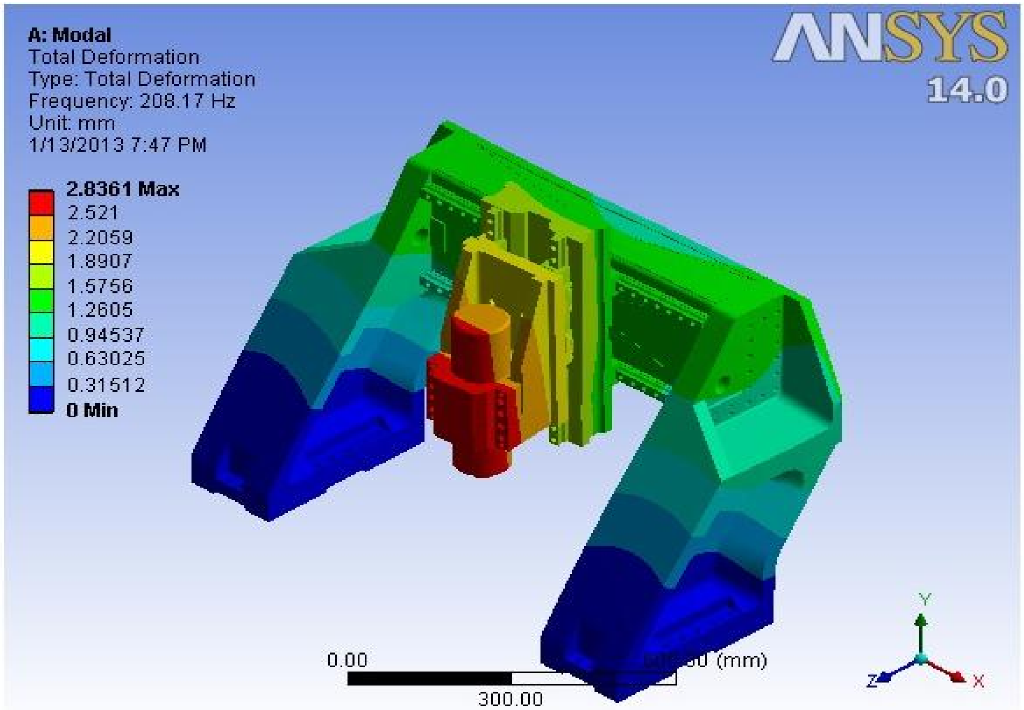

Figure 4.21: Modal Analysis of the Gantry when the Spindle Holder is in the Middle of the Spindle Carriage

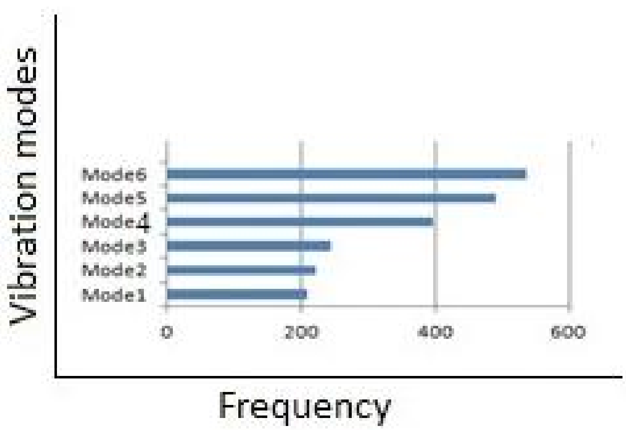

Mode	Frequency [Hz]
1.	208.17
2.	220.59
3.	245.19
4.	395.34
5.	490.79
6.	536.7

Frequency Modes

Figure 4.22: Modal Analysis Results for the Gantry with New Moving Part Positions

4.4.2 Static Analysis of the Modified Gantry

To identify the static behavior of the gantry, two evaluations were performed. The total deformation of the gantry under its total weight, which increased during modification, was extracted via static analysis. In this process, the total gantry weight was applied onto the middle of the gantry crossbeam. The total deformation under the weight is shown in Figure 4.23.

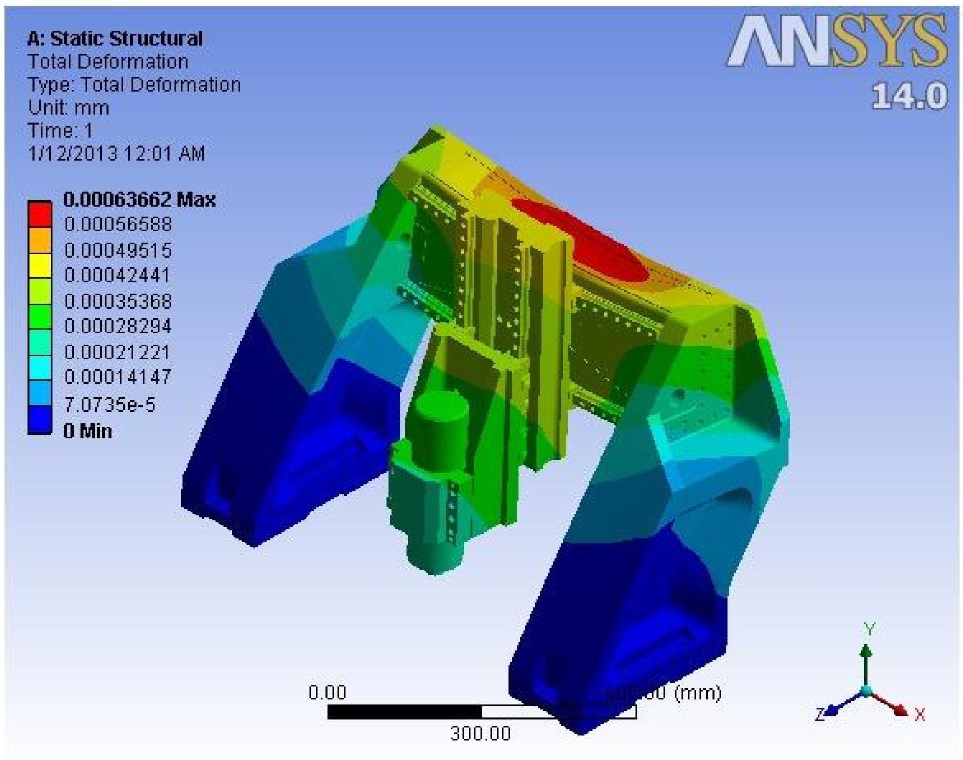

Figure 4.23: Total Deformation under the Weight

Figure 4.23 shows the total crossbeam deformation under the weight acquired in the red area, which is 6.3662e-4 mm -- less than the minimum required error of 10 µm.

The standard, high-speed CNC machine spindle was chosen. It has 3.3 N-m torque and more than 12,000 rpm. An end mill was used for cutting at high-speed machining to calculate cutting force. The cutting force generated by spindle torque can be calculated. An end mill with 8 mm diameter served as the cutting tool in this process. The amount of cutting force on the edge of the end mill based on the torque equation (M=F*r) was 825 N. The cutting pressure in a milling operation can be obtained from the (KS=F/A) equation and Figure 4.24. For calculating KS, the cross section of a milling chip was selected (1 mm depth and 0.3 mm feed rate, then A = 0.3 mm^2) to find the maximum cutting pressures that can be obtained from the spindle torque with the selected tool. If the force already calculated is (F=825 N), then the amount of KS will be 2750 N/mm^2. According to this information, the type of material that can be machined with this tool is obtained as per Figure 4.24, hence the selected tool is able to machine steel (ST 34-37).

The selected spindle can clamp 4-16 mm diameter and different end mill sizes. This calculation method can be used for various end mill sizes.

The cutting speed (Eq. 4.1) according to 8 mm diameter end mill and 12,000 RPM spindle speed was 301.44 m/min. According to KS (2750 N/mm^2) and (A= 0.3 mm^2) the spindle must be able to produce 4.144 kW of power using (Eq. 4.2) for a machining operation in this case. However, the selected spindle can produce 6 kW of power, so it is easily capable of this cutting operation.

$$V = \frac{\pi * d * n}{1000} \tag{4.1}$$

$$\mathrm{P} = \frac{A * KS * \mathrm{v}}{60000} \tag{4.2}$$

In order to evaluate the gantry behavior under the cutting force of finishing steel material, the total amount of force must be multiplied by a 1.2 safety factor.

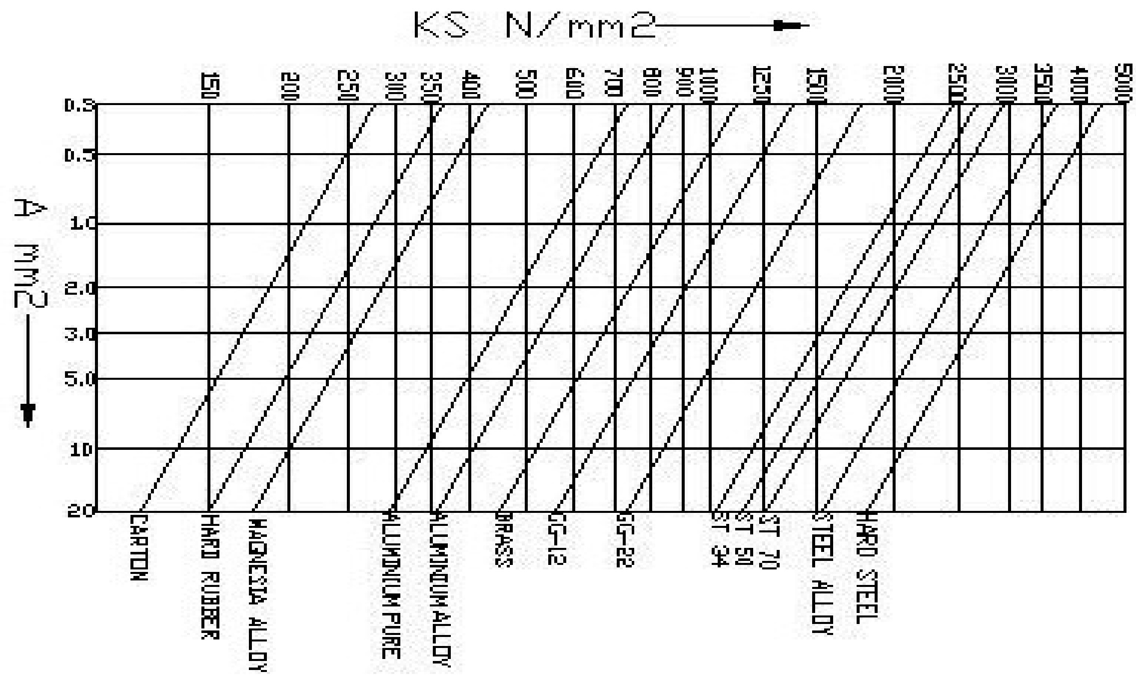

Figure 4.24: Material Cutting Pressures (Graham, 2008)

This amount of force (F=990N) is located on the tip of the end mill and the undesirable deformation under cutting force is identified via static analysis (Figure 4.25).

As shown in Figure 4.25, the maximum structure deformation under the maximum force produced by the spindle (when the spindle holder is in critical position) is 0.0099 mm. Thus, the expected accuracy of 10 microns is achievable in critical condition.

4.4.3 **Harmonic Analysis**

In the next step, the total amount of deformation when the gantry vibrates under cutting force of F=825 N must be identified using harmonic analysis. 300 Hz frequency was evaluated to observe the maximum gantry deformation during vibration. Furthermore, the existing cutting force of F=825 N was applied to the spindle tip for analysis. The harmonic analysis result is shown in Figure 4.26.

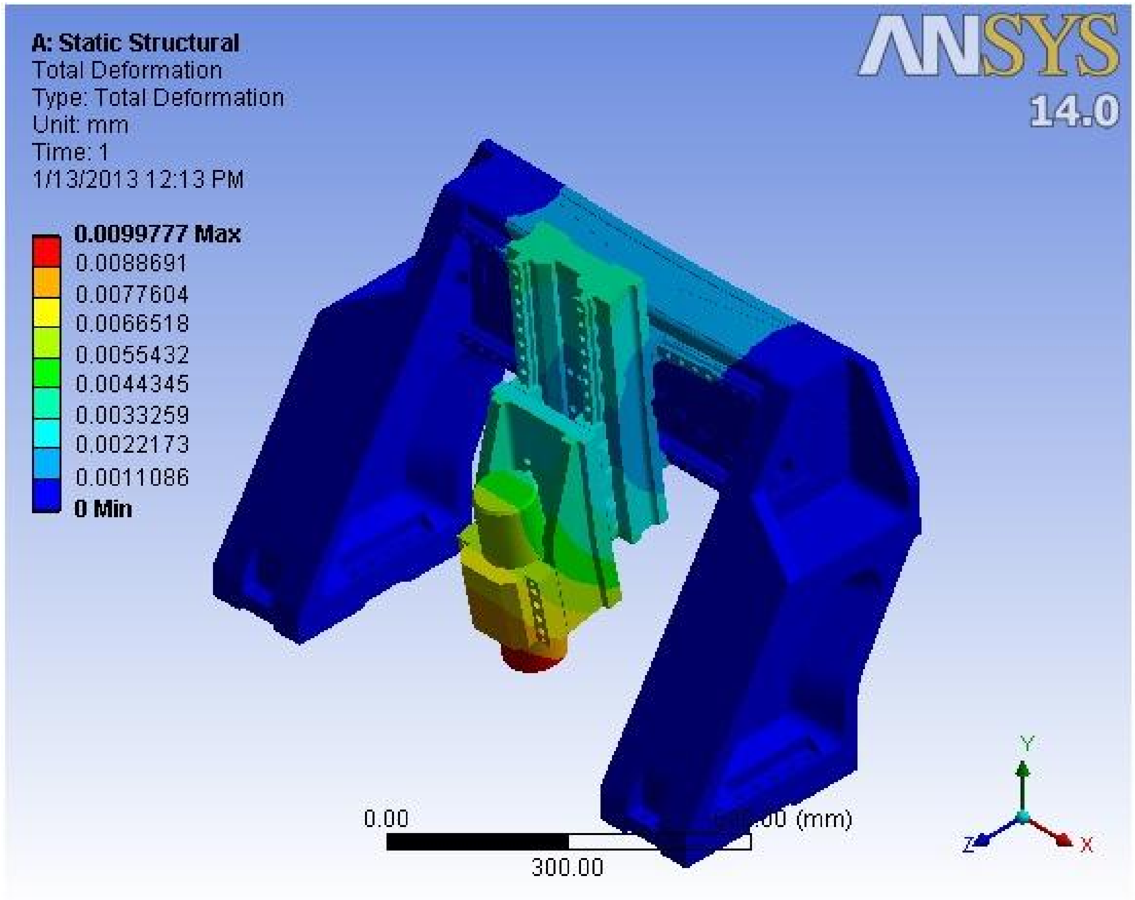

Figure 4.25: Maximum Deformation of the Gantry under Cutting Force

The frequency response from the harmonic analysis is shown in Figure 4.27. Evidently, the maximum deformation (nearly 150 microns) of the spindle tip occurred when the spindle was rotating at nearly 12600 rpm; however, at less than 11530 rpm the maximum deformation was 10 microns. Hence, the required 10micron accuracy for the gantry machine can be achieved at around 11530 rpm spindle speed.

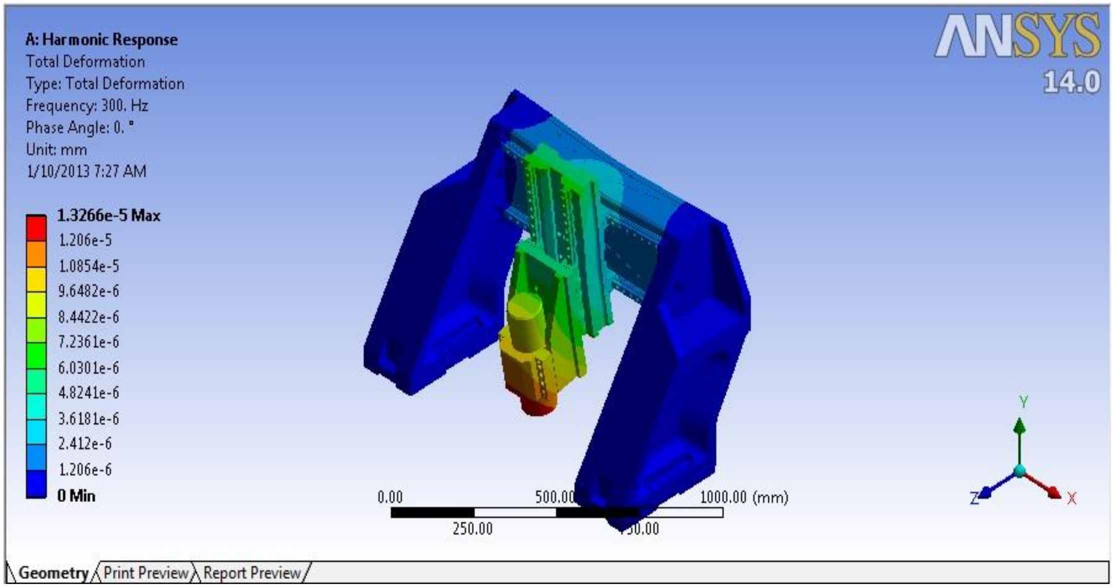

Figure 4.26: Harmonic Analysis Resul

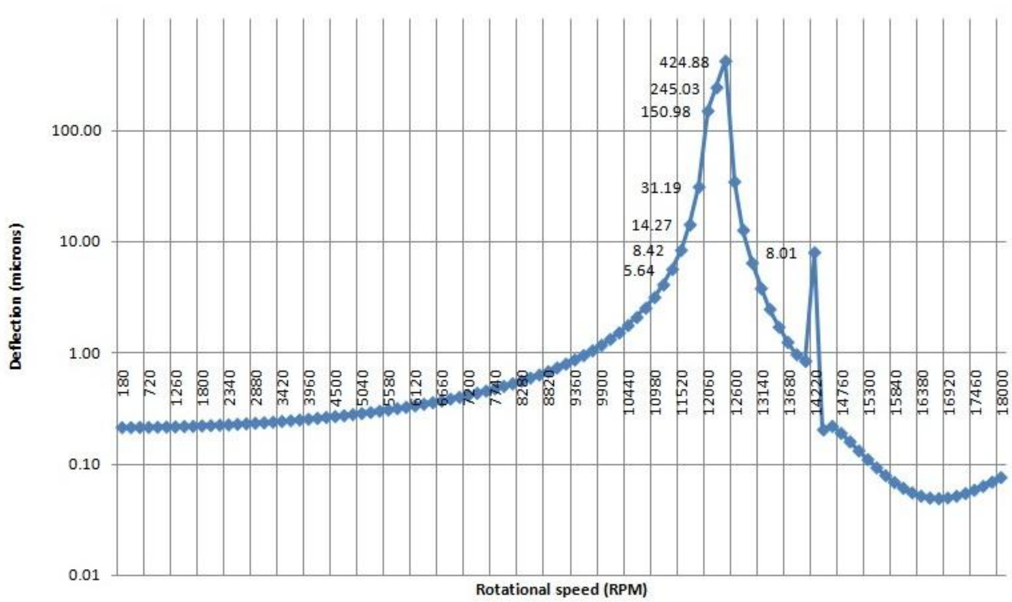

Figure 4.27 : Frequency response from the harmonic analysis

4.4.4 **Fourth and Fifth Proposed Designs based on Static and Dynamic Analysis**

After once again modifying the design of the new type of CNC gantry machine, the fourth design obtained is shown in Figure 4.28.

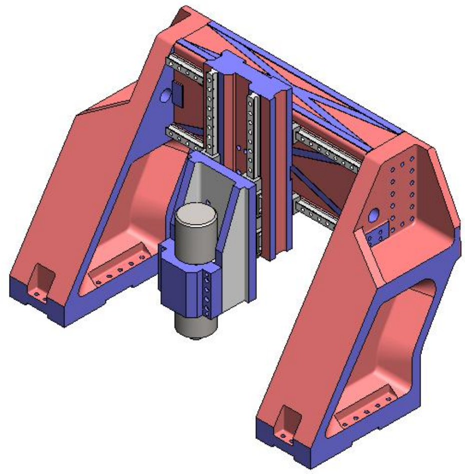

Figure 4.28: The Fourth Proposed Design in the Modification Process

Since the gantry weight increased during the modification process, a new crossbeam was designed to reduce the weight. This design reduced the gantry's weight by up to 3.8%. Figure 4.29 shows the fifth proposed design (lightweight gantry).

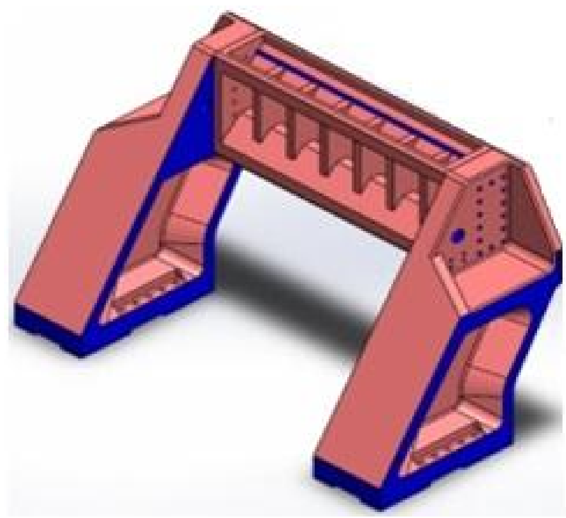

Figure 4.29 : The Fifth Proposed Design (lightweight gantry)

Both last two designs satisfy the design requirement. The fifth design is lighter than the fourth design but the fifth design has been shown lower natural frequency than the fourth design. In addition, the fifth design is more difficult to be manufactured using the available facilities on prototyping process. However, in selection process some of the important criteria of the existing designs will be evaluated via the proper method.

4.5 Best Design Selection

Five gantry designs have been developed based on experience and modification processes. Each step of the process focused on one or two gantry design criteria, such as stiffness or natural frequency. There are other criteria, including light weight and manufacturing cost that cannot be achieved at the same time in the design process but are nonetheless important to selecting the best option. There are several scientific methods to find the ideal option among several designs with different criteria.

Figure 4.30 illustrates the design obtained from the gradual design and modification process. In the selection process for the best gantry design, the four main criteria considered were manufacturing cost, natural frequency, the total deformation of each gantry under its weight and cutting force and weight.

4.5.1 Cost Evaluation

Cost is an important factor in the selection process. To evaluate the cost of the obtained designs, four cost sources (modeling, casting, machining and assembling) were defined based on existing experience and manufacturers' quotations, such as casting cost (cast iron per Kg), modeling cost (cost of patterns) and casting process, machining and assembly cost. The costs were estimated by industrial experts, as presented in Table 4.1.

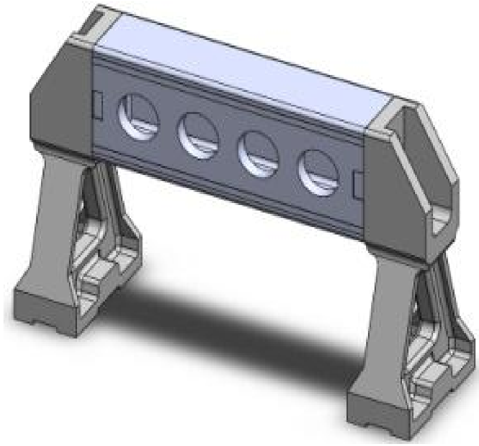

1. The First Design

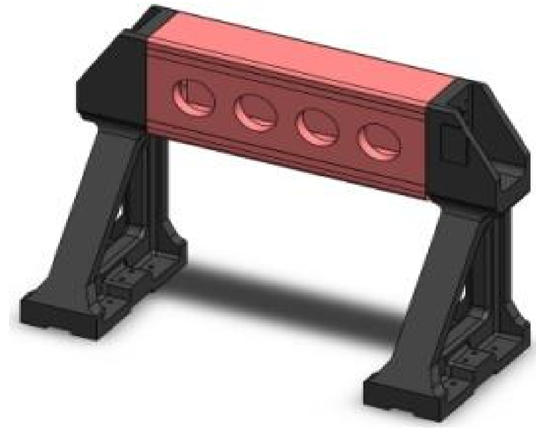

2. The Second Design

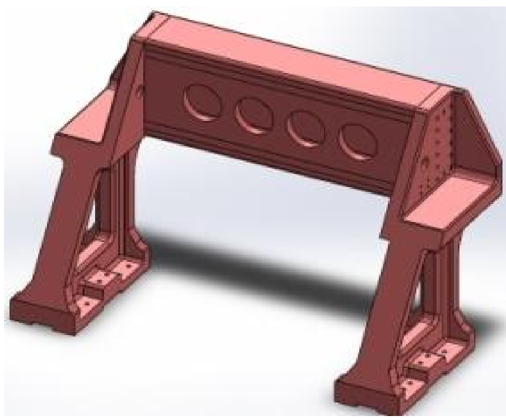

3. The Third Design

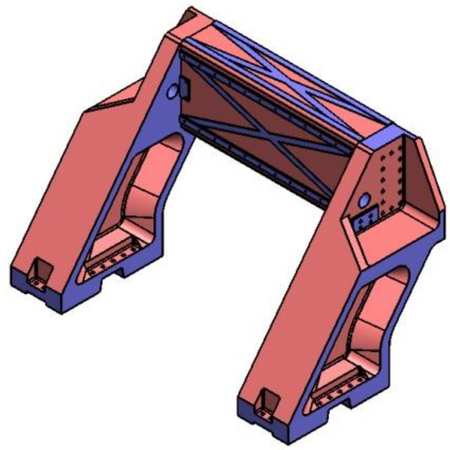

4. The Fourth Design

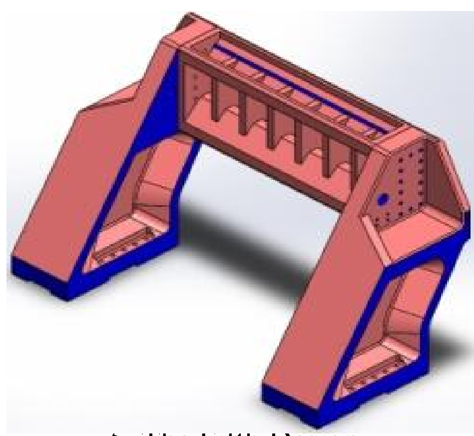

5. The Fifth Design

Figure 4.30: Five Proposed Designs

Table 4.1: Cost Estimation Results for Five Gantry Designs

Parameters	Model1	Model2	Model3	Model4	Model5
Modeling	2100$	2500$	3000$	2800$	3100$
Casting/Kg	492$	685$	765$	1224$	1161$
Machining	4500$	5900$	5800$	6500$	6000$
Assembly	350$	400$	400$	500$	600$
Total Cost	7442$	9485$	9965$	11024$	10861$

4.5.2 Evaluation of Gantry Designs

The initial gantry design evaluation was conducted based on designer experience and analysis. An attempt was made for each configuration to offer unique characteristics with respect to performance indices. The initial results of static and dynamic analysis evaluations as well as prototyping costs are shown in Table 4.2

Table 4.2: Performance Index Values for the Five Gantry Models

	Model 1	Model 2	Model 3	Model 4	Model 5
Deformation (μm)	6.63	6.32	8.53	3.60	4.41
1^{th} N.F.	215.1	157.54	135.5	286.69	250.47
2^{ed} N.F.	216.49	194.54	202.98	303.17	307.71
3^{rd} N.F.	403.29	370.24	320.23	479.38	441.69
4^{th} N.F.	525.7	381.87	368.08	631.56	507.22
Mass (kg)	273.2	244	292.1	492.6	473.5
Approximated Manufacturing Cost (Unit)	7633	9410	9930.25	11031.5	1088.75

The performance indices are: the gantries' maximum deformation under their weight and cutting force, anti-vibration characteristics for high speed operation, mass and fabrication cost. The conditions for five alternatives of gantry performance indices for each configuration are presented in Figure 4.31.

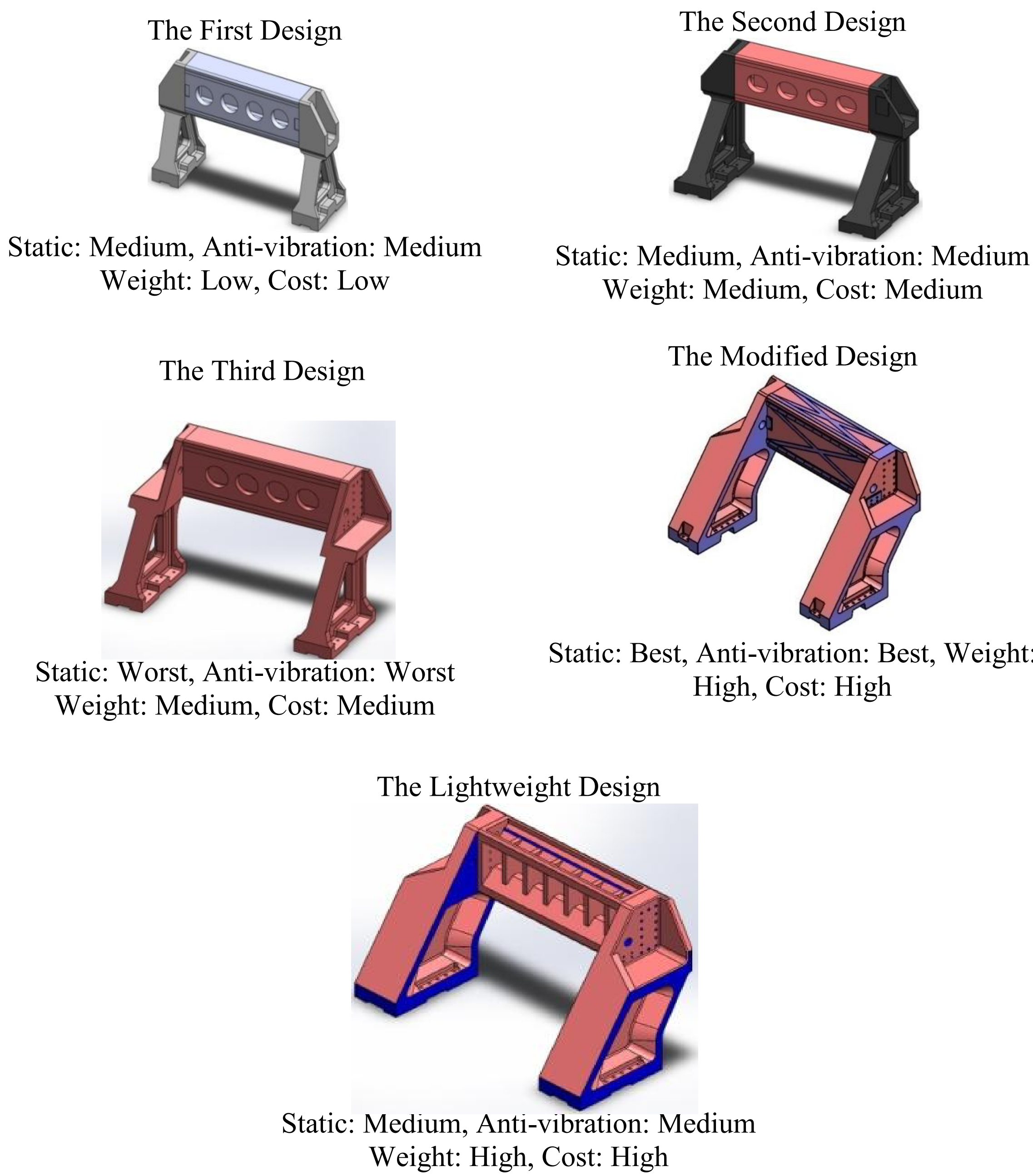

Figure 4.31 : The Five CNC Gantry Machine Design Alternatives

Because there are many criteria affecting the ultimate selection, it is indeed difficult to choose among these five candidate designs. This problem leads to using special methods that help find out which candidate is more appropriate and appealing. In the next chapter, the MCDM (Multi-criteria decision making) is introduced and exploited to select the best overall design.

4.6 Conclusion

In this section the double motion mechanism was converted from a rack and pinion to a ball screw system. The three gradual designs of the new type of CNC gantry machine were presented. All CNC gantry machine components were designed and completed in the machine assembly. Most changes were dependent on the gantry columns. Several different machine designs were evaluated to improve the machine design. The third design of the new CNC gantry machine was presented and enhanced center of gravity was found.

To evaluate the gantry's behavior and modification with desired characteristics, modal analysis was performed. The natural frequency of the gantry was 102.36 HZ and the gantry's frequency was 131.95 Hz when the material was changed to steel. The results showed that the gantry was improving. Modification was also done to increase stiffness. For this, the minimum natural frequency of the gantry was increased slightly, to more than 200 Hz. This gantry modification process increased its weight. The results indicate that the Z-axis position had no significant effect on the gantry's dynamic behavior. The range of machining materials and cutting force was calculated for the selected spindle. According to the static analysis results, the cutting force did not have any negative effect on machining precision. The harmonic results show that deformation was around 10 microns at the spindle tip at 11530 rpm. The fourth proposed design of a new CNC gantry machine was patented

(S. R. Besharati, et al., 2013) as a special gantry machine of three different types. The fourth and fifth designs were proposed and the fifth design was a lightweight gantry, with gantry weight reduction by up to 3.8%.

As pointed out, due to the difficulty in selecting the best design, it was necessary to employ the MCDM method to discover the best overall design. In the next chapter, the MCDM is introduced and two methods, AHP and PEG-MCDM, are used to help obtain the best overall design. The optimum gantry selection process in light of the different designs and the optimization of the ultimately chosen one will be discussed in the next chapter as well.

CHAPTER 5

5 OPTIMUM GANTRY DESIGN USING MULTI-CRITERIA DECISION MAKING (MCDM) METHOD AND MULTI-OBJECTIVE STRUCTURAL OPTIMIZATION OF GANTRY

5.1 Introduction

The gantry design is an important part of the CNC gantry machine tool, as the gantry plays a crucial role in supporting the spindle as well as influencing the gantry's static and dynamic characteristics. This is reflected in the final machining precision and ultimate allowable cutting speed and feed rate.

In this section, selecting the best gantry alternative using Multi-Objective design is considered through the analytical hierarchy process (AHP) and PEG-MCDM method. The objectives include the maximum static deformation of the gantry, the first four natural frequencies, mass and fabrication cost. The AHP method is applied to quantify the significance of each criterion according to experts' judgment. The five proposed gantry configuration designs are selected based on experts' experience and the engineering modification process.

Upon selecting the best among five proposed designs, the multi-objective genetic algorithm is employed to further enhance the performance indices. However, due to the complexity involved in automatic cost evaluation, these indices are not considered during the optimization process. The optimization results offer several solutions. The PEG-MCDM is used to select the best candidate and the final solution offers good static, dynamic and weight performance.

5.2 Optimum Gantry Design using AHP and PEG-MCDM

In practice, gantry design is a multi-criteria decision making problem aimed to achieve the ultimate design that exhibits higher stiffness, less deflection, low cost and light weight performance (Ayağ, et al., 2006). Improper machine design and selection may cause inefficient design with low performance and weak competitive capabilities. Due to conflict between the design criteria, selecting the best solution without using quantitative methods is not appropriate. Several MCDM methods introduced by many researchers can be used successfully in machine tool design selection (G-H Tzeng, 2011). A number of the MCDM (Multi-Criteria Design Making) methods are based on the Decision Maker's (DM) preference, which stems from the DM's wisdom and experience.

5.2.1 **Analytical Hierarchy Process (AHP)**

The Analytical Hierarchy Process (AHP) proposed by Saaty (Saaty, 1980) is based on a pair-wise comparison of alternatives or criteria according to a DM's judgment. Ease and applicability of this method lead to its exploitation in many diverse applications, especially in machine tool selection. After obtaining the evaluation matrix based on the DM's preference, a consistency test must be performed to ensure consistent results. Finally, this method reveals the weight of each alternative or criterion, which may later be applied for the decision making process.

In order to convert the judgment of a DM to a corresponding numerical value, Table 5.1 serves as a guide.

The AHP method must be used separately for each group of criteria or alternatives that are on the same level. Thereafter, an evaluation matrix $I=(a_{ij})_{n\times n}$ is established, where n is the number of criteria or alternatives.

Due to inconsistence in DMs' judgment, further result evaluation with AHP is necessary to obtain confident results. Consistency Index $(C.I.)$ and Consistency Ratio $(C.R.)$ are two indices applicable to assessing final results. These two indices must be lower than 0.1 to ensure reliable assessment (G-H Tzeng, 2011).

Table 5.1: Qualitative Numerical Conversion Guide

Number	Qualitative meaning
1	Equal
3	Moderate
5	Strong
7	Demonstrated
9	Extreme
2, 4, 6, 8	Intermediate values

A pair-wise comparison of the gantry's performance indices and natural frequency order is presented in Table 5.2 and 5.3, respectively. Also, the weights of the criteria calculated using the AHP method, are presented in the two tables as well. The consistency index and consistency ratio are well below 0.1 (Boadway, 1984), implying confident results.

In order to compare the values of performance indices, the indices must be normalized prior to analysis using Eq. (5.1). Obviously the goal is to minimize deformation, cost and mass and maximize the natural frequencies.

Table 5.2: Pair-Wise Comparison of Performance Indices and Calculated Weights using AHP $(C.I.=0.017,\ C.R.=0.019)$

	Deformation	Anti-vibration performance	Mass	Estimated fabrication Cost	AHP estimated Weight (%)
Deformation	1	2	2	3	43
Anti-vibration performance	1/2	1	2	3	25.4
Mass	1/2	1/2	1	1	17.3
Estimated fabrication Cost	1/3	1/3	1	1	14.2

Table 5.3: Pair-Wise Comparison of Gantry Resonance Frequencies and Calculated Weights using AHP $(C.I.=0.08,\ C.R.=0.089)$

	1^{st} N.F.	2^{nd} N.F.	3^{rd} N.F.	4^{th} N.F.	AHP esti-mated Weight (%)
1^{st} N.F.	1	2	2	2	40.4
2^{nd} N.F.	1/2	1	2	3	26.8
3^{rd} N.F.	1/2	1/2	1	3	19.6
4^{th} N.F.	1/2	1/3	1/3	1	13.1

The relative ranking of each alternative can be obtained by calculating the sum of the multiplication of the normalized performance indices with the corresponding criteria weights. Table 5.4 presents the normalized performance indices, weights and final gantry evaluation. In this table, the overall anti-vibration performance indices of each design are calculated according to the normalized natural frequencies in Table 4.2 (chapter 4) and the corresponding weights are ultimately normalized using Eq. (5.1). According to the final evaluation results presented in Table 5.4, the fourth gantry is the best choice. This design provides the best performance in terms of deformation and anti-vibration index, but it is worth one for mass and cost index.

To decide on the preferred design according to MCDM analysis, further geometry optimization on the selected design was applied using the multi-objective optimization method.

Table 5.4: Normalized Performance Indices, Weights and Final Evaluation of Gantries

		Normalized Performance Indices of Gantries				
	Weight	1	2	3	4	5
Deformation	0.43	0.385	0.448	0	1	0.835
Overall Anti-Vibration performance	0.254	0.436	0.110	0	1	0.909
Mass	0.173	1	0.735	0.627	0	0.084
Cost	0.142	1	0.429	0.295	0	0.268
Final evaluation		0.591	0.408	0.150	0.684	0.643

5.2.2 **PEG-MCDM Method**

Accomplishing an evaluation based on DM preference would be time consuming and may contain mistakes, especially for MCDM problems consisting of many alternatives.

The PEG-MCDM method proposed by Grierson (Grierson, 2008) in 2008 is a MCDM method used to discover the optimum choice among Pareto solutions without requiring DM preference. The method is based on a trade-off analysis technique adapted from the theory of social welfare economies (Boadway, 1984).

Originally, Grierson (Grierson, 2008) developed the method for a two-criteria problem and then advanced it for a general multi-criteria problem. In this thesis, this method is applied to select among Pareto solutions resulting from multi-objective structural optimization of a gantry based on MOGA (Konak, 2006). The procedure of applying PEG-MCDM is as follows (Grierson, 2008):

5.2.2.1 Initial Normalization

Since the criteria are often non-commensurable and there may large numerical differences among them, the first step is to map all criteria vectors in the range of [0, 1] where 1 corresponds to the designer's need.

The criteria vector $\mathbf{f}_i^* (i = 1, n)$ contains the value of each criterion for all alternatives, where n is the number of criteria. In order to normalize the criteria vector, the following relation is applicable:

$$X_{i,j} = (f_{i,j} - \max(\mathbf{f}_i)) / (\max(\mathbf{f}_i) - \min(\mathbf{f}_i)); \quad (i = 1, n) \ (j = 1, m) \qquad (5.1.a)$$

$$X_{i,j} = (f_{i,j} - \min(\mathbf{f}_i)) / (\max(\mathbf{f}_i) - \min(\mathbf{f}_i)); \quad (i = 1, n) \ (j = 1, m) \qquad (5.1.b)$$

For the higher-is-better and lower-is-better rules, Eqs. (5.1.a) and (5.1.b) are used, respectively.

5.2.2.2 **Calculating the ordinarily-maintained primary-aggregate vector** $\mathbf{x}_i, \mathbf{y}_i\, (i = 1, n)$

First, the ordinarily-maintained primary criterion vectors are formed by sequentially re-ordering them from their minimum to maximum values,

$$\mathbf{x}_i = [X_i^{\min}, \ldots, X_i^{\max}]^T = [0, \ldots, 1]^T; \quad (i = 1, 2, \ldots, n) \tag{5.2}$$

The aggregate vector for each criterion $\mathbf{Y}_i$ is calculated as:

$$\mathbf{Y}_i = (\sum_{k=1}^{n} \mathbf{x}_k - \mathbf{x}_i) / (n-1); \quad (i = 1, 2, \ldots, n) \tag{5.3}$$

Then the ordinarily-maintained aggregate criterion vector $\mathbf{y}_i$ will be formed by sequentially reordering $\mathbf{Y}_i$ form the maximum to minimum values.

$$\mathbf{y}_i = [Y_i^{\max}, \ldots, Y_i^{\min}]^T = [1, \ldots, 0]^T; \quad (i = 1, 2, \ldots, n) \tag{5.4}$$

5.2.2.3 **Calculating the shifted vectors**

In this step, the shifted vectors $\mathbf{x}_i^*, \mathbf{y}_i^*\ (i = 1, n)$ are calculated according to the primarily-aggregate vectors by using the following shifting relation:

$$\mathbf{x}^* = (\mathbf{x} + \delta\mathbf{x}) / (1 + \delta x) = [1 - \sqrt{2}/2, \ldots, 1]^T \tag{5.5.a}$$

$$\mathbf{y}^* = (\mathbf{y} + \delta\mathbf{y}) / (1 + \delta y) = [1, \ldots, 1 - \sqrt{2}/2]^T \tag{5.5.b}$$

where $\delta x = \delta y = \sqrt{2} - 1$.

5.2.2.4 **Calculating radial shift** Δr_i

The following relation is used to calculate radial shift:

$$\Delta r_i = \sqrt{2}\Delta x_i = \sqrt{2}\Delta y_i \tag{5.6}$$

where $\Delta x_i = \Delta y_i$ is calculated according to the following relation:

$$\Delta x_i = \Delta y_i = 0.5 - (x_j^* + x_{j+1}^*)(y_j^* + y_{j+1}^*) / (x_j^* + x_{j+1}^* + y_j^* + y_{j+1}^*) \tag{5.7}$$

where j is such that $x_j^* / y_j^* \leq 1$ while $x_{j+1}^* / y_{j+1}^* \geq 1$.

5.2.2.5 **Evaluating the PEG function**

The PEG-function estimates the optimum value of each criterion based on the PEG theory. The following relation is used to calculate PEG functions:

$$f_i^0 = f_i^{\max} - (f_i^{\max} - f_i^{\min})(\Delta r_i + \sqrt{2}/2); \;\; (i = 1, n) \tag{5.8}$$

5.2.2.6 **Calculating the mean-square-error (MSE) for each alternative**

In obtaining the PEG functions of criteria, the closeness of each alternative to the optimum value is determined by the following relation:

$$MSE_i = 1/n \sum (1 - f_i^* / f_i^0)^2; \quad (i = 1, n) \tag{5.9}$$

The alternative with the lowest MSE is set as the best alternative design.

5.3 Multi-objective Structural Optimization of a Gantry

In this section, the fourth gantry design was optimized using MOGA to improve all objectives excluding cost. Sensitivity analysis was conducted to identify the most effective parameters among fourteen initial geometrical parameters from Table 5.6 selected intuitively. After determining the most effective parameters, MOGA was performed using the Design Exploration toolbox of ANSYS workbench to obtain the Pareto-optimal solutions. In order to choose the final configuration, PEG-MCDM was applied.

For gantry optimization ANSYS software was used. First, some gantry dimension parameters were defined for the optimization process. These parameters were changed during the process to achieve a new design with new dimensions. Moreover, the results of dynamic and static behavior of the new design were investigated via ANSYS, after which the objectives were optimized by the special method.

5.3.1 **Optimization Objectives**

In this process, four objectives were defined for optimization using the ANSYS optimization package. Initially, four natural frequencies of the gantry related to CNC machine performance and gantry mass were calculated. Gantry mass must be minimized while the natural frequencies of the machine must be maximized. Mass is usually opposite the high natural frequency of the structure, which signifies that the machine's performance is related to the natural frequency. The objectives and future conditions (after optimization) are shown in Table 5.5.

5.3.2 **Optimization Method**

The ANSYS software offers several optimization methods such as Screening, MOGA, Adaptive Multiple-Objective methods which are suitable for multi-objective optimization [Appendix G]. The genetic algorithm is one such method that finds wide applications for multi-objective optimization problems. Therefore, the method applied was the multi-objective genetic algorithm (MOGA).

Table 5.5: Technical Parameters and Conditions

Name	Technical Parameters	Objective	Type
P15	Reported Frequency (mode1)	Maximize	No constraint
P16	Reported Frequency (mode2)	Maximize	No constraint
P17	Reported Frequency (mode3)	Maximize	No constraint
P18	Reported Frequency (mode4)	Maximize	No constraint
P19	Total Deformation	Minimize	No constraint
P20	Gantry Mass	Minimize	No constraint

5.3.3 Optimization Process

This process entails the following steps.

1. Changed the design dimensions between the lower and upper bounds according to the variable steps
2. The modified design was automatically created by SolidWorks software
3. Performance indices were calculated using ANSYS Workbench
4. All of the results were collected for the optimization process
5. A new-generation gantry was constructed according to the dimensions proposed by the optimization algorithm
6. Optimization was done based on the MOGA method to achieve convergence.

5.3.4 Structural Multi-Objective Optimization of a Gantry using MOGA (Multi-Objective Optimization Algorithm)

Upon selecting the preferred configuration, the structural optimization of the gantry is a valuable task for further improving the performance indices. Each performance index indicates an objective that the optimization algorithm attempts to improve. Since in gantry optimization more than one objective takes part in overall performance, a multi-objective optimization algorithm must be employed.

Unlike a single-objective optimization problem that contains a single, global optimum solution, multi-objective optimization problems contain many optimum solutions. The definition of an optimal solution is not straightforward, as it defines a single-objective optimization problem. Pareto-optimal solutions or non-dominant solutions are multi-objective optimization problem solutions. A Pareto-optimal solution is achieved when it is not possible to further improve a single selected objective without causing at least one other objective to deteriorate (Deb, 2001).

Design Exploration of the ANSYS workbench provides many important and practical means for design optimization, including several algorithms for multi-objective optimization. Among the numerous multi-objective optimizations, MOGA has been exploited in many engineering design problems (Andersson, 2003). In this thesis, MOGA is employed to explore the design space and identify Pareto-optimal solutions. Due to the gantry's configuration complexity, initial parameter selection was carried out intuitively. Figure 5.1 shows the initial design parameters.

5.3.5 **Parameters Range**

As illustrated in Figure 5.1, fourteen parameters were defined for the optimization process and each parameter had an initial value in the main design. The parameters had two variable values and these changed during the process to automatically modify the new gantry design. These changing parameters altered the gantry's dynamic and static behavior. Next, the optimization domain of parameters was estimated. This estimation (lower and upper bound) was limited to the initial design requirements, such as the final dimensions of the machine workspace or axes and the designer must be considered.

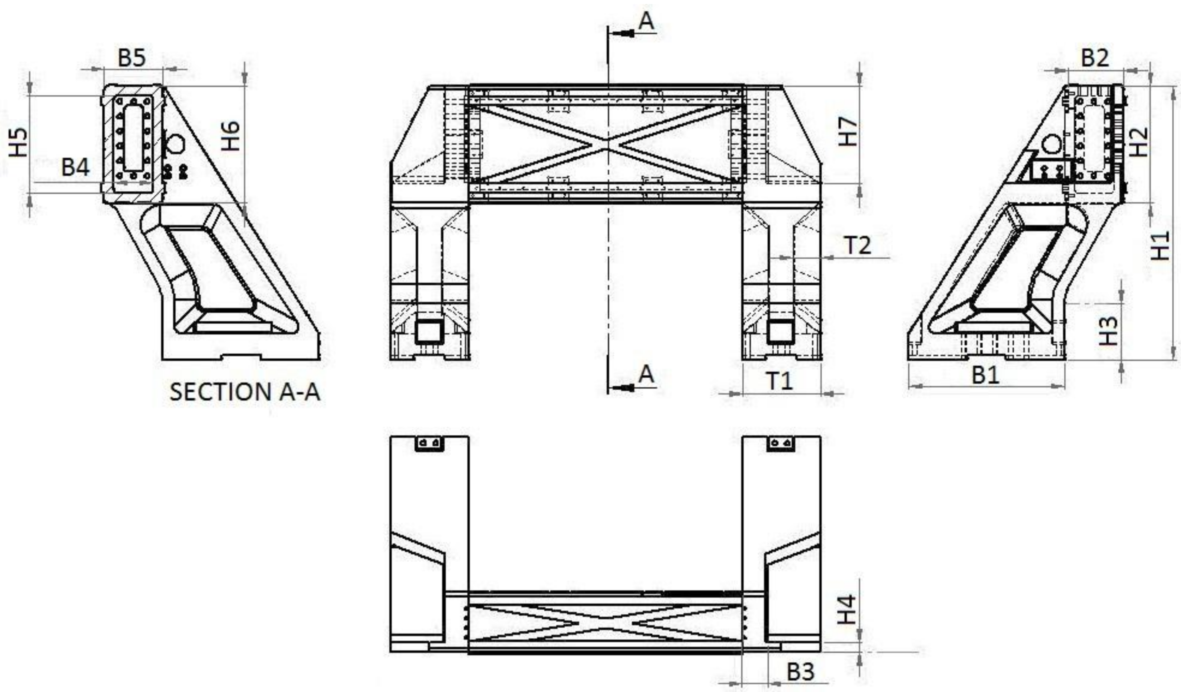

Figure 5.1: Initial Selected Parameters for Structural Optimization

According to this estimation constraint for each parameter variable, the lower and upper bound dimensions (minimum and maximum) were defined and are shown in Table 5.6.

The parameter ranges for sensitivity analysis and optimization are as follows (all units are in millimeters):

The Pareto analysis is a formal technique where many possible courses of action are competing for attention. In fact, the problem solver estimates the value delivered by each action, then selects a number of the most effective actions that deliver a total value reasonably close to the maximal possible one. Table 5.7 shows the organization of the ANSYS optimization process carried out in this work.

Table 5.6: The Lower and Upper Bounds of Parameters (Gantry Dimensions)

No.	Optimization Domain	Base Dimension	Lower Bound	Upper Bound
1	T1	200	180	220
2	B4	100	90	110
3	H5	250	240	260
4	H6	300	285	315
5	B5	150	140	160
6	T2	70	60	80
7	H7	250	225	270
8	B3	60	54	66
9	H4	25	22.5	27.5
10	B1	400	380	420
11	H1	700	675	725
12	B2	150	140	160
13	H2	300	280	320
14	H3	170	160	180

5.3.6 **Sensitivity Analysis of the Parameters and Optimization**

Sensitivity analysis reveals the significance of each parameter. Figure 5.2 presents the sensitivity analysis results obtained using the Design Exploration toolbox of ANSYS.

Table 5.7: The ANSYS Technical Parameters and Conditions

No.	Property	Value
1	Optimization Method	MOGA
2	Number of Initial Samples	100
3	Number of Samples per Interaction	50
4	Maximum Allowable Pareto Percentage	80
5	Maximum Number of Interactions	20
6	Maximum Number of Candidates	3

It is clear from this figure that some of the parameters did not contribute significantly. Therefore, parameters H3, H4 and H6 were omitted from the optimization procedure. Column parameters, such as T1, have great influence on the static and dynamic characteristics, even more than the crossbeam parameters. This implies the significant influence of design parameters associated with the columns.

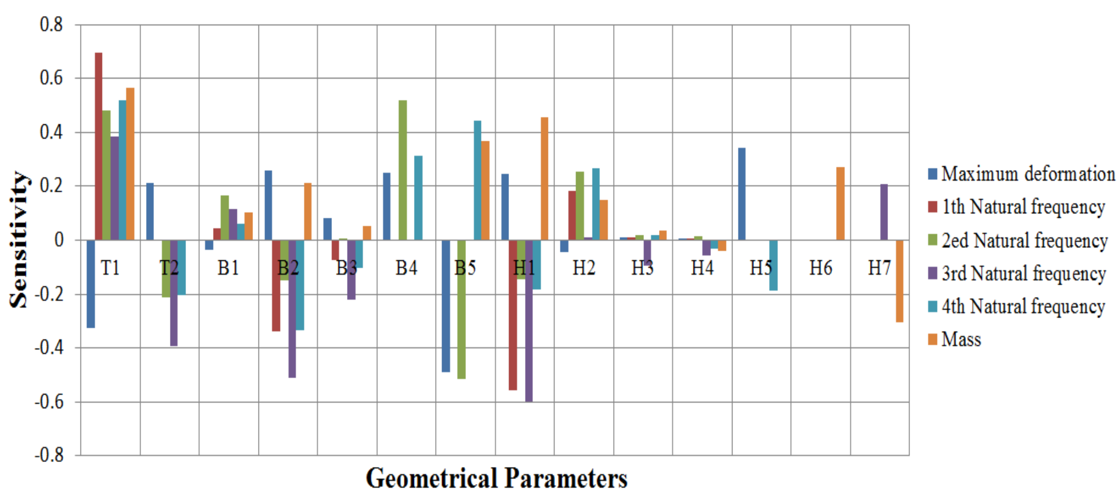

Figure 5.2: Sensitivity Analysis Results of the Gantry Geometrical Parameters on Static and Dynamic Characteristics

MOGA was performed using the design exploration toolbox of ANSYS workbench. As convergence criteria, the maximum allowable Pareto percentage was set to 80%. The populations of the first and later generations were 100 and 50 (Sensitivity Analysis of the Parameters and Optimization

Sensitivity analysis reveals the significance of each parameter. Figure 5.2 presents the sensitivity analysis results obtained using the Design Exploration toolbox of ANSYS.

Table 5.7 MOGA converged automatically after 243 evaluations. The five candidate points selected among the Pareto-optimum solutions are shown in Table 5.8. These are non-dominated solutions. In order to select the final optimal solution, PEG-MCDM was employed as described in section 5.2. Following the previously outlined procedure, the normalization of criteria values, primary-aggregate vectors, radial shifts and PEG-functions were evaluated for each criterion as shown in Table 5.9. Accordingly, the MSE (Mean-Square-Error) value of each candidate point was calculated using Eq. (5.9). Table 5.10 reveals the MSE values of the design alternatives.

According to the results, the fifth solution offers the least MSE and is the best option introduced by the PEG-MCDM method. Therefore, this option was considered the final choice. Upon finalizing the multi-criteria design stage, the prototype was fabricated according to the geometrical parameters of the fifth design. This prototype was used to investigate and ensure the accuracy of the FE model.

Table 5.8: Candidates Revealed by MOGA

Candidates	1	2	3	4	5
T_1	215.4	215.4	212.2	212.2	209.64
T_2	61.75	61.75	66.25	66.25	65.57
B_1	399.51	418.99	385.71	385.71	394.18
B_2	148.85	148.85	142.6	142.6	142.75
B_3	54.54	55.022	60.917	60.917	63.15
B_4	102.27	102.27	93.57	93.53	100.72
B_5	156.57	156.81	144.80	144.80	141.58
H_1	682.25	689.27	677.25	677.28	681.74
H_2	312.79	311.85	297.97	297.97	313.78
H_5	254.83	254.83	244.31	244.41	251.84
H_7	237.86	237.86	241.58	239.69	229.64
Max Deformation (mm)	0.0032	0.0033	0.0033	0.0033	0.0035
1^{st} natural frequency (Hz)	315.13	314.59	313.09	313.10	315.97
2^{nd} natural frequency (Hz)	321.55	318.57	318.63	318.37	322.48
3^{rd} natural frequency (Hz)	507.05	504.18	503.93	503.57	497.94
4^{th} natural frequency (Hz)	655.98	656.19	640.02	640.34	640.55
Mass (kg)	544.95	556.24	517.99	519.13	513.88

Table 5.9: Maximum, Minimum, Radial shift Δr_i and PEG-functions of Design Criteria

	$f_i^{\min}$	$f_i^{\max}$	Δr_i	f_i^{0}
Max deformation	0.0032	0.0035	-0.27008	0.003442
1st Natural freq. (Hz)	385.7172	418.998	-0.08545	398.5451
2nd Natural freq. (Hz)	313.0993	315.9777	-0.20628	314.5566
3rd Natural freq. (Hz)	318.3707	322.4886	-0.13778	320.1734
4th Natural freq. (Hz)	497.9459	507.0545	-0.33448	503.7251
Mass (kg)	640.0225	656.1948	-0.22875	648.5735

Table 5.10: MSE Values of Design Alternatives Introduced by MOGA

Candidates	1	2	3	4	5
MSE	0.000436	0.000635	0.000464	0.000478	0.000308

5.3.7 **The Final Design Obtained with Optimization**

Based on the modification process, the final modified gantry machine design is shown in Figure 5.3 and three views of the “FINAL” new type of CNC gantry machine are shown in Figure 5.4. Defining the technology for fabricating the components with available facilities, ease of fabrication and low cost fabrication are the targets of the next stage. The design team has prepared documents, such as 3D and detailed drawing files for fabrication. All CNC design documentation is attached in the index.

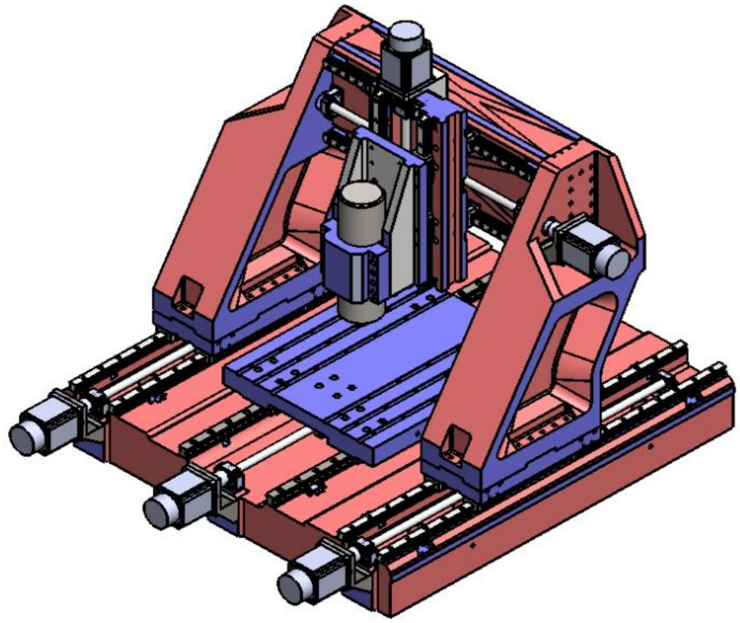

(a) Optimized CNC Gantry Machine without Cover

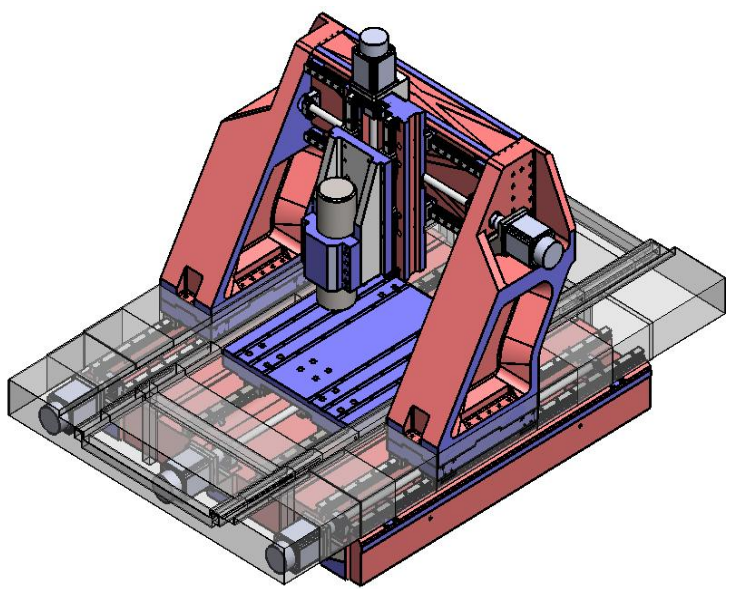

(b) The New CNC Gantry Machine with Cover

Figure 5.3: The Optimized Design of the New CNC Gantry Machine

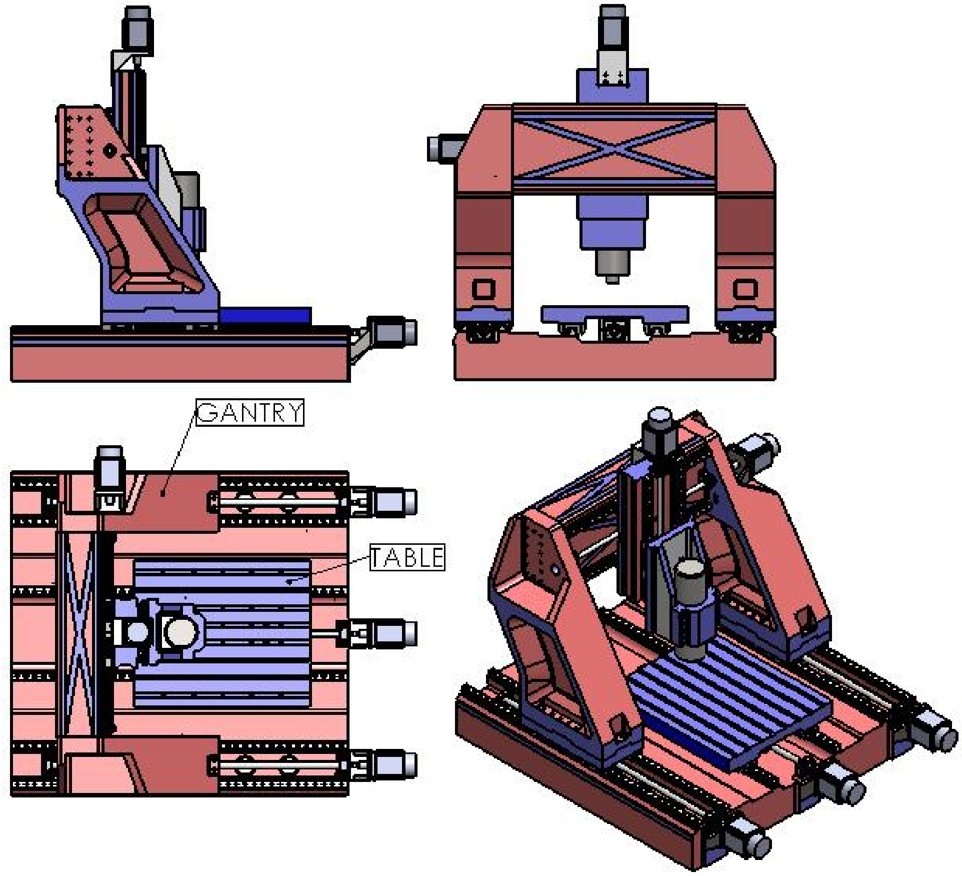

Figure 5.4: Three Views of the “FINAL” New CNC Gantry Machine

5.4 Conclusion

Improving static and dynamic characteristics may ultimately cause higher mass and cost. This implies that in the design stage, many conflicting criteria must be taken into consideration to meet the machine performance indices as well as fulfill market demand. Combining experts’ knowledge and experience along with well-developed MCDM methods served as a guide in the design stage, which further yielded confidence regarding the final design configuration.

The performance indices used were the maximum static deformation of the gantry, the first four natural frequencies, mass and fabrication cost. According to the designers’ judgment, the significance of the criteria was determined using the AHP method. After normalizing the performance indices, the optimal configuration was selected based on merit as calculated by aggregating the weighted normalized performance indices.

MOGA was employed to additionally improve the performance indices. Prior to optimization, sensitivity analysis was done to eliminate insignificant parameters. The sensitivity analysis results signified a major contribution of the columns on the static and dynamic characteristics of the gantry relative to the crossbeam's contribution. Five design points were chosen through Pareto-optimal solutions revealed by MOGA. These non-dominated design points were examined by PEG-MCDM technique to identify the ultimate configuration. The manufacturing process of the new type of CNC gantry machine designed and discussed in the last chapters will be presented in the subsequent chapter.

CHAPTER 6

6 GANTRY MACHINE MANUFACTURING PROCESS AND TESTING

6.1 Introduction

In this chapter, all gantry documents are prepared for the prototyping process. The prototyping steps, namely gantry modeling, casting, machining and assembly are portrayed. The modal experimental test of the gantry is presented and the FE model's accuracy is validated with the analysis results following gantry assembly. The final machine assembly is also discussed.

6.2 Documentation

All necessary documents based on the design and manufacturing processes have been prepared and attached to the [APPENDICES], including:

1. All drawings of the CNC gantry machine design with overall dimensions [Appendix A].
2. Quality control report from the casting process by SIRIM Company [Appendix B].
3. Quality control report from the machining process by TPM Company [Appendix C].
4. Drawing of CNC gantry machine assembly [Appendix D].
5. Quality control reports from assembly and alignment process by TPM [Appendix E].
5. Detail specifications of standard components and calculation [Appendix F].
6. Servomotor detail specifications [Appendix F].
7. Spindle detail specifications [Appendix F].
8. General information [Appendix G]

6.3 Prototyping Process

The prototyping process with modeling (patterns making), casting, machining and assembly of the gantry and machine is introduced in this section.

6.3.1 The Materials and Methods for Manufacturing the CNC Machine Structure

Gray cast iron is the most commonly employed material for casting mass production. The high damping ratio and self-lubrication are two important advantages of this material.

For low production or large machine structures, welding technology is suitable. The low damping ratio is a disadvantage for welding. To improve damping, the hollow area in the frame must be filled with specific sand or polymer. Figure 6.1 shows a structure made by welding.

Figure 6.1 : Welding Technology Machine Structure

Residual stress, distortion and non-homogeneity are other problems associated with welding parts. Therefore, grinding machines and other highly accurate finishing machines, such as glass turning and polishing machines can be used (L.N, 2009). To overcome these issues, casting technology is more suitable for machine prototyping. The casting process is introduced in the next section.

6.3.2 **Casting Process**

In this step, the design of the main machine components, i.e. structure, columns, cross-beam, worktable, Y and Z-axis carriages, spindle holder and column base is prepared for pattern-making. The patterns are made by special CNC machine based on a calculation of the shrinkage requirement. The patterns are made of expanded Polystyrene (EPS) material, which is suitable for easy and fast casting. EPS is also cheaper than other materials, but it can only be used once. The crossbeam pattern is shown in Figure 6.2.

Figure 6.2 : The Crossbeam Pattern

The component patterns are placed in a mold for casting. Some special sand is strewed in the mold. The molding process of a CNC machine structure is shown in Figure 6.3.

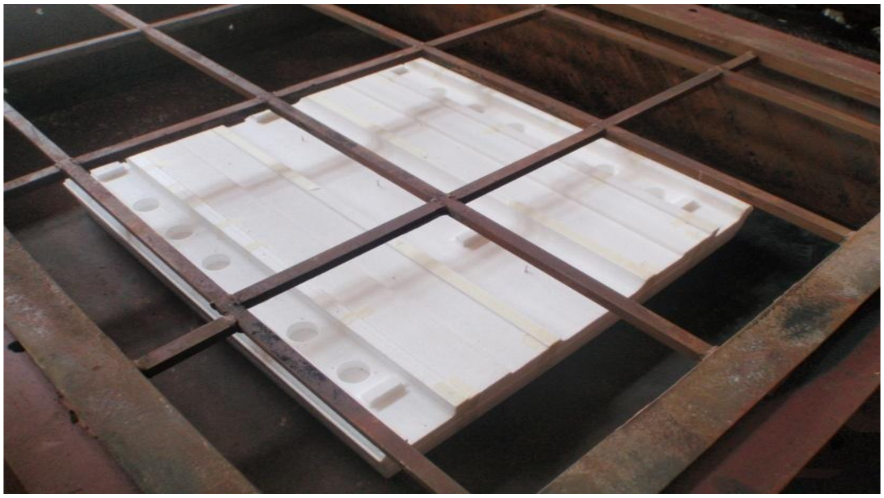

(a) Sand Mold of the Machine Structure

The Molding Process

Figure 6.3: The Molding Process of the Machine Structure

For casting, gray cast iron material is suggested for gantry prototyping. The specifications of this material are given in Table 6.1.

Table 6.1: Specifications of Casting Material

Property	Value	Units
Elastic Modulus	66178.1	N/mm^2
Poisson's Ratio	0.27	N/A
Shear Modulus	50000	N/mm^2
Density	7200	kg/m^3
Tensile Strength	151.66	N/mm^2
Compressive Strength	572.17	N/mm^2
Yield Strength		N/mm^2
Thermal Expansion Coefficient	1.2e-005	/K
Thermal Conductivity	45	W/(m·K)
Specific Heat	510	J/(kg·K)
Material Damping Ratio		N/A

All components were produced by casting method with EPS patterns. The molding process was very difficult and took time because the patterns were not rigid enough. The different casted components are illustrated in Figure 6.4.

6.3.3 Machining Process

For machining the components, the methods and manufacturing technologies must be prepared as detailed drawings. Quality control and assembly instruction are two important steps. To prepare these requirements and prototype the CNC machine, one of the best governmental companies in Malaysia, TPM (Technology Park Malaysia) with good experience in producing CNC milling machines, was chosen. TPM prepared the technical instructions for machining, quality control and assembly based on the CNC machine documents submitted to them. Thus, all components were fabricated by CNC machine at TPM.

(a) Columns, Spindle carriage, Spindle clamp and Base columns

(b) Crossbeam, Spindle holder, Worktable

(c) Machine bed

Figure 6.4: Casted CNC Machine Components

The CNC **vertical** machine was used for some components and the CNC horizontal machine for others. The machine components fabricated at TPM are shown in Figure 6.5**.**

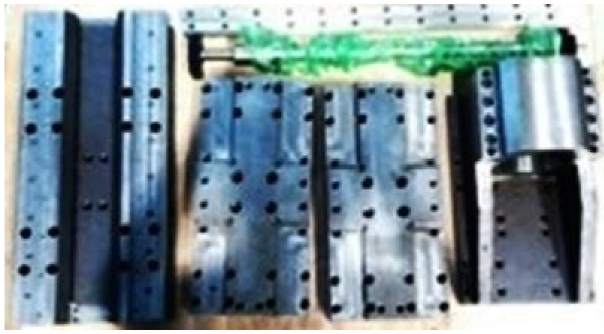

(a) Spindle carriage, Base columns and Spindle holder

(a) Machine Worktable

(a) Machine Structure

(d) The Column

Figure 6.5 : CNC Machine Components in the Machining Process

6.4 Modal Testing and Analysis of the Manufactured Gantry

Before final machine assembly, the CNC machine gantry was assembled for modal testing and analysis. A gantry vibration test was required to verify the gantry's dynamic behavior as investigated via modal analysis in ANSYS software. The assembled gantry is shown in Figure 6.6.

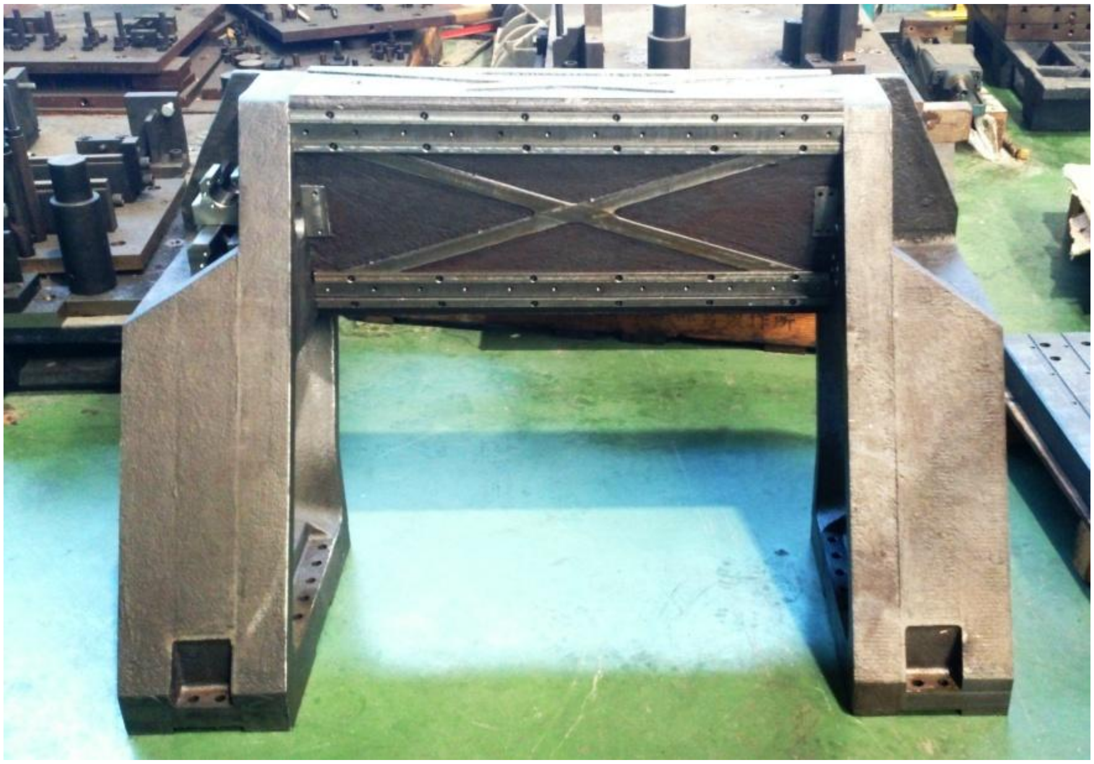

Figure 6.6: The Gantry of the CNC Machine

During the test the gantry was hanged by a lift to fulfill the free-free boundary condition (Figure 6.7). The free natural frequency of four modes was extracted. This type of boundary condition was chosen as it is convenient to attain. In order to excite the structure, a force sensor-embedded hammer and three-axis acceleration sensor were used to capture the gantry's structural dynamic response.

An impulse force test hammer was used to excite the gantry structure and thereafter the accelerometer measured the point of vibration acceleration. For this test, a PCB impact hammer model 086D20 and accelerometer model 604B 31 were used (Table 6.2). The experimental setup and equipment involved including the hammer, 3-axis accelerometer, DAQ and PC for processing the data are shown in Figure 6.8.

Table 6.2: Descriptions of the Instruments employed in the Experimental Modal Analysis

INSTRUMENTS	DESCRIPTION
PCB Impact Hammer, Model 086D20	Sensitivity: 0.23 mv/N Tip type: medium tip
IMI ICP Tri-axial Accelerometer, Model 604B31	Sensitivity: 100 mv/g
NI USB Dynamic Signal Acquisition Module, Model NI-USB 9234	Number of channels: 4 ADC resolution: 24 bits
DASYLab v11.0	Sampling rate: 2048
Me'Scope v4.0	To process acquired data To define the structural geometry To determine the natural frequencies, damping and animated mode shapes after the curve fitting process

The hammer gives a vibration signal via impact while the vibration signal response is detected by sensors attached to the gantry body. The four-channel detector collects the vibration response for analysis in a special program on the computer.

In this test a total of 32 points were selected on the machine gantry (Figure 6.9). Experimental Modal Analysis (EMA) with SIMO (single-input, multiple-output) modal identification algorithm was used. The impact hammer was connected to channel 1 of the dynamic analyser and a tri-axial accelerometer was connected to channels 2, 3 and 4. The impact hammer was set at point 5 as the fixed excitation. The experiment was carried out by fixing the impact hammer and roving the tri-axial accelerometer from point 1 until point 32. The sampling rate used was 2048 samples/sec with block size of 4096.

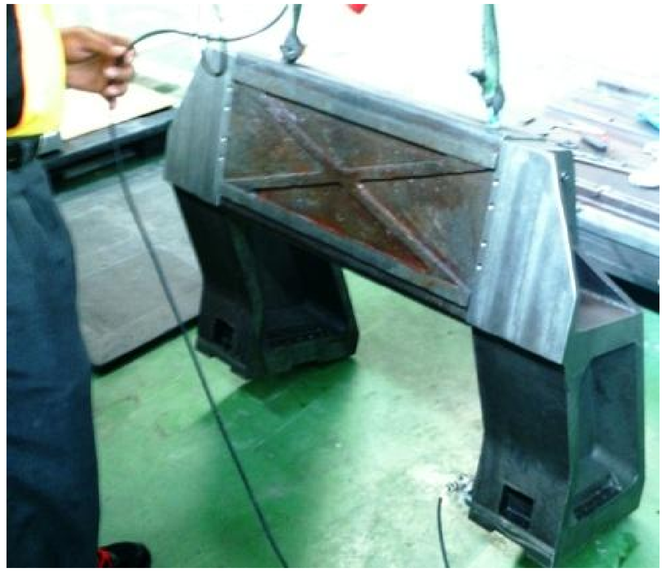

Figure 6.7: The hanging gantry

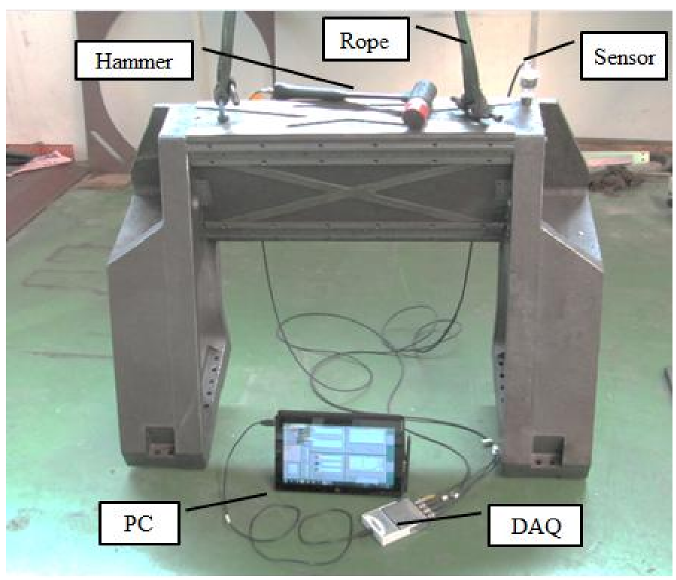

Figure 6.8: Experimental Setup and Equipment Involved:
Hammer 3-axis Accelerometer, DAQ and PC for Processing Data

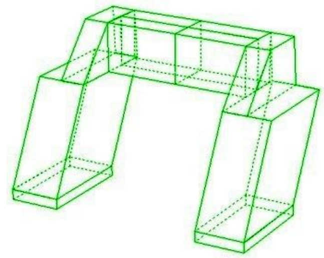

Structural Wire-mesh Model of machine tool gantry columns

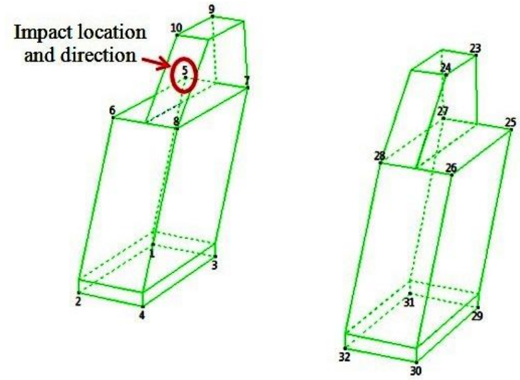

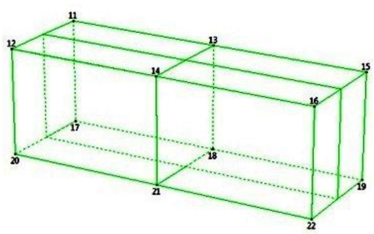

Measurement Points and Locations of crossbeam on the machine tool gantry

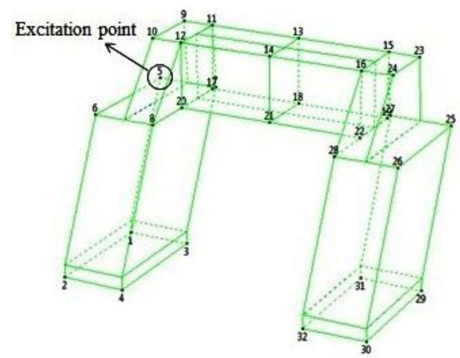

Figure 6.9: Excitation Points and Sensor Locations

The free natural frequency of the gantry's four modes of vibration was extracted via modal analysis in ANSYS software before the testing process. The experimental results were compared with the FE. The gantry's natural frequency results from modal analysis are shown in Table 6.3.

The results show that the mode shape of frequency response in both analyses (FE and EME) was the same. The FE results for the gantry compared with experimental modal analysis (EMA) are given in Table 6.3. It can be seen the results are close to each other, meaning that the modification process of the gantry design was acceptable.

Table 6.3: The Results of Finite Element and Experimental Modal Analysis of the Gantry

Mode shapes	FE (Finite Element) Modal Analysis	EMA (Experimental Modal Analysis)
Frequency of Mode1	117.50Hz	101Hz
Frequency of Mode2	179.55Hz	175Hz
Frequency of Mode3	238.38Hz	210Hz
Frequency of Mode4	333.38Hz	300Hz

Experimental and FE-predicted mode shapes and associated natural frequencies are compared in Table 6.4. According to these results, the FE model adequately represents the actual experimental structural behavior, meaning the model can be used to predict the structure's behavior.

6.5 Assembly of the CNC Gantry Machine

The CNC gantry machine was assembled in four steps as follows:

1. Investigated suitable standard components for the machine
2. Assembled the structure including the worktable and base columns
3. Assembled the gantry to the machine bed
4. Assembled the spindle carriage holder to the gantry

Table 6.4: Experimental and FE Mode Shapes and Corresponding Natural Frequencies

Mode No.	FE Predicted Mode Shapes	Experimental Mode Shapes	Error%
1	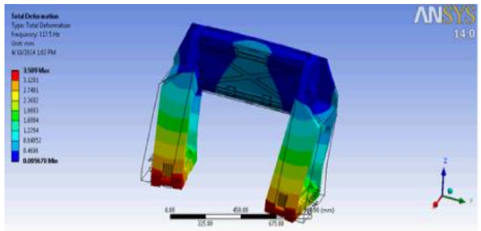 117.5 Hz	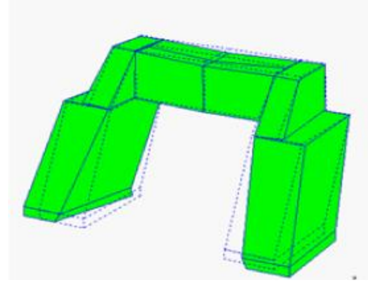 101Hz	16.33
2	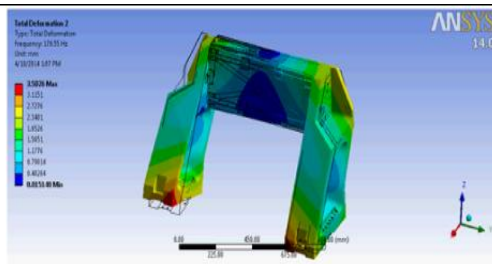 179.55 Hz	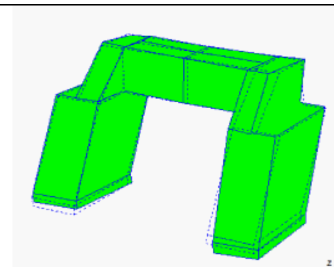 175 Hz	2.6
3	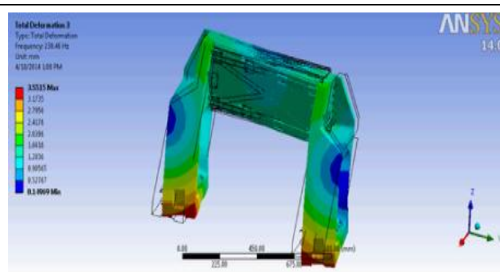 238.46 Hz	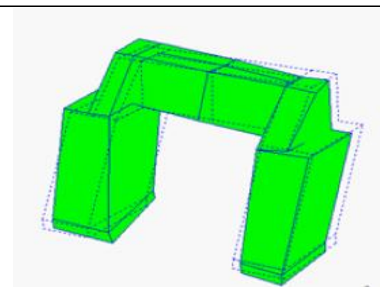 210 Hz	13.55
4	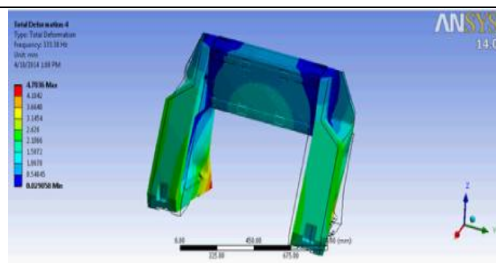 333.38 Hz	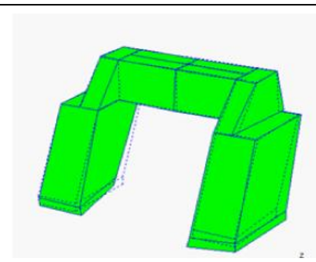 300 Hz	11.12

6.5.1 Standard Components of the CNC Machine

6.5.1.1 Selection of Guideways

The guideways are directly responsible for the precision and smoothness of the machine's axis movements. The required functional parameters for the longitudinal guideways are:

- Geometric perfection -- any guideway defect will be transferred into the moving part and create non-accuracy.

- Stiffness -- the guide must withstand the cutting forces and inertial loads without deformations.

- Wear resistance -- good frictional feature is valued for guideway surface or rolling elements.

- Sufficient toughness -- to withstand small impacts from the machining process, especially in case of highly interrupted cutting. Figure 2.21Based on the requirements, standard linear guides were chosen for the CNC gantry machine. Two types of linear guide were selected for this machine, namely "RGW25CC" and "RGW30CC" of the rolling circulation system type from HIWIN Company. This type of linear guide is suitable for heavy loads, as rollers are used instead of balls for circulation in the linear block.

Figure 6.10 shows the rolling type of linear guides and Figure 6.11 presents the RGW-CC/ RGW-HC series of linear guides. According to the information of standard CNC machine components from a linear guide catalogue, suitable linear guides were selected for the machine. The RGW25 CC was selected for the U-axis (the gantry) and Y- and Z-axis feed drive motions and RGW30 was chosen for the X-axis feed drive motion of the CNC gantry machine (Figure 6.12).

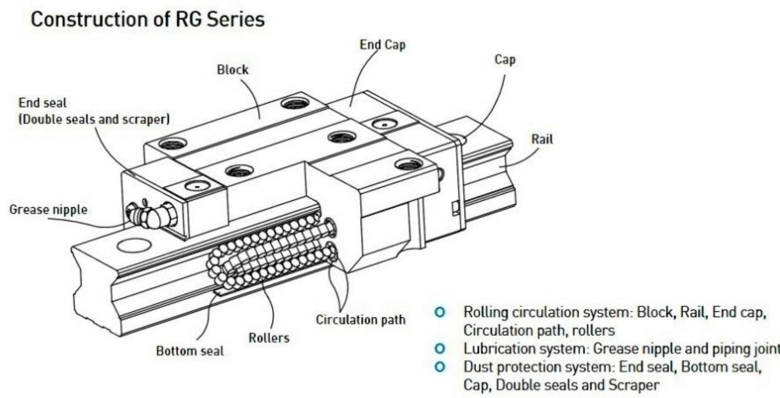

Figure 6.10: Rolling Circulation System in the RG Type of Linear guide (Hiwin technologies corp, 2011)

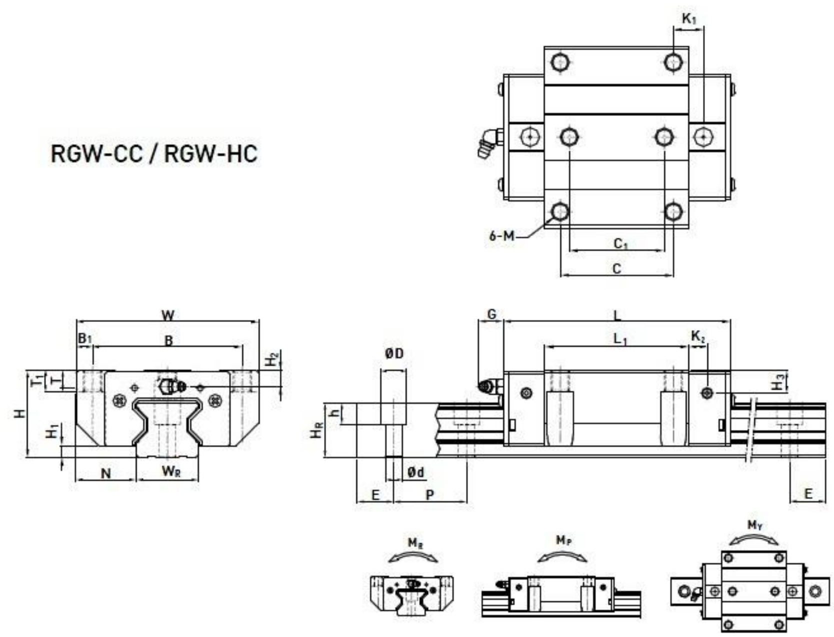

Figure 6.11: The RGW-CC/ RGW-HC Series of Linear Guide (Hiwin technologies corp, 2011)

The detailed specifications of the linear guides are provided in Table 6.5 and the technical information for these linear guides of two sizes, such as dimensions, basic dynamic load rating, basic static rating, static rated moment and calculation of applied loads are shown in [Appendix F]

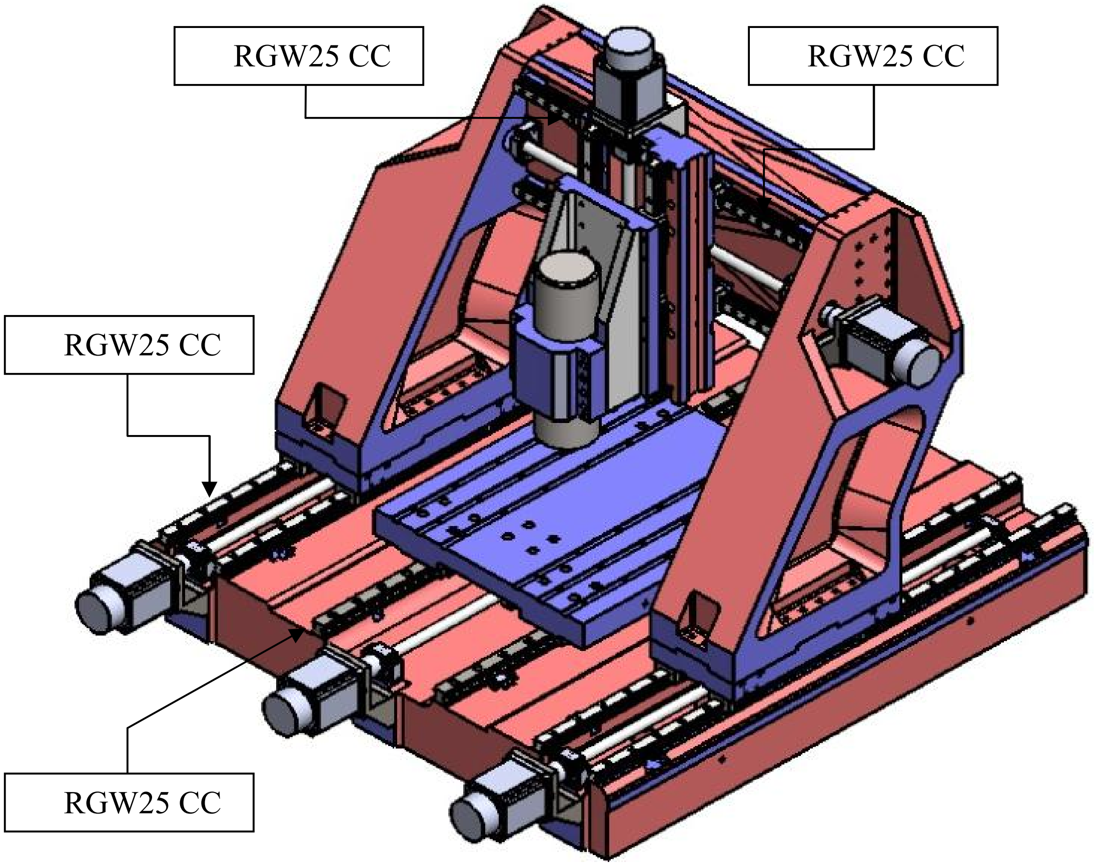

Figure 6.12: Installation of the Linear guides

Table 6.5: The Linear Guides Selected for the CNC Gantry Machine

	AXES	Model	W_R	H_R	W	L
1	X-axis	RGW30CC	28	28	90	109.8
2	U-axis	RGW25CC	23	23.6	70	97.9
3	Y-axis	RGW25CC	23	23.6	70	97.9
4	Z-axis	RGW25CC	23	23.6	70	97.9

6.5.1.2 **Selection of CNC Gantry Machine Ball screws**

To select the ball screw, the initial information of CNC machine feed drive motion must first be prepared based on two ball screw system installation schematics, namely horizontal and vertical systems. The horizontal system installation schematic is provided in Figure 6.13 and it shows the standard CNC gantry machine equipment, such as ball screw, motor and bearings. The vertical ball screw installation schematic is shown in Figure 6.14.

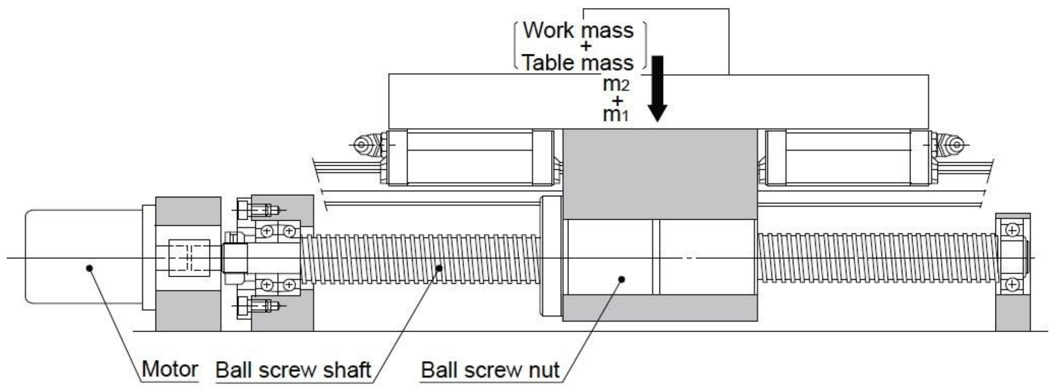

Figure 6.13: Horizontal Ball Screw Installation Schematic (THK A-679, 2014)

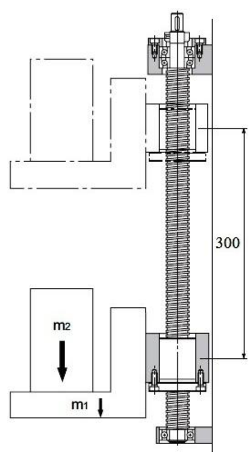

Figure 6.14: Vertical Ball Screw Installation Schematic (THK A-679, 2014)

The CNC machine feed drive information for selecting suitable ball screws of the axes based on the horizontal and vertical systems is prepared in Table 6.6.

Table 6.6: The Initial Information for CNC Gantry Machine Ball Screws

Options	Abb.	Z-axis	Y-axis	X-axis	U-axis
Table Mass	m_1	52kg	66kg	103 kg	627kg
Work Mass	m_2	15kg	52kg	20 kg	-
Stroke length	l_s	300mm	500mm	600 mm	600 mm
Maximum speed	V_{max}	0.2m/s	0.2m/s	0.2m/s	0.2m/s
Acceleration time	t_1	0.15s	0.15s	0.15s	0.15s
Deceleration time	t_3	0.15s	0.15s	0.15s	0.15s
Backlash	b	0.1mm	0.1mm	0.1mm	0.1mm
Positioning accuracy		0.06mm /1000mm	0.06mm /1000mm	0.06mm /1000mm	0.06mm /1000mm
Positioning Repeatability		0.05mm	0.05mm	0.05mm	0.05mm
Feed resolu-tion	s	0.01 mm/pulse	0.01 mm/pulse	0.01 mm/pulse	0.01 mm/pulse
Speed of AC servomotor	n	1000 min^{-1}	1500 min^{-1}	1500 min^{-1}	1500 min^{-1}
Moment of servomotor inertia	J_m	1×10^{-3} kg•m^2	1×10^{-3} kg•m^2	1×10^{-3} kg•m^2	1×10^{-3} kg•m^2
Frictional co-efficient	μ	0.003	0.003	0.003	0.003
Cutting force	f	825N	825N	825N	825N
Service life time	h	2000h	2000h	2000h	2000h

In this step, several important technical specifications of ball screws that can be used in CNC gantry machine assembly are investigated via standard methods offered by the manufacturer, including type of ball screw based on accuracy, shaft diameter, maximum axial load and buckling load of the ball screws. The maximum axial load and buckling load of the ball screws which will be selected must be compared with the permissible compressive and tensile load of the screw shaft for selection process approval.

1) **Selecting Lead Angle Accuracy**

According to the positioning accuracy requirement defined as ±0.06 mm/1000 mm, this precision can be obtained with a (C5) type ball screw, which comes in 30 µm for 500-630 mm long ball screws [Index Table A-696 THK].

1) Selecting Ball Screw Lead

For calculating ball screw lead, the maximum revolution of the servomotors and maximum speed of the machine feed drive system can be used. Ball screw lead is calculated by Eq. 6.1:

$$Ballscrew\ Lead = \frac{v=0.2m/s \times ls\ mm \times 60}{n\ mm^{-1}} = 4.8mm \tag{6.1}$$

$$X\ and\ Uaxes\ Lead = \frac{v=0.2m/s \times 600mm \times 60}{1500mm^{-1}} = 4.8mm$$

$$Y\ axis\ Lead = \frac{v=0.2m/s \times 500mm \times 60}{1500mm^{-1}} = 4mm$$

$$Z\ axis\ Lead = \frac{v=0.2m/s \times 300mm \times 60}{1000mm^{-1}} = 3.6mm$$

Based on the calculation, the standard selected lead can be 4 mm or longer for the Y- and Z-axis and 5 mm or longer for the X- and U-axis. Therefore, 5 mm of lead was selected for all axes. In addition, the ball screws were mounted onto the servomotor directly by coupling.

3) **Selecting a Screw Shaft Diameter**

In the standard catalog for ball screws with 5 mm of lead, several different diameters (14, 16, 20, 25 mm) [Index A-711THK] for shaft are offered by manufacturers. According to the design limitations, 20 mm diameter was selected for the CNC gantry machine axes, but the selected diameter must be supported by calculation. The maximum axial and buckling loads of the selected ball screw are calculated in the next step. Both loads must be less than the permissible load.

5) Calculating the Maximum Axial Load of the X-axis Ball screw

The calculation process will only be done for the X and U axes, but the results can be used for all axes because the condition of these two ball screws is more critical than the Y and Z axes.

Considering Table 6.6 where the cutting force (section 4.4.2) is f=825N, mass is m_1 =130 kg, work mass is m_2 = 20 kg, frictional coefficient of the guide surface is μ= 0.003, maximum speed is V_{max}=0.2 m/s, gravitational acceleration is g = 9.807 m/s^2 and acceleration time is t_1 = 0.15s; then the maximum acceleration and maximum axial load are obtained by Eq. 6.2-6.8 respectively:

$$\alpha = \frac{V_{max}}{t_1} \tag{6.2}$$

$$\alpha = \frac{0.2}{0.15} = 1.33 m/s^2$$

The maximum axial load during forward acceleration will be obtained by Eq. 6.3:

$$Fa_1 = \mu \times (m_1 + m_2)\, g + f + (m_1 + m_2) \times \alpha \tag{6.3}$$

$Fa_{1\,(X\ axis)}$ = 0.003× (130+20) ×9.807+825+ (130+20) ×1.33=1028.9N

$Fa_{1\,(U\ axis)}$ = 0.003× (627/2) ×9.807+825+ (627/2) ×1.33=1251.1N

The maximum axial load during forward uniform motion will be obtained by Eq. 6.4:

$$Fa_2 = \mu \times (m1 + m2)\ g + f \tag{6.4}$$

$Fa_{2\ (X\ axis)} = 0.003\times (130+20) \times 9.807+825 = 829.4N$

$Fa_{2\ (U\ axis)} = 0.003\times (627/2) \times 9.807+825 = 834.2N$

The maximum axial load during forward deceleration will be obtained by Eq. 6.5:

$$Fa_3 = \mu \times (m_1 + m_2) \times g + f - (m_1 + m_2) \times \alpha \tag{6.5}$$

$Fa_{3\ (X\ axis)} = 0.003\times (130+20) \times 9.807+825- (130+20) \times 1.33= 629.9N$

$Fa_{3\ (U\ axis)}\ 0.003\times (627/2) \times 9.807+825- (627/2) \times 1.33= 417.2N$

The maximum axial load during backward acceleration will be obtained by Eq. 6.6:

$$Fa_4 = -\mu \times (m_1 + m_2) \times g - f - (m_1 + m_2) \times \alpha \tag{6.6}$$

$Fa_{4\ (X\ axis)} = -0.003\times (130+20) \times 9.807-825- (130+20) \times 1.33= -1028.9\ N$

$Fa_{4\ (U\ axis)} = -0.003\times (627/2) \times 9.807-825- (627/2) \times 1.33= -1251.1\ N$

The maximum axial load during uniform backward motion will be obtained by Eq. 6.7:

$$Fa_5 = -\mu \times (m_1 + m_2) \times g - f \tag{6.7}$$

$Fa_{5\ (X\ axis)} = -0.003\times(130+20) \times 9.807- 825= -829.4\ N$

$Fa_{5\ (U\ axis)} = -0.003\times(627/2) \times 9.807- 825= -834.2\ N$

The maximum axial load during backward deceleration will be obtained by Eq. 6.8:

$$Fa_6 = -\mu \times (m_1 + m_2) \times g - f + (m_1 + m_2) \times \alpha \tag{6.8}$$

$Fa_{6\ (X\ axis)} = -0.003\times (130+20) \times 9.807- 825+ (130+20) \times 1.33= -629.91\ N$

$Fa_{6\ (U\ axis)} = -0.003\times (627/2) \times 9.807- 825+ (627/2) \times 1.33= -417.2\ N$

Thus, the maximum axial load applied on the ball screw is Fa max for $Fa_{1(X\ axis)} = 1028.9$ N and $Fa_{1\ (U\ axis)} = 1251.1$N.

6) Buckling Load on the Screw Shaft

According to the minor thread diameter of the ball screw (17.5 mm), the distance between two bearings $L_{a\ X\ axis} = 820$mm, $L_{a\ U\ axis} = 757$ mounted on the ball screw and the mounting method factor ($\eta_2=10$) related to the fixed-supported condition [Index A-712 THK], the buckling load (P1) will be obtained by Eq.6.9:

$$P_1 = \eta_1 \times \frac{d_1^4}{L_a^2} \times 10^4 \tag{6.9}$$

$$P_{1\ X\ axis} = 2 \times \frac{17.5^4}{820^2} \times 10^4 = 2789.6\text{N}$$

$$P_{1\ Uaxis} = 2 \times \frac{17.5^4}{757^2} \times 10^4 = 3273.3\text{N}$$

7) Permissible Compressive and Tensile Load of the Screw Shaft

According to the minor thread diameter of the ball screw shaft ($d_1 = 17.5$ mm), the permissible compressive and tensile load of the ball screw can be obtained from Eq. 6.11.

$$P_2 = 116 \times d_1^2 \tag{6.11}$$

$$P_2 = 116 \times (17.5)^2 = 35525\text{ N}$$

However, the calculation result shows that the maximum axial load ($Fa_{1(X\ axis)} = 1028.9$N, $Fa_{1\ (U\ axis)} = 1251.1$N) is less than buckling load ($P_{1(X\ axis)} = 2789.6$N, $P_{1\ (U\ axis)} = 3273.3$N). Also, this load is less than the permissible compressive and tensile load ($P_2=35525$N), hence these ball screws can work with no problem.

6.5.1.3 **Slelection of Ball Screw End Support**

The end supports are standard bearings that can facilitate easy ball screw installation. The two types of end support are fixed and free end support. Figure 6.15 shows a fixed end support and Figure 6.16 shows a free end support.

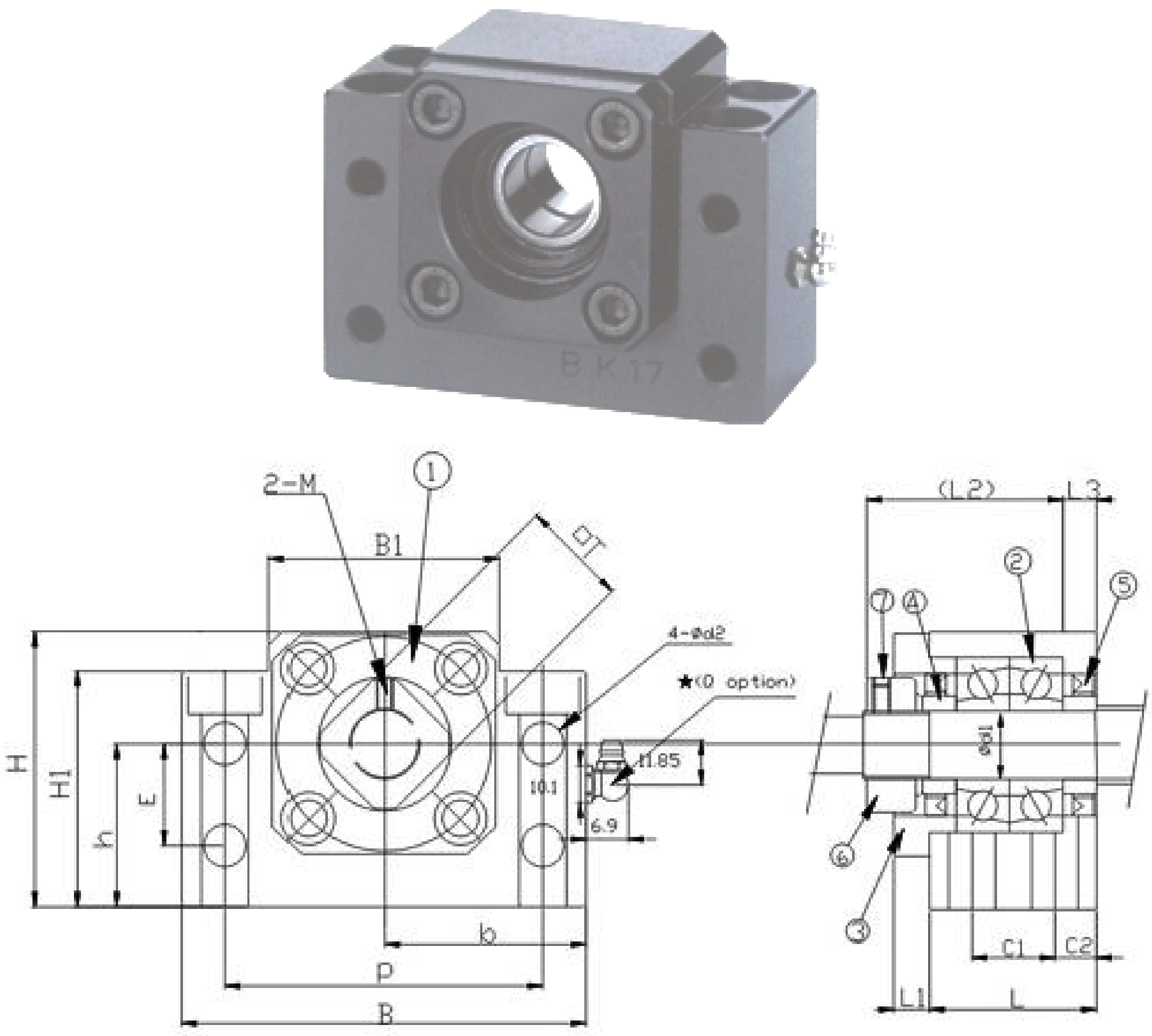

Figure 6.15: Fixed End Support (BK type) (Hiwin Company)

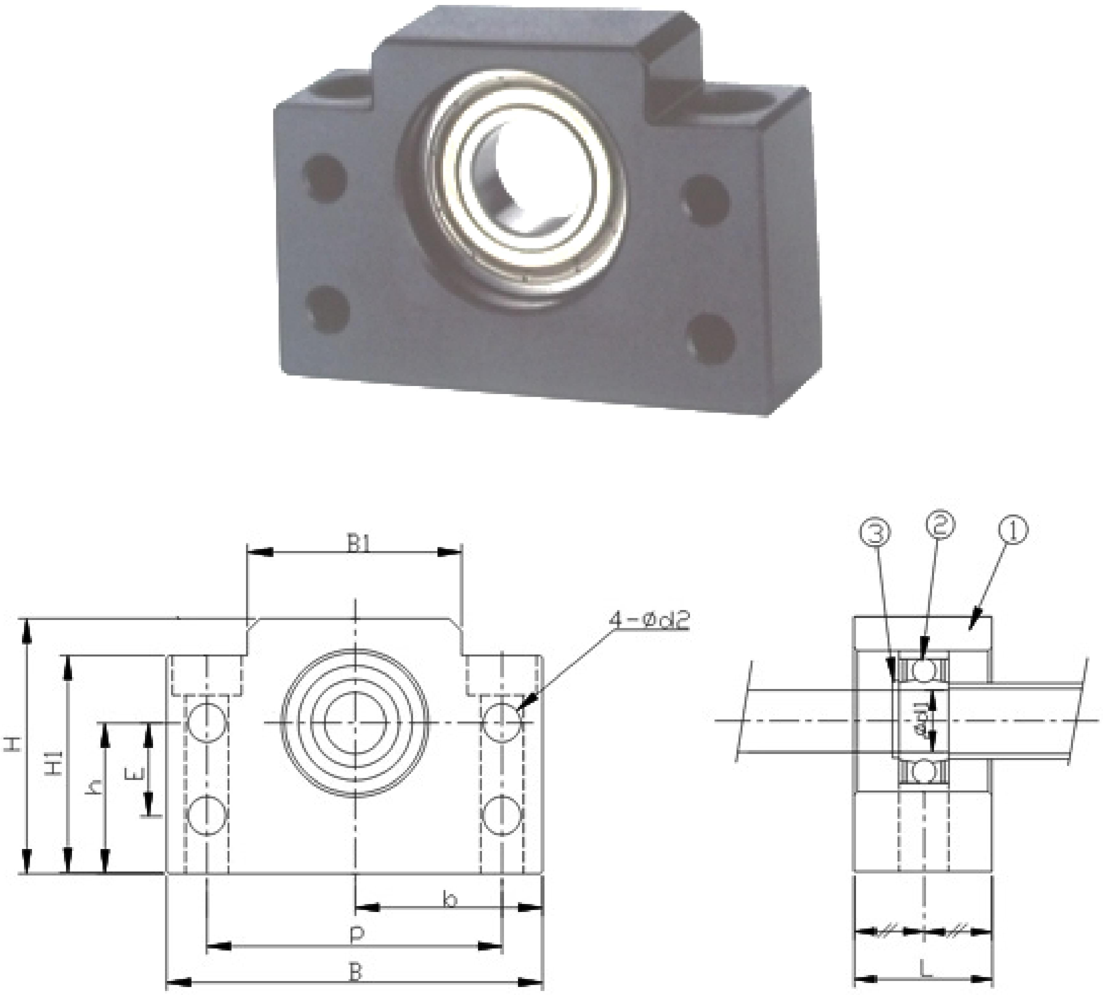

Figure 6.16 : Free End Support including Radial Bearing (BF type) (Hiwin Company)

BK 15 and BF 15 were selected for the ball screws of the CNC gantry machine axes. The internal diameter of these bearings is d1=15 mm. The technical information of these end supports is attached in [Appendix F].

6.5.2 **Assembling the Linear Guides, Ball screws, Column Bases and Worktable**

The machine structure assembly includes the machine bed, worktable and column bases. They were installed and aligned on the ball screw [the alignment documents are attached in the appendix]. Figure 6.17 shows the assembly of the CNC gantry machine structure.

Figure 6.17: Assembly of the New Type of CNC Gantry Machine Structure

6.5.3 **Assembly of gantry and machine structure**

Prior to assembling the gantry on the machine structure, the Y-axis linear guide and ball screw were aligned on the ground. Figure 6.18 illustrates the Y-axis feed drive motion linear guides and ball screw alignment [the alignment documents are attached to the Appendix]. Following Y-axis accessory alignment, the gantry was assembled to the machine structure (Figure 6.19)

6.5.4 Assembling the spindle carriage and holder to the gantry

In this step the spindle carriage is assembled to the gantry (Figure 6.20) and the spindle holder is assembled to the spindle carriage (Figure 6.21).

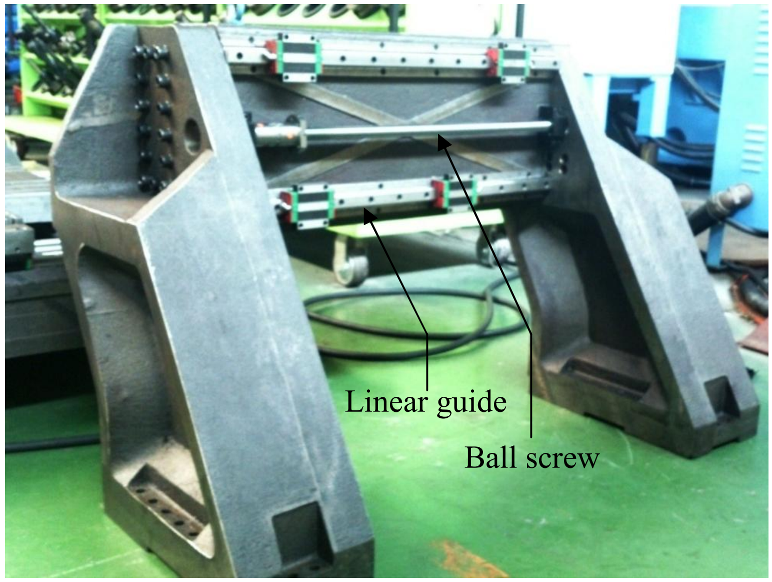

Figure 6.18 : Y-axis linear guide and ball screw alignment

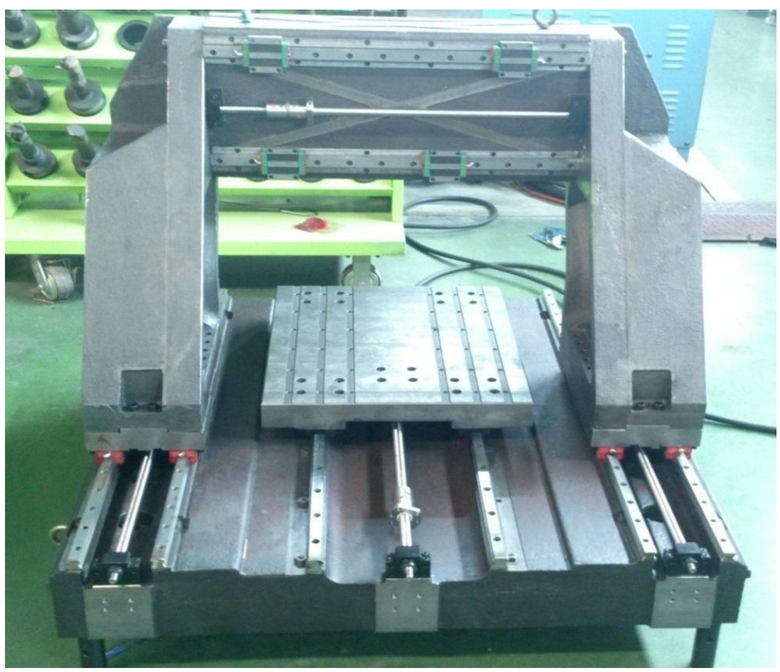

Figure 6.19 : Assembly of the entire gantry and structure

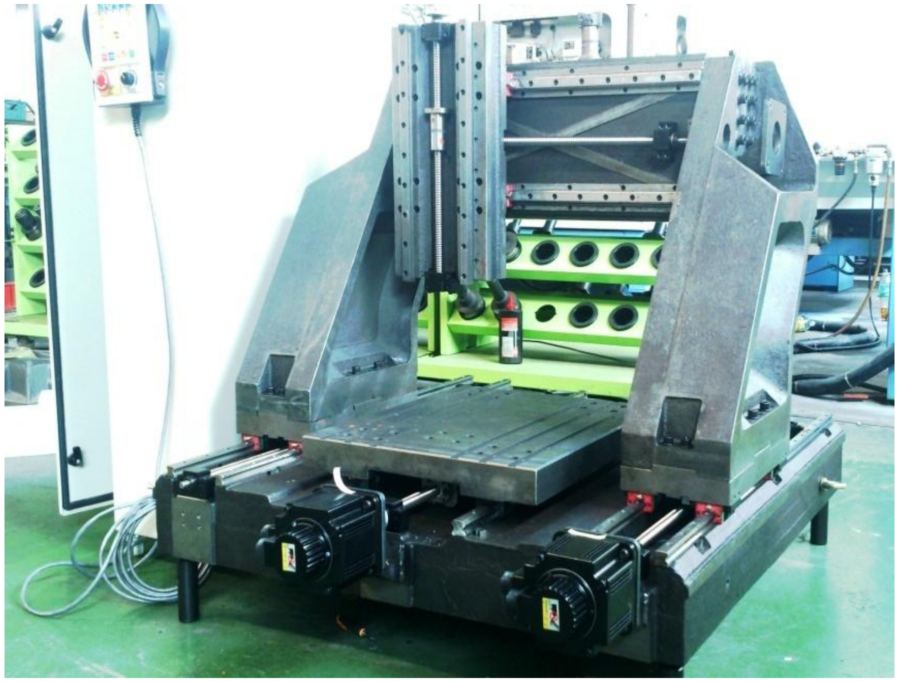

Figure 6.20 : Assembly of Y-axis part to the gantry

Figure 6.21: Assembly of Z-axis part to the Y-axis

Clearly, all axes are aligned [the alignment documents are attached to the appendix] and the machine's angular accuracy was investigated with relevant instruments [the quality control (Q.C) documents are attached to the appendix]. Finally, the CNC machine spindle was assembled to the holder (Figure 6.22).

6.6 CNC Gantry Machine Controller

The control for the new CNC gantry machine is a separate project undertaken by a Master's student from University of Malaya. However, the CNC controller selected for the machine is briefly introduced next. There are two types of CNC controller (PC- and PLC-based) The PC-based system has been chosen to control the machine because it is flexible and applicable in the academic field.

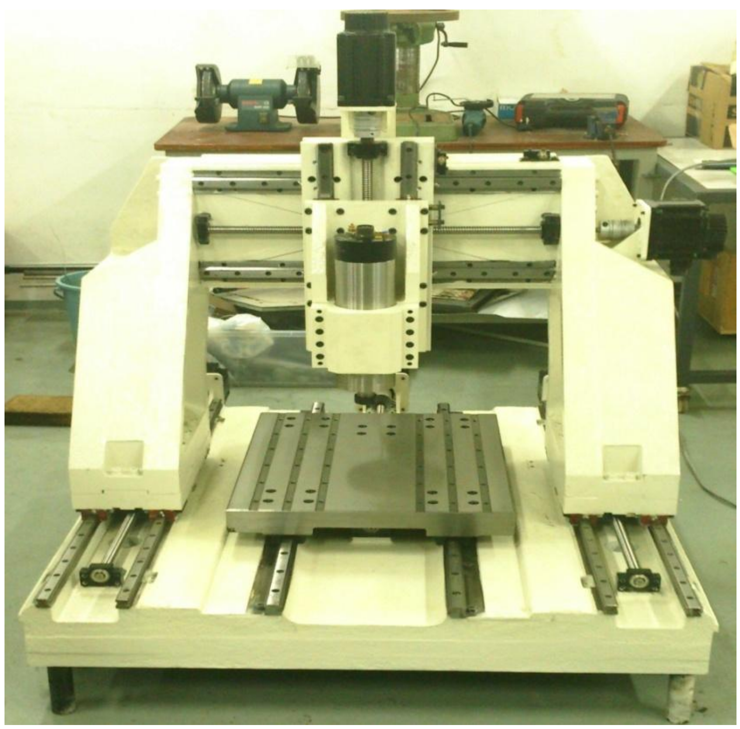

Figure 6.22 : Final Assembly of the New Type of CNC Machine(S. R. Besharati, et al., 2014)

The CENTROID is a PC-based controller, made in the USA, All-in-One-DC (Display Console) control card that is the pinnacle of CNC control technology. The CENTROID's CNC CPU, Servo Drive and PLC have been brought together in one amazing printed circuit card. The All-in-One-DC CNC control card combines the CENTROID's renowned digital DC Servo motor drive with its powerful MPU11 CNC CPU (the 11th in a long reliable linage of CNC CPU cards) and its own CNC PLC (designed with functions geared towards machine tools). The All-in-One-DC provides reliable operation with simple installation. A block diagram of the CENTROID for the CNC is shown in Figure 6.23 .

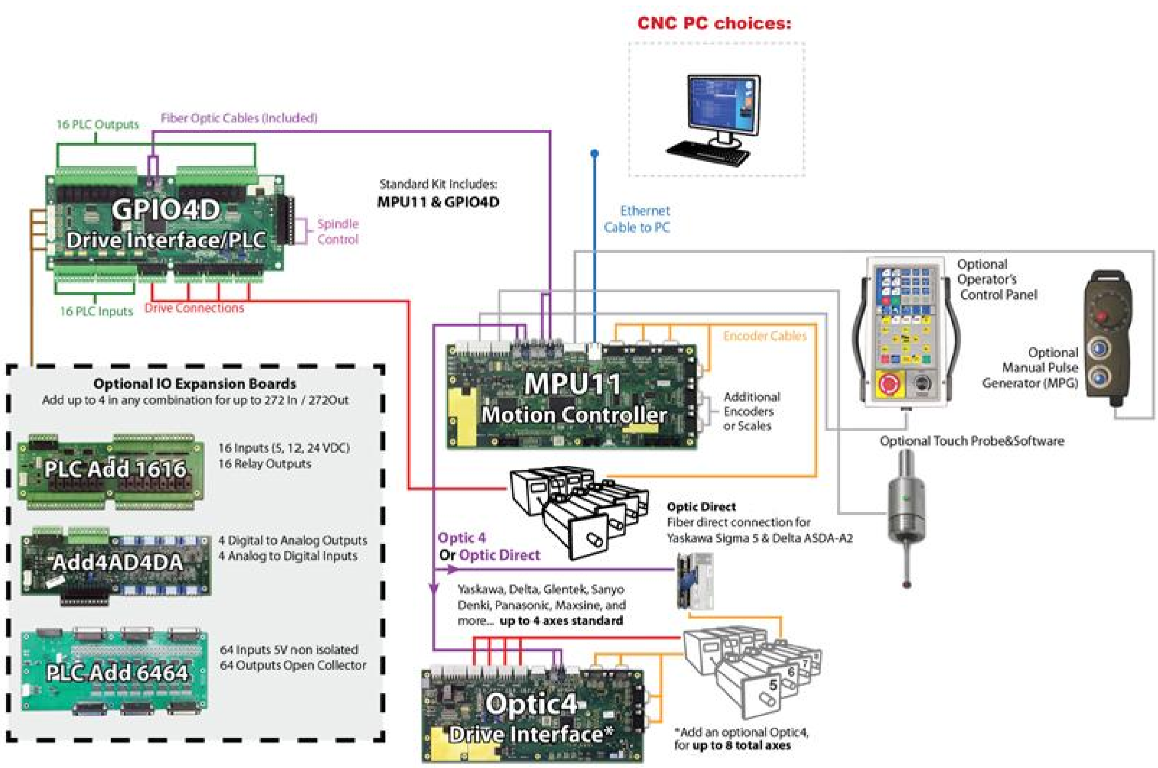

Figure 6.23: Block diagram of the CENTROID for the CNC (Centroid Controler, CNC Controler technology)

The CENTROID comes in several series, with the M39S series selected for this purpose. The M39S uses the CENTROID's new ALLIN1DC CNC control card along with a new

Windows 7-based Tablet PC that runs the reliable CNC11 software. The big screen and keyboard with built-in mouse pad. This combination yields many advantages and useful tools to make CNC jobs easier and faster to complete. In addition to all the great CENTROID features, CNC software can be used. Windows 7 familiarity helps with easy file transfers and networking, running Windows-compatible 3rd party software tools on the control, such as G code editors, CAD systems, CAD/CAM systems etc., using any PC-compatible keyboard or mouse, background editing, running another program while the machine is doing a job, Internet-based remote control for fast, accurate tech support and fast and reliable Solid State Hard Drive (no moving parts).Figure 6.24 shows the CENTROID CNC controller unit. The remote control panel can be hand-held or mounted and has clearly labeled controls for each axis and direction.

Figure 6.24 : The CENTROID CNC controller unit (Centroid Controler, CNC Controler technology)

There are buttons dedicated for spindle and coolant controls. Also, there is spindle speed override and feed rate override. Tool Check, Feed Hold, Cycle Start, Rapid override, Incremental and Continuous Jog and Single Block are additional capabilities. Extra auxiliary buttons are programmable for special applications. Figure 6.25 shows the control panel.

Figure 6.25: Control Panel for Common Milling Functions (Centroid Controler, CNC Controler technology)

The CNC controller was installed onto the CNC gantry machine at TPM by the Master’s student undertaking the machine controller project. The complete CNC gantry machine with DOBELE motion mechanism is shown in Figure 6.26.

Figure 6.26: New Type of CNC Gantry Machine with Double Motion Mechanism

6.7 Conclusion

The CNC gantry machine documents were prepared for manufacturing purposes. Pattern manufacturing, casting, machining and assembly were subsequently done.

The machine gantry was assembled for an experimental test. In order to ensure the accuracy of the FE model employed while obtaining the performance indices as well as during the optimization stage, experimental modal analysis was exploited. The first four natural frequencies and associated mode shapes were obtained and compared against the FE results. The experimental results showed that the average error was less than 11% between dynamic analysis and the experimental test. Before assembling the CNC gantry machine, standard components including linear guides, ball screws and bearing supports were selected. The CNC controller selected for the machine was introduced and explained. This CNC controller is able to control eight axes of the CNC gantry machine. Four linear motions were used via the X, U, Y and Z axes, two rotational motions can be used via the CY spindle if requested for future functions and two extra axes for other requirements. Considering the machine and CNC controller's capabilities, the final machine configuration can be LLLLRR. The CNC controller selected for the machine was introduced. The final thesis conclusions are discussed in the next chapter.

CAPTER 7

7 THESIS CONCLUSION

7.1 Conclusion

The CNC gantry machine is presently one of the most valuable machine tools for industrial manufacturing purposes, as it is useful in many fields. The CNC gantry machine is functional for machining large and long components. Up until now, two such machine types have been invented. The first type has a moving worktable and fixed gantry while the second type has a moving gantry and fixed worktable. Both types have advantages and disadvantages.

In this study, for improving the specifications and applications of the existing types of CNC gantry machine, a new, innovative CNC gantry machine has been proposed. The advantage of the proposed gantry machine is the reciprocal (simultaneous) motion of the gantry and worktable, which is called a double motion mechanism.

Initially, the double motion mechanism was designed as a rack and pinion system. Due to backlash (gear mechanism error), a new anti-backlash gear mechanism comprising three spur gears and a rack was explained and a nonlinear dynamic system model was introduced to gain insight into the system's dynamic behavior. Validity of the concept of eliminating backlash was examined using Motion Analysis (MA) in Solidworks software. The mesh stiffness of mated gears and rack-pinion was evaluated with the finite element method and was considered by solving a motion equation. Assuming that the gear and rack teeth are rigid and static transmission error is negligible, the total transmission error of the new mechanism will be near zero.

The minimum amount of preload at which the system remains anti-backlash while operating was estimated. This depends on applied torque, external load on the rack and varied mesh stiffness behavior. Total system transmission error was obtained by solving the differential equation of motion using the Runge-Kutta method.

However, due to difficulties in manufacturing gear systems, a new double motion mechanism was proposed with a ball screw system. Three different designs of a new CNC gantry machine were then proposed.

To evaluate the behavior and modifications of the gantry with desired characteristics, modal analysis was performed. The gantry's natural frequency was 102.36 Hz, but it changed to 131.95 Hz when the material was changed to steel. The results showed that the gantry was improving.

A modification process was done to increase stiffness. The minimum natural frequency of the gantry increased slightly to above 200 Hz. The deformation of the CNC machine's spindle tip was around 10 microns at 11530 rpm. This modification process increased the gantry's weight. The results indicated that the Z-axis position has no significant effect on the gantry's dynamic behavior.

The range of machining materials and cutting force was calculated for the selected spindle. According to the static analysis results, cutting force did not have any negative effect on machining precision. It appeared that the new CNC gantry machine could function at 11,530 rpm in the machining process without a problem. The final design of the new CNC gantry machine was patented as a special gantry machine of three different types.

After modifying the third gantry machine design, the fourth design was obtained.

Since the gantry weight increased during modification, a new crossbeam was designed to decrease the weight. Hence, a fifth design was proposed by changing the gantry cross-beam. This design reduced the gantry's weight by up to 3.8%.

The increasing natural frequency of the gantry during design modification affected complexity and increased the weight and manufacturing cost of the gantry. For these reasons, five different gantry designs were selected and compared. Four parameters, namely the first four natural mode frequencies, total deformation under mechanical forces and weight and manufacturing cost were considered for the comparison. One was selected among five designs using a mathematical method. The selected design was optimized by MOGA (multi-objective genetic algorithm) in ANSYS software.

In the optimization process, the gantry's natural frequency was maximized and total deformation against mechanical forces and its weight was minimized.

The CNC gantry machine documents for manufacturing were prepared. Subsequently, pattern manufacturing, casting, machining and assembly were done, respectively.

To evaluate and verify the design and analysis processes, an experimental test was performed with related instruments. The experimental results indicated that that the average error was less than 11% between the dynamic analysis and experimental test.

Before assembling the CNC gantry machine, standard components, such as linear guides, ball screws and bearing supports were selected, after which they were assembled respectively.

The selected CNC machine controller was introduced and explained. This CNC controller is able to control eight axes of the CNC gantry machine. Four linear motions were used through the X, U, Y and Z axes, two rotational motions will be used via the CY spindle if requested for future functions and two extra axes can be applied for other requirements. In light of the capabilities of the machine and CNC controller, the final machine configuration can be LLLLRR. The controller is a separate project done by a Master's student at University of Malaya. To control the machine, there are two types of CNC controller (PC- and PLC-based). A PC-based system, the CENTROID, was chosen for machine control because it is flexible. Ultimately, the complete, new type of CNC gantry machine was presented in this study.

7.2 Directions for Future Research

Considering the advantages of the double motion mechanism discussed in this study, other advantages should be investigated further in future research works. The topics addressed in this case, such as improving "machine efficiency," simplifying "machine manufacturing," and decreasing the "total cost" of the machine, need more investigation as well. In addition, considering the capability of the CNC gantry machine designed and made in three types, experimentally testing the machining process of the new type (simultaneously moving gantry and worktable) and comparing the results with other types, is subject to potential, significant new research.

7.3 Future Works

According to the machine tool errors which affected the machining accuracy, such as geometric and thermal errors, for finding the geometrical errors, the metrological test of the machine will be needed in the future works. In addition the total thermal errors of spindle of the CNC gantry machine must be evaluated due to the large amounts of the heat, which is produced by its high-speed revolution.

7.4 Recommendation

Throughout this project, the researcher worked very hard to innovate, design and prototype the machine. This is an original type of gantry machine, which will significantly affect the machining process and CNC gantry machine manufacturing. Therefore, recommends commercializing this machine.

REFERENCES

158 JIXIE, Available from: "158jixie.com/news-detail/256/256275.html".

Abdel-Malek, et al. . (2000). Algorithm based decision support system for the concerted selection of equipment in machining/assembly cells. *International journal of production research, 38*(2), 323-339.

Abdi, M. (2009). Fuzzy multi-criteria decision model for evaluating reconfigurable machines. *International Journal of Production Economics, 117*(1), 1-15.

Allan, et al. (1980). The determination of minimum pre-load torque for anti-backlash gears in a positional servomechanism. *IEEE Transactions on Industrial Electronics and Control Instrumentation, 27*(1), 26-29.

Altintas, et al. (2011). *Machine tool feed drives*. Paper presented at the CIRP Annals-Manufacturing Technology.

Altintas, Y. (2000). Manufacturing Automation *Cambridge University Press, London, UK 2000*.

Andersson, J. (2003). *Applications of a multi-objective genetic algorithm to engineering design problems.* Paper presented at the Evolutionary Multi-Criterion Optimization.

Arnold, et al. (2001). The recent history of the machine tool industry and the effects of technological change. *Münchner Betriebswirtschaftliche Beiträge, 14*.

Atlanta Drive Systems Inc. (2013). Ultra-High Precision Rack & Pinion Drive Systems Available From: "atlantadrives.com" (Vol. (800) pp. 505-1715).

Ayağ, et al. (2006). A fuzzy AHP approach to evaluating machine tool alternatives. *Journal of intelligent manufacturing, 17*(2), 179-190.

Ayağ, et al. (2011). An intelligent approach to machine tool selection through fuzzy analytic network process. *Journal of intelligent manufacturing, 22*(2), 163-177.

Ayağ, Z. (2007). A hybrid approach to machine-tool selection through AHP and simulation. *International journal of production research, 45*(9), 2029-2050.

B. Sencer, et al. (2008). Feed optimization for five-axis CNC machine tools with drive constraints. *Machine Tools*.

Baker, et al. (2002). Finite Elem. Anal. Des.*, 38* 1029-1046.

Baradie, et al. (1991). Statistical theory of machine tool stability. *Journal of Engineering Manufacture 205*, 195–206.

Be´zier, P. (1972). *Numerical Control Mathematics and Applications*: Wiley & Sons.

Boadway, et al. (1984). *Welfare economics*: Pablised by "Blackwell Oxford".

Bohez, Erik LJ. (2002). Five-axis milling machine tool kinematic chain design and analysis. *International Journal of Machine Tools and Manufacture, 42*(4), 505-520.

Boyuan, et al. (2001). Drive Chain Return difference analysis and estimate of spring-loaded anti-backlash Gear. *Mechanical Design, 6*, 40-42.

Brauer, et al. (2003). *Investigation of transmission error, friction and wear in anti-backlash involute gear transmissions: A finite element approach.* (C815490 Ph.D.), Kungliga Tekniska Hogskolan (Sweden), Ann Arbor.

Budak, E. (2004). A decision support system for machine tool selection. *Journal of Manufacturing Technology Management, 15*(1), 101-109.

C. W. Cairnes, Anti-backlash gearing "US Patent 2,663,198, 1953". (1953).

C.Yongqing, W. Xunchi. (Jan. 2007). Finite element analysis of 2400t gantry crane. *Construction machinery*, 7-73.

Centroid Controler, Available From: "centroidcnc.com/cnc_technology.html". (CNC Controler technology).
Chen, et al. (2000). A ballscrew drive mechanism with piezo-electric nut for preload and motion control. *International Journal of Machine Tools and Manufacture, 40*(4), 513-526.
Cheng, et al. (2005). Design of a six-axis high precision machine tool and its application in machining aspherical optical mirrors. *International Journal of Machine Tools and Manufacture, 45*(9), 1085-1094.
Clark, Norman G. Roller Pinion System -- The Linear Drive Alternative
corp., Hiwin technologies. (2011). HIWIN "Motion control and System Technology".
Dağdeviren, M. (2008). Decision making in equipment selection: an integrated approach with AHP and PROMETHEE. *Journal of intelligent manufacturing, 19*(4), 397-406.
Deb, K. (2001). *Multi-objective optimization using evolutionary algorithms*: John Wiley & Sons Chichester.
Dhupia, et al. (2007). Dynamics of the arch-type reconfigurable machine tool. *International Journal of Machine Tools and Manufacture, 47*(2), 326-334.
Díaz, et al. (2009). Machines for the Aeronautical Industry *Machine Tools for High Performance Machining,Springer, 399-420*.
E. Budak, Y. Altintas. (1994). Peripheral milling conditions for improved dimensional accuracy. *International Journal of Machine Tools and Manufacture, 34*(7), 907-918.
EI Baradie, et al. (1976). Dynamic acceptance tests for horizontal milling machine based on a statistical theory of machine tool chatter. *Journal of Engineering for Industry Transactions of ASME, 98*(3), 919-929.
EI Baradie, M.A. . (1993). Statistical analysis of the dynamic cutting coefficients and machine tool stability. *Journal of Engineering for Industry Transactions of ASME 115, 115*(2), 205-215.
Eman, et al. (1983). Modal analysis of machine tool structures based on experimental data. *Journal of manufacturing science and engineering, 105*(4), 282-287.
Eritenel, et al. (2012). Three-dimensional nonlinear vibration of gear pairs. *Journal of Sound and Vibration, 331*(15), 3628-3648.
Erkorkmaz, et al. (2010). *Precision machine tool X–Y stage utilizing a planar air bearing arrangement*. Paper presented at the CIRP Annals - Manufacturing Technology.
Ertuğrul, et al. (2007). Fuzzy Multi-criteria Decision Making Method for Machine Selection. *Analysis and Design of Intelligent Systems using Soft Computing Techniques, 41*, 638-648.
FJunlian. (2006). Bridge crane girder optimization design based on ANSYS. *Science & Technology Association Forum*, 21-22.
G-H Tzeng, J-J Huang. (2011). Multi-attribute decision making: methods and applications. *CRC Press*.
Gill-Jeong, Cheon. (2007). WITHDRAWN: Nonlinear behavior analysis of spur gear pairs with a one-way clutch. *Journal of Sound and Vibration, 304*(1), 18-30.
Gimenez, et al. (1995). A Step by Step Approach to the Dynamic Behavior of Centreless Grinding Machines. *Int. J. Maeh. Tools Manuf, 35*(9), 1291-1307.

Gordon, et al. (2005). Development of a high-speed CNC cutting machine using linear motors. *Journal of Materials Processing Technology, 166*(3), 321-329.
Graham, T.Smith. (2008). *Cutting tool technology*: Published by "Springer".
Gregory, et al. (1963). *Dynamic behaviour of spur gears*. Paper presented at the Proceedings of the institution of mechanical engineers.
Grierson, Donald E. (2008). Pareto multi-criteria decision making. *Advanced Engineering Informatics, 22*(3), 371-384.
Guan, et al. (2010). *Analysis and optimization of crossbeam of gantry machining center.* Paper presented at the Information Engineering and Computer Science (ICIECS), 2010 2nd International Conference on.
Guang-Yuan, et al. (1985). Fuzzy optimum design of structures. *Engineering optimization, 8*(4), 291-300.
Guoming, L. I. (2001). Calculation and analysis of double gear's inherent frequency. *Electro-Mechanical Engineering, 3*, 11-12.
Hale, et al. (1994). Design of anti-backlash transmissions for precision position control systems. *Precision Engineering, 16*(4), 244-258.
Han, et al. (2011). *Structural analysis and optimization on crossbeam of heavy NC gantry moving boring & milling machine.* Paper presented at the Electronic and Mechanical Engineering and Information Technology (EMEIT), 2011 International Conference on.
He, et al. (2007). Effect of sliding friction on the dynamics of spur gear pair with realistic time-varying stiffness. *Journal of Sound and Vibration, 301*(3), 927-949.
Held, M. (1991). A geometry-based investigation of the tool path generation for zigzag pocket machining. *The Visual Computer, 7*(5-6), 296-308.
Hiwin Company, Available From: "hiwin.com/html/ball%20screws/support_units.html".
Hiwin technologies corp, available from "hiwin.com". (2011). Motion control and System Technology.
Holland, J. M. (1975). Adaptation in natural and artificial systems. *Ann Arbor*.
Imasaki, Naoki. (1995). *Adaptive control of robot manipulators with anti-backlash gears.* Paper presented at the Robotics and Automation, 1995. Proceedings., 1995 IEEE International Conference on.
IOS. (2001). Industrial automation systems and integration – Numerical control of machines – Coordinate system and motion nomenclature (Vol. International Standard ISO 84).
Jianrun, et al. (2005). Dynamic optimization design of 5 axis numerical control gantry machining center. *China Mechanical Engineering, 16*(21), 1949-1953.
K Fansen, Y Junyi (1999). Fuzzy dynamic response analysis of machine tool structure *International Journal of Machine Tools and Manufacture, 39*(12), 1993–2002.
Kahraman, et al. (1991a). Interactions between time-varying mesh stiffness and clearance non-linearities in a geared system. *Journal of Sound and Vibration, 146*(1), 135-156.
Kahraman, et al. (1991b). Non-linear dynamics of a geared rotor-bearing system with multiple clearances. *Journal of Sound and Vibration, 144*(3), 469-506.
Khuberyan, et al. (1972). Analysis of the arches of underground powerhouses with crane-supporting beams. *Hydrotechnical Construction, 6*(4), 376-382.

Konak, et al. (2006). Multi-objective optimization using genetic algorithms: A tutorial. *Reliability Engineering & System Safety, 91*(9), 992-1007.
Koza, J. R. (1992). *Genetic programming: on the programming of computers by means of natural selection* (Vol. 1): MIT press.
Krishna, V. (2009). Structural optimization using ANSYS classic and radial basis function based response surface models.
Krulewich, Debra A. (1998). Temperature integration model and measurement point selection for thermally induced machine tool errors. *Mechatronics, 8*(4), 395-412.
Kwon, et al. (2004). *Rate loop control based on torque compensation in anti-backlash geared servo system.* Paper presented at the American Control Conference, 2004. Proceedings of the 2004.
L.N, et al. (2009). *machine tools for high performance machining*: Springer press.
Lamikiz, et al. (2009). Machine Tool Performance and Precision. In L. N. López de Lacalle & A. Lamikiz (Eds.), *Machine Tools for High Performance Machining* (pp. 219-260): Springer London.
Lan, T.-S. (2010). Parametric deduction optimization for surface roughness. *American Journal of Applied Sciences, 7*(9), 12-48.
Lassâad Walha, et al. (2009). Nonlinear dynamics of a two-stage gear system with mesh stiffness fluctuation, bearing flexibility and backlash. *Mechanism and Machine Theory, 44*, 1058–1069.
Lee, et al. (2006). Dynamic analysis of a mesoscale machine tool. *Journal of manufacturing science and engineering, 128*(1), 194-203.
Lei, et al. (2007). Double ballbar test for the rotary axes of five-axis CNC machine tools. *International Journal of Machine Tools & Manufacture, 47* 273–285.
Li, S. (2007). Finite element analyses for contact strength and bending strength of a pair of spur gears with machining errors, assembly errors and tooth modifications. *Mechanism and Machine Theory, 42*(1), 88-114.
Lin, et al. (1996). Evaluation of machine selection by the AHP method. *Journal of Materials Processing Technology, 57*(3), 253-258.
Lin, et al. (2001). CAD-based CMM dimensional inspection path planning – a generic algorithm. *Robotica, 19*(2), 137-148.
Liu, et al. (1995). Damping Identification of the Mechanical Structural Jiont Surface. *Journal of Vibration and Shock, 14* (3), 61-65.
Liu, et al. (2014). Structural optimization of the cross-beam of a gantry machine tool based on grey relational analysis. *Structural and Multidisciplinary Optimization, 50*, 297-311.
Liu Fang, et al. (2007). Dynamic finite element analysis of the high speed gantry machine center GMC3000[J],. *Modern Manufacturing Engineering*, 113-116.
LNL de Lacalle, et al. (2009). Machine Tools for Removal Processes: A General View *Machine Tools for High Performance Machining, Springer, 1-45* .
Luo, et al. (2006). Design and research of the structural of cross-rail in the planer type machines. *Mech Electr Eng Technol, 35*(3), 45-47.
Macrotec Machine tools LTD, Available from. *google.com.my/?gws_rd=cr&ei=e0U1VKuTC4WSuAT9jIJ4#q=Macrotec+Machine+tools+LTD*.

Maia, et al. (1997). *Theoretical and Experimental Modal Analysis (John Wiley & Sons, New York, NY, USA 1997).*
Majid, Kamal Izeldeen. (1974). Optimum design of structures.
Mayr, et al. (2014). *Cutting Fluid Influence on Thermal Behavior of 5-axis Machine Tools*. Paper presented at the Procedia CIRP.
Ming, et al. (2010, 26-28 June 2010). *Influence of different boundary constraint in static and dynamic analysis.* Paper presented at the Mechanic Automation and Control Engineering (MACE), 2010 International Conference on.
Moradi, et al. (2012). Analysis of nonlinear oscillations in spur gear pairs with approximated modelling of backlash nonlinearity. *Mechanism and Machine Theory, 51*, 14-31.
Myers, A. (2005). Measurement techniques for determining the static stiffness of foundations for machine tools. *Journal of Physics, 13*, 410–413.
Nevzat Özgüven, et al. (1988). Mathematical models used in gear dynamics—a review. *Journal of Sound and Vibration, 121*(3), 383-411.
Newmana, et al. (2008). Strategic advantages of interoperability for global manufacturing using CNC technology. *Robotics and Computer-Integrated Manufacturing, 24* 699–708.
Ni Xiangyang, et al. (2005). features analysis of 5 axis numerical control gantry machining center[J]. *Precision with the automation*, 12-16.
Nsk Ltd. (2013). *Patent Application Titled "Rack and Pinion Steering Gear Unit" Under Review.* NewsRx, Atlanta. ABI/INFORM Complete database.
O. Durán, J. Aguilo. (2008). Computer-aided machine-tool selection based on a Fuzzy-AHP approach. *Expert Systems with Applications, 34*(3), 1787-1794.
Önüt, et al. (2008). A hybrid fuzzy MCDM approach to machine tool selection. *Journal of intelligent manufacturing, 19*(4), 443-453.
Padmanabhan, et al. (1996). Analysis of periodically forced nonlinear Hill's oscillator with application to a geared system. *The Journal of the Acoustical Society of America, 99*(1), 324-334.
Patwari, et al. (2010). Dynamic modal analysis of vertical machining centre components. *Advances in Acoustics and Vibration*.
Pedrammehr, et al. (2012). Modal analysis of the milling machine structure through FEM and experimental test. *Advanced Materials Research, 383*, 6717-6721.
Qi, J.. (2010). Machine tool selection model based on fuzzy MCDM approach. *In,. IEEE*, 282-285.
R. Kalantari, M. Saadat Foomani. (2009). Backlash Nonlinearity Modeling and Adaptive Controller Design for an Electromechanical Power Transmission System. *Sharif University of Technology, 16*, 463-469.
Ra Jeev S. (2003). *Vibration analysis of machine tool structure*. Paper presented at the VIII International Conference on Recent Advances in Structure Dynamics, Southampton, UK.
Rahman, et al. (2001.Bazul,). Non-conventional materials for machine tool structures. *Int. J. JSME., 44: 1-11, DOI: 10.1299/jsmec.44.1*.
Rao, S. S. (2009). *Engineering optimization: theory and practice*: John Wiley & Sons.
Rechenberg, Evolutionsstrategie. (1973). Optimierung technischer Systeme nach Prinzipien der biologischen Evolution. *Frommann-Holzboog Verlag, Stuttgart*.

Reuleaux. (2007). Theoretische Kinematik. *Verlag Dr. Müller.*

S. Haranath, et al. (1987). Dynamic analysis of machine tool column with layer finite element approach. *International Journal of Machine Tools and Maunfacture*, 27-41.

S. R. Besharati, et al. (2012). Malaysia Patent No. PI 2012 701279. Patent title "Gear Backlash Compensation Mechanism (GBCM) in Rack and Pinion System", UMCIC.

S. R. Besharati, et al. (2013). Malaysia Patent No. PI 2013 001205 Patent title "A Newly Efficient, Accurate and Precision CNC Gantry Machine with Double Motion", UMCIC.

S. R. Besharati, et al. (2014). Malaysia Patent No. PCT: UM.TNC2/UMCIC/603/536. Patent title "A Newly Efficient, Accurate and Precision CNC Gantry Machine with Double Motion", UMCIC.

S. R. Besharati, M. Hamdi. (2011). Malaysia Patent No. PI 2011700176. Patent title "CNC Double Motion Gantry Machine", UMCIC.

Saaty, T. L. (1980). *The analytic hierarchy process* New York: McGraw-Hill.

Sematech. (1997). Computer Integrated Manufacturing (CIM) Application Framework Specification *2706 Montopolis Drive, Austin, TX 78741 U.S.A* (Vol. 7, pp. 17-21).

Shevchuk, S.A. (2008). Cast iron in machine tools. *Russian. Eng. Rese., 29*, 901-903.

Shibly, H. A. (1988). *Performance evaluation and efficient control of trajectory following robots with friction and backlash. (Volumes I and II).* (8813721 Ph.D.), Carnegie Mellon University, Ann Arbor. ProQuest Dissertations & Theses Full Text database.

Shim, et al. (2008). Reduction of PTO rattle noise of an agricultural tractor using an anti-backlash gear. *Biosystems engineering, 100*(3), 346-354.

Shubo Xu, et al. (2010). Study on Modeling Simulation of Long-span Gantry NC Machining Center Structure. *International Conference of Digital Manufacturing & Automation*.

Sorokin, et al. (2001). Analysis and optimization of energy flows in structures composed of beam elements–Part I: problem formulation and solution technique. *Structural and Multidisciplinary Optimization, 22*(1), 3-11.

Stamper, et al. (1997). *Optimization of a three DOF translational platform for well-conditioned workspace.* Paper presented at the Robotics and Automation.

Stecke, K. E. (1983). Formulation and solution of nonlinear integer production planning problems for flexible manufacturing systems. *Management Science, 29*(3), 273-288.

T. Murakami, et al. (2006). Damping and tribological properties of Fe–Si–C cast iron prepared using various heat treatments. *Materials Science and Engineering, 2006*, 113 - 119.

Taha, et al. (2012). A hybrid fuzzy AHP-PROMETHEE decision support system for machine tool selection in flexible manufacturing cell. *Journal of intelligent manufacturing, 23*(6), 2137-2149.

Taha, et al. (2011). A fuzzy AHP-ANN-based decision support system for machine tool selection in a flexible manufacturing cell. *The International Journal of Advanced Manufacturing Technology, 57*(5-8), 719-733.

Teo, et al. (2007). Dynamic modeling and adaptive control of a H-type gantry stage. *Mechatronics, 17*, 361–367.

THK A-679, Available from "THK.com". (2014). Ballscrew *General Catalog*.

Tlusty, M. Polacek. (1963). Proceedings of the ASME International Research in Production Engineering. *Pittsburgh, USA*, 465-474.

Tobias, S.A. . (1965). Machine Tool Vibration. *Wiley New York*.

Tomasent, Availabl from: . "news.thomasnet.com/fullstory/CNC-Machining-Finishing-System-offers-5-axis-flexibility-565843"

Tsann-Huei Chang, et al. (2004). US 10/011,487. Patent title" Gantry type hybrid parallel linkage five-axis machine tool".

Van Dooren, R. (2001). Comments on non-linear dynamics of gear-pair systems with periodic stiffness and backlash. *Journal of Sound and Vibration, 244*(5), 899-903.

Verl, et al. (2014). Double nut ballscrew with improved operating characteristics. *CIRP Annals - Manufacturing Technology, 63*(1), 361-364.

W.T. Lei, Y.Y. Hsu. (2002). Accuracy test of five-axis CNC machine tool with 3D probe–ball. Part I: design and modeling. *International Journal of Machine Tools & Manufacture, 42*, 1153–1162.

Wang, et al. (2003). Survey of nonlinear vibration of gear transmission systems. *Applied Mechanics Reviews, 56*(3), 309-329.

Wang, et al. (2007). Dynamics of a hypoid gear pair considering the effects of time-varying mesh parameters and backlash nonlinearity. *Journal of Sound and Vibration, 308*(1), 302-329.

Wang XY, et al. (2009). The topological optimization design and analysis for gantry machine tool crossbeam component. *Manuf Technol Mach Tool, 56(11)*, 64–67.

Weule, et al. (2003). *Structural Optimization of Machine Tools including the static and dynamic Workspace Behavior.* Paper presented at the The 36th cirp-international seminar on manufacturing systems.

Wu, et al. (2003). Thermal analysis for the feed drive system of a CNC machine center. *International Journal of Machine Tools and Manufacture, 43*(15), 1521-1528.

Xiuheng, et al. (2010). *Structural Optimization on Beam Parts of Bridge Type Five Axis Linkage Gantry Machining Center.* Paper presented at the Intelligent Networks and Intelligent Systems (ICINIS), 2010 3rd International Conference on.

Xu, et al. (2006). Making CNC machine tools more open, interoperable and intelligent—a review of the technologies. *Computers in Industry, 57* 141–152.

Y. Guan, et al. (2010). Finite Element Analysis of Five-Axis Gantry Milling Machine Main Structure. *International Conference on E-Product E-Service and E-Entertainment (ICEEE),*, 1-4.

Y.T. Ic, et al. (2012). Development of a component-based machining centre selection model using AHP.

Y.T. İç, M. Yurdakul. (2009). Development of a decision support system for machining center selection. *Expert Systems with Applications, 36*(2), 3505-3513.

Yanhua, S. (2009). Beam Parts Dynamic Characteristic Analyse of GS5200 Gantry Five-face Machining Center. *Manufacturing Technology & Machine Tool, 5*, 32.

Z. Ayağ, et al. (2006). A fuzzy AHP approach to evaluating machine tool alternatives. *Journal of intelligent manufacturing, 17*(2), 179-190.

Z. Taha, S. Rostam. (2011). A hybrid fuzzy AHP-PROMETHEE decision support system for machine tool selection in flexible manufacturing cell. *Journal of intelligent manufacturing*, 1-13.

Z.Dewen, et al. (2006). Bridge type crane girders deflection analysis based on the finite element method. *Water transportation science research,*, A-7.
Zhang, et al. (1996). The theory of response analysis of fuzzy stochastic dynamical systems with a single degree of freedom. *Science Press*.
Zhao, et al. (2008). Structural bionic design for high-speed machine tool working table based on distribution rules of leaf veins. *SCIENCE CHINA Technological Sciences, 55*(8), 2091-2098.
Zhao, et al. (2011). Lightweight Design and Verification of Gantry Machining Center Crossbeam Based on Structural Bionics. *Journal of Bionic Engineering, 8*(2), 201-206.
Zrnić, et al. (2014). Dynamic responses of a gantry crane system due to a moving body considered as moving oscillator. *Archives of Civil and Mechanical Engineering*(0).

APPENDICES

Appendix A:

All Drawing and Manufacturing Components of CNC Gantry Machine Design with overall Dimension

No.	Name	App. No.	DWG No.
1	Machine Bed	A1	Machine Bed-CNC-G.M-V1-No.01-1
2	Left Column	A2	Left Column-CNC-G.M-V1-No.02-1
3	Right Column	A3	Right Column-CNC-G.M-V1-No.03-1
4	Crossbeam	A4	Crossbeam-CNC-G.M-V1-No.04-1
5	Worktable	A5	Worktable-CNC-G.M-V1-No.05-1
6	Spindle Carriage	A6	Spindle Carriage-CNC-G.M-V1-No.06-1
7	Spindle Holder	A7	Spindle Holder-CNC-G.M-V1-No.07-1
8	Spindle Clamp	A8	Spindle Clamp-CNC-G.M-V1-No.08-1
9	Column Bases	A9	Column Bases-CNC-G.M-V1-No.09-2
10	Y&U axis Servomotor Bases	A10	Y&U axis Servomotor Bases -CNC-G.M-V1-No.10-3
11	X axis Servomotor Bases	A11	X axis Servomotor Bases-CNC-G.M-V1-No.11-1
12	Z axis Servomotor Bases	A12	Z axis Servomotor Bases -CNC-G.M-V1-No.12-1
13	Nut Holder(U,X axis)	A13	Nut Holder(U&X axis)-CNC-G.M-V1-No.13-3
14	Nut Holder(Y axis)	A14	Nut Holder(Y axis)-CNC-G.M-V1-No.14-1
15	Nut Holder(Z axis)	A15	Nut Holder(Z axis)-CNC-G.M-V1-No.15-1
16	Cover	A16	Cover-CNC-G.M-V1-No.16-1

Appendix B:

Report of Quality Control of Casting Process (from SIRIM Company)

No.	Name	App. No.	DWG No.
1	Base X	B1	Machine Bed-CNC-G.M-V1-No.01-1
2	Test	B2	Left Column-CNC-G.M-V1-No.02-1
3	Test2	B3	Right Column-CNC-G.M-V1-No.03-1
4	MD1	B4	Crossbeam-CNC-G.M-V1-No.04-1
5	Y beam Base	B5	Worktable-CNC-G.M-V1-No.05-1
6	MD2XT	B6	Spindle Carriage-CNC-G.M-V1-No.06-1
7	MD3-2	B7	Spindle Holder-CNC-G.M-V1-No.07-1
8	MD3	B8	Spindle Clamp-CNC-G.M-V1-No.08-1
9	G1-1&G1-2	B9	Column Bases-CNC-G.M-V1-No.09-2

Appendix C:

Report of Quality Control from Machining Process by TPM (Technology Park Malaysia)

No.	Name	App. No.	DWG No.
1	Machine Bed	C1	Machine Bed-CNC-G.M-V1-No.01-1
2	Left Column	C2	Left Column-CNC-G.M-V1-No.02-1
3	Right Column	C3	Right Column-CNC-G.M-V1-No.03-1
4	Crossbeam	C4	Crossbeam-CNC-G.M-V1-No.04-1
5	Worktable	C5	Worktable-CNC-G.M-V1-No.05-1
6	Spindle Carriage	C6	Spindle Carriage-CNC-G.M-V1-No.06-1
7	Spindle Holder	C7	Spindle Holder-CNC-G.M-V1-No.07-1
8	Spindle Clamp	C8	Spindle Clamp-CNC-G.M-V1-No.08-1
9	Column Bases	C9	Column Bases-CNC-G.M-V1-No.09-2

Appendix D:

Assembly Drawing of the CNC Gantry Machine

No.	Name	App. No.	DWG No.
1	New type of CNC gantry Machine	D1	CNC-G.M-V1-Ass.01
2	Machine Structure	D2	CNC-G.M-V1-Ass.02
3	Gantry	D3	CNC-G.M-V1-Ass.03
4	Y and Z Axes of Gan-try Machine	D4	CNC-G.M-V1-Ass.04
5	Spindle Carriage	D5	CNC-G.M-V1-Ass.05
6	Spindle Holder	D6	CNC-G.M-V1-Ass.06

Appendix E:

Report of Quality Control from Assembly and Alignment Process by TPM (Technology Park Malaysia)

No.	Name	App. No.	DWG No.
1	Q.C. 1	E1	Ballscrew Alignment
2	Q.C. 2	E2	Linear guides Alignment
3	Q.C. 3	E3	Squareness X-Y
4	Q.C. 4	E4	Squareness X-Z

Appendix F:

Specifications and Calculation of Standard CNC Machine Components

No.	Name	App. No.	DWG No.
1	List of the components	F1	Standard components
2	Calculation	F2	Applied load of linear guide
3	Specification	F3	End support (BK)
4	Specification	F4	End support (BF)
5	Specification	F5	Servomotor

Standards CNC Gantry Machine Components

Name	Specification	quantity	documents
Servomotor	Delta type	4	Attachment
Spindle	Up to 24000 RPM	1	Attachment
Linear guide X axis	28/1150	1	Attachment
Linear guide U axis	23/1150	2	Attachment
Linear guide Y axis	23/700	1	Attachment
Linear guide Z axis	23/510	1	Attachment
Ballscrew X axis	20/760	1	Attachment
Ballscrew U axis	20/995	2	Attachment
Ballscrew Y axis	20/636	1	Attachment
Ballscrew Z axis	20/470	1	Attachment
Flexible Coupling	16/48	5	standard
Bearing	BK -15	5	Attachment
Bearing	Bf -15	5	Attachment
M8	L=40	28	Structure linearguide
M6	L=30	76	Gantry linearguide
M6	L=50	6	Workable bearings
M6	L=50	12	Gantry bearings
M8	L=40	12	For lock linear
M8	L=35	12	Motor brackets

M8	L=25	20	Motors
M6	L=25	24	For lock linear
M12	L=80	28	Crossbeam to columns
M12	L=95	12	Columns to base
M12	L=80	8	Columns to base
M12	L=60	8	Columns to base
M10	L=65	4	Gantry motor Bracket
M6 ***	L=20	16	Crossbeam lock
M6	L=30	24	Crossbeam linearguide
M6	L=50	6	Crossbeam bearing
M6	L=25	32	Crossbeam lock
M6	L=30	18	Y axis linear
M8	L=50	16	Y axis linear block
M8	L=55	4	Y axis nut holder
M6	L=30	6	Y axis nut
M6	L=50	6	Y axis bearing
M8	L=30	4	Y axis motor bracket
M6	L=25	8	Y axis linear lock
M4	L=15	16	Lock linear
M8	L=40	16	Z axis linear block
M8	L=50	4	Z axis nut holder
M6	L=30	6	Z axis nut

M6	L=25	8	Z axis linear lock
M8	L=55	8	Spindle holder
M8	L=45	32	Base linear block
M10	L=60	8	Base nut holder
M6	L=25	16	Base lock block
M6	L=30	16	Base lock block
M6 ***	L=15	16	Base lock block
M10	L=65	16	Worktable linear block
M10	L=70	4	Worktable Nut holder
M6	L=30	6	Nut to holder
M10	30	12	Lock linear columns
Lifting eye bolt M12		4	structure
Lifting eye bolt M10		2	Y axis body
Lifting eye bolt M12		2	crossbeam
Lifting eye bolt M12		2	gantries
Lifting eye bolt M10		1	Z axis body
Lock linear	D=11	12	Worktable linear
Lock linear	D=9	12	Y axis linear
Pine d=10	L=50	4	Spindle holder

Applied load of linear guide

The applied load of linear guide of CNC gantry X axis motion have been calculated in the following as an example to verifying of selected standard LM guides. The Figure 1 is shown the X axis LM guide installation schematic. This is radial condition of installation of LM guides and CNC gantry machine worktable will be considered for the evaluation process. The Figure 2 is shown real dimension of the X axis LM position. The requirement information of calculation is shown if Table 1. Two types of linear guide have selected for this machine “RGW25CC”, “RGW30CC” of rolling circulation system type from HIWIN Company (Table 2)

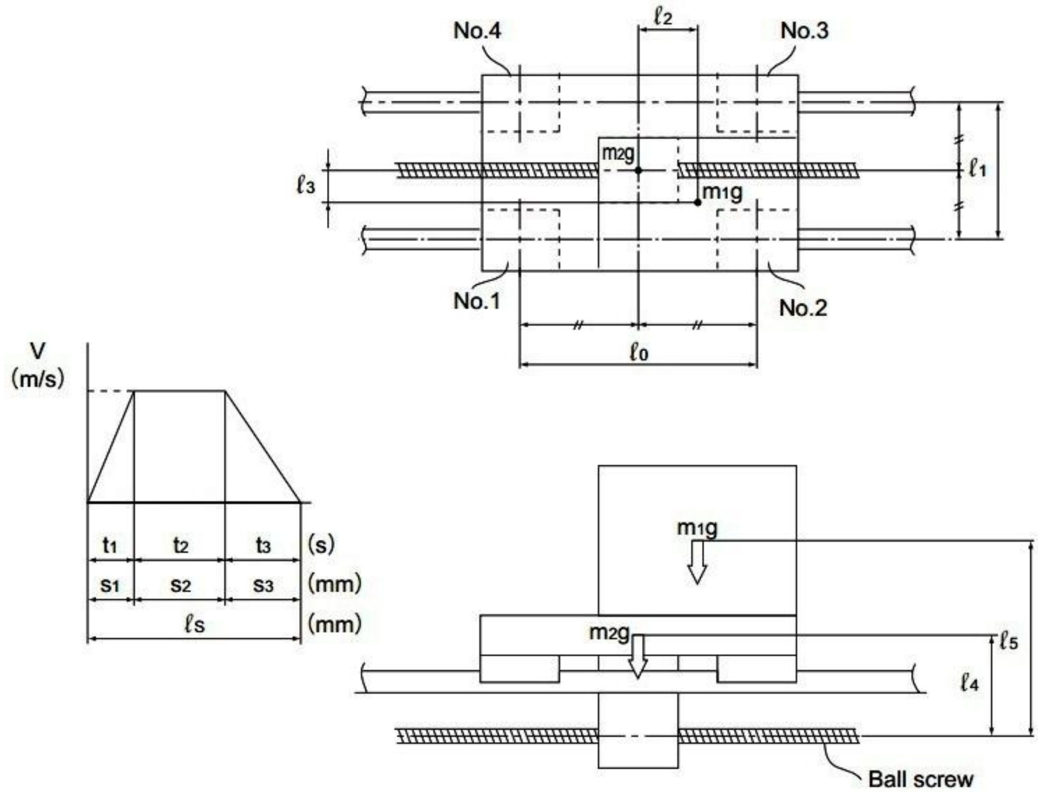

Figure 1: The X axis LM guide installation schematic

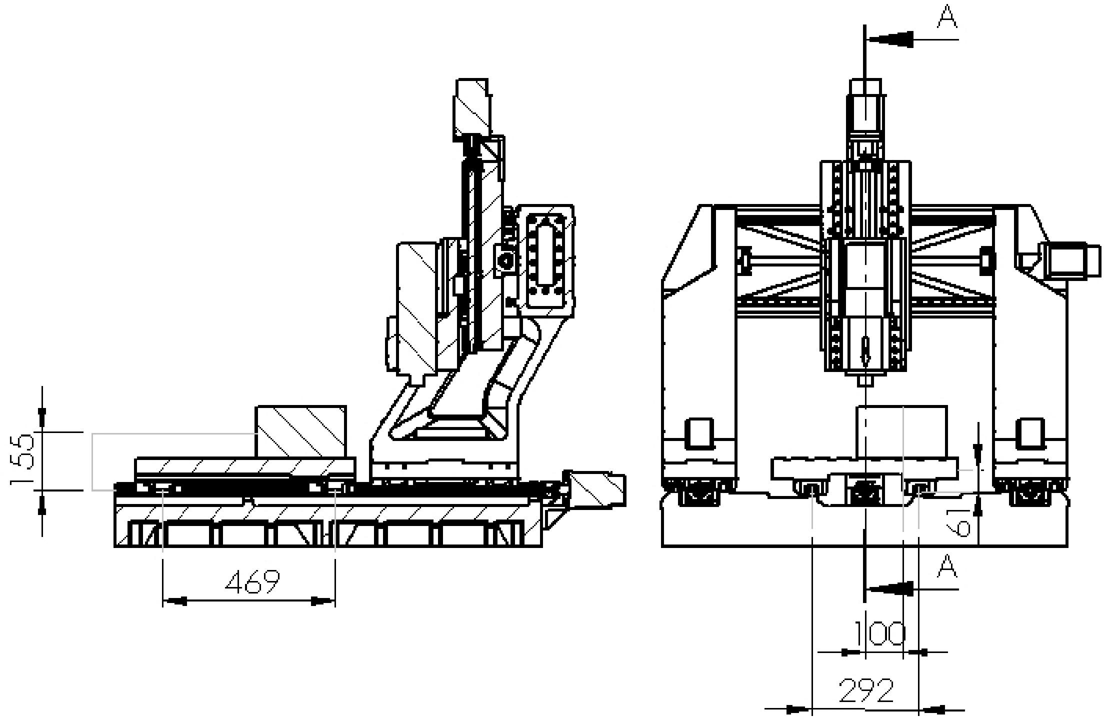

Figure 2: Linear guide positions

Table 1: Requirement Information for Calculation

Options	Abb.	Z axis	Y axis	X axis	U axis
Table Mass	m_1	52kg	66kg	103 kg	627kg
Work Mass	m_2	15kg	52kg	20 kg	-
Stroke length	l_s	300mm	500mm	600 mm	600 mm
Maximum speed	V_{max}	0.2m/s	0.2m/s	0.2m/s	0.2m/s
Acceleration time	t_1	0.15s	0.15s	0.15s	0.15s
Deceleration time	t_3	0.15s	0.15s	0.15s	0.15s

1- The applied load (radial direction) can be obtained via Eq. (7.1). Where, m_1=103, m_2=20, V=0.2 m/s, t_1, t3=0.15s, t_2=2.7, acceleration a_1=10 m/s^2 , a_3=1.333 m/s^2, ls= 600 mm. According Figure 2, l_0=469 mm, l1=292 mm, l_2=150 mm, l_3=100 mm, l_4=85(61) mm, l_5=155.

$$P1 = +\frac{m_{1\times g}}{4} - \frac{m_{1\times g\times l_2}}{2\times l_0} + \frac{m_{1\times g\times l_3}}{2\times l_1} + \frac{m_{2\times g}}{4} = 337.1 \quad (7.1\text{ a})$$

$$P2 = +\frac{m_{1\times g}}{4} + \frac{m_{1\times g\times l_2}}{2\times l_0} + \frac{m_{1\times g\times l_3}}{2\times l_1} + \frac{m_{2\times g}}{4} = 666.5 \quad (7.1\text{ b})$$

$$P3 = +\frac{m_{1\times g}}{4} + \frac{m_{1\times g\times l_2}}{2\times l_0} - \frac{m_{1\times g\times l_3}}{2\times l_1} + \frac{m_{2\times g}}{4} = 313.9 \quad (7.1\text{ c})$$

$$\mathrm{P3} = +\frac{m_{1\times g}}{4} - \frac{m_{1\times g\times l_2}}{2\times l_0} - \frac{m_{1\times g\times l_3}}{2\times l_1} + \frac{m_{2\times g}}{4} = -15.5 \quad (7.1\text{ d})$$

2- The applied load (radial direction) during leftward acceleration can be obtained via Eq. (7.2):

$$Pla_1 = p_1 - \frac{m_1 \times a_1 \times l_5}{2\times l_0} - \frac{m_2 \times a_1 \times l_4}{2\times l_0} = 153.9 \quad (7.2\text{ a})$$

$$Pla_2 = p_2 + \frac{m_1 \times a_1 \times l_5}{2\times l_0} + \frac{m_2 \times a_1 \times l_4}{2\times l_0} = 849.7 \quad (7.2\text{ b})$$

$$Pla_3 = p_3 + \frac{m_1 \times a_1 \times l_5}{2\times l_0} + \frac{m_2 \times a_1 \times l_4}{2\times l_0} = 497.1 \quad (7.2\text{ c})$$

$$Pla_4 = p_4 - \frac{m_1 \times a_1 \times l_5}{2\times l_0} - \frac{m_2 \times a_1 \times l_4}{2\times l_0} = 198.7 \quad (7.2\text{ d})$$

3- The applied load (lateral direction) can be obtained via Eq. (7.3):

$$Ptla_1 = -\frac{m_1 \times a_1 \times l_3}{2\times l_0} = -170.2 \quad (7.3\text{ a})$$

$$Ptla_2 = +\frac{m_1 \times a_1 \times l_3}{2\times l_0} = 170.2 \quad (7.3\text{ b})$$

$$Ptla_3 = +\frac{m_1 \times a_1 \times l_3}{2\times l_0} = 170.2 \quad (7.3\text{ c})$$

$$Ptla_4 = -\frac{m_1 \times a_1 \times l_3}{2\times l_0} = -170.2 \quad (7.3\text{ d})$$

4- The applied load (lateral direction) during leftward acceleration can be obtained via Eq. (7.4):

$$Pld_1 = P1 + \frac{m_1 \times a_3 \times l_5}{2 \times l_0} + \frac{m_2 \times a_3 \times l_4}{2 \times l_0} = 362.1 \quad (7.4\ a)$$

$$Pld_2 = P2 - \frac{m_1 \times a_3 \times l_5}{2 \times l_0} - \frac{m_2 \times a_3 \times l_4}{2 \times l_0} = 642.2N \quad (7.4\ b)$$

$$Pld_3 = P3 - \frac{m_1 \times a_3 \times l_5}{2 \times l_0} - \frac{m_2 \times a_3 \times l_4}{2 \times l_0} = 289.6N \quad (7.4\ c)$$

$$Pld_4 = P4 + \frac{m_1 \times a_3 \times l_5}{2 \times l_0} + \frac{m_2 \times a_3 \times l_4}{2 \times l_0} = 8.8N \quad (7.4\ d)$$

5- The applied load (lateral direction) via Eq. (7.5):

$$Ptld_1 = +\frac{m_1 \times a_3 \times l_3}{2 \times l_0} = +14.6 \quad (7.5\ a)$$

$$Ptld_2 = -\frac{m_1 \times a_3 \times l_3}{2 \times l_0} = -14.6 \quad (7.5\ b)$$

$$Ptld_3 = -\frac{m_1 \times a_3 \times l_3}{2 \times l_0} = -14.6 \quad (7.5\ c)$$

$$Ptld_4 = +\frac{m_1 \times a_3 \times l_3}{2 \times l_0} = +14.6 \quad (7.5\ d)$$

6- The applied load (lateral direction) during rightward acceleration can be obtained via Eq. (7.6):

$$Pra_1 = P1 + \frac{m_1 \times a_3 \times l_5}{2 \times l_0} + \frac{m_2 \times a_3 \times l_4}{2 \times l_0} = 361.4 \quad (7.6\ a)$$

$$Pra_2 = P2 - \frac{m_1 \times a_3 \times l_5}{2 \times l_0} - \frac{m_2 \times a_3 \times l_4}{2 \times l_0} = 642.2 \quad (7.6\ b)$$

$$Pra_3 = P3 - \frac{m_1 \times a_3 \times l_5}{2 \times l_0} - \frac{m_2 \times a_3 \times l_4}{2 \times l_0} = 289.6 \quad (7.6\ c)$$

$$Pra_4 = P4 + \frac{m_1 \times a_3 \times l_5}{2 \times l_0} + \frac{m_2 \times a_3 \times l_4}{2 \times l_0} = 8.8 \quad (7.6\ d)$$

7- The applied load (lateral direction) during rightward acceleration can be obtained via Eq. (7.7):

$$Ptra_1 = +\frac{m_1 \times a_1 \times l_3}{2 \times l_0} = +109.8 \quad (7.7\text{ a})$$

$$Ptra_2 = -\frac{m_1 \times a_1 \times l_3}{2 \times l_0} = -109.8 \quad (7.7\text{ b})$$

$$Ptra_3 = -\frac{m_1 \times a_1 \times l_3}{2 \times l_0} = -109.8 \quad (7.7\text{ c})$$

$$Ptra_4 = +\frac{m_1 \times a_1 \times l_3}{2 \times l_0} = +109.8 \quad (7.7\text{ d})$$

8- The applied load (radial direction) during rightward acceleration can be obtained via Eq. (7.8):

$$Prd_1 = P1 - \frac{m_1 \times a_3 \times l_5}{2 \times l_0} - \frac{m_2 \times a_3 \times l_4}{2 \times l_0} = 312.8 \quad (7.8\text{ a})$$

$$Prd_2 = P2 + \frac{m_1 \times a_3 \times l_5}{2 \times l_0} + \frac{m_2 \times a_3 \times l_4}{2 \times l_0} = 690.8 \quad (7.8\text{ b})$$

$$Prd_3 = P3 + \frac{m_1 \times a_3 \times l_5}{2 \times l_0} + \frac{m_2 \times a_3 \times l_4}{2 \times l_0} = 338.2 \quad (7.8\text{ c})$$

$$Prd_4 = P4 - \frac{m_1 \times a_3 \times l_5}{2 \times l_0} - \frac{m_2 \times a_3 \times l_4}{2 \times l_0} = -39.8 \quad (7.8\text{ d})$$

9- The applied load (lateral direction) can be obtained via Eq. (7.9):

$$Ptrd_1 = -\frac{m_1 \times a_1 \times l_3}{2 \times l_0} = -109.8 \quad (7.9\text{ a})$$

$$Ptrd_2 = +\frac{m_1 \times a_1 \times l_3}{2 \times l_0} = +109.8 \quad (7.9\text{ b})$$

$$Ptrd_3 = +\frac{m_1 \times a_1 \times l_3}{2 \times l_0} = +109.8 \quad (7.9\text{ c})$$

$$Ptrd_4 = +\frac{m_1 \times a_1 \times l_3}{2 \times l_0} = -109.8 \quad (7.9\text{ d})$$

10- Combined radial and thrust load (during uniform motion) can be obtained:

P_{E1}=P1=337.1N

P_{E2}=P2=666.5N

P_{E3}=P3=313.9N

$P_{E4}=P4=15.5N$

11- Combined radial and thrust load (during leftward acceleration) can be obtained via Eq. (7.10):

$P_E la_1=|Pla_1|+|Ptla_1|=624.1N$ (7.10 a)

$P_E la_2=|Pla_2|+|Ptla_2|=1019.9N$ (7.10 b)

$P_E la_3=|Pla_3|+|Ptla_3|=667.3N$ (7.10 c)

$P_E la_4=|Pla_4|+|Ptla_4|=368.9N$ (7.10 d)

12- Combined radial and thrust load (during leftward acceleration) can be obtained via Eq. (7.11):

$P_E ld_1=|Pld_1|+|Ptld_1|=376.7N$ (7.11 a)

$P_E ld_2=|Pld_2|+|Ptld_2|=656.8N$ (7.11 b)

$P_E ld_3=|Pld_3|+|Ptld_3|=301.2N$ (7.11 c)

$P_E ld_4=|Pld_4|+|Ptld_4|=23.4N$ (7.11 d)

13- Combined radial and thrust load (during rightward acceleration) can be obtained via Eq. (7.12):

$P_E ra_1=|Pra_1|+|Ptra_1|=471.2N$ (7.12 a)

$P_E ra_2=|Pra_2|+|Ptra_2|=752N$ (7.12 b)

$P_E ra_3=|Pra_3|+|Ptra_3|=399.4N$ (7.12 c)

$P_E ra_4=|Pra_4|+|Ptra_4|=118.6N$ (7.12 d)

14- Combined radial and thrust load (during rightward acceleration) can be obtained via Eq. (7.13):

$P_E rd_1=|Prd_1|+|Ptrd_1|=422.6N$ (7.13 a)

$P_E rd_2=|Prd_2|+|Ptrd_2|=800.6N$ (7.13 b)

P_Erd_3=|Prd_3|+|$Ptrd_3$|=448N (7.13 c)

P_Erd_4=|Prd_4|+|$Ptrd_4$|=149.6N (7.13 d)

15- The average load of each linear guide can be obtained via Eq. (7.14):

$$P_{m1=}\sqrt[3]{\frac{1}{2\times l_s}}\times(p_E la_1{}^3\times S_1+P_{E1}{}^3\times S_2+P_E ld_1{}^3\times S_3+P_E ra_1{}^3\times S_1+P_{E1}{}^3\times S_2+ P_E rd_1{}^3\times S_3)=359.3 \quad (7.14\ a)$$

$$P_{m2=}\sqrt[3]{\frac{1}{2\times l_s}}\times(p_E la_2{}^3\times S_1+P_{E2}{}^3\times S_2+P_E ld_2{}^3\times S_3+P_E ra_2{}^3\times S_1+P_{E2}{}^3\times S_2+ P_E rd_2{}^3\times S_3)=686.3 \quad (7.14\ b)$$

$$P_{m3=}\sqrt[3]{\frac{1}{2\times l_s}}\times(p_E la_3{}^3\times S_1+P_{E3}{}^3\times S_2+P_E ld_3{}^3\times S_3+P_E ra_3{}^3\times S_1+P_{E3}{}^3\times S_2+ P_E rd_3{}^3\times S_3)=341.3 \quad (7.14\ c)$$

$$P_{m4=}\sqrt[3]{\frac{1}{2\times l_s}}\times(p_E la_4{}^3\times S_1+P_{E4}{}^3\times S_2+P_E ld_4{}^3\times S_3+P_E ra_4{}^3\times S_1+P_{E4}{}^3\times S_2+ P_E rd_4{}^3\times S_3)=111.2 \quad (7.14\ d)$$

Table 2: The RGW-CC/RGW-HC Series of Linear Guides(corp., 2011)

Model No.	Dimensions of Assembly (mm)			Dimensions of Block (mm)															Dimensions of Rail (mm)							Mounting Bolt for Rail	Basic Dynamic Load Rating	Basic Static Load Rating	Static Rated Moment			Weight	
																													M_R	M_P	M_Y	Block	Rail
	H	H_1	N	W	B	B_1	C	C_1	L_1	L	K_1	K_2	G	M	T	T_1	H_2	H_3	W_R	H_R	D	h	d	P	E	(mm)	C(kN)	C_0(kN)	kN-m	kN-m	kN-m	kg	kg/m
RGW15CC	24	4	16	47	38	4.5	30	26	45	68	11.4	4.7	5.3	M5	6	6.95	3.6	6.1	15	16.5	7.5	5.7	4.5	30	20	M4x16	11.3	24	0.311	0.173	0.173	0.23	1.8
RGW20CC	30	5	21.5	63	53	5	40	35	57.5	86	13.8	6	5.3	M6	8	10	4.3	4.3	20	21	9.5	8.5	6	30	20	M5x20	21.3	46.7	0.647	0.46	0.46	0.44	2.76
RGW20HC									77.5	106	23.8																26.9	63	0.872	0.837	0.837	0.62	
RGW25CC	36	5.5	23.5	70	57	6.5	45	40	64.5	97.9	15.75	7.25	12	M8	9.5	10	6.2	6	23	23.6	11	9	7	30	20	M6x20	27.7	57.1	0.758	0.605	0.605	0.67	3.08
RGW25HC									81	114.4	24																33.9	73.4	0.975	0.991	0.991	0.86	
RGW30CC	42	6	31	90	72	9	52	44	71	109.8	17.5	8	12	M10	9.5	10	6.5	7.3	28	28	14	12	9	40	20	M8x25	39.1	82.1	1.445	1.06	1.06	1.06	4.41
RGW30HC									93	131.8	28.5																48.1	105	1.846	1.712	1.712	1.42	
RGW35CC	48	6.5	33	100	82	9	62	52	79	124	16.5	10	12	M10	12	13	9	12.6	34	30.2	14	12	9	40	20	M8x25	57.9	105.2	2.17	1.44	1.44	1.61	6.06
RGW35HC									106.5	151.5	30.25																73.1	142	2.93	2.6	2.6	2.21	
RGW45CC	60	8	37.5	120	100	10	80	60	106	153.2	21	10	12.9	M12	14	15	10	14	45	38	20	17	14	52.5	22.5	M12x35	92.6	178.8	4.52	3.05	3.05	3.22	9.97
RGW45HC									139.8	187	37.9																116	230.9	6.33	5.47	5.47	4.41	
RGW55CC	70	10	43.5	140	116	12	95	70	125.5	183.7	27.75	12.5	12.9	M14	16	17	12	17.5	53	44	23	20	16	60	30	M14x45	130.5	252	8.01	5.4	5.4	5.18	13.98
RGW55HC									173.8	232	51.9																167.8	348	11.15	10.25	10.25	7.34	
RGW65CC	90	12	53.5	170	142	14	110	82	160	232	40.8	15.8	12.9	M16	22	23	15	15	63	53	26	22	18	75	35	M16x50	213	411.6	16.20	11.59	11.59	11.04	20.22
RGW65HC									223	295	72.3																275.3	572.7	22.55	22.17	22.17	15.75	

Note : 1 kgf = 9.81 N

Appendix G:

Optimization Methods:

The ANSYS Design Xplorer offers the following Goal Driven Optimization methods

Method	Description	Response Surface Optimization	Direct Optimization
Screening	Shifted-Hammersley Sampling	X	X
NLPQL	Nonlinear Programming by Quadratic Lagrangian	X	X
MISQP	Mixed-Integer Sequential Quadratic Programming	X	X
MOGA	Multi-Objective Genetic Algorithm	X	X
Adaptive Single-Objective	Hybrid optimization method using Latin Hypercube Sampling, a Kriging response surface, NLPQL and domain reduction in a Direct Optimization system		X
Adaptive Multiple-Objective	Hybrid optimization method using a Kriging response surface and MOGA in a Direct Optimization system		X

Performing a Screening Optimization

The Screening option can be used for both Response Surface Optimization and Direct Optimization. It allows you to generate a new sample set and sort its samples based on objectives and constraints. It is a non-iterative approach that is available for all types of input parameters. Usually the Screening approach is used for preliminary design, which may lead you to apply the MOGA or NLPQL options for more refined optimization results.

Performing a MOGA Optimization

The MOGA (Multi-Objective Genetic Algorithm) option can be used for both Response Surface Optimization and Direct Optimization. It allows you to generate a new sample set or use an existing set for providing a more refined approach than the Screening method. It is available for continuous input parameters only and can handle multiple goals.

Performing an Adaptive Multiple-Objective Optimization

The Adaptive Multiple-Objective (Kriging + MOGA) option can be used only for Direct Optimization systems. It is an iterative algorithm that allows you to either generate a new sample set or use an existing set, providing a more refined approach than the Screening method. It uses the same general approach as MOGA, but applies the Kriging error predictor to reduce the number of evaluations needed to find the global optimum.

The table below shows the general capabilities of each method

Method	Single Objective	Multiple Objectives	Local Search	Global Search	Discrete & Manufacturable Values
Screening		X		X	X
NLPQL	X		X		
MISQP	X		X		X
MOGA		X		X	
Adaptive Single-Objective	X			X	
Adaptive Multiple-Objective		X		X	